Armed Forces Institute of Regenerative Medicine

Annual Report 2012
Technical Progress Reports

ARMED FORCES INSTITUTE OF REGENERATIVE MEDICINE

AFIRM

our science for their healing

Armed Forces Institute of Regenerative Medicine

Annual Report 2012 Technical Progress Reports

This report contains technical progress reports of all currently funded Armed Forces Institute of Regenerative Medicine research projects. Nontechnical summaries of these projects are contained in the AFIRM Annual Report 2012.

Ms. Kathleen Berst
AFIRM Acting Director
kathleen.berst@us.army.mil

Table of Contents

III: Craniofacial Reconstruction

Bone Regeneration

Soft Tissue Regeneration

Cartilage Regeneration (Focus: Ear)

IV: Scarless Wound Healing

Control of Wound Environment and Mechanics

Therapeutic Delivery to Wounds

Table of Contents

Clinical Trials

VI: Compartment Syndrome

Cellular Therapy of CS

Biological Scaffold-Based Treatment of CS

I: Introduction

Background

The wars in Iraq and Afghanistan have resulted in more than 6,600 U.S. military fatalities and nearly 50,000 injuries.[1] The use of improvised explosive devices in Operation Iraqi Freedom/Operation Enduring Freedom/Operation New Dawn has led to a substantial increase in severe blast trauma; explosive injury mechanisms have accounted for approximately 75% of all combat-related injuries.[2] Advances in body armor to protect the torso and vital organs, faster evacuation from the battlefield after injury, and major advances in trauma resuscitation save wounded warriors who would have died of their injuries in previous conflicts. However, those who survive often have seriously debilitating injuries to unprotected structures of the face, neck, head, and limbs, causing massive trauma and tissue loss.

[1] As of October 4, 2012 http://www.defense.gov/news/casualty.pdf.
[2] Belmont, et al. *J Trauma Acute Care Surg.* 2012 Jul;73(1):3-12.

WFPC researchers Sean Murphy and Muhammad Albanna inspect the printhead mechanism for the mobile bioprinter.

The emerging field of regenerative medicine focuses on (1) restoring the structure and function of tissues and organs that have been damaged and (2) finding methods of curing previously untreatable injuries and diseases. Regenerative medicine holds great potential for healing military personnel with debilitating, disfiguring, and disabling injuries. Scientists working in the area of regenerative medicine are applying a variety of approaches to prompt the body to regenerate cells and tissues, often using the patient's own cells combined with degradable biomaterials. Use of a patient's own cells eliminates the possibility of tissue rejection. Technologies for engineering tissues are developing rapidly. The ultimate goal is to deliver advanced therapies, such as whole organs and engineered fingers and limbs, to injured members of the military as well as civilians.

Research Goals

The AFIRM is a multi-institutional, interdisciplinary network focused on developing advanced treatment options for severely wounded warfighters. The mission of the AFIRM is to accelerate the delivery of regenerative medicine therapies to treat the most severely injured U.S. service members. Clinical trials of several AFIRM products, including advanced transplantation strategies and engineered skin replacement applications, are under way. Inclusion of military patients in these trials is the first step in delivering advanced technologies to wounded warriors.

The AFIRM Has Five Major Research Programs:

Limb and Digit Salvage
Saving the limb, also referred to as "limb salvage," at a minimum requires (1) bridging large bony defects to restore skeletal integrity; (2) bridging soft tissues, such as muscle, nerves, tendons, and ligaments, to lend stability and enable movement; and (3) covering the injured area with healthy skin. The AFIRM Limb and Digit Salvage Program is dedicated to developing regenerative medicine therapies to help health care providers save and rebuild injured limbs. Enabling victims of severe extremity trauma to recover rapidly, reliably, and completely so they can return to productive lives is the ultimate goal of the program.

Craniofacial Reconstruction
Massive bone and soft tissue loss to the face and head due to blast forces is a devastating injury. The AFIRM Craniofacial Reconstruction Program is designing and developing therapies that health care providers can use to return form and function of the face, head, and neck to warfighters with severe craniofacial injuries. These therapies will (1) regenerate functional bone and cartilage to levels of the face; (2) restore motor and sensate competencies through muscle, vascular, and nerve regeneration; (3) mitigate scar formation; (4) prevent infection; and (5) eliminate skin coverage deficits through tissue engineering. The creation and delivery of new polymers and tissues will preserve and regenerate bone and soft tissue capable of administering stem cells, growth factors, bone derivatives, and therapeutic drugs.

Scarless Wound Healing
Military trauma burns often heal with large scars that may impair normal function and cause significant disfigurement. Scars are the result of the body's complex series of wound-healing processes that begin at the onset of injury and can continue for months. This AFIRM program is investigating all phases of wound healing and scar formation

to find new treatment strategies to prevent and mitigate scars.

Burn Repair
Severe burns are associated with substantial morbidity and mortality in spite of many advances in medical care. The AFIRM Burn Repair Program is leveraging regenerative medicine technology to (1) prevent wound infection, (2) prevent burn inflammation and injury progression, (3) speed generation of a viable wound bed and reduce reharvest time of autograft donor sites, (4) improve skin substitutes for burn wound grafting when autografts are not immediately available, and (5) prevent and manage scars.

Compartment Syndrome
Compartment syndrome is often a secondary sequela resultant from blast injuries, severe blunt or penetrating trauma, fractures, and vascular injuries. Muscles are encased in compartments of nonyielding tissue called fascia. Bleeding or tissue swelling within a muscle compartment raises the pressure in the compartment that, if unchecked, can become high enough that blood flow into the compartment is reduced or completely stopped. Prolonged interruption of blood flow can destroy the nerves and muscles within the compartment. Restoration of those damaged or destroyed tissues has no satisfactory solution with current surgical options. This AFIRM program focuses on advancing effective therapies to stabilize tissue and reduce the onset of late effects of nerve and muscle damage.

History

In 2005, Dr. Anthony Atala presented some of the latest advances in the field of regenerative medicine at the Advanced Technology Applications in Combat Casualty Care Conference. This talk alerted the combat casualty care research community to the near-term potential for regenerative medicine products that could make a substantial difference in the care of our wounded warriors. The following year, the Army's Director of the Combat Casualty Care Research Program, COL Bob Vandre, developed the idea of a regenerative medicine institute similar to the Department of Defense's (DoD's) Multidisciplinary University Research Initiatives but aimed at near-term, translational research. COL Vandre received U.S. Army Medical Research and Materiel Command (USAMRMC) approval in 2006 to pursue funding for the project. He subsequently briefed the DoD Technology Area Review and Analysis panel, which reviews medical research and development for the DoD. The concept received high approval from the panel.

In 2007, USAMRMC, the Office of Naval Research, the U.S. Air Force Office of the Surgeon General, the National Institutes of Health (NIH), and the Veterans Health Administration of the Department of Veterans Affairs (VA) agreed to co-fund the new institute. Taking their funds and adding in $10 million (M) from the 2007 War Supplemental bill provided $8.5M per year in funding for the AFIRM, which was deemed sufficient to proceed.

A Program Announcement was released in August 2007, and seven proposals were received in October 2007. In December 2007, two finalists were selected for oral presentations. Both received scores of "excellent," and one was selected for funding. White House staffers heard about the AFIRM and invited representatives from USAMRMC to come and discuss the new institute.

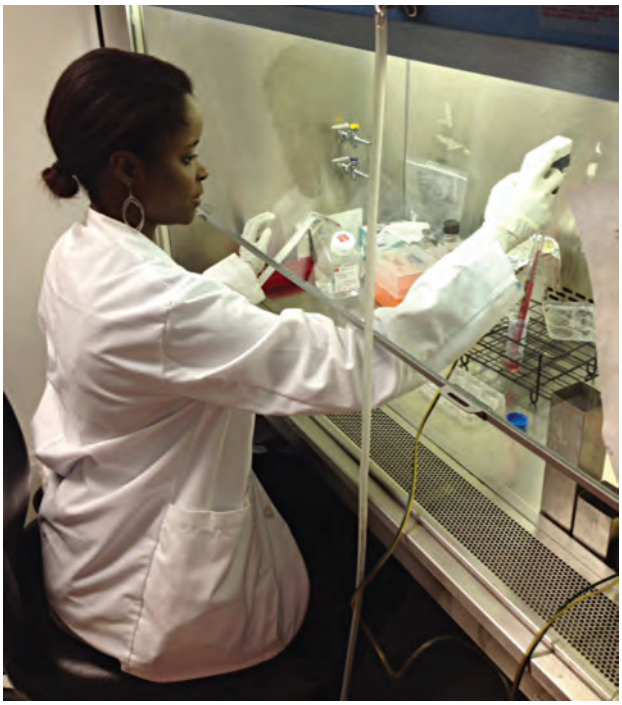

RCCC researcher Olive Mwizerwa is producing sterile muscle constructs.

After two meetings and upon hearing that there was funding for only one AFIRM finalist, the DoD was tasked to provide funding for the second AFIRM finalist. Within 1 week, an additional $8.5M per year was transferred to USAMRMC's budget lines. Both AFIRM finalists signed USAMRMC cooperative agreements in March 2008.

Funding – A Six-Way Partnership

The AFIRM is financed with basic research through exploratory development funds and is expected to make major advances in the ability to understand and control cellular responses in wound repair and organ/tissue regeneration. The program is managed and funded through USAMRMC with funding from the following organizations:

- U.S. Army
- U.S. Navy, Office of Naval Research
- U.S. Air Force, Office of the Surgeon General
- Veterans Health Administration
- Defense Health Program
- NIH
- Total funding for the first 5 years of the AFIRM amounts to more than $300M:
  - $100M from U.S. Government funding (Army, Navy, Air Force, VA, and NIH).
  - $80M from matching funds received from state governments and participating universities.
  - $109M from pre-existing research projects directly related to deliverables of the AFIRM from the NIH, Defense Advanced Research Projects Agency, congressional special programs, the National Science Foundation, and philanthropy.
  - $25M in additional funds provided by the Defense Health Program.

Structure

The AFIRM is composed of two independent civilian research consortia working with the U.S. Army Institute of Surgical Research (USAISR) at Fort Sam Houston, Texas. USAISR, which includes the San Antonio Military Medical Center – North (formerly Brooke Army Medical Center), serves as the AFIRM's primary government component and is home to the DoD's only burn unit. The two AFIRM research consortia are responsible for executing the management of overall therapeutic programs and individual projects within their consortia. One consortium is led by Rutgers, the State University of New Jersey, and the Cleveland Clinic, and the other is led by the Wake Forest Institute for Regenerative Medicine and the McGowan Institute for Regenerative Medicine in Pittsburgh. Each of these civilian consortia is itself a multi-institutional network, as described in the following paragraphs.

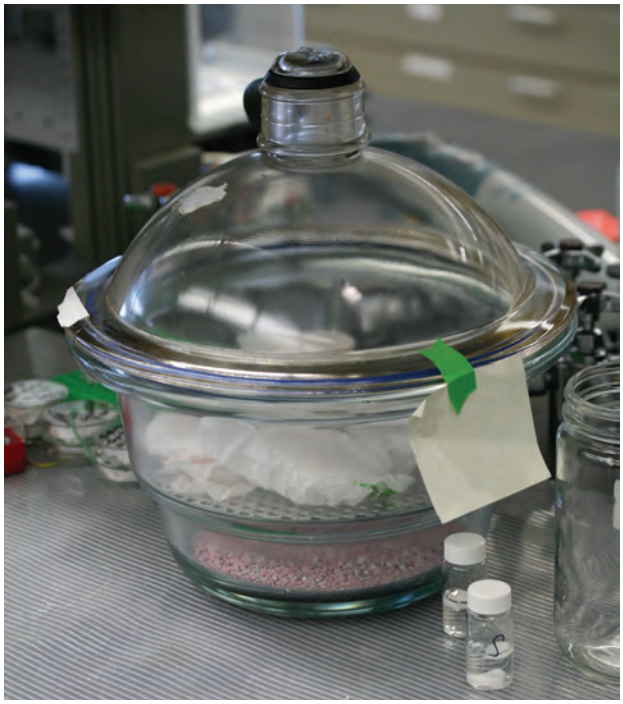

Degassing of bone regeneration scaffolds in an AFIRM laboratory .

Rutgers-Cleveland Clinic Consortium

The Rutgers-Cleveland Clinic Consortium (RCCC) is directed by Joachim Kohn, PhD, Director of the New Jersey Center for Biomaterials and Board of Governors Professor of Chemistry at Rutgers University, and co-directed by Linda Graham, MD, Staff Vascular Surgeon at the Cleveland Clinic and Professor in the Department of Biomedical Engineering at the Lerner Research Institute at Case Western Reserve University.

The RCCC consists of the following member institutions:

- Rutgers the State University of New Jersey/ New Jersey Center for Biomaterials
- Cleveland Clinic

- Brigham and Women's Hospital
- Carnegie Mellon University
- Case Western Reserve University
- Cooper Medical School of Rowan University
- Dartmouth Hitchcock Medical Center/Thayer School of Engineering
- Massachusetts General Hospital/Harvard Medical School
- Massachusetts Institute of Technology
- Minnesota Medical Research Foundation
- Mayo Clinic College of Medicine
- Northwestern University
- Stony Brook University
- University of Cincinnati
- University of Florida
- University of Medicine and Dentistry of New Jersey
- University of Minnesota
- University of Michigan
- University of Pennsylvania
- University of Virginia
- Vanderbilt University

Wake Forest–Pittsburgh Consortium

The Wake Forest–Pittsburgh Consortium (WFPC) is directed by Anthony Atala, MD, Director of the Wake Forest Institute for Regenerative Medicine and Professor and Chair of the Department of Urology at Wake Forest University, and co-directed by Rocky Tuan, PhD, Director of the Center for Cellular and Molecular Engineering at the University of Pittsburgh.

The WFPC consists of the following member institutions:

- Wake Forest Institute for Regenerative Medicine/ Wake Forest University
- McGowan Institute for Regenerative Medicine/ University of Pittsburgh
- Allegheny-Singer Research Institute
- Carnegie Mellon University
- Georgia Institute of Technology
- Institute for Collaborative Biotechnologies (includes University of California, Santa Barbara; Massachusetts Institute of Technology; and California Institute of Technology)
- Johns Hopkins University School of Medicine
- Oregon Health and Science University
- Rice University
- Sanford-Burnham Medical Research Institute/ University of California, Santa Barbara
- Stanford University
- Tufts University
- University of California, Berkeley
- University of Chicago
- University of Texas Health Science Center at Houston
- University of Wisconsin
- Vanderbilt University

Additional Collaborators to the AFIRM

AFIRM researchers have established more than 90 national and international partnerships with academia and industry, which has contributed to the success of the program to date. A complete list of AFIRM collaborators can be found

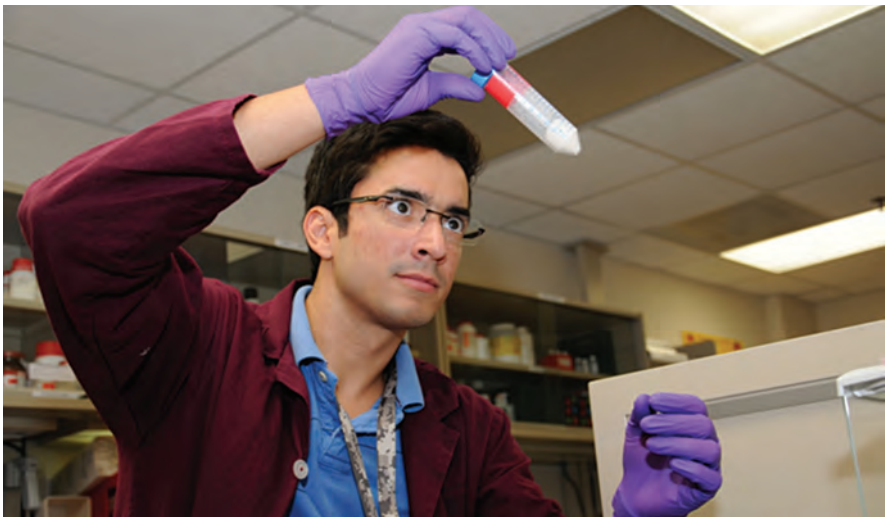

Graduate student researcher Ramon E. Coronado at USAISR analyzes an extracellular matrix powder from decellularized human adipose tissue.

AFIRM researcher fabricating polymer films in the laboratory.

in the Introduction chapter of the AFIRM Annual Report 2012.

Programs and Projects

Within each consortium, research activities are organized into programs. Some of the consortia programs are directly comparable to the AFIRM's major research programs (e.g., RCCC's CranioMaxilloFacial Program) while other consortia programs consolidate expertise such as WFPC's Extremity Injury Program that integrates experts in the areas of limb and digit salvage and compartment syndrome. Each program consists of multiple projects and is coordinated by a scientist or clinician Program Leader. Each project is directed by one or more Project Leaders and can vary in size from a single laboratory to a collaboration spanning multiple institutions.

Consortium members evaluate all levels of the operation annually to monitor progress and guide the consortium's activities. Active project management by each consortium has reshaped the programs, leading to the termination or reduced funding of some projects and the addition of projects that are more promising for accelerated development. The consortia also engage external scientific program and product development consultants who provide advice about clinical trials, product development plans and other recommendations for commercialization. Additionally, information for the public, including clinical trial opportunities, has been made available through web sites developed and maintained by the consortia.

In addition to the three core groups (RCCC, WFPC, and USAISR), intramural researchers from the NIH and/or the Veterans Health Administration can participate in the AFIRM Program although none have chosen to do so as of yet. With the approval of a program leader, these intramural researchers can lead projects.

Management and Oversight

Day-to-day execution of the AFIRM's Science and Technology and Translational Science portfolio is managed by the AFIRM Project Management Office (PMO), located within the U.S. Army Medical Materiel Development Activity at Fort Detrick, Maryland. The AFIRM PMO works as part of an integrated project management team, across the AFIRM consortia, to incorporate the strategic, developmental, and tactical aspects of product management. The AFIRM PMO also functions as an accountability model to ensure execution of the AFIRM portfolio.

The AFIRM is guided by a Board of Directors and an Integrated Project Team, which contains a Steering Group. A Program Synergy Group is responsible for research coordination and communication between the three components of the AFIRM. Details of the roles and membership of each of these entitles can be found in the Introduction chapter of the AFIRM Annual Report 2012.

II: Limb and Digit Salvage

Bone Repair and Regeneration

Advanced 3D Scaffolds for Large Segmental Bone Defects: Non-Load-Bearing Tyrosine-Derived Polycarbonate Scaffolds

Project 4.2.1a, RCCC

Team Leader(s): Ophir Ortiz, PhD (New Jersey Center for Biomaterials at Rutgers University)

Project Team(s): Aniq Darr, PhD, Koustubh Dube, MS, and Durgadas Bolikal, PhD (New Jersey Center for Biomaterials at Rutgers University)

Collaborator(s): Racquel LeGeros, PhD (New York University, NYU)

Therapy: Advanced Regeneration of Segmental Bone Defects

Deliverable(s): Tyrosine-derived polycarbonate (TyrPC) scaffolds containing calcium phosphates (CaPs)

TRL Progress: 2010, TRL 3; 2011, TRL 3; 2012 (Current), TRL 4; 2013 (Target), TRL 4/5

Key Accomplishments: The researchers synthesized four CaPs with varying solubilities and incorporated them into the TyrPC terpolymer to produce composite scaffolds. They tested the CaP-containing scaffolds in vivo in a rabbit calvarial critical-size defect model and found that three of the four TyrPC/CaP composite scaffolds regenerated bone as well as or better than a commercially available bone scaffold control. The best performer of these three scaffolds will be biologically enhanced and evaluated in vivo.

Key Words: Bone repair, bone defect, bone graft, scaffold, osteogenesis

Introduction

The repair of large bone defects and fracture non-unions in extremity injury is a key objective of the AFIRM Limb and Digit Salvage Program. Treating these injuries is an ongoing need because high-energy blast injuries from improvised explosive devices (IEDs) have become increasingly common. Extremity injuries traditionally comprise the majority (58%–88%) of traumatic injuries in the U.S. armed conflicts. The contemporary standards of care for bone defects and complex fractures, in both civilian and military practice, include many options for wound management, fixation, and bone grafting. One potential option for bone replacement is the use of ceramic-based grafts. RCCC's Limb Salvage and Transplantation Program will provide injured warriors with one or more new clinical methods that significantly improve bone regeneration, particularly, healing of bone defects greater than 3 cm or bone non-unions quickly and reliably. This project specifically focuses on developing advanced scaffolds to treat these large segmental bone defects.

During the first year of the project, the researchers designed and fabricated four distinct families of copolymer-based osteoconductive scaffolds and determined that the tyrosine-based copolymer and poly(alkyl ester) composites provided the best in vivo performance. In the second year, they completed competitive assessment and down-selection of scaffold materials in the canine femoral multidefect (CFMD) model. Of the materials they tested, the porogen-leached TyrPC with beta tri-calcium phosphate (TCP) performed best. The researchers also established historical performance standards that can be used to rapidly measure the performance of new or competing scaffold materials in the CFMD model. In the third year, the researchers found that a rapidly resorbing, porogen-leached TyrPC scaffold containing TCP granules and a slowly resorbing, structural poly(propylene fumarate) (PPF) scaffold coated with poly(lactic-co-glycolic acid) (PLGA) and hyaluronan acid (HA) represented the best performing polymer scaffolds tested to date.

In Year 4, this project was divided into Projects 4.2.1a (focus: TyrPC scaffolds) and 4.2.1b (focus: PFF scaffolds).

Research Progress – Year 4

Screening/Selection of New Composite Scaffolds in Animal Models

TyrPC terpolymers were used as a platform to test the bone-regenerating performance of four CaP minerals, which were produced in consultation with Dr. Racquel LeGeros at New York University. TyrPC was selected for its nontoxicity and osteoconductivity. CaPs, which mimic the compositions of natural bone, were added to TyrPC as a bioactive component. Each of the four different CaP minerals were incorporated into TyrPC scaffolds (referred to as composite scaffolds) and evaluated in the rabbit calvarial critical-size defect model. One scaffold was implanted per animal. At 6 weeks post implantation, the defect area was assessed for new bone formation using microcomputed tomography (microCT). MicroCT data revealed that three of the four composite scaffolds regenerated bone as well as or better than a commercially available bone scaffold control (**Figure 1**).

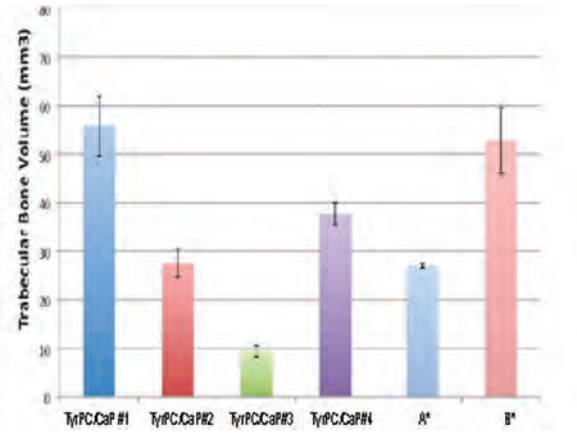

Figure 1. Trabecular bone volume resulting from treatment with each of the four TyrPC/CaP formulations evaluated. Data from two commercially available bone grafts (A and B) were added for comparison purposes.

TyrPC/CaP 1 was identified as the best performer in the test group. Based on these results, TyrPC/CaP 1 will be biologically enhanced (as described in Project 4.2.3) and evaluated in vivo.

Conclusions

In Year 4, the Rutgers team utilized CaPs to enhance the performance of TyrPC bone regeneration scaffolds. Analysis with microCT revealed that three TyrPC/CaP composite scaffolds regenerated bone as well as or better than a commercially available bone scaffold control. The team identified TyrPC/CaP 1 as the best performer in the test group.

Research Plans for Year 5

In Year 5, the enhancement of TyrPC bone regeneration scaffolds with calcium minerals will continue to be optimized. The researchers will focus on TyrPC/CaP 1, based on the Year 4 results. They will biologically enhance TyrPC/CaP 1 by integrating cell sourcing/delivery (Project 4.2.2) and molecular surface design (Project 4.2.3) strategies. These strategies will be evaluated in the rabbit critical size-segmental defect model.

Planned Clinical Transitions

A 510(k) is planned for a TyrPC bone pin made of the same polymer used in the TyrPC bone regeneration scaffold. A Phase 1 clinical trial has been designed and the team is seeking funding. Another 510(k) is planned for the first-generation bone regeneration scaffold. Subsequent combination products that include a soluble or tethered biologic will be pursued on the premarket application pathway. Concurrently, product development feasibility studies will be accelerated to ensure a fast and seamless transition to industry to provide a new treatment option for military and civilian patients suffering from severe bone injury.

Bone Repair and Regeneration

Advanced 3D Scaffolds for Large Segmental Bone Defects: Partial Load-Bearing Poly(Propylene Fumarate) Scaffolds

Project 4.2.1b, RCCC

Team Leader(s): Michael Yaszemski, MD, PhD, (Mayo Clinic [MC])

Project Team(s): Mahrokh Dadsetan, PhD, Brett Runge, PhD, Suzanne Segovis, MBA, and Lichun Lu, PhD (MC)

Collaborator(s): Pamela Brown Baer, PhD, Joseph Wenke, PhD, U.S. Army Institute of Surgical Research (USAISR); Ralph Carmichael, JD, MBA (BonWrx, Inc.); and Raquel LeGeros, PhD (New York University)

Therapy: Treatment of segmental bone defects

Deliverable(s): PPF scaffolds with CaP surface coating for bone regeneration

TRL Progress: 2010, TRL 3; 2011, TRL 3; 2012 (Current), TRL 4; 2013 (Target), TRL 4

Key Accomplishments: The researchers fabricated PPF scaffolds for the rabbit calvarial defect model, loaded the scaffolds with recombinant human bone morphogenetic protein-2 (rhBMP-2) via a collagen-based hydrogel for controlled delivery, and quantified (in vitro) the delivery kinetics of the rhBMP-2 from the hydrogels in the scaffold pores. The group then demonstrated an increase in bone formation in an in vivo rabbit calvarial model, via a combination of CaP surface coating on the scaffold and rhBMP-2-controlled delivery from the scaffold.

Key Words: Bone repair, bone defect, bone graft, scaffold, osteoinduction, calcium phosphate, osteoconduction

Introduction

The conflicts in Iraq and Afghanistan have seen improvements in body protection, with a resulting increase in the frequency of extremity injuries in our war wounded. Two-thirds of the extremity fractures are Grades 2 and 3 (severe) and frequently have segmental skeletal defects as a component of injury. The repair of segmental bone defects and fracture non-unions is a key target of the AFIRM Limb and Digit Salvage Program. Often, the injuries also include damaged or missing soft tissues and a compromised skeletal base, which is an essential platform for the healing of the injured soft tissues. Current skeletal reconstruction methods appropriately address many of these injuries. However, there is a need for additional surgical options for those wounded warriors for whom the existing methods do not result in a healed skeletal defect. Current bone graft options include autogenous cancellous bone (ACB), allograft bone, addition of bone marrow-derived cells (with or without cell processing), bone transport, and local delivery of osteoinductive proteins. The novel therapies that become available via AFIRM to our war wounded will be immediately translatable to our civilian population.

The RCCC solution to the unmet need of bone regeneration in segmental skeletal defects or non-unions is to develop skeletal implants that can (1) be processed into any desired size and geometry, (2) have an internal architecture that is macroporous, microporous, and interconnected, (3) have an osteoconductive CaP surface coating on all internal and external surfaces, and (4) have the property of being able to deliver a variety of biomolecules in a controlled, sustained manner that will direct the cellular processes that result in bone formation. This solution offers precise implant geometry to match that of the missing bone. The shape-specific scaffold has appropriate mechanical strength to physically prevent the encroachment of adjacent soft tissues into the reconstruction volume, to bear load immediately after implantation so that joint and muscle rehabilitation can occur during bone healing, and to effect bone healing.

In addition, the ability to include controlled delivery of antibiotics and osteoinductive proteins, when the clinical situation calls for them, does not exist in any of the currently available therapies.

During the first 2 years of the project, the researchers designed and fabricated four distinct families of copolymer-based osteoconductive scaffolds and completed competitive assessment and down-selection of scaffold materials in the CFMD model. Of the materials they tested, the porogen-leached TyrPC with β-tricalcium phosphate (BTCMP) performed best. In Year 3, the researchers found that a rapidly resorbing, porogen-leached TyrPC scaffold containing TCP granules and a slowly resorbing, structural PPF scaffold coated with PLGA and HA represented the best performing polymer scaffolds tested to date.

Research Progress – Year 4

PPF Synthesis and Scaffold Fabrication

PPF was used to fabricate scaffolds for in vivo studies in the rabbit calvarial defect model. PPF undergoes shrinkage during the laser stereolithography scaffold fabrication process. PPF scaffold surfaces were coated with three different coating materials: magnesium substituted BTCMP, carbonate hydroxyapatite (synthetic bone mineral, SBM), and a BTCMP: hydroxyapatite blend (biphasic calcium phosphate, BCP). The coated scaffolds were characterized using scanning electron microscopy (SEM), energy dispersive x-ray analysis (EDXA), and x-ray photoelectron spectroscopy (XPS).

Characterization of PPF Scaffolds Coated with CaPs

Surface coating the polymeric scaffolds alters their surface topography in that the smooth PPF surface becomes a rough CaP surface. Previous work by the Yaszemski group has shown that the presence of scaffold surface roughness improves cell attachment, as compared to a smooth scaffold surface of similar composition. The CaP coating did not affect the PPF scaffolds' pore interconnectivity.

Recombinant Human Bone Morphogenetic Protein-2 Incorporation and Release

Recombinant human bone morphogenetic protein 2 (rhBMP-2) at concentrations of 0, 50, and 100 µg was loaded onto PPF scaffold surfaces, using a bovine collagen-based (3 mg/mL) hydrogel as a delivery vehicle, for studies of loading efficiency and release kinetics (using the 50 µg rhBMP-2 concentration), and for implantation in rabbit calvarial defects. The researchers found that only 20% of the rhBMP-2 was released from the scaffolds that were coated with SBM (carbonate hydroxyapatite). Moreover, measurements of the alkaline phosphatase (ALP) activity of the osteoblasts revealed that rhBMP-2 released from all scaffolds remained biologically active. This rhBMP-2 biologic activity manifested itself via an increase in the ALP activity of the cells when they were exposed to the released rhBMP-2. The magnesium substituted BTCMP scaffolds have the same composition as the "BTCMP/trim" scaffolds. The latter scaffolds have been trimmed with a nail file after loading with rhBMP-2, but prior to beginning the release experiments, to simulate the trimming necessary for some specimens to obtain a secure fit in the rabbit calvarium implantation study.

Rabbit Surgery

PPF scaffolds with the three different CaP coatings and the three rhBMP-2 levels (n=10 scaffolds per group for each of the nine groups in this full factorial experimental design) were implanted in 90 rabbit calvarial defects at USAISR at the San Antonio Military Medical Center. Briefly, critical-size calvarial defects (15 mm in diameter) were created in skeletally mature New Zealand White male rabbits. The 3D PPF scaffold was placed in the defect and the wound was closed in anatomic layers. Some of the scaffolds were slightly (about 0.2–0.6 mm) larger than the 15 mm defects. To fit them in the defect, they were trimmed prior to the surgery using autoclaved nail files. The Mayo laboratory has previously demonstrated in vitro, as described previously, that when trimming, some of the rhBMP-2 is removed from the scaffold surfaces resulting in inconsistent bone regeneration within defects in vivo. After 6 weeks, the rabbits were euthanized, and the calvaria were recovered. Calvaria were analyzed by microCT. The micro-CT data show that

scaffolds without rhBMP-2 had 36% bone volume. The addition of 50 and 100 µg of rhBMP-2 to the scaffolds increased the bone volume to 69% of the void space available for bone growth. The bone volume was similar on scaffolds coated with BTCMP and SBM (carbonate hydroxyapatite). These volumes, expressed as a percentage of the available space that is filled with new bone, contained three times the amount of bone found in normal trabecular bone (23%). The bone volume was slightly less on scaffolds coated with the biphasic HA/TCP blend (BCP). PPF is, by design, a slowly degrading polymer that provides immediate structural support to a skeletal defect and had not begun to degrade at 6 weeks after implantation. Therefore, at 40% scaffold porosity, only 40% of the total specimen volume of 442 mm^3 (that is, 176.8 mm^3) is available for tissue ingrowth. In previous work by the Mayo laboratory with another critical-size defect model (rat femoral defect), the total regenerated bone volume in PPF scaffolds increased by 60% during the interval from 6 weeks to 12 weeks. The bone growth into the scaffolds in the current study should behave similarly with time in vivo beyond 6 weeks.

Conclusions

The CaP-coated PPF scaffolds fabricated via stereolithography have interconnected pores, appropriate mechanical properties for the treatment of segmental skeletal defects, and are promising candidates for further scaffold development. The combination of CaP coating and rhBMP-2 controlled delivery improves the in vivo performance of 3D porous PPF scaffolds. The anticipated additional advances include the controlled delivery of other bioactive molecules from the scaffolds, the tethering of signaling molecules to the scaffold surfaces, and the selective retention of cells on the scaffolds.

Research Plans for Year 5

The CaP-coated PPF scaffolds with controlled rhBMP-2 delivery will be evaluated in the rat femoral defect model. The implants will be press-fitted into femoral segmental defects in 45 rats (5 rats/group x 9 groups). After 12 weeks, the specimens will be harvested, and micro-CT, mechanical testing, and histology will be performed.

Planned Clinical Transitions

The Mayo Clinic is currently working with the AFIRM industry partner, BonWrx, Inc., to establish protocols for the manufacturing and filing for FDA device Investigational Device Exemption (IDE) approval. The researchers will work collaboratively with BonWrx, Inc. to scale up the synthesis of PPF and fabricate the scaffolds via Good Manufacturing Practice (GMP) and to begin the tests that the FDA will require (e.g., toxicology) in a commercial testing laboratory. BonWrx, Inc. currently licenses several of the Yaszemski group's patents. The novel materials used in this study have entered the patent approval process.

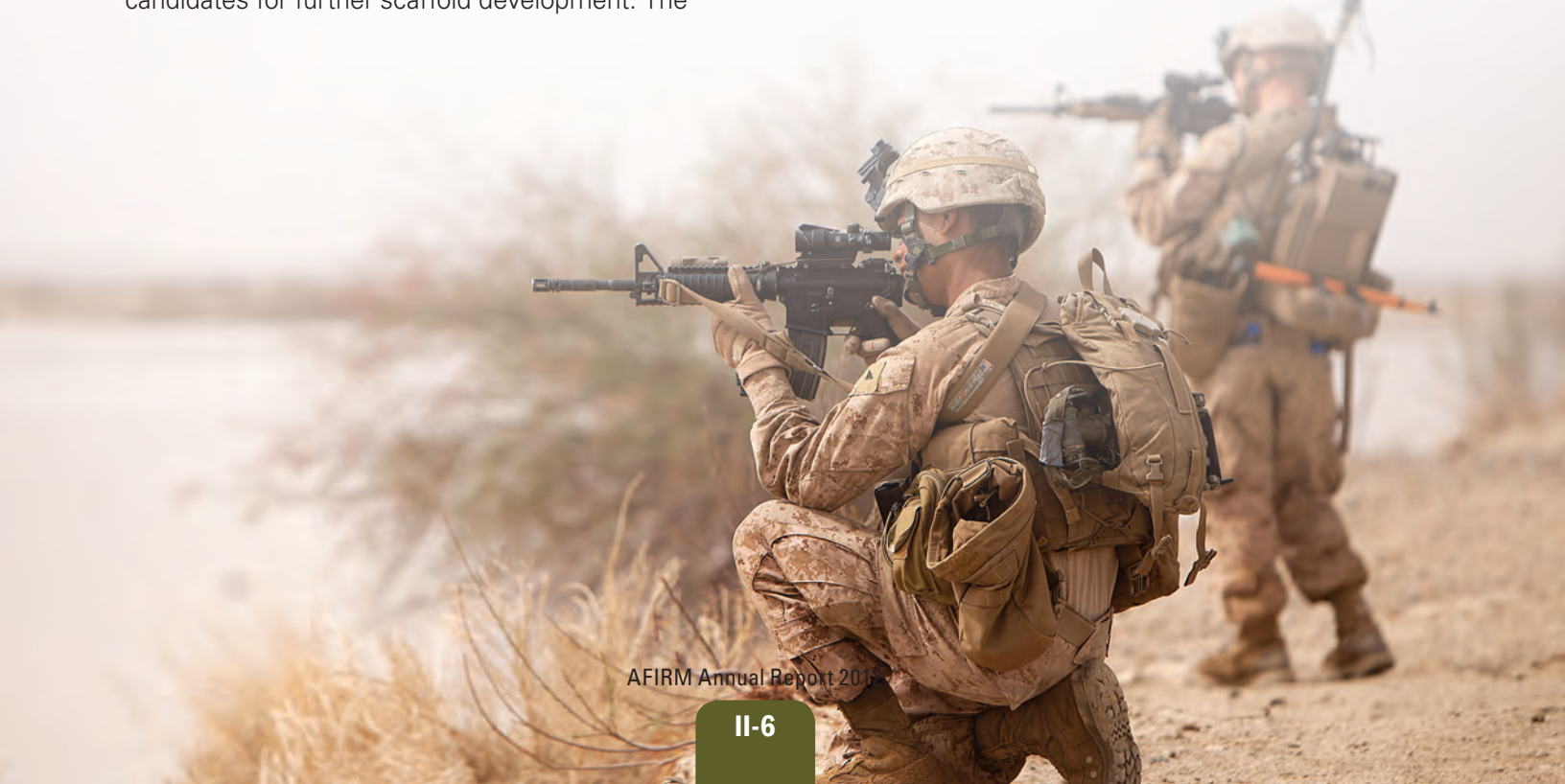

Bone Repair and Regeneration

Optimizing Cell Sources for Repair of Bone Defects

Project 4.2.2, RCCC

Team Leader(s): George Muschler, MD (Cleveland Clinic, [CC])

Project Team(s): Viviane Luangphakdy, MS, Cynthia Boehm, BS, Hui Pan, MD, PhD, Kentaro Shinohara, PhD, MD, Tess Henderson, BS, and Powrnima Joshi, PhD (CC)

Collaborators(s): Maciej Zborowski, PhD (CC)

Therapy: Advanced regeneration of segmental bone defects

Deliverable(s): Preferred clinical method for progenitor cell concentration, selection, and delivery

TRL Progress: 2010, TRL 3; 2011, TRL 3; 2012 (Current), TRL 4; 2013 (Target), TRL 4

Key Accomplishments: The researchers showed that magnetic separation based on HA, as a marker for osteogenic connective tissue progenitors (CTP-Os), increased bone regeneration in the CFMD model, which remains the most effective model for assessment of cell therapy methods. In addition, the research team established effective methods for percutaneous access to the goat pelvis for marrow aspiration or excavation. The researchers then determined that the Spanish-Boer goat is an inappropriate breed in which to evaluate marrow harvest and cell-processing strategies. A goat breed with more human-like hematopoietic marrow needs to be identified.

Key Words: Osteogenic, progenitors, bone graft, selective retention

Introduction

Regeneration of bone tissue requires the presence of CTP-Os—cells that are capable of making new bone. In many severe injuries, CTP-Os are present in numbers that are less than optimal for bone repair. Therefore, to optimize bone regeneration, it is desirable to define methods that allow a surgeon to replenish the population of CTP-Os by harvesting CTP-Os from another site and transplanting them at a concentration and in an environment that optimizes their survival and their performance.

CTP-Os are found in many tissues, but particularly in bone and bone marrow. They can be harvested and processed in many ways, and many factors may improve the environment in which they are transplanted. The use of platelet-rich plasma (PRP) has been proposed as one such method, as have specialized scaffolds and local drug delivery.

In this project, the researchers are addressing the need to define and competitively assess promising methods for harvesting, processing, and transplanting CTP-Os in appropriate models, so the best possible methods can be made available for the treatment of wounded warriors, and other victims of severe limb, spine, or craniofacial trauma. The research objective is to compare three different methods for marrow processing: Density separation (DS) (using a centrifuge to remove red blood cells and serum), selective retention (SR) (using the fact that CTP-Os attach very readily to some surfaces as a means for concentration and selection), and magnetic separation (MS) (magnetically labeling CTP-Os and then preferentially collecting them with a magnet). All of these methods can increase CTP-O concentration. SR and MS processing can also increase CTP-O prevalence (i.e., reduce the number of non-CTP-Os).

During the first 3 years of the project, the researchers defined methods to increase the surgical yield of bone marrow harvest procedures without an increase in morbidity; evaluated two DS devices for their ability to concentrate bone marrow cells; tested one of the preferred degradable scaffolds from Project 4.2.1a and found that it showed modest performance as a substrate for SR; downselected the option of CD45 depletion in favor of

HA-positive selection as a means of enhancing the prevalence of CTP-Os; and designed, fabricated, and validated a new MS system for the selection of CTP-Os. In addition, the research team's in vitro testing of magnetically separated cells demonstrated no loss of selective adherence behavior on the allografts, suggesting that a combination of MS and SR processing is clinically feasible. The researchers also found that bone formation using mineralized cancellous allograft (MCA) is very robust, regardless of the cell source and is not different from the performance of MCA alone in the CFMD model.

The researchers used two animal models to assess cell-sourcing methods:

- The CFMD model was used in Years 3 and 4 to evaluate the performance of MS processing based on HA as a surface marker for CTP-Os. This is the same model that was used in Years 1–3 of AFIRM to compare and select the most effective bone scaffold materials.
- The chronic caprine tibial defect (CCTD) model, a model that is currently under development in AFIRM in Project 4.8.1, was also used in Years 3 and 4, in an attempt to assess the efficacy of SR.

Thus far, no in vivo assessment of DS has been completed.

Research Progress – Year 4

Histomorphometric Results of the Assessment of MS in the CFMD Model

Intraoperative processing of bone marrow using HA for positive selection of CTP-Os was shown to significantly improve bone regeneration. Histomorphometric analysis performed at Mayo Clinic demonstrated that the area of bone formation and vascular sinusoids was significantly greater when MS processing was used, compared to unprocessed bone marrow. This was associated with a decrease in the area of residual allograft and a decrease in marrow fibrosis. These findings validate that MS processing may be a viable strategy to improve clinical bone regeneration in a more stringent clinically relevant model. The researchers have also determined that the CFMD model is suitable for screening, evaluating, and assessing CTP-O harvest and processing strategies.

Evaluation of Bone Regeneration in the CCTD Model

The researchers have further refined their CCTD model in collaboration with their colleagues on Project 4.8.1, who were charged with the task of developing and validating the CCTD model. Surgical and husbandry protocols and methods for quantitative outcome assessment have been greatly advanced (see Project 4.8.1 report). In this project, the researchers over the past 2 years have attempted to validate the CCTD model as a viable tool for advanced assessment of cell harvest and processing strategies. Progress with the assessment of cell therapy strategies has been thwarted, however, by the finding that the marrow space of the Spanish-Boer goat is unsuitable for effective harvest of CTP-Os.

MicroCT results. Seven of 12 goats completed the 12-week follow-up. The researchers found that bone formation was much less than expected or desired in all 7 animals. Although preliminary analysis suggested that there was greater bone formation in the SR graft sites, statistical analysis has not yet been completed and will likely be limited by statistical power. **Figure 1** illustrates the mean percentage of bone volume (%BV) for bone marrow aspirate (BMA) and SR groups and also includes data for ungrafted defects and autogenous cancellous bone graft (ACBG) from Project 4.8.1 goats that were treated by the same surgical team. These data confirm that the CCTD model is very

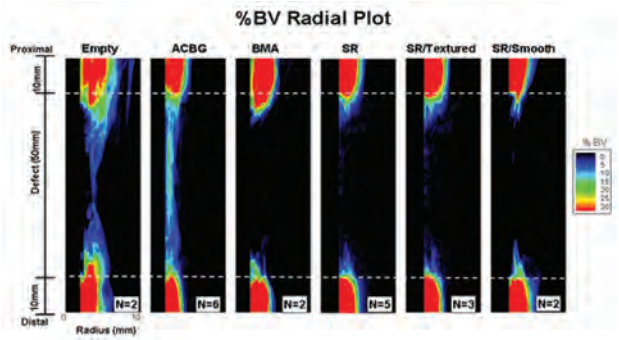

Figure 1. Percentage of bone volume based on microCT analysis plotted versus radial position.

stringent, as intended; only 1 in 12 goats treated with ACBG regenerated bone across the defect.

Characterization of marrow from the Spanish-Boer goat . An important part of the development of any model is to confirm that it is as similar as possible to the human biology. Without this confirmation, the results from the model are less likely to answer clinically relevant questions. Therefore, as part of this assessment, the quality of the marrow samples that were collected from the Spanish-Boer goats in this study were evaluated and compared to prior experience with human and canine marrow.

The striking observation is that the marrow obtained from Spanish-Boer goats is exceptionally fatty (Spanish-Boer goats are bred for meat and their ability to be fattened). The excessive fat and fibrous tissue composition required that changes be made in established cell-processing methods to remove the fatty and fibrous debris. In addition, the prevalence of colony-forming connective tissue progenitors (CTPs) was found to be significantly lower than human or canine marrow (**Table 1**).

These findings demonstrate that the Spanish-Boer goat is an unsuitable breed for the evaluation of marrow harvest and cell-processing strategies. A goat breed with more human-like hematopoietic marrow needs to be identified.

Conclusions

This research showed that MS based on HA as a marker for osteogenic CTPs increased bone regeneration in the CFMD model (a suitable model for the assessment of cell therapy methods). The evaluation of SR methods was limited in the CCTD model; a goat breed with more human-like hematopoietic marrow needs to be identified. Overall, the CFMD model used during Years 1–3 has proven to be a suitable model for the assessment of cell therapy strategies and will be used in Year 5 to complete the comparison between DS, SR, and MS processing.

Research Plans for Year 5

In Year 5, the Cleveland Clinic will complete the assessment of DS and SR processing with mineralized cancellous allograft (MCA) in the CFMD model.

Planned Clinical Transitions

The most effective sourcing and processing methods will be advanced from initial assessment in the CFMD model into appropriate assessment in the CCTD model, once an appropriate age and breed of goat are identified. The most effective methods for cell sourcing will be evaluated alone and in combination with advanced scaffolds, surgical methods, and/or drug delivery systems to identify the most promising therapies to advance into clinical trials. Clinical trials may involve either new products or methods and are most likely to be performed in collaboration with the Major Extremity Trauma Research Consortium.

Corrections/Changes Planned for Year 5

The research team will complete the comparison of DS, SR, and MS processing in the dog model instead of the goat model.

Table 1. Comparison of marrow samples from spanish-boer goats, coonhounds, and from human patient subjects undergoing arthroplasty procedures.

	Goat [Mean Age = 5 yr]	Human [Mean Age = 61 yr]	Canine [Mean Age = 1.5 yr]
Cells (millions/cc)	20.0 ± 4.2 (17.5,22.5)	21.9 ± 8.9 (19,25.2)	35.7 ± 9.0 (29.0,42.0)
CTPs per million cells plated	11.3 ± 11.2 (4.27,17.9)	38.1 ± 69.0 (25.7,56.6)	51.8 ± 37.1 (24.3,79.3)
Total CTPs per mL	222.8 ± 266.4 (65.4,380.0)	834.5 ± 1811.0 (506.4,1374.9)	1851.0 ± 8586.0 (791.0,2912.0)

Bone Repair and Regeneration

Advancing Bone Repair Using Molecular Surface Design (MSD): Biodegradable Scaffolds with Tethered Osteoinductive Biomolecules

Project 4.2.3, RCCC

Team Leader(s): Jared Bushman, PhD (Rutgers University)

Project Team(s): Zheng Zhang, PhD, Sven Sommerfeld, and Richard Farias (Rutgers University)

Collaborator(s): Ophir Ortiz, PhD (Rutgers University) and Jeffrey Hollinger, PhD (Carnegie Mellon University)

Therapy: Advancing regeneration of bone in large bone defects and cartilage in joint defects

Deliverable(s): Scaffold with tethered osteoinductive and chondrogenic proteins to enhance regeneration, increase safety through controlled presentation of proteins, and reduce costs associated with recombinant proteins.

TRL Progress: 2010, TRL 2; 2011, TRL 3; 2012 (Current), TRL 3; 2013 (Target), TRL 4

Key Accomplishments: The researchers developed standard operating procedures (SOPs) for modifying and tethering recombinant human bone morphogenetic protein-2 (rhBMP-2) to three-dimensional (3D) scaffolds, and demonstrated tethering efficiency in complex 3D scaffolds. They developed polymers for chondrogenic differentiation and scaffold fabrication that enabled a single contiguous scaffold with a discrete and well-defined transition area and showed that different proteins could be regionally tethered. They also developed biphasic scaffolds that regionally promoted bone and cartilage formation and determined that proteins could be tethered in distinct localizations. They found that the tethering components did not promote a disproportionate inflammatory response in vitro or in vivo. Finally, they initiated animal studies to determine safety and efficacy of the tethered scaffolds in a rabbit critical-size bone defect model.

Key Words: Tether, rhBMP-2, bone, cartilage, scaffold, biphasic

Introduction

The Rutgers group is seeking to advance the treatment of injured service members by improving control over the cell and tissue response to an implant material using MSD, in which specific bioactive ligands (recombinant proteins) are tethered on a scaffold surface. The use of recombinant proteins to induce bone formation has gained a strong footing in the market with Medtronic's Infuse™, Mastergraft™, and Amplify™, Stryker's OP-1™, and Biomimetic's Augment™. The pitfalls of these technologies are the high cost of the recombinant proteins, the safety concerns of ectopic bone and male sterility linked to poor localization of the proteins, and the inability to create well-defined scaffolds with biphasic physical and biological characteristics. Tethering of such biomolecules via MSD to scaffold surfaces has the potential to greatly reduce the necessary quantity of the biomolecules, thereby decreasing the cost and increasing potential use of the device. Tethering prevents biomolecules from diffusing out of the injury site, reducing the potential for ectopic bone formation. Tightly tethered biomolecules would also be less susceptible to receptor-mediated endocytosis, prolonging the duration of activity.

During the first 3 years of this project, the researchers modified a biodegradable polymer so that large osteoinductive biomolecules osteoinductive biomolecules (e.g., rhBMP-2 or rhBMP-7) could be efficiently tethered to the polymer surface. They confirmed that the polymer could be fabricated into a scaffold material and that proteins

could be efficiently tethered in a complex 3D scaffold. The researchers also modified an osteoinductive protein for tethering, purified the modified protein, and showed equivalent activity.

Research Progress – Year 4

Activity of Modified and Tethered rhBMP-2

To determine if the modification made to rhBMP-2 to enable it to be tethered to scaffolds alters its capacity to induce bone formation, modified rhBMP-2 was compared to control rhBMP-2 for the ability to induce alkaline phosphatase (ALP) expression in mouse calvarial MC3T3-E1 osteoblasts. Modified rhBMP-2 showed no decline in activity compared to control rhBMP-2 at the doses administered (**Figure 1A**). The researchers performed a second set of experiments comparing a single administration of adsorbed rhBMP-2 to the same dose of tethered rhBMP-2 (**Figure 1B**). In these experiments, 1/30th the concentration of tethered rhBMP-2 stimulated cells several-fold more than control rhBMP-2. Subsequent experiments determined a tethering efficiency of greater than 96% in complex 3D scaffolds, indicating that very little of this expensive protein is lost during the tethering procedure. This high efficiency meets the target for commercialization. The researchers conducted animal experiments and found a lack of a disproportionate immune response in vitro and in vivo. Additional animal experiments are currently in progress to determine the safety and efficacy of the device in a 15 mm rabbit critical-size calvarial defect model.

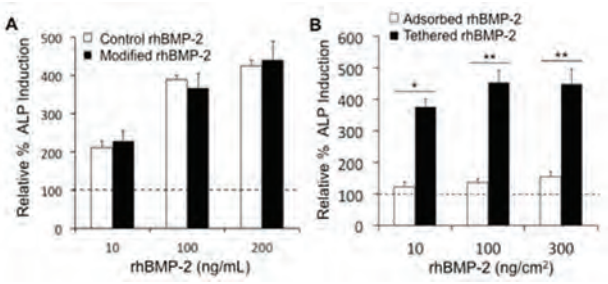

Figure 1. Activity of modified rhBMP-2 compared to control rhBMP-2 (A) and activity of rhBMP-2 when adsorbed versus tethered to the culture surface (B). *p < 0.05, **p < 0.005

Development of Biphasic Scaffolds with Localized Protein Tethering

In Year 4, the Rutgers group began to apply the versatile tethering platform to osteochondral regeneration where it is necessary to create scaffolds with biphasic properties to support bone and cartilage growth. The tethering can be superimposed upon these features to create scaffolds that are not only mechanically or physically biphasic but can now also contain localized regions of tethered proteins. The ability to apply the Rutgers group's tethering platform technology to this application was tested by tethering two separately labeled model proteins into a single contiguous scaffold. As depicted in **Figure 2**, the results showed that the two signals were discretely localized, supporting the researchers' goal of creating a strict interface of biological stimuli.

The next step was to develop scaffolds with biphasic physical and mechanical properties (hard and large pores for bone, soft and small pores for cartilage) that would support the tethering technology. A polymer was developed for the pro-chondrogenic portion and combined with the pro-osteogenic portion previously developed. Porogen leaching yielded a single contiguous scaffold composed of both materials (**Figure 3**). In aqueous conditions the scaffold's soft portion swells, takes on characteristics of a semihydrogel, and is supportive of chondrogenic differentiation of human

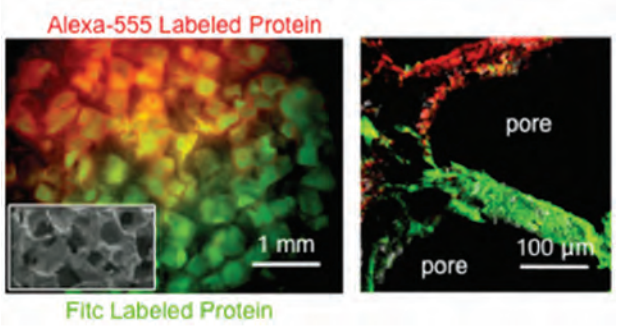

Figure 2. Images of differently labeled model proteins tethered in discrete locations within a single scaffold. (A) Low magnification image showing interface of FITC and Alexa-555 from different proteins, with inset scanning electron micrograph to show scale and configuration of pore structure. (B) Higher magnification image of interface of Alexa-555 and FITC-labeled proteins in a single pore.

mesenchymal stem cells (MSC), whereas the bottom layer (optimized for bone formation) does not promote any degree of chondrogenesis.

Conclusions

In Year 4, the team focused on two aspects of the MSD technology: bone regeneration and osteochondral regeneration. With respect to bone regeneration, a great portion of the effort was devoted to scaling up and assessing efficiency. Biocompatibility was demonstrated in vivo. Subsequent animal studies were initiated to assess the efficacy and safety of scaffolds tethered with rhBMP-2 in a rabbit critical-size calvarial defect model. The Rutgers group was able to leverage past experience and rapidly evolve the technology for bone into biphasic scaffolds for osteochondral regeneration, a construct that fully leverages the tethering technology.

Research Plans for Year 5

The goal of Year 5 is to further assess the tethering of rhBMP-2 onto bone scaffolds to maximize regeneration at the lowest dose of rhBMP-2 possible. For osteochondral regeneration, rhBMP-2 will be tethered in combination with pro-chondrogenic proteins to create a biphasic scaffold, which will be studied in the rabbit joint defect model. Potential commercial partners have been identified as suppliers of GMP-grade recombinant proteins.

Planned Clinical Transitions

Pathways toward clinical transitions are currently being evaluated and are expected to take place in Year 6 using leveraged funds.

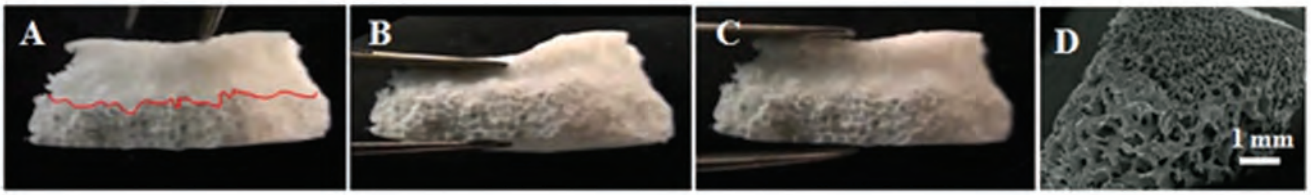

Figure 3. Images of biphasic scaffolds. (A) Scaffold with red line added to demark different phases of the scaffold. (B) Scaffold when compressed by forceps. (C) Scaffold immediately following release of forceps compression. (D) Scanning electron microscope image depicting top and bottom layers prepared via leaching salt particles with size range 45–150 µm and 212–450 µm, respectively.

Bone Repair and Regeneration

Improved Preclinical Model for Orthopedic Trauma

Project 4.8.1, RCCC

Team Leader(s): G. Elizabeth Pluhar, DVM, PhD (University of Minnesota); Joan Bechtold, PhD (Minnesota Medical Research Foundation); and George Muschler, MD (Cleveland Clinic)

Project Team(s): Anne Nicholson, DVM, Cathy Carlson, DVM, PhD, Michelle Goulart, DVM, Charles Seiler, BS (University of Minnesota); Viviane Luangphakdy, MS, Hui Pan, PhD, MD, Kentaro Shinohara, MD, and Cynthia Boehm, BS (Cleveland Clinic)

Collaborator(s): Joseph Wenke, PhD, Kinton Armmer, and Douglas Cortez (USAISR)

Therapy: Advanced regeneration of segmental bone defects

Deliverable(s): New large animal model of a critical bone defect

Key Accomplishments: The researchers created a bone defect in the tibia of 20 Spanish-Boer goats. They treated 16 of the animals 4 weeks later with fresh autogenous cancellous bone graft (ACBG). At 12 weeks post treatment, radiographic analysis of the ACBG-treated animals revealed little to no bone formation. The researchers showed that the goats tolerated both surgeries well and used the treated limb well. They also found major differences in the quantity and quality of ACBG between young goats and those over 5 years of age. In addition, the researchers observed less bone formation in the defects when muscle was excised from around the bone defects during creation of the wounds, as compared to defects without muscle excision.

Key Words: Bone defect, caprine (goat) model, chronic, bone graft

Introduction

Large bone defects and chronic bone defects represent a difficult and, as yet, unsolved clinical challenge. The contemporary standards of care for bone defects and complex fractures (i.e., fractures with considerable damage of surrounding soft tissue) or fracture non-unions (i.e., fractures that permanently fail to heal) in civilian and military practice include many options for wound management, fixation, and bone grafting. Bone grafting is a surgical procedure in which missing bone in complex fracture non-unions is replaced. Despite substantial advances in the availability of bone graft substitute materials and continuous development of new bone regeneration technologies, these wounds often fail to heal completely. Information gained from testing materials in animal models often does not translate well to human clinical practice. There are numerous animal models with critical-size defects in a variety of species and anatomic sites. But to date, preclinical testing in these models has resulted in complete defect healing when current standard of care treatments are used. This does not translate well to human clinical practice as these wounds often fail to heal in humans. Hence, more challenging and biologically relevant models are needed to compare improvements in the regenerative therapies that may become available to injured warriors and civilians whose injuries do not heal as readily as those in animal models.

Research Progress – Year 1 (Project Began in Year 4)

Characterization of the Time Course and Outcome of Chronic Defects That Are Left Empty/Not Grafted or Are Treated with Fresh Autogenous Cancellous Bone Graft (ACBG)

Demonstrate a nonhealing defect that does not heal 12 weeks after treatment. Five-year-old Spanish-Boer goats were used to create the chronic caprine tibial defect model. This model involves removing a 5 cm piece of bone from the tibia (shin bone) and 10 grams of muscle from around the defect, filling the defect with bone

cement to induce the formation of a membrane, removing the bone cement 4 weeks later, and filling the defect with bone graft. The original site for bone graft harvest was the proximal humerus, which was found to be filled with fatty tissue and had a poor quality graft. Therefore, the bone graft was taken from the iliac crest (hip bone) that had more cancellous (spongy) bone and hematopoietic stem cells within the bone.

There was little to no bone formation in the 4 goats that served as a negative control with defects that were left empty or not grafted. In the 16 goats treated with ACBG, 15 goats had little or no bone healing after 12 weeks (**Figure 1**). In one goat, the defect was considered to be healed with new bone filling the defect on 3 of 4 sides of the bone, as assessed with x-rays. Overall, the radiographic assessment of bone healing showed that the model does "raise the bar" with less than 10% of the defects healing when treated with fresh ACBG.

Assess the impact of local muscle loss on bone healing in this model. Goats were divided into two groups. In the first group of 8 goats, 10 g of muscle was removed when the bone defect was created. These goats had approximately half the volume of bone (mean = 15.7% of the defect area filled with bone), relative to the second group of 8 goats that had bone injury but no muscle removed (mean = 32.4% of the defect area filled with bone). Therefore, it appears that muscle excision that simulates soft tissue loss, which occurs in most military trauma, should be included during future experiments using this chronic defect model.

Demonstrate that the pain caused by this procedure can be controlled. All goats survived and tolerated the first surgery (creation of bone defect) and second surgery (filling of the gap with bone graft) and were using the limb within a few days of both surgeries (**Figure 2**). Compared to the first surgery, the goats were not as lame after the second "treatment" surgery, where the bone cement spacer was removed and the defect was either filled with ACBG (treatment group) or left empty (control group). These results demonstrate that the proposed procedure does not cause uncontrollable

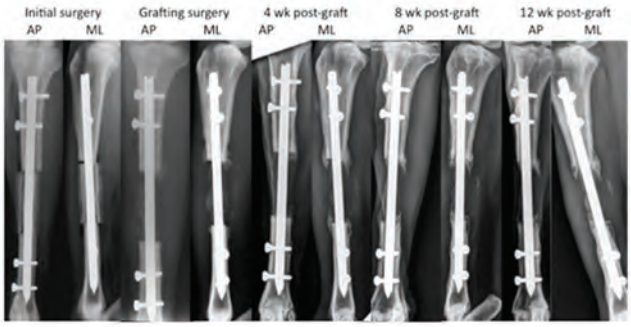

Figure 1. Serial radiographs from a goat that was treated with ACBG show very little bone formation in the defect over a 12-week time frame.

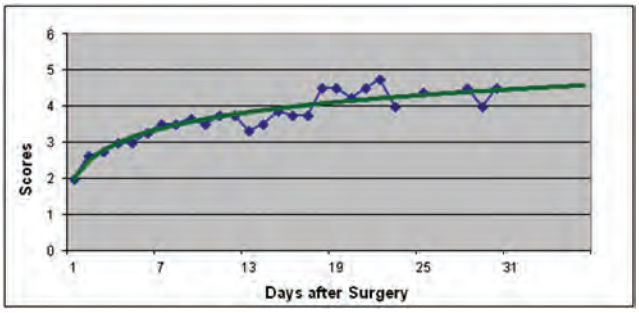

Figure 2. Graph showing the average score for weight bearing or use of the treated leg over time after creating the bone and muscle defect. A score of four indicates that the goat bore weight on the leg most of the time.

and unrelenting pain that would lead to severe lameness in these goats.

Define the variation in experimental outcomes between research centers. Three centers are collaborating on this project: the University of Minnesota, the Cleveland Clinic, and the USAISR. There were differences in the incidence of post-operative infections at the centers due to differences in sterile preparation techniques. Another difference was in the average amount of bone formation observed that may have been due to the degree of soft tissue injury caused by varying usage of electrocautery or from differences in the quality and fat content of bone graft. A detailed description of the surgical preparation and surgical procedures has been developed to minimize variation moving forward.

Characterization of the Intrinsic Properties of the Induced Membrane in This Chronic Caprine Model

Placing a bone cement spacer in the bone defect induces local inflammation and leads to a chronic defect as well as the formation of a soft tissue membrane within 1 month. This membrane helps to retain graft material in the defect site and may provide factors that promote healing.

Assess the concentration/prevalence of osteogenic progenitors in the membranes. The average number of nucleated cells per gram of digested membrane tissue was 35 million and did not vary significantly between goats or between different regions of the membrane. The assays for determining the concentration and prevalence of osteogenic progenitors use a technique that causes cells to differentiate into osteogenic or bone-forming cells. These assays are in progress.

Assess the histological and biochemical properties of the membranes. The induced membranes are basically composed of fibrous connective or scar tissue with no evidence of inflammation. The analysis of all membrane samples collected from the University of Minnesota and the Cleveland Clinic is currently ongoing.

Conclusions

The chronic caprine (goat) tibial defect model "elevates the bar" of biological challenge to a level where improvements over current standards of care or treatment can be detected. While this protocol provides adequate pain relief for the animals, the surgical preparation and procedure will need to be better defined to limit variations among research centers.

Research Plans for Next Year

The University of Minnesota/Cleveland Clinic/USAISR team will further characterize the chronic tibial defect in mature goats and use the model to test novel bone regeneration technologies.

Planned Clinical Transitions

This project is aimed at developing a large animal model in which novel bone regeneration technologies can be tested before moving into Phase 1 or 2 human trials.

Corrections/Changes Planned for Next Year

A detailed description of the entire procedure including animal preparation and surgical technique will be produced to minimize variance in data using the model. An instructional video will also be produced demonstrating the procedures. The bone marrow obtained from these 5-year-old Spanish-Boer goats was extremely fatty and fibrous. Hence, a different breed of goat with less fatty tissue in the long bones (e.g., pure Spanish goats) and younger animals (3.0 ± 0.5 years old) will be assessed during the upcoming year. Cancellous bone graft and bone marrow aspirates obtained from these goats should more closely mimic those obtained from humans.

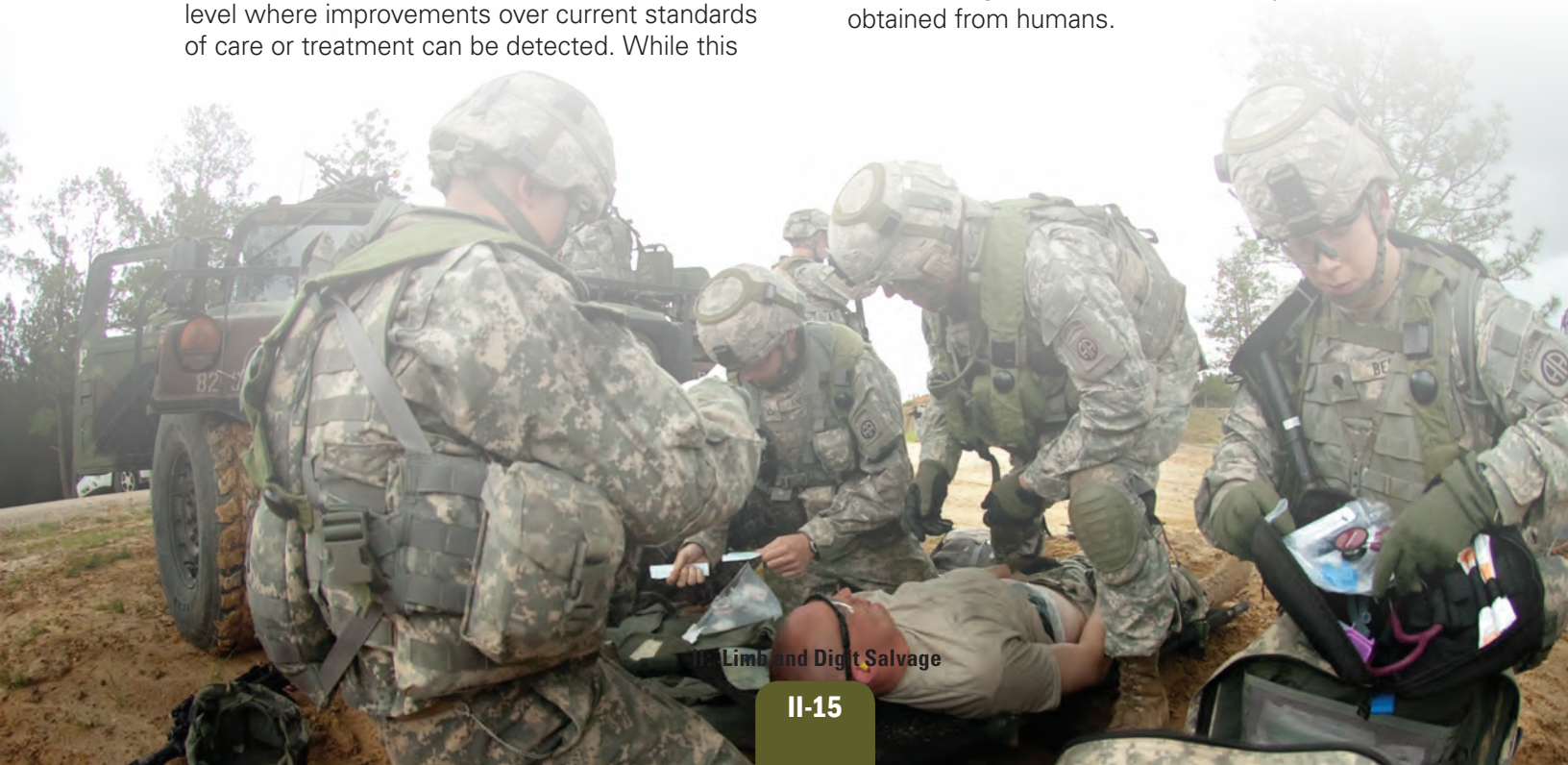

Soft Tissue Repair and Regeneration (excluding nerve)

Development of Tissue (Peritoneum)-Lined Bioabsorbable and Fracture-Resistant Stent Graft for Vessel Trauma

Project 4.3.2, RCCC

Team Leader(s): Timur Paul Sarac, MD (Cleveland Clinic)

Project Team(s): Malika Satirraju, MS (Cleveland Clinic); Ilia Koev, PhD (Biogeneral, Inc.); and Keith Platenyk (Evonics)

Collaborator(s): Craig Bonsignore, MBA, Minh Shin, PhD (Nitinol Development Corp.); Elliot Sanders, PhD, Keith Platenyk (Evonics, Inc.); Brian Hrouda (Norman Noble Inc.); and Diwalker Ramanathan, PhD (Resonetics Inc.)

Therapy: Minimally invasive treatment of arterial and venous trauma

Deliverable(s): Fracture-resistant and bioabsorbable tissue-lined stent graft

TRL Progress: 2010, TRL 3; 2011, TRL 2; 2012 (Current), TRL 3; 2013 (Target), TRL 4

Key Accomplishments: The researchers made several bioabsorbable stents with polylactic acid (PLA) subtypes or polydioxanone (PDO) using a fracture-resistant stent design. They cut the PLA stent with an athermal laser and are in the process of optimizing the PDO athermal laser cut.

Key Words: Stent, peritoneum, polydioxanone (PDO), polylactic acid (PLA), mineral oil, blood vessel trauma, delivery system and catheter

Introduction

Over the past 15 years, there has been a transformation in vascular surgery toward minimally invasive therapy. Currently, the best minimally invasive therapy available to treat injured blood vessels is a stent lined with the synthetic material "expanded polytertafluoroethylene" (ePTFE). However, the long-term success rates of these "off label" stent grafts are suboptimal as they are highly susceptible to infection and failure. There is no minimally invasive stent graft specifically designed to treat blood vessel injuries that considers the particular issues related to the trauma theater in military and civilian populations. This is even more important as published reports from recent conflicts indicate that blood vessel injuries to U.S. troops are five times higher than previously thought.

During the first 3 years of this project, the researchers constructed prototypes of several bioabsorbable PDO fiber-based, tissue-lined stents for the treatment of traumatic arterial and venous injuries. They first evaluated the tensile strength of several polymers. They chose PDO as an appropriate polymer for their bioabsorbable tissue-lined stents. They identified a 3–6-month window for the degradation time line of the polymers. They discovered that mineral oil will serve as an effective storage emollient for the stent graft. They placed fracture-resistant, nitinol-based, tissue-lined stents into a canine iliac artery injury animal model; this model is the same as the predicate device use and accepted by the FDA for the IDE. All animal implants were successful after 30 days. The research team also developed a second-generation, user-friendly catheter delivery system.

Research Progress – Year 4

Manufacture PDO and Polylactic Acid

The researchers' first goal was to identify sources of PDO and PLA. With the assistance of Evonics, Inc. and Biogeneral, Inc., they were able to find both suppliers.

Extrude Polymer Tubes

The research team was able to extrude polymer tubes in collaboration with Biogeneral, Inc. The resin is gravity fed from a top-mounted hopper into the barrel of the extruder as shown in **Figure 1**.

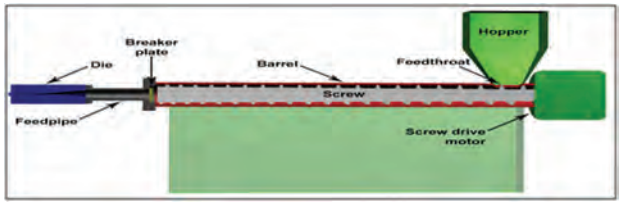

Figure 1. Mechanical design for extruding polymer tubes.

After passing through the breaker plate, molten plastic enters the die. The die is what gives the final product its profile and must be designed so that the molten plastic evenly flows from a cylindrical profile to the product's profile shape. The product polymer is then cooled. **Figure 2** shows extruded PDO tubes, which were then etched with an athermal laser.

Figure 2. PDO tubes and laser-etched tubes with fracture-resistant design.

Athermal Laser Stent Manufacture

The stents are designed to accommodate tissue and take into account the intricacies of flow. This includes different resistive forces along the path of the stent and a 10° flare for flow eddies (**Figure 3**).

Athermal Laser Cut

The Sarac group is still in the process of optimizing the PDO athermal laser cut by varying the laser application time. This strategy is based on its durometer readings and the ability to cut the struts and islets. However, the team is excited to report that it has produced its first athermal cut, fracture-resistant, self-expanding stent design made of PLA (**Figure 4**). The technology is proprietary and is developed in conjunction with Noble UltraLight. Its advantages are: (1) uses an ultra short pulse laser that does not generate any heat-affected zone; (2) reduces, and in some cases, eliminates costly deburring and post-processing steps; and (3) increases product quality and yield.

The next steps for PDO athermal laser cut are to heat set the stent and examine its radial resistive force. If any modifications have to be made to the athermal laser cut, the team will fix it based on heat setting, strut thickness, and stent architecture.

Delivery System

The research team has made substantial changes to the delivery system, which allows it (or the surgeon) to crimp the stent into the delivery catheter in about 30 seconds. In conjunction with Peritec Biosciences, the team is now progressing to design verification and design freeze.

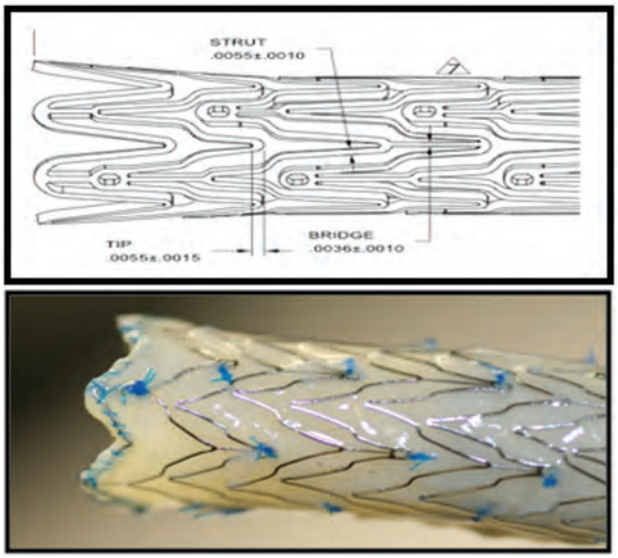

Figure 3. Fracture-resistant stent design and fracture-resistant nitinol stent.

Figure 4. PLA fracture-resistant stent.

Conclusions

The Sarac group has successfully manufactured and extruded tubes of PDO and PLA. They have also now cut a fracture-resistant stent design made of PLA with an athermal laser. The researchers are in the process of doing the same for PDO.

Research Plans for Year 5

In Year 5, the Sarac group will complete design verification and mechanical testing of the stents. This will include the final selection of either one or two polymers. In addition, they will histologically evaluate the stents in a preliminary canine iliac artery injury animal model; this model is the same as the predicate device use and accepted by the FDA for the IDE. In the future, the team plans to perform a Good Laboratory Practice (GLP)-compliant animal study.

Planned Clinical Transitions

The clinical transition will be done through Peritec Biosciences, who will obtain funding for an IDE and a Humanitarian Device Exemption.

Corrections/Changes Planned for Year 5

The Year 5 corrections will be based on final radial force testing of the self-expanding stents. This will allow the team to focus on one polymer.

Soft Tissue Repair and Regeneration (excluding nerve)

Functional Scaffold for Musculoskeletal Repair and Delivery of Therapeutic Agents

Project 4.4.3a, RCCC

Team Leader(s): Kathleen Derwin, PhD (Cleveland Clinic)

Project Team(s): Sambit Sahoo, MD, PhD, and Joseph Iannotti, MD, PhD (Cleveland Clinic)

Collaborator(s): Michael Rosen, MD (University Hospitals, Cleveland)

Therapy: Repair of large abdominal wall defects and hernias

Deliverable(s): A fiber-reinforced allograft or xenograft scaffold (dermis) or a combination dermis plus synthetic mesh device

TRL Progress: 2010, N/A; 2011, TRL 2; 2012 (Current), TRL 3; 2013 (Target), TRL 4/5

Key Accomplishments: Using an in vitro enzymatic degradation model that simulates weakening of implanted biologic grafts, the researchers showed that fiber reinforcement helped to reduce the stretching of the grafts after they were enzymatically digested and subjected to forces that patients would experience after implantation in the abdominal wall. The researchers licensed the fiber reinforcement technology to a commercial partner for development of therapeutic products. They are currently transitioning to semiautomated scaffold fabrication and assessing candidate fibers and reinforcement designs using biaxial and burst testing.

Key Words: Extracellular matrix, abdominal wall, hernia, allograft, xenograft

Introduction

Researchers have experienced major challenges in designing methods to repair abdominal wall defects and hernias that result from traumatic injuries, surgery, or chronic diseases. Abdominal wall injuries sustained during military trauma are typically large (with massive loss of tissue) and infected, and one in every three cases fails to heal. Abdominal wall hernias also complicate nearly one-third of all abdominal surgeries in the civilian population, and an estimated 350,000 hernia repairs costing a total of U.S. $3.2 billion are performed each year in the United States alone (2006 data). Currently available synthetic and biologic grafts have demonstrated limited success. While the use of synthetic meshes has reduced hernia recurrence, these repairs often require repeat surgery as a result of complications, such as mesh infection, bowel adhesion, extrusion, and fistulation. These complications can largely be avoided through the use of biologic grafts for hernia repair.

Biologic dermal grafts are commonly used in clinical practice since they possess biomechanical properties similar to abdominal wall fascia. However, implanted dermal grafts lose mechanical strength and integrity over time, leading to complications such as bulging and hernia recurrence. Hence, engineered improvements to biologic grafts are necessary to make them more suitable for abdominal wall repair and reconstruction. Hernia recurrence rate is very high, with 24%–43% of hernia repairs resulting in repair failure and hernia recurrence. It is estimated that a 1% reduction in recurrence rate would result in a cost saving of $32 million dollars in the United States.

During the first 3 years of this project, the researchers developed a rat subcutaneous model for evaluating the in vivo host response, degradation, and loss of suture retention following implantation of large (4 x 4 cm) scaffolds and used the model in pilot studies. They developed a human cadaver model for testing the extent to which augmentation with scaffolds improves the biomechanical outcomes of rotator cuff repairs. They developed and validated a fluoroscopic method for measuring tendon repair gap formation. They

identified a candidate material for fiber reinforcement and demonstrated how fiber reinforcement can be used to alter the mechanical properties of biological grafts derived from ECM.

Research Progress – Year 4

The Derwin group demonstrated that dermal grafts stretch significantly and irrecoverably when loaded. Strips and patches of dermal grafts were reinforced using the group's proprietary fiber reinforcement technique, and the grafts' mechanical properties were evaluated. The group also used an in vitro enzymatic degradation model to simulate weakening of biologic grafts implanted in the body. Fiber reinforcement improved the stiffness and increased the maximum load that could be borne by the dermis patches and also mitigated their weakening due to enzymatic degradation. Fiber reinforcement also helped to reduce the stretching of the grafts after the grafts were enzymatically digested and pulled to forces that they would experience after implantation in a patient's abdominal wall. These results support the concept that fiber-reinforced biologic grafts could reduce bulging and recurrence and improve the long-term outcome of hernia repairs.

The Derwin group is now transitioning from a manual to a semiautomated scaffold fabrication process for dermal graft reinforcement and is also establishing a preclinical large animal model of hernia repair with the help of surgeon collaborators. The research team is also developing test protocols and analytical methods that will allow a better and more meaningful evaluation of the biomechanical properties of the graft and the repaired abdominal wall.

Conclusions

Biologic grafts stretch significantly with loading and after remodeling. Biologic grafts could be fiber-reinforced, using the group's proprietary technology to improve their stiffness and strength. Fiber reinforcement also reduced the weakening and stretching of graft at physiologic loads and increased the total amount of load the graft could endure.

Research Plans for Year 5

In Year 5, the Derwin group will transition to a semiautomated scaffold fabrication process for dermal graft reinforcement and screen multiple scaffold designs to optimize the reinforced grafts for abdominal wall repair applications. The biomechanics of the candidate-reinforced grafts will be evaluated using the in vitro degradation model and burst and biaxial testing. The reinforced grafts will be evaluated in a preclinical large animal hernia model. In addition, the industrial collaborator will conduct manufacturing, toxicity, packaging, and shelf-life studies.

Planned Clinical Transitions

The researchers have identified potential clinical collaborators and are in the process of establishing a formal collaborative partnership. Based on guidance from consulted clinicians, they developed a preclinical large animal study, which will be initiated in Year 5. As the device moves into product development and a regulatory path is defined, human trials will be initiated.

Corrections/Changes Planned for Year 5

The researchers are performing a series of pilot studies with the goal of establishing the surgical repair model that will be used in the large animal study in Year 5. They also aim to develop a computed tomography imaging protocol that will allow monitoring of hernia progression in the animal model.

Soft Tissue Repair and Regeneration (excluding nerve)

Functional Scaffolds for Soft Tissue Repair and Joint Preservation

Project 4.4.3b, RCCC

Team Leader(s): Charles J. Gatt, Jr., MD and Michael G. Dunn, PhD (University of Medicine and Dentistry of New Jersey [UMDNJ])

Project Team(s): Aaron Merriam, BS, Michael Dunn, PhD, and Charles Gatt, MD (UMDNJ)

Collaborator(s): Joachim Kohn, PhD and Sanjeeva Murthy, PhD (Rutgers University)

Therapy: Regeneration of fibrocartilaginous tissue such as the meniscus of the knee

Deliverable(s): An implantable scaffold composed of biodegradable polymer fiber-reinforced collagen sponge for repair of knee meniscus

TRL Progress: 2010, TRL 3; 2011, TRL 3; 2012 (Current), TRL 4; 2013 (Target), TRL 4

Key Accomplishments: Based on data obtained from the nonfunctional rabbit model, the researchers finalized their second-generation meniscus scaffold design for a functional evaluation in sheep. They completed implantation of the second-generation scaffold in the functional sheep model and have recovered all 16-week implants. They found that scaffolds integrate into the surrounding tissue, and cells rapidly infiltrate the device and lay down new collagen. Most importantly, the meniscus scaffold protects the articular surface.

Key Words: Meniscus, scaffold, degradable polymeric fibers, collagen, regeneration, joint preservation

Introduction

This project addresses a large burden to the military and its personnel: injuries to the musculoskeletal system, specifically, the meniscus and cartilage of the knee joint. Severe damage to the knee meniscus can significantly impair the normal activity of a military member. Due to limited healing capabilities of meniscal injuries, these are often treated with surgical resectioning. This treatment leads to symptom relief but in many cases results in the development of degenerative arthritis of the knee. The pain associated with damaged meniscal tissue and arthritis in the knee is debilitating and inhibits the short- and long-term operational capacity of service members.

The focus of this project is the development of a tissue-engineered meniscus scaffold for the treatment of moderate to severe meniscal damage. The overall goal is to develop an off-the-shelf clinical device that can be implanted at the site of a meniscal resection and results in knee joint preservation. The clinical role of the device is twofold: (1) to provide symptom relief and rapid return of function for active military personnel and (2) to prevent progression to degenerative knee arthritis, which commonly requires costly total knee replacement surgery later in life.

During the first year of the study, the researchers developed a novel meniscus scaffold consisting of high-strength, resorbable, tyrosine-derived polymeric fibers arranged within a collagen matrix. They completed full meniscal scaffold implantation surgeries in sheep; however, half of the implants failed due to improper positioning of the posterior anchor attachment of the scaffold. To address this issue, researchers developed a new surgical procedure. They demonstrated a new synthesis of collagen at 8 weeks after meniscal scaffold implantation. During the second and third years of the study, the researchers designed, fabricated, and tested a second-generation meniscal scaffold. They began testing the scaffold in a nonfunctional small animal model, which demonstrated its biocompatibility.

Research Progress – Year 4

In Vivo Nonfunctional Rabbit Model

The objective of the nonfunctional rabbit model was to observe the in vivo response to the scaffold and determine its ability to initiate cellular infiltration, proliferation, and protein deposition within the construct. Wedge-shaped sections of the meniscus scaffold were implanted in synovial pockets of 10 New Zealand White rabbits (one per knee, 20 implants). Animals were euthanized at either 4 or 8 weeks post implantation. The excised scaffolds were then processed for standard histological analysis.

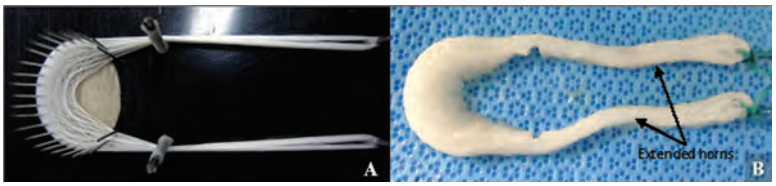

Figure 1. (A) woven polymer fiber and (B) completed meniscus scaffold.

Gross observations of the excised scaffolds showed no negative host response to the implants. The implants were firm and showed signs of good tissue in-growth. Results from the in vivo study suggest that the scaffold with HA or HA and chondroitin sulfate elicits a biological response conducive to its incorporation, degradation, and eventual replacement with native tissue. While the collagen portion of the scaffold is almost completely replaced by cells and amorphous tissue at 8 weeks, the continued presence of the polymer fibers shows that, despite the harsh synovial environment of the joint, the primary load-bearing portion of the scaffold persists through the early remodeling phase. This is important for a meniscus scaffold, which needs to provide mechanical function for a relatively extended period of time as new collagen is deposited and organized into a structurally sound tissue.

In Vivo Functional Sheep Model

Evaluation of the meniscus scaffold in a functional sheep model will determine its ability to promote new fibrocartilaginous tissue growth and minimize degenerative changes to the articular surfaces of the knee joint. Based on the combined data from the mechanical testing in Year 3 and the nonfunctional rabbit model, the scaffold design containing bovine tendon collagen with HA and poly(desaminotyrosyl-tyrosine dodecyl dodecanedioate) poly(DTD DD)) fibers was chosen as the optimal meniscus implant for this functional evaluation (**Figure 1**).

The medial menisci of 20 sheep were removed, and 16 were replaced with a polymer fiber/collagen/glycosaminoglycan (GAG) meniscus scaffold; four were left as meniscectomy controls. The animals were allowed recovery times of either 16 or 32 weeks post operatively.

The researchers have completed all ovine surgeries with minimal complications. They found that animals regained full function of the surgical leg by 2 weeks post operation. Animals were then transported to a sheep farm and were allowed unrestricted mobility for the duration of their recovery. All implants and controls from the 16-week time point have been recovered to date. Harvest of implants and controls from the animals given 32 weeks of post-operative recovery is pending.

At 16 weeks, recovered scaffolds were fully intact and firmly adhered to the surrounding tissue (**Figure 2**; top). Scaffold anchor attachments to the tibial plateau were structurally sound. Even at a gross level, the tissue integration and in-growth

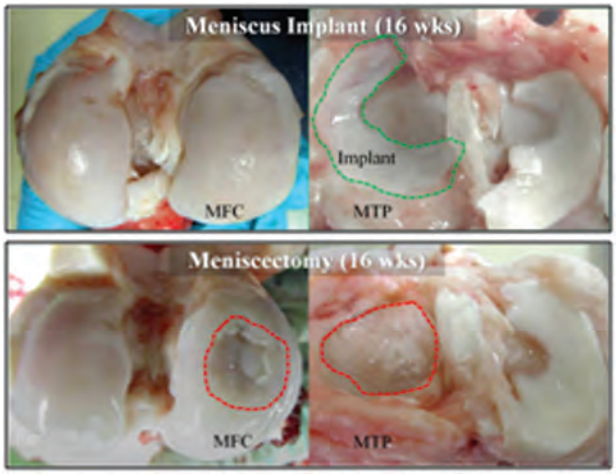

Figure 2. Ovine knee joint (left: Medial femoral chondial, right: Tibial Plateau), (A) implanted meniscus scaffold, (B) control full meniscectomy.

into the scaffolds were obvious. There were no gross degenerative changes in the articular cartilage surfaces in knees with meniscal implants (Figure 2; top). In sharp contrast, the cartilage was severely damaged in the control total meniscectomy knees with no implant (Figure 2; bottom; red circles).

This evaluation of the scaffold thus far demonstrates that the design has the potential to function as a load-bearing device when implanted at the site of a total meniscectomy. Cells within the scaffold should receive appropriate mechanical stimuli, promoting neo-tissue formation similar to that of fibrocartilage. Early results from this study are promising. Scaffolds are integrating into the surrounding tissue, and cells are rapidly infiltrating the device and laying down new collagen. Perhaps most importantly, the meniscus scaffold protects the articular surface.

Conclusions

Overall, the research team has shown that this novel hybrid meniscus scaffold promotes the synthesis of organized, new tissue when implanted as a meniscal replacement. The second-generation meniscus replacement is currently being evaluated in a sheep model, and the results so far have been extremely positive. Therefore, preparations for a 1-year meniscus replacement study using the second-generation scaffold are in progress.

Research Plans for Year 5

In Year 5, the team plans to determine the efficacy of the scaffold in a total meniscus replacement model in sheep after 1 year. The new meniscus tissue and articular cartilage will be evaluated using biomechanical testing and histological analyses, and data will be compared to control knees (without operations).

Planned Clinical Transitions

Transition to clinical trials will be dependent on the results of the 1-year implantation studies and planned longer term studies through 2 years post implantation. The team is in discussions with several companies who have expressed interest in partnering or codeveloping the technology. They also plan to meet with representatives of the FDA to determine the best regulatory strategy for this novel medical device.

Soft Tissue Repair and Regeneration (excluding nerve)

Oxygen-Generating Biomaterials for Large Tissue Salvage

Project 4.4.6, WFPC

Team Leader(s): Benjamin Harrison, PhD (Wake Forest University)

Project Team Member(s): Benjamin Rowe, MS and Catherine Ward, PhD (Wake Forest University)

Collaborator(s): George Christ, PhD, James Yoo, MD, PhD, and Shay Soker, PhD (Wake Forest University)

Therapy: Supply temporary oxygen to hypoxic tissue

Deliverable(s): Injectable oxygen-generating materials for tissue salvage

TRL Progress: 2008, TRL 2; 2009, TRL 2; 2010, TRL 3; 2011, TRL 3

Key Accomplishments: The researchers have created a controllable, injectable, oxygen-generating biomaterial. They have tested the particulate oxygen generators (POGs) for sustained release of oxygen in vitro and feasibility of injection in vivo. They demonstrated that POGs can preserve skeletal muscle structure and function in vivo in an ischemic environment.

Key Words: Oxygen, tissue engineering, tissue salvage, hypoxia, ischemia

Introduction

Replacement or restoration of tissue loss caused by traumatic injury, congenital defects, tumor removal, or severe burns is a challenge. For example, current treatment for reconstruction of volumetric muscle loss (VML) is associated with donor-site morbidity and limited functional restoration. In addition, following traumatic injury or chronic peripheral vascular disease, vascular integrity is compromised (or absent) and the metabolic needs of downstream organs/tissue are not met. Both scenarios produce an ischemic environment, which if not corrected, can result in decreased organ/tissue function and, ultimately, tissue necrosis. Restoring blood flow can take time, as natural angiogenesis is a slow process, so intervention is needed to preserve tissue while the body heals itself.

Since metabolically active cells can only survive up to a few hundred micrometers away from a blood supply due to oxygen diffusion limitations, investigators have used a variety of biological approaches to promote angiogenesis. While such approaches are able to stimulate host tissue responses associated with neovascularization, the extended time needed to establish the vascular network may be inadequate.

Preparing an injectable oxygen-generating material would allow delivery of oxygen in controlled amounts to engineered tissue scaffolds or pre-existing tissue. The ability to control the amount of oxygen delivered is important because different cell types can have different biological oxygen demands, and different oxygen tensions can trigger different biological effects in cells.

POGs Are Particles That Can Release Oxygen When Placed in Aqueous Environments Such as in Culture or in the Body

Previously published work has shown that these materials can provide oxygen in an ischemic skin flap model in mice and in cell culture. The Harrison group has shown that POGs can provide a supplemental source of oxygen for cells and tissue in a hypoxic environment and increase their viability and minimize apoptosis and necrosis. The team's ultimate goal is to develop a method to maintain cell and tissue viability during the time it takes for a vascular network to be established or repaired.

The aims of the project include characterizing the novel biomaterial both in vitro and in vivo for optimal characteristics for tissue salvage and

regeneration to establish their utility as an enabling technology, providing oxygen in several situations.

POGs May Overcome One of the Major Limitations in Muscle Salvage and Tissue Engineering by Acting as a Supplemental Oxygen Source in Several Regenerative Models

Therefore, the goal is to provide oxygen at a therapeutic concentration and not necessarily to replicate standard cell culture conditions. The materials used are based on encapsulated solid peroxides that decompose upon contact with water to oxygen, water, and other biocompatible byproducts. Examples of the chemical equations governing oxygen generation are shown below:

$$4Na_2CO_3 \bullet 6H_2O_2 \rightarrow 8Na^+ + 4HCO_3^- + 3O_2 + 2H_2O + 4OH^-$$

During the first year of the project, efforts were primarily focused on identifying formulations capable of generating oxygen that were nontoxic to cells and could be injected. During Year 2, the laboratory began to establish collaborations with other AFIRM investigators and use the POG technology in relevant in vivo models. During Year 3, the researchers demonstrated that their POG technology could be well tolerated and could improve the functional muscle responses over nontreated controls. Optimization of their in vivo models needed to be continued to move their research forward.

Research Progress – Year 4

Development and Optimization of Hind Limb Ischemia Model to Evaluate the Utility of POGs for Preservation of Tissue Structure and Function

Skeletal muscle is a highly metabolic tissue at major risk of irrecoverable functional loss following traumatic injury and development of peripheral vascular disease in both military and civilian populations. As such, skeletal muscle provides an excellent model system for evaluating the ability of POGs to preserve tissue structure and function. An extended series of studies were conducted using leveraged funding from the National Institutes of Health that led to establishment of the boundary conditions for POG-mediated preservation of skeletal muscle tissue structure and function in vitro (Ward et al., manuscript in preparation).

The goal of this past year of investigations was to establish an in vivo model for evaluating the applicability of POGs. In this regard, several experimental procedures were reviewed as potential candidates for development of a hind limb ischemia model to test the POG technology. For example, the research team previously placed a pressure cuff on the hind limb for 3 hours to create an ischemic injury and 14 days later recorded force measurements. These initial studies showed no significant differences in the functional responses between the injured and noninjured animals, and moreover, the researchers determined that using a pressure cuff produces a tourniquet effect resulting in unwanted nerve damage; this neuropathy, in turn, impedes the researchers' ability to study the impact of POGs. To avoid this complication, they redesigned their experimentation.

The research team's reworked experimental design created ischemia to the rat hind limb via arterial ligation. Through multiple iterations, they concluded that to counter the robust collateral vascularization inherent in rodents, they needed to ligate the iliac artery and vein directly distal to the abdominal bifurcation. Moreover, this approach also allows the animal's contralateral limb to serve as an internal control for future experiments. After a 24-hour post-ligation recovery period, the researchers depleted the oxygen reserve in the tibialis anterior muscle via electrical stimulation of the peroneal nerve. The experimental setup is shown in **Figure 1**. The researchers performed functional assessments in vivo using a customized servomotor (Aurora Scientific) with a foot pedal. They placed electrodes in the limb, surrounding the common peroneal nerve, to elicit muscle contraction.

The initial results show the promising potential of the POG technology (**Figure 2**). In this pilot study, the research team evaluated three different experimental groups: (1) a noninjured control, (2) an ischemic injury group that did not receive POG treatment, and (3) an ischemic injury group that received a single POG injection. As illustrated in Figure 2, the tibialis anterior muscle in POG-treated animals exhibited a 25%–35% functional

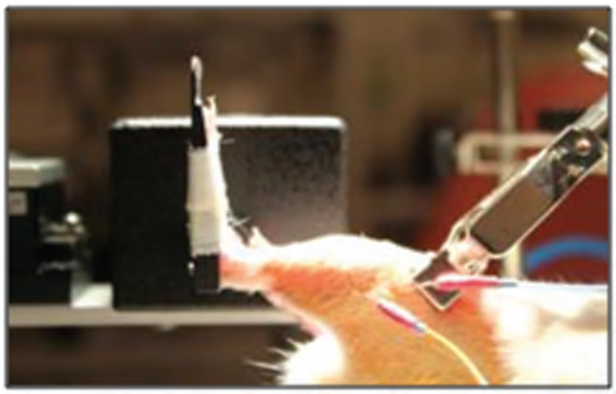

Figure 1. In vivo servomotor with foot pedal, illustrating stimulus through electrodes positioned around nerve. Contraction of hind limb muscles (anterior crural compartment) is measured as torque.

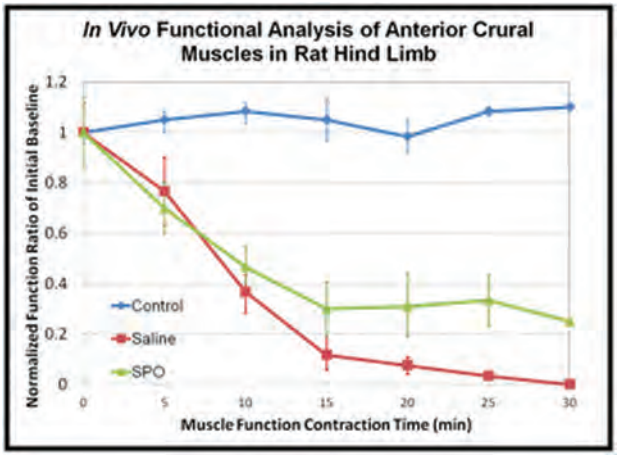

Figure 2. Force Measurement Comparison between noninjured, POG-treated, and saline-treated ischemic animals. POG-treated animals showed a 25%–35% functional reserve as compared to nontreated injuries.

contractile reserve for up to 30 minutes of stimulation (i.e., stimulating every 5 minutes).

Morphological differences were also documented between experimental groups. The POG-treated experimental group showed similar fiber morphology to the noninjured control while the nontreated (saline injection) injury group had irregularly shaped muscles in cross-section and early signs of necrosis (**Figure 3**). Consistent with these findings, the initial studies also showed that the POG-treated group maintained similar glycogen levels to uninjured animals while nontreated groups displayed significant glycogen depletion (**Figure 4**). This

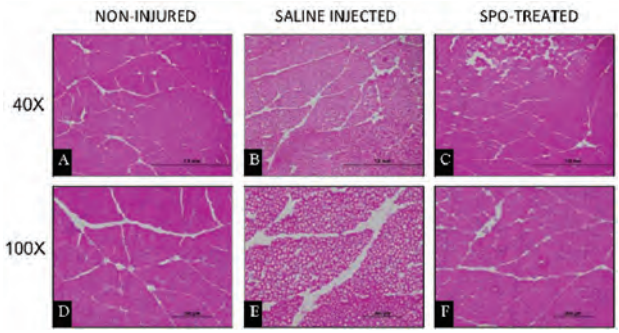

Figure 3. H&E Staining. POG-treated VML injured animals (C, F) showed similar muscle-fiber morphology to noninjured control (A, D). Nontreated injuries (B, E) showed irregular-shaped fibers and early signs of necrosis.

clearly suggests that the POG-treated group can more efficiently metabolize glycogen via the aerobic respiration pathway while the nontreated group is relegated to anaerobic respiration.

While further studies are clearly required, this pilot study shows that POGs have the potential to preserve skeletal muscle structure and function in an acute ischemic environment in vivo.

To further expand the utility and "signal-to-noise" ratio in the in vivo studies, the researchers wanted to develop an animal model that would better mimic a clinically relevant injury, i.e., compromised or injured vasculature requiring limb salvage from, for example, battlefield casualties, peripheral arterial disease, or extremity thrombosis. The above-mentioned pilot study utilized a periodic maximal tetanic contraction, which suboptimally addresses this more realistic scenario. Therefore, the research team's near-term goal is to standardize an

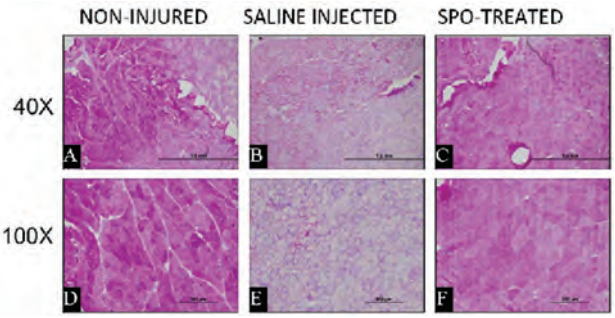

Figure 4. Glycogen staining. POG-treated VML injuries (C, F) retained a significantly higher amount of glycogen than nontreated injuries (B, E).

experimental protocol that induces ischemia in a two-step process by (1) removing blood flow to the hind limb via arterial ligation (as described previously) and (2) fatiguing the tibialis anterior muscle through submaximal contraction.

The initial findings have been promising. Following a 24-hour post-ligation surgical recovery time period, the researchers saw similar tetanic responses from both noninjured and ligated hind limb animal groups. After fatiguing the hind limb via a continual submaximal stimulation protocol, they saw a significant decrease in a second tetanic stimulus from the ischemic injury group compared to noninjured controls (**Figure 5**). More work is needed to increase group size and to monitor a time-course recovery of injured versus noninjured experimental groups.

Conclusions

This project has been focused on developing a chemically based oxygen delivery system. As this technology matures, the laboratory has increasingly become focused on testing the feasibility of delivering oxygen for assisting in tissue preservation or salvage in vivo. The results suggest that this could be used as a readily available treatment to delay the onset of additional tissue damage resulting from compromised blood flow.

Research Plans for Year 5

The researchers will continue to evaluate the efficacy of the material in animal studies. They will test the technology in multiple systems where ischemia/hypoxia may cause detrimental effects and POGs may be most beneficial. Because organs are composed of multiple cell types, the researchers will continue to analyze several different tissues systems including skeletal muscle, bone, nerve, and skin. The primary focus in Year 5 will be to optimize the model and delivery protocol for POGs to demonstrate physiologically relevant

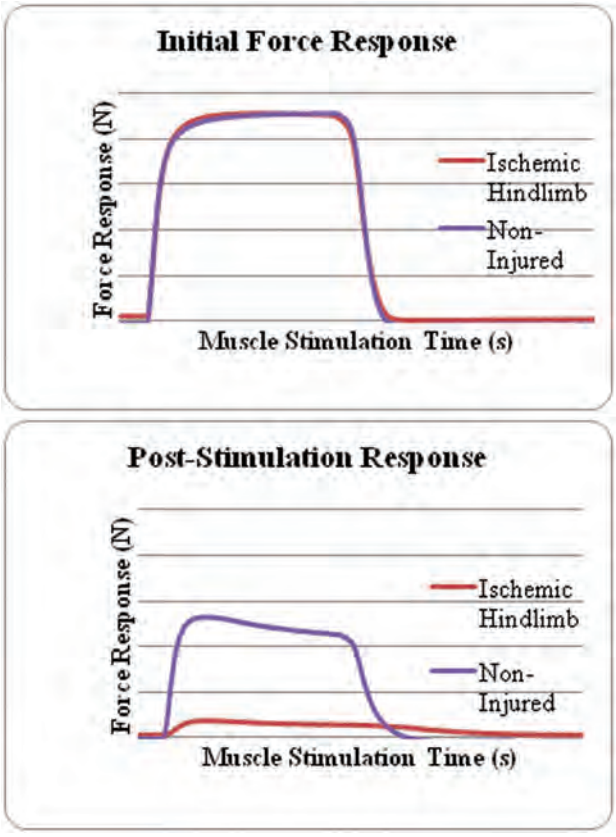

Figure 5. Initial tetanic force measurement curves of ischemic versus noninjured hind limb TA muscles before and after a fatigue-inducing submaximal stimulation protocol.

improvement in skeletal muscle structure and function under clinically relevant experimental conditions.

Planned Clinical Transitions

While no immediate human clinical trials are currently slated under this AFIRM project, multiple pathways are being explored to incorporate this technology into other AFIRM research, as well as to leverage other funds to accelerate the time to clinic.

Soft Tissue Repair and Regeneration (excluding nerve)

Isolation and Expansion of Native Vascular Networks for Organ-Level Tissue Engineering

Project 4.5.8, WFPC

Team Leader(s): Geoffrey C. Gurtner, MD (Stanford University)

Project Team Member(s): Michael T. Longaker, MD, MBA (Stanford University) and Robert Langer, ScD (Massachusetts Institute of Technology)

Collaborator(s): None

Therapy: Vascularized tissue engineering

Deliverable(s): Hydrogel-encased vascularized networks for organ-level engineering

TRL Progress: 2008, TRL 1; 2009, TRL 1; 2010, TRL 2; 2011, TRL 3

Key Accomplishments: During the past year, the Stanford group further developed and improved their technique to isolate and maintain explantable microvascular beds (EMBs), based on the rat superficial inferior epigastric vessels, on an ex vivo bioreactor system. They achieved EMB viability during the bioreactor period with thermoreversible gel for tissue protection and demonstrated reanastomosis of EMB into the native vascular circulation. They improved the decellularization process of the native vascular network that preserved a structural matrix but removed the majority of the adipose cells. As proof-of-concept they established that human adipose-derived stem cells (hASC) seeded onto intact flaps after a decellularization process remain viable 14 days after reanastomosis into the native circulation.

Key Words: Tissue engineering, explantable microvascular beds, decellularization, bioreactor

Introduction

Injured or missing extremities, failing organs, and significant burn injuries continue to place a huge burden on wounded soldiers and society. Tissue engineering holds the promise of creating replacement organs outside the human body. However, two major obstacles have hindered the development of techniques to fabricate replacement organs: (1) the inability to adequately vascularize tissue constructs in vitro and (2) the inability to reintegrate these tissues into the systemic circulation. Researchers have successfully applied tissue-engineering approaches based on the implantation of cells onto resorbable matrices for the replication of simple, relatively avascular structures such as cartilage or bone but not for the creation of more complex parenchymal organs, such as liver. Despite the obvious promise that stem cell technology holds to "regenerate" partially damaged organs in vivo, it is difficult to envision the creation of new organs in vitro using existing methodologies.

To address this problem, the Stanford group has developed a novel approach to engineering constructs of organ-level complexity by using pre-existing EMBs to fabricate autologous, vascularized neo-organs in vitro. This approach starts with the vascular system and surrounding stromal support as the scaffold and builds tissue from the "inside-out" as compared to existing paradigms of tissue engineering. The research team has constructed a novel perfusion bioreactor system that permits the cultivation of EMBs for extended periods ex vivo. The researchers have demonstrated extremely efficient seeding of cultivated EMBs with primitive progenitor and stem cells after a decellularization process. The technology has advanced beyond proof-of-principle toward a flexible regenerative environment based on a bioreactor system. This innovative approach has allowed utilization of the pre-existing vascular system as a scaffold that can be manipulated ex vivo and subsequently reconnected to the circulatory system in vivo using standard microsurgical techniques.

During the first 2 years of the study, the researchers used detergents and enzymes to isolate the vascular network of rat superficial inferior epigastric artery flaps. They also worked on defining the native matrix surrounding the explanted vessels. They made plans to test various decellularization strategies.

Research Progress – Year 4

The Stanford group has focused on optimizing the perfusion rates and perfusate composition to maximize EMB survival and vascular potency. They have further developed and improved the technique to isolate and maintain EMBs based on the rat superficial inferior epigastric vessels on an ex vivo bioreactor system. They have continued to refine the surgical protocol to maximize preservation of microvascular structures. Previous studies by the Hagey laboratory have established, as proof-of-concept, that stem cells can be seeded onto intact flaps. However, the persistence of pre-existing mature cells appears to limit the ability to guide stem cell differentiation for neo-organ fabrication. As such, a major goal of this study was to remove the pre-existing parenchymal cells while maintaining the vasculature and matrix scaffolding for progenitor cell seeding. The Stanford group first improved the decellularization process of the native vascular network with the external administration of trypsin (enzymatic digestion) that preserved a structural matrix but removed the majority of the adipose cells (**Figure 1**).

Figure 1. Processed autologous scaffold (explantable microcirculatory bed) after multiple decellularization steps with external administration of trypsin. The vasculature architecture remains intact.

The vascular architecture was concurrently subjected to the external enzymatic digestion and perfused internally with Dulbecco's Modified Eagle Medium (DMEM) to limit vascular decellularization and thereby preserve the vascular architecture. The research team examined a wide variety of detergents, but after multiple iterations they found the trypsin-DMEM protocol to be the most effective in removing parenchymal cells while preserving the microcirculation. They were able to decellularize the tissue while preserving the matrix architecture and nearly all vascular structures, most importantly, the microcirculation. They were therefore able to perfuse the EMBs for longer than 48 hours on the bioreactor and maintain the viability of the matrix. This was never possible with fully cellular explantable microvascular beds even with exogenous oxygen carrier perfusion, which created a host of secondary problems.

Finally, as illustrated in **Figure 2**, the research team further optimized the mechanical protection of the EMB with the application of a thermoreversible gel, which is a solid mass at 37°C during the bioreactor period and is transformed into a liquid at room temperature. This preserves the microvascular pedicle and allows re-anastomosis to the host vasculature for in vivo experiments and mimimizes mechanical damage of these delicate structures during manipulation.

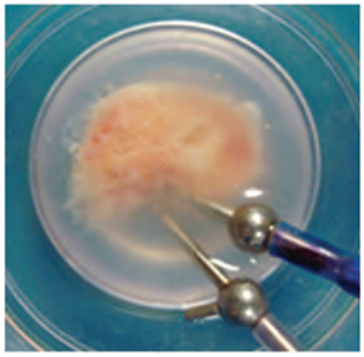

Figure 2. The explanted microvascular bed is covered and secured with a thermoreversible gel (Thermogel) for overnight protection during ex vivo perfusion on the bioreactor.

The Stanford group has continued to determine the optimal seeding and differentiation conditions for different infused stem cells. Since the EMB is encased in a gel during the ex vivo period, the researchers examined the feasibility of using this opportunity to further augment cell delivery in vivo. They examined the capacity of a biomimetic pullulan-collagen hydrogel (developed by the Hagey lab) to create a functional biomaterial-based stem cell niche for the delivery of MSC in vivo. Bioluminescence imaging and fluorescence-activated cell-sorting analysis of MSC that are positive for both luciferase and green fluorescent protein indicated that stem cells delivered within the hydrogel remained viable longer (up to 2 weeks) and demonstrated enhanced engraftment efficiency, suggesting that this would be a viable way

to increase cell delivery around the EMB and may provide a method for creating laminated structures composed of two or more different cell types as would be required for organ replacement. For example, one population of cells could be delivered perivascularly via perfusion while simultaneously a second distinct population could be delivered to the EMB via delivery in the encasing gel.

In preliminary studies to simulate the extravascular environment of neo-liver constructs, the researchers seeded MSC into the pullulan collagen hydrogel. Pluripotency gene expression and expression of hepatic growth factor (HGF) and insulin-like growth factor (IGF) were increased (data not shown). This may therefore be a viable strategy to increase hepatocyte cell mass. This preliminary work is ongoing and focuses on describing the differences between mature adult hepatocytes and differentiating hepatocyte-like progenitor cells. If adult hepatocytes are the preferred cell type, then the hydrogel delivery mechanism will be required for seeding as prior work has shown that these cells cannot be seeded via perfusion.

In a parallel effort, the Stanford group has demonstrated for the first time the ability to seed luciferase+ hASC on the EMB and confirm the survival of the cells during and after perfusion on the bioreactor (**Figure 3**). Furthermore, they reattached the EMB into the original femoral vessels of an immune-compromised rat (**Figure 4**). They demonstrated that hASC can engraft and remain functional for extended periods in vivo following seeding onto processed EMBs and reintegration into the host (**Figure 5**). The research team has continued to refine the protocol for hASC administration on the decellularized EMB matrix. Detection of bioluminesence with an in vivo imaging system allows the non-invasive monitoring of cell survival and has allowed the researchers to achieve engraftment of the cells into the scaffold and cell viability for greater than 14 days after replantation of the EMB back into the native vascular circulation. Thus, they have demonstrated that extrinsic seeding of hASC onto EMBs is possible, providing a new and readily available cell source for eventual translation.

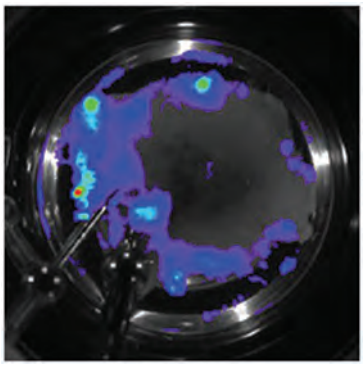

Figure 3. Bioluminescence imaging of the EMB 24 hours after perfusion on the bioreactor. The EMB was seeded with luciferase+ hASC. The image shows that the luciferase+ human ASC are viable and persistent after perfusion on the bioreactor.

Figure 4. Successful re-anastomosis ("replant") of the EMB back into the native femoral vessels of the nude rat after 24 hours with the seeded luciferase+ hASC.

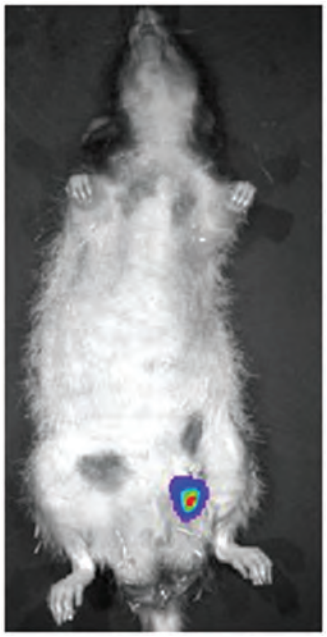

Figure 5. Bioluminescence imaging 14 days after replantation of the EMB back into the native rat circulation. The EMB was seeded with luciferase+ hASC. These data demonstrate that hASC can engraft and remain functional for extended periods following seeding onto processed EMBs and reintegration into the vascular circulation.

While the effort to optimize a cell seeding protocol that is scalable and potentially translatable for human applications has been under way, the researchers continue to develop alternative approaches to replace physiologic function in vivo that have the potential to be translated into human trials in a reasonable time frame. Broadly, these approaches fall into two categories: either replace a single protein using gene therapy or replace cells to provide for more diverse

functionality. It is currently unclear which of these approaches is more feasible; therefore, preliminary efforts are under way exploring both approaches.

The easiest goal to accomplish in the short term is to replace a single protein. The translational target for this approach is human factor IX deficiency, which is a single gene defect that has proven difficult to reverse using standard gene therapy techniques. The researchers used EMBs without decellularization along with a novel minicircle DNA delivery technique. They achieved significant progress using the vascularized adipose tissue flaps (EMB) engineered with minicircle DNA, which provides significantly enhanced and sustainable transgene expression and results in significantly higher levels of protein production than standard in vivo techniques. Adipose tissue flaps (such as human omentum) are ideal candidates for minicircle transfection due to their excellent vascularization, peripheral location, and expendability. The researchers demonstrated that transfection with minicircle DNA provides efficient mid-term transgene expression with minimal adverse effects. This technology appears to provide safe and sustainable systemic protein release.

Conclusions

The Stanford group established proof-of-principle and optimized its protocol for the isolation and maintenance of EMBs based on the rat superficial inferior epigastric vessels on an ex vivo bioreactor system. The researchers developed a decellularization protocol that achieves complete decellularization of tissue while preserving the matrix architecture and the macroscopic vascular structure. They have successfully seeded decellularized rat tissue flaps with ASC, and studies indicate that engrafted cells persist in a functional capacity for extended time periods. Also, the group reanastomosed the EMB into the native vascular circulation and showed a long-term survival of the engrafted ASC after the reanastomosis. Together, these studies suggest that progenitor cell-seeded vascularized scaffolds are a promising approach to fabricate complex organ-level constructs. The potential of this technology is tremendous, and the research team continues to make significant strides toward refining this novel paradigm for organ-level engineering and regenerative medicine.

Research Plans for Year 5

In the upcoming year, the Stanford group will continue to modify the perfusion protocols to optimize EMB tissue survival ex vivo, in particular, the degree of decellularization. They will focus on refining amounts of trypsin and duration of the enzymatic step, as well as the perfusion rate during the internal perfusion with the culture medium to maximize the decellularization. Another goal is to preserve completely the microvascular pedicle of the adipose tissue flap during the decellularization process, which is critical for the microsurgical reanastomosis of the artery and vein back into the systemic circulation of the rat.

The researchers will concentrate on refining the thermoreversible gel as a protective agent of the vascular pedicle. They will also continue to improve the stem cell seeding efficiency and post-implantation survival by examining both intravascular and extravascular approaches and will determine the "ideal" amount of stem cells to administer. Repeated applications of the stem cells with intravascular and extravascular approaches appear to be important for further optimization of the engraftment rate. Therefore, the researchers will refine their protocol involving repeated applications of cells.

Modification of the parenchymal tissues may allow for improved stem cell survival. This will be investigated in the upcoming year. Due to loss of immunocompetence that occurs in a nude rat model with human cells, the researchers will transition this work to employ ASC from a luciferase-expressing rat species. Two different strategies to replace essential hepatic function will be investigated to enable a gradual transition from replacement of single proteins to replacement of cells and fabrication of a true vascularized neo-liver construct. Initially, these efforts will focus on albumin production in their seeded flap in a hypoalbuminemia rat model as a surrogate for global liver function although this is an oversimplification. The essential task over the next year will be to determine the ideal cell type (progenitor vs. differentiated) to use in these studies.

Nerve Repair and Regeneration

Repair of Segmental Nerve Defects: Prevention of Muscle Atrophy

Project 4.4.1, RCCC

Team Leader(s): Robert S. Langer, ScD and Daniel G. Anderson, PhD (Massachusetts Institute of Technology [MIT])

Project Team(s): Liang Guo, PhD and Paulina S. Hill, PhD (MIT)

Collaborator(s): Anthony Windebank, MD and Michael Yaszemski, MD, PhD (Mayo Clinic)

Therapy: A theragnostic solution for promoting peripheral nerve repair by epimysial electrical stimulation and recording from denervated muscle

Deliverable(s): Techniques for in vivo tracking of nerve regeneration and estimating number of motor units to assess reinnervation; technique for reducing denervated muscle atrophy using an implanted, epimysial, stretchable microelectrode array

TRL Progress: 2010, N/A; 2011, TRL 2; 2012 (Current), TRL 3; 2013 (Target), TRL 3/4

Key Accomplishments: The researchers developed an implantable, organic, stretchable microelectrode array (OSMEA) for epimysial stimulation and recording. Preliminary biocompatibility assessments using both PC12 cell culture and rat subcutaneous implantation proved positive for the conducting polymer used in the OSMEA.

Key Words: Peripheral nerve repair, muscle denervation and atrophy, OSMEA, microelectrode array, epimysial stimulation and recording

Introduction

The course of peripheral nerve repair can take from a few months to more than 1 year. Denervated muscles quickly undergo atrophy, which can significantly affect functional recovery of motor reinnervation. The common clinical method to treat muscle atrophy uses functional electrical stimulation. However, conventional transcutaneous electrodes are not optimal for peripheral nerve repair and can induce significant tissue damage. Intramuscular electrodes are rarely used in a clinical setting to treat muscle denervation atrophy, primarily because of the invasiveness of the approach and the need for a large electrode area capable of delivering the current required to elicit contraction of the denervated muscle. Conventional epimysial (i.e,. on the muscle surface) electrodes are sometimes bulky and unable to meet the stringent needs of peripheral nerve repair. Meanwhile, little information with regard to the time course of nerve regeneration and motor reinnervation has been collected.

Therefore, there remains a need for an effective, continuous interface that is suitable for stimulation of denervated muscle and for the real-time in vivo monitoring of the nerve regeneration time course. Additionally, though many efforts have been devoted to this end, it is still unclear what the optimal stimulation protocols should be. Variations in experimental methods and animal models used in the literature make cross-comparisons even more difficult.

During the first 3 years of the study, the researchers fabricated a series of biocompatible nerve conduits with mechanical properties that mimicked peripheral nerve and exhibited a degradation rate superior to conventional nerve conduits. They tested their conduits in a 1 cm long rat sciatic nerve defect model and determined that the first-generation conduit showed better functional nerve regeneration than the commercially available collagen conduit, as assessed by electrophysiological response and muscle weight. The researchers also developed a method for incorporating aligned electrospun fibers inside the lumen of their nerve conduits. They found that encapsulation of anti-inflammatory agents into the electrospun fibers decreased the local host immune response and

resulted in considerably less fibrosis around the implant. Intraluminal scaffolds of these electrospun fibers were tested in rat sciatic nerves and were found to promote functional nerve regeneration.

Research Progress – Year 4

In Year 4, the researchers focused on the preservation of denervated muscles during the course of nerve repair using electrical stimulation. The team developed an implantable OSMEA for epimysial stimulation and recording. In addition, they set up a new animal experiment platform for treating muscle atrophy following denervation by using electrical stimulation. They also acquired devices and equipment for the upcoming animal experiments.

The OSMEA was developed using biocompatible materials so that FDA approval can be obtained in the future. While in-depth characterization of the technology is ongoing, data from preliminary evaluations on the materials and OSMEA is promising for the intended application.

Conclusions

The OSMEA technology developed by the MIT team shows promise for the intended application of treating muscle atrophy during the course of nerve repair following denervation. Of note, the OSMEA technology is also applicable to many other exciting neural interfacing applications, including spinal cord surface stimulation, electrocorticogram-based brain-computer interfaces, and retinal prostheses.

Research Plans for Year 5

The researchers plan to fully characterize the OSMEA and prepare a manuscript for publication. They will connect the entire system (OSMEA, head stage/stimulator, data acquisition system) for use in short-term rat experiments, involving epimysial recording and stimulation. The research team will also test the long-term in vivo performance of OSMEA as an epimysial interface. Both short- and long-term experiments will be conducted to develop the proposed theragnostic solution. In addition, the MIT team will develop diagnostic and therapeutic techniques using a rat sciatic nerve transection model.

Planned Clinical Transitions

The research team is currently focused on demonstrating the safety and efficacy of this novel approach in a preclinical animal study. It is expected that the preclinical stage of development will take at least 3 years. Once proof-of-concept is validated in a defined animal model, an IDE application will be submitted and a human clinical trial will be designed.

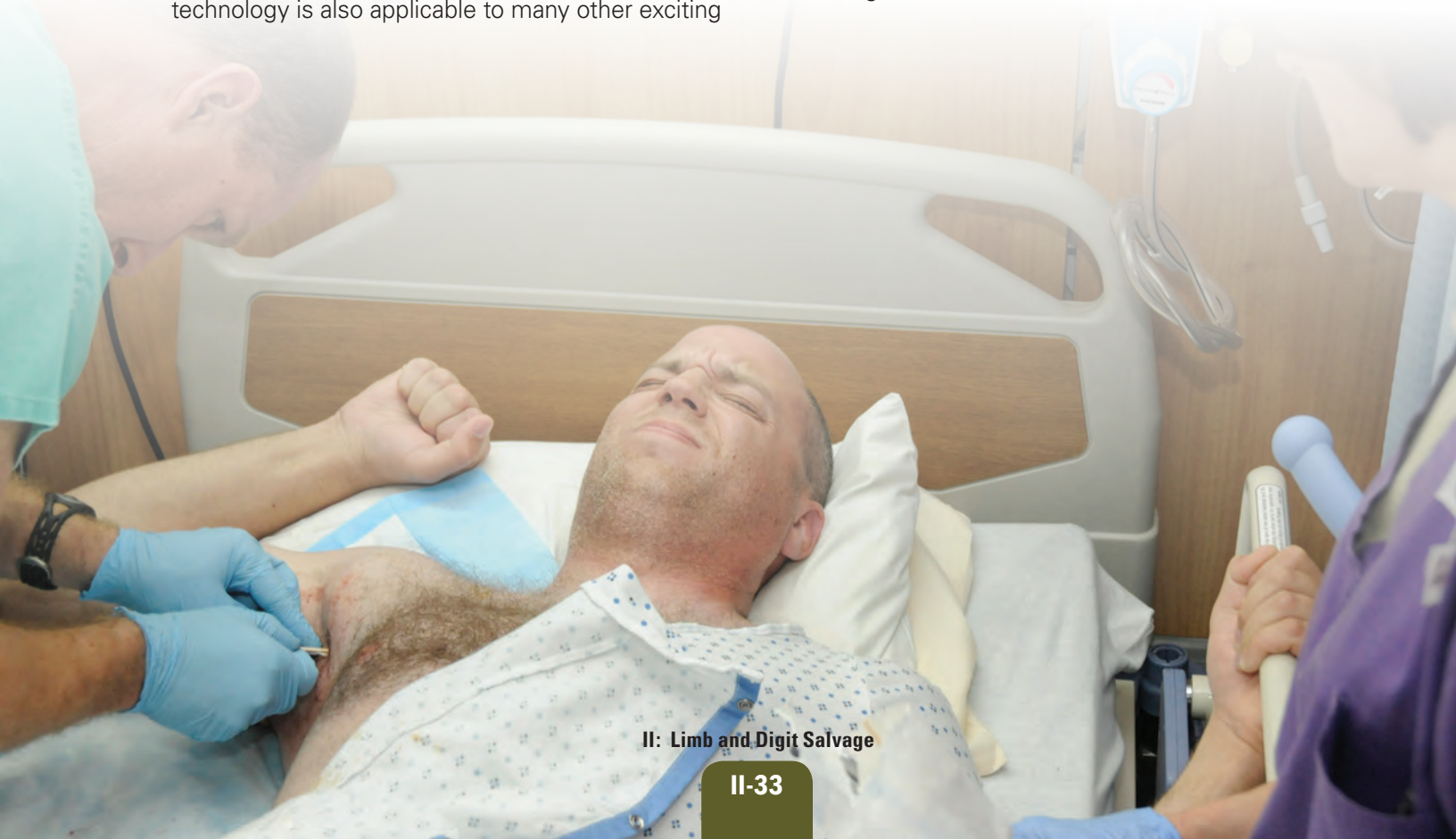

Nerve Repair and Regeneration

Repair Segmental Nerve Defects

Project 4.4.2, RCCC

Team Leader(s): Anthony J. Windebank, MD and Michael J. Yaszemski, MD, PhD (Mayo Clinic)

Project Team(s): Robert J. Spinner, MD, Huan Wang, MD, PhD, Peng Wu, MD, Chandan Reddy, MD, Aditya Chawla, Joaquin Hidalgo, MD, Shuya Zhang, Glenda Evans, Jarred Nesbitt, Brett Runge, PhD, and Suzanne Segovis (Mayo Clinic)

Collaborator(s): BonWrx™; Joachim Kohn, PhD, Basak Clements, PhD, Jack Hershey, PhD, Ijaz Ahmed, PhD, Mikel Ehntholt, and Sruti Golthi (Rutgers University)

Therapy: Treatment of peripheral nerve injuries

Deliverable(s): Tissue-engineered scaffolds suitable to repair large, motor nerve defects

TRL Progress: 2010, TRL 3; 2011, TRL 2; 2012 (Current), TRL 3; 2013 (Target), TRL 4

Key Accomplishments: The researchers established and validated a delayed nerve repair model and a noninvasive isometric muscle force measurement device. They demonstrated that polycaprolactone fumarate (PCLF) nerve conduits supplemented with vascular endothelial growth factor (VEGF) microspheres induced better nerve functional recovery than PCLF nerve conduits filled with empty microspheres. They also reduced fibroblast attachment by modulating braided conduit porosity through a hyaluronic acid (HA) coating and improved histological and electrophysiological outcomes in vivo compared to uncoated braided conduits.

Key Words: Peripheral nerve, conduit, scaffold, biodegradable polymer, growth factors, braiding, tyrosine-derived polycarbonate

Introduction

The Mayo Clinic team established and validated a delayed nerve repair model and a 1.5 cm critical-size nerve defect model. A noninvasive muscle force measurement technology and device were also being developed to longitudinally track the restoration of motor function. The researchers' goal is to be able to effectively reconstruct a motor nerve with a long defect using their synthetic nerve conduits. While their PCLF conduit is entering a Phase 1 safety clinical trial (see Project 4.4.1a), the researchers also aim to enrich the conduit with growth factors and supporting cells. VEGF, an angiogenic and neurotrophic factor, was encapsulated within microspheres and introduced into the PCLF conduits. The microspheres offer the potential to deliver VEGF in a dose- and rate-controlled manner. The Mayo Clinic team is also going to supplement PCLF conduits with Schwann cells, the normal supporting cell of peripheral nerves that produces extracellular matrix and myelin and is essential for regeneration. The team is collaborating with the Miami Project to obtain adequate quantities of autologous Schwann cells.

During the first 3 years of this project, the researchers effectively encapsulated and released neuronal growth factors from fumarate-derived polymer scaffolds and polymer microspheres. They also showed that MSC provide a potential cell-based delivery platform for growth factor delivery. They screened candidate polymers by comparing the effectiveness of nerve regeneration after implanting synthetic polymer conduits in 1 cm nerve gap in rats. They found that PCLF performed better than any other polymer. The researchers demonstrated that sterilization by autoclaving is compatible with the material properties of their PCLF conduits. They fabricated second-generation conduits that allowed delivery of electric stimulation and demonstrated that electrical stimulation via a conductive polymer promoted axon growth in vitro. The researchers also created an ischemic/

fibrosis model for nerve injury and repair that mimics the real clinical scenario and allows for studies of complex nerve injury.

Research Progress – Year 4

Standardized Preclinical Models and Motor Function Evaluation Modality

Delayed nerve repair model. In this more critical and clinically relevant model, the sciatic nerve was repaired in a second stage after various post-transection intervals (1, 4, 6, and 8 weeks). The incidence of successful direct coaptation without tension was calculated to be over 80%. This level of efficiency makes the model applicable for future studies of combat-related peripheral nerve injuries. Functional outcomes were evaluated for nerves that were repaired in a delayed fashion. Wet muscle weight of the gastrocnemius muscle (histological assessment), maximum isometric muscle force recovery (functional assessment), and nerve conduction (physiological assessment) were measured. These three classes of outcome measures consistently showed a decreased capacity of regeneration and recovery when the nerve repair was delayed; the longer the delay, the weaker the recovery. These phenomena closely match the clinical scenario.

Noninvasive isometric muscle force measurement: A custom device and technology. A custom rat dynamometer that is capable of registering plantar flexion force generated by the lower leg muscles was developed. The isometric forces generated during plantar flexion of the ankle were in the range of values reported in the literature. One-way ANOVA showed that interanimal variability, interobserver variability and day-to-day variability were not statistically significant. Data tested on the left and right hind limbs were also not significantly different.

The researchers used two animal cohorts to validate this test. One cohort consisted of 10 rats with sciatic nerve transection and repair while the other cohort was composed of 10 rats with tibial nerve transection and repair. These represent the most commonly used nerve repair models. The sensitivity of this test was demonstrated by the close correlation of the return of measure forces with the post-nerve repair time course and the close correlation of the forces elicited by both direct and indirect stimulation.

Conditioning PCLF Conduit with VEGF: Effects on Vascularity and Nerve Regeneration

The researchers established poly(lactic-co-glycolic acid) microspheres as a novel system for controlled release of VEGF. This system is capable of high encapsulation efficiency and sustained release of bioactive VEGF for 4 weeks. Importantly, when VEGF-containing microspheres were placed in synthetic (PCLF) nerve conduits, robust angiogenesis and nerve regeneration were observed.

Braiding Nerve Conduits: A Technology to Introduce Porosity and Flexibility

The Rutgers team hypothesized that the macropores of the braided conduits are detrimental for nerve regeneration and limiting the porosity will decrease the fibrotic infiltration and allow for the formation of an epineurium around the axons. Therefore, studies were conducted in Year 4 to optimize braided conduit design with minimized porosity while maintaining permeability, which is essential for successful nerve regeneration.

Coating of braided conduits with secondary layers to reduce porosity. Braided conduits were fabricated from a relatively slow degrading TyrPC (E0000) for optimization of conduit design. During Year 4, the Rutgers team used the single layer braided conduits as well as three coating strategies to minimize the conduit porosity. These strategies involved coating the conduits with a nanofibrous electrospun (ES) polymer layer as well as coating them with cross-linked HA hydrogels, which have been shown to be cell-repellent and led to improved nerve regeneration in a 6-week study.

Optimizing the braid design. Second-generation braided conduits fabricated from a faster degrading TyrPC composition, (E1001) were also tested in this study. These conduits were macroporous, like the first-generation conduits but had a smaller fiber diameter forming a tighter braid with a uniform pore-size distribution. These conduits were also heat formed at the end of braiding, which rendered them highly elastic and flexible. To realize

the effect of conduit porosity on nerve regeneration, nonporous, dip-coated conduits were also fabricated and tested as controls. These conduits did not have the favorable flexibility or kink-resistance of the braided conduits and were therefore disqualified from the conduit fabrication criteria for long nerve gaps but served as a test bed for understanding the effect of conduit porosity on nerve regeneration.

In vivo testing of braided conduits. All conduits were implanted in the 1 cm rat sciatic nerve defect model and evaluated during a 16-week study. The outcome measures were recovery of the electromyography (EMG) signal, muscle mass, and nerve histomorphometry.

Electrophysiology. Electrophysiological measurements were recorded every 4 weeks after surgery, and average compound muscle action potential (CMAP) amplitude and latency of three consecutive measurements for all the responding animals in a given treatment group were plotted. The earliest post-operative CMAP signals were detected by 8 weeks for the autografts and 12 weeks for the conduit groups. Autografts had the largest amplitude followed by nonporous E1001 dip-coated conduits and HA-coated braided conduits. HA coating alone doubled the CMAP amplitude of uncoated braided E0000 conduits, but additional ES coating was detrimental.

Muscle weight recovery. The TA and gastrocnemius muscles of both hind limbs were harvested and weighed, and the ratios of injured muscle weights to healthy muscle weights at 16 weeks were calculated. Muscle weight recovery was greatest in the autograft group, followed by the HA-coated E0000 braids. TA muscle weight recovery for HA-coated E0000 braids was significantly higher ($p<0.05$) than uncoated E0000 braids.

Nerve histology. The size and density of the nerve cable appeared to be larger in E1001 dip-coated and E0000 uncoated and HA-coated braided conduits. The nerve cables in the dip-coated and HA-coated braided conduits were densely packed with axons with a well-defined epineurium surrounding the fascicles while the nerve cable in the uncoated conduits appeared loosely packed without an epineurium. This suggests that limiting porosity allows for the formation of an epineurium and leads to a more organized and densely regenerated nerve cable. This is the case with the HA-coated braided conduits even though fibrotic tissue eventually co-occupies the lumen, suggesting that the HA layer around the conduits is effective long enough to promote the formation of the epineurial layer but fails to act as a nonporous barrier throughout the duration of the study.

Conclusions

Repairing nerve injury in a delayed method led to a decreased capacity for nerve regeneration. As such, the delayed repair model is designed to be more clinically relevant than immediate repair by: (1) mitigating the discrepancy between rodent nerve growth and human nerve growth, the former being much more potent; (2) mimicking the clinical scenario when primary nerve repair is seldom done; and (3) providing the opportunity to choose different levels of challenge by timing various delay intervals and applying them to test a wide range of treatment strategies. Supplementing the PCLF nerve conduit with VEGF-loaded microspheres could increase vascularity of the regenerating nerve and thus improve functional return. Using a custom-made dynamometer, longitudinal tracking of muscle force recovery is possible. The isometric plantar flexion force generated by direct stimulation of the gastrocnemius muscle or indirect stimulation of the sciatic nerve was indicative of the extent of nerve recovery.

Flexible, HA-coated braided conduits provide a mechanically optimized nerve conduit, and the Rutgers group is ready to apply the same fabrication methodology to PCLF fibers. By combining such conduits with biologically active fillers or cells, it may be possible to create a nerve regeneration conduit capable of bridging long nerve gaps.

Research Plans for Year 5

The Mayo Clinic group will continue to examine the acquisition of gene expression profile and neuromuscular junction changes and muscle fiber-type characteristics that are part of the delayed nerve repair experiments aimed at understanding key events in denervation muscle atrophy. Such

information will allow the group to identify key components in muscle reinnervation that it can target in future studies to achieve better functional recovery with regeneration strategies.

The Mayo Clinic group will utilize the Miami Project's IRB-approved GMP protocol to isolate and expand autologous human Schwann cells from waste nerve. The same protocol will be applied to isolate and expand rat autologous Schwann cells to be used as fillers in PCLF nerve conduits to repair critical-size nerve defects.

The Rutgers group expects to scale up the conduit prototype for large animal testing and long nerve gaps in Year 5. Braided conduits will be fabricated to bridge long gaps (>5 cm) in the pig model of peripheral nerve injury in collaboration with University of Pennsylvania. Biodegradable conduits will be used to support stretch grown human dorsal root ganglia axons and then evaluated in long nerve gaps in a peripheral nerve injury model.

Planned Clinical Transitions

In conjunction with BonWrx, the Mayo Clinic group has filed an IDE application for the safety evaluation of PCLF conduits in humans. Once the application is approved, the research team will secure IRB and HRPO approval for the clinical protocol. The Phase 1 clinical trial will then commence.

The Rutgers group has an exclusive license with Trident Biomedical, Inc. for the library of TyrPCs, and discussions have been initiated to define required funding to advance planned animal studies. The Rutgers team is also working with two separate industrial partners for the large-scale cGMP synthesis of TyrPCs and the fabrication of the braided conduits.

Nerve Repair and Regeneration

Cells and Bioactive Molecules Delivery in Peripheral Nerve Restoration

Project 4.4.2a, RCCC

Team Leader(s): Maria Siemionow, MD, PhD (Cleveland Clinic)

Project Team(s): Can Ozturk, MD, Miroslaw Lukaszuk, MD, Maria Madajka, PhD, Halil Uygur, MD, and Joanna Cwykiel, MSc (Cleveland Clinic)

Collaborator(s): N/A

Therapy: Long nerve gap repair

Deliverable(s): Method of cellular therapeutics by local administration of bone marrow stromal cells (BMSC) into transplanted epineural nerve conduits

TRL Progress: 2010, TRL 3; 2011, TRL 3; 2012 (Current), TRL 4; 2013 (Target), TRL5

Key Accomplishments: The researchers established a protocol for the isolation of BMSC from sheep. They performed BMSC phenotypic characterizations and determined epineural sheath surface markers. They developed naturally occurring epineural sheaths supported with BMSC conduits and tested them for the repair of long nerve gap defects (6 cm) in 18 sheep.

Key Words: Epineural sheath, stromal cells, sheep model, long nerve repair, conduit

Introduction

Injured warfighters in the U.S. military have special needs, as their injuries are likely to be penetrating or large open wounds. The use of autograft nerve (e.g., sural nerve) is not always feasible in the multiextremity amputees often seen in combat-related traumatic injury due to limited source and length of autologous nerves available for grafting, especially in multiextremity amputees often seen in combat-related traumatic injury. In addition, autologous nerve grafting can cause pain, sensory loss, neuroma formation, and infection at the harvest site. As an alternative to nerve autografts, a number of natural and synthetic materials have been explored; however, their efficacy in repair of long nerve defects is limited.

Severe limb injuries frequently require complex bone, muscle, and nerve reconstruction. This setting is ideal for the application of an epineural sheath conduit, which could contribute to better nerve regrowth. An epineural sheath conduit is composed of a naturally occurring epineural sheath tube filled with BMSC. BMSC are an important source of growth factors and provide crucial structural support.

During the first 3 years of this project, the researchers developed several biological nerve conduits and tested them in a rat nerve repair model using a combination of in vitro and in vivo methods. They demonstrated that allogeneic epineural tube repair without immunosuppression is a feasible method of peripheral nerve gap repair. They identified the most effective conduit and selected it for use in the repair of a long nerve defect in a large animal (sheep) model.

Research Progress – Year 4

BMSC Isolation and Characteristics

BMSC were purified by the buffy coat technique and cultured for 2 weeks. BMSC were then fluorescently labeled with PKH-26 red prior to their injection into the empty epineural tube. No clotting or cell lysis was observed after cell injection. Cells were uniformly distributed inside the epineural tube directly before the transplantation of the conduit into the recipient animal (**Figure 1**). BMSC do not express immunological markers, which make them applicable for nerve repair conduits without the need of supportive immunosuppression therapy.

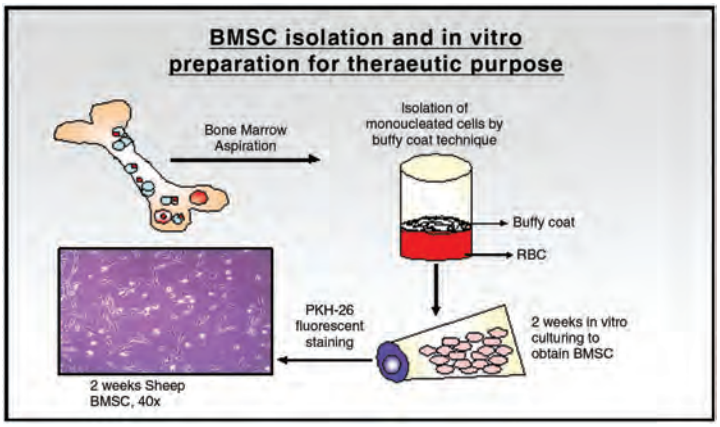

Figure 1. BMSC in vitro isolation and culturing procedure for transplantation into the epineural tube.

Epineural Sheath Conduit Preparation and Transplantation

Empty epineural tubes were created from sheep median nerves. Nerves were exposed and dissected, and all internal structures were removed by the use of surgical forceps. The epineural sheath tube was then filled with fluorescently labeled BMSC to create a conduit, which was then transplanted into recipient animals that had a 6 cm median nerve gap. The following experimental groups were prepared: autologous conduit with autologous BMSC, allogenic conduit with allogenic BMSC, and saline-filled conduit. Autograft technique served as a control.

Sheep Surgical Procedure

In total, 18 animals underwent the stated median nerve surgery. Both legs were utilized to complete autogenic or allogeneic BMSC, saline controls, and nerve autograft experimental groups. Each animal underwent bone marrow collection to isolate and culture BMSC. Animals were able to ambulate immediately after surgery. There were no signs of inflammation or discomfort. Animals carrying the conduit are still under observation. Based on collected samples, histomorphometric analysis will be performed as well as fluorescent staining of neurotrophic, angiogenic, and immunological markers. These analyses will determine the quantity and quality of nerve growth in the epineural sheath conduit.

Conclusions

The use of the epineural tube technique is a feasible method of peripheral large nerve gap repair. This technique does not require lifelong immunosuppression as compared to nerve allografts. Epineural tubes provide a neuropermissive environment for axonal growth. The analysis of histomorphometric measurements and immunological evaluation of nerve samples after epineural tube transplantation are under investigation.

Research Plans for Year 5

During Year 5, the researchers will complete over 20 surgical procedures of epineural conduit transplantation. They will analyze collected nerve samples to evaluate the growth, density, and quality of regenerated neurons. Fluorescent staining of nerve sections will determine the release of nerve growth factors, and proangiogenic and immunological markers. Somatosensory evoked potential analysis will be completed to determine the quality of the conductivity of the conduit. All collected data will be statistically analyzed and compared to the currently used gold standard of autograft.

Planned Clinical Transitions

The clinical transition plan will be initiated after preclinical studies have been completed and data analyzed. The researchers are currently performing human cadaver studies to develop the best method for collecting and preparing the epineural tube. They are taking measurements to determine the size of the epineural tubes, as well as its volume capacity. Final clinical transition is expected in the next 2 years.

Nerve Repair and Regeneration

Peripheral Nerve Repair for Limb and Digit Salvage

Project 4.4.4, WFPC

Team Leader(s): Kacey Marra, PhD (University of Pittsburgh); David Kaplan, PhD (Tufts University); and Tom Smith, PhD (Wake Forest University)

Project Team Member(s): YenChih Lin, PhD, Mostafa Ramadan, MD, Lauren Kokai, PhD, Amir Mahan Ghaznavi, MD, Ryan Nolan, Samantha Beckowski, and Danielle Minteer, BS (University of Pittsburgh); Marie Tupaj, PhD, James White, PhD, and Lee Tien, BS (Tufts University); Jonathan Barnwell, MD, Zhongyu John Li, MD, PhD, Mark Van Dyke, PhD, and Lauren Pace (Wake Forest University)

Collaborator(s): Tirrell Laboratory at University of California, Santa Barbara, Harrison Laboratory at Wake Forest Institute for Regenerative Medicine, University of Virginia Department of Orthopaedic Surgery (Hand Surgery)

Therapy: Combined strategy for regeneration over long (>3 cm in human) peripheral nerve gaps

Deliverable(s): Proactive biodegradable nerve guide system for peripheral nerve regeneration

TRL Progress: 2008, TRL 1; 2009, TRL 2; 2010, TRL 2; 2011, TRL 4; 2012, TRL 4

Key Accomplishments: The researchers completed a study focused on examining the thermal stability and activity of chondroitinase ABC (chABC) released from silk films and lyogels for the reduction of scar tissue proteoglycan formation during nerve regeneration. They found that chABC is compatible with silk material processing, that altering the silk's crystallinity affects the release kinetics, and that incorporating trehalose significantly enhances recovery. They quantitatively characterized the mechanical properties of the silk nerve conduits by determining Young's modulus and ultimate tensile strength. From their measurements, the nerve guides were more elastic than native peripheral nerve in the longitudinal direction. The researchers prepared silk microspheres encapsulating growth factors for controlled release from silk nerve conduits. They improved the gradient design and delivery of neurotrophic factors from the conduits. Finally, the research team completed a nonhuman primate (NHP) study using keratin gel-filled conduits. The data confirmed earlier studies and showed that peripheral nerve regeneration is significantly improved with the addition of keratin over the use of a conduit alone.

Key Words: Limb regeneration, silk fibroin, nerve guides, drug delivery, keratin, functional electrical stimulation

Introduction

Approximately 1.9 million people are living with limb loss in the United States as a result of trauma, cancer, vascular problems, or congenital defects. A copious nerve supply is a key factor in the ability of some amphibians to regenerate appendages following amputation. Peripheral nerve regeneration is a critical issue as 2.8% of trauma patients present with this type of injury. Following trauma, incomplete nerve regeneration and permanent demyelination may lead to lifelong disability. Several regeneration strategies are currently being employed including biophysical guidance, biochemical applications, and protein modification.

The research teams at Tufts University, University of Pittsburgh, and Wake Forest University seek to create a biodegradable nerve guidance system that delivers neurotrophic growth factors (NGF, GDNF, NT-3) and biophysical guidance to regenerating peripheral nerves and (2) move this nerve guidance system to the in vivo level.

During the first 3 years of the project, the researchers developed biodegradable custom-designed nerve guides consisting of collagen, silk, and polycaprolactone (PCL) and demonstrated enhanced nerve repair with the nerve guides in a critical-size rat defect model. They established methods for

incorporating pores, patterned silk films, electrospun silk fibers, neurotrophic growth factors, and electronics into their biodegradable nerve guides. Neurotrophic growth factors were encapsulated in double-walled polymer microspheres for extended, long-term release. The researchers demonstrated that porous silk fibroin-based nerve conduits, infused with bioactive neurotrophic factors in a controlled manner, represent a potential conduit for Schwann cell migration and proliferation during regeneration of peripheral nerves. They achieved promising results with keratin-filled nerve guides in NHPs, which have prompted further evaluations in additional NHPs.

Research Progress – Year 4

Chondroitinase ABC (chABC) Stabilization and Release from Silk

chABC-Silk Encapsulation: Films and lyogels. The enzyme chondroitinase has therapeutic potential to improve the outcome of peripheral nerve regeneration by degrading chondroitin sulfate proteoglycans, which are known to inhibit axon outgrowth during peripheral nerve regeneration. However, the activity of chABC drops dramatically under physiologic conditions, and current use requires bolus delivery every other day for 10–14 days to achieve clinical efficacy. The research team first incorporated chABC into the silk-based nerve guides as a means of increasing their stability and providing sustained localized delivery. The researchers monitored the cumulative effective release of chABC that was incorporated into silk fibroin films and lyogels over a 2-week period. They observed nearly linear release of chABC at 4°C, indicating active enzyme encapsulation. Varying the water annealing time allowed the researchers to alter the crystallinity of the silk films, which provided control over the release kinetics of the enzyme. Total enzyme activity was diminished upon heating to 37°C, with no active chABC released after day 3.

Additives for chABC stabilization. The researchers blended poly(ethylene glycol) (PEG), trehalose, and lipid microtubes with the silk fibroin/chABC mixture to improve the thermal stability of chABC. Trehalose and lipid microtubules have been shown to be effective for the thermal stabilization of chABC. The researchers found that dissolving chABC in 1 M trehalose before dilution into silk solution significantly improved recovery and overall enzyme activity. However, trehalose treatment did not appear to stabilize the enzyme at 37°C beyond day 3. Combinations of trehalose with lipid microtubules led to a small improvement in enzyme efficacy, increasing the active release of the chABC for up to 4 days (**Figure 1**). Current experiments will assess the activity of chABC/antibody complexes released from silk fibroin and study the thermal stability of PEG-chABC conjugates. The researchers aim to achieve both controlled release of chondroitinase from the silk nerve guide and improvement in the thermal stability of the enzyme.

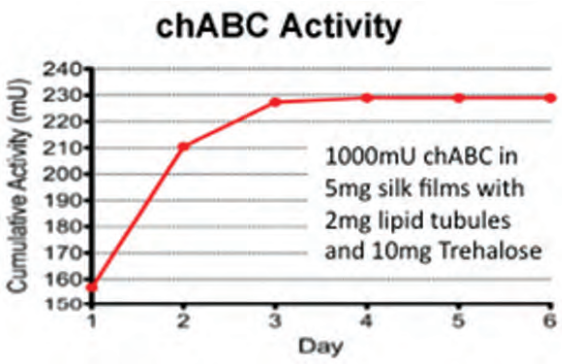

Figure 1. chABC activity for enzyme stabilized in silk fibroin film containing both trehalose and lipid microtubules.

Mechanical Testing of Silk Fibroin Conduits

Nerve guide elasticity. The researchers measured Young's modulus for the patterned silk nerve guides using an Instron materials testing system. They obtained Young's modulus values ranging from 0.058 MPa to 0.243 MPa following 3 days of hydration by varying the porosity of the silk fibroin nerve guide during processing. Young's modulus in the longitudinal direction for peripheral nerves has been reported as approximately 8.5–40 MPa. From their measurements, the research team's nerve guides were more elastic than native peripheral nerve in the longitudinal direction.

Nerve guide strength. The researchers determined that the ultimate tensile strength of the silk fibroin guides was ~0.4–3.15 MPa following 3 days of hydration. Ultimate tensile strength in the nerve guides varied depending on porosity. Maximum

stress on peripheral nerves was reported as 11.7 MPa.

Neuron growth on guides with varying Young's modulus. SH-SY5Y derived neurons were grown onto the guides with varying Young's modulus values and varying porosities. Live-dead staining was conducted to compare cell viability on each of the guides. **Figure 2** shows representative results and indicates that guides with an approximate Young's modulus of ~0.06 MPa afford optimal neuron attachment and growth.

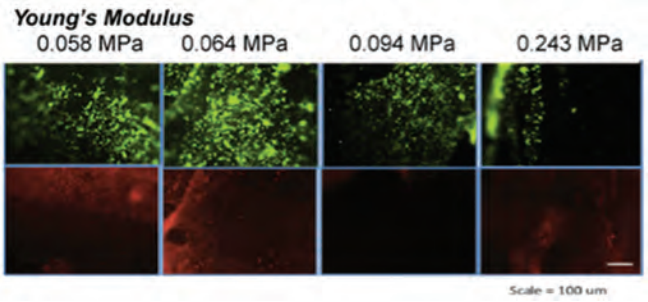

Figure 2. Live-dead staining of SH-SY5Y derived neurons grown on silk fibroin nerve guides with varying Young's modulus ranging from 0.06–0.24 MPa. Optimal cell viability was observed for cells grown on guides of lower stiffness.

Growth Factor Gradient Concentration Studies

Growth factor gradient formation. To study growth factor release, the researchers generated silk microspheres encapsulating NGF. ELISA showed ~90% incorporation of positively charged NGF into the anionic silk biopolymer spheres. Controlled release of NGF from sectioned guides indicated ~1% growth factor release (picogram level) over a period of 2 weeks. A simple dip-coating procedure was used to establish a gradient of NGF from high to low from the distal to the proximal end, respectively. Following gradient formation, the guides were sectioned and dissolved in hexafluoroisopropanol to release the encapsulated growth factor, and NGF was quantified using ELISA.

The researchers found that the dip-coating procedure was effective at creating a concentration gradient. However, the processing conditions led to detection of only ~25% of the loaded growth factor. As an alternative strategy, the research team developed silk films containing gradients of growth factors. These films could be rolled into a cylinder, inserted into preformed silk fibroin nerve guides, and water-annealed to set the shape. The researchers quantified gradient formation on the films using fluorescently labeled FITC-poly(lysine) as a model growth factor. The films displayed gradients similar to those obtained for the dip-coating procedure. Importantly, the film method did not expose encapsulated growth factors to methanol during guide fabrication and allow for other biophysical strategies of improving peripheral nerve regeneration, including patterning and electrode incorporation to be tested in in vivo studies.

Polymer-based tubes containing GDNF. The University of Pittsburgh group received IACUC approval to utilize a NHP model for peripheral nerve repair and began negotiations with both a drug company and a biomaterials company to manufacture GMP guides for clinical trials. The researchers are conducting a NHP median nerve defect study to further investigate the hypothesis that the PCL conduit containing GDNF embedded in double-walled microspheres will improve the functional recovery of critical-size peripheral nerve deficits compared to nerve autografts. They operated on the first two NHPs, which were treated with two different technologies: (a) autograft and (b) clinical control (decellularized nerve allograft) in a 5 cm median nerve gap.

The researchers are conducting functional testing on animals 14 days following surgery. All functional testing is completely noninvasive, harmless, and does not limit motion for the animal. As shown in **Figure 3**, prior to surgery the NHPs were extensively trained by Marra laboratory members to pick up treats in the right hand (the arm to be operated on) from Klüver Board using only their finger and thumb, which are directly affected by a median nerve injury. The researchers measured each NHP's ability to retrieve food pellets from the Klüver Board at least 50 times (**Figure 4**).

Keratin Gel-Filled Nerve Guide Study

The Smith group completed the initial NHP nerve gap repair study, which was initiated in 2010. Ten female macaque monkeys underwent a median nerve injury with a 1 cm gap. This gap was repaired using a commercially available nerve guide,

Neuragen®, with either a human hair keratin hydrogel matrix filler or a physiological saline filler, the clinical standard. Functional and histological assessments of recovery in the monkeys were made for 1 year post repair. The keratin hydrogel accelerated functional and histologic recovery from the critical-size nerve injury. Final histologic and statistical analyses are being completed for manuscript submission. These data were submitted to the FDA to obtain approval for a funded clinical study. The pre-Investigational New Drug (IND) data package was well received, and a clear path to the full IND application was outlined at a subsequent pre-IND meeting with the FDA. Additional preclinical testing will be required before the IND can be filed, and funding to support these studies has been requested from multiple sources including AFIRM.

Figure 3. Functional behavior test. That test involved the training of a monkey to pick up 5 mm diameter 50 mg, roughly spherical food pellets from small wells on a modified Klüver Board.

Conclusions

Overall, these three teams of researchers are demonstrating that novel, porous silk fibroin-based nerve conduits, infused with growth factors in a controlled manner, represent a potential conduit for Schwann cell migration and proliferation in the regeneration of peripheral nerves.

Research Plans for Year 5

The three research teams will begin integrating electrode, drug delivery, and chemical coupling techniques with natural biodegradable polymer nerve guides and testing them in the NHP model. Studies will be carried out with natural biodegradable polymer nerve guides in vitro. In the NHP model, implantations modified by porosity, multiple growth factors, and biophysical stimulation will continue with the next-generation biodegradable polymer nerve guides.

Planned Clinical Transitions

All three research teams have begun planning a pathway to clinical studies. At the University of Pittsburgh, Dr. Marra has met with members of the Clinical Translation Science Institute twice to begin the process of transitioning from preclinical to clinical studies and has had numerous discussions with members of the FDA, as has the Wake Forest University group. After completion of the NHP model, Dr. Marra will be able to conduct a Phase 1 clinical trial. The Wake Forest University group's multicenter clinical trial will begin as soon as IRB approval is received. Funding has been requested to fulfill keratin fate and distribution studies and studies to verify the GMP standards of the keratin hydrogel requested by the FDA.

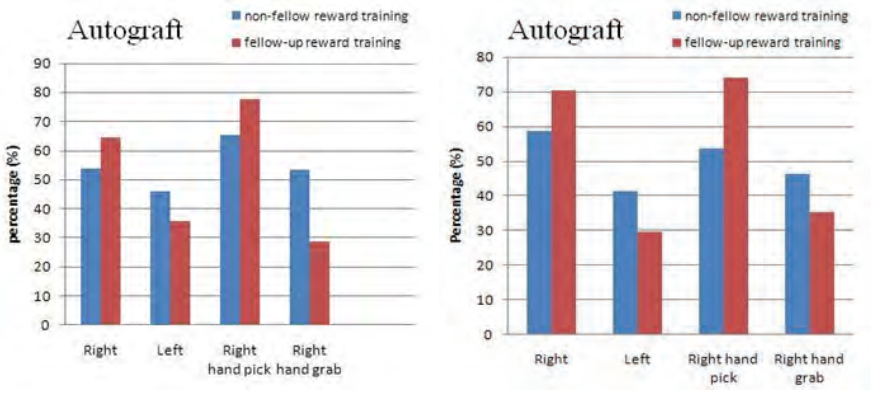

Figure 4. Baseline measurement of functional behavior test. NHP performances improved continuously with practice. After 30 days of limited daily practice (30 pellet retrievals/day), NHPs successfully retrieved and carried these small round pellets to the mouth by right hand at an average rate of 70%–78% retrieval.

Corrections/ Changes Planned for Next Year and Rationale for Changes

Important changes include the removal of the rabbit tibial nerve defect model and the rapid progression into the NHP median nerve defect model. These will permit earlier clinical translation.

Nerve Repair and Regeneration

Modular, Switchable, Synthetic Extracellular Matrices for Regenerative Medicine

Project 4.4.5, WFPC

Team Leader(s): Matthew Tirrell, PhD (UC Berkeley, University of Chicago)

Project Team Member(s): Katie Megley, BS and Won H. Suh, MS/PhD (UC Berkeley); Brian Lin, MS, Dan Krogstad, BS (UCSB), Nickesh Viswanathan, BS and Seema Desai (UC Berkeley)

Collaborator(s): Kacey Marra (UPMC)

Therapy: Injectable synthetic extracellular matrices for regenerative medicine

Deliverable(s): Peptide-based injectable, biocompatible, pH-responsive hydrogel system

TRL Progress: 2008, TRL 1; 2009, TRL 1; 2010, TRL 2; 2011, TRL 2; 2012, TRL 2

Key Accomplishments: The researchers have developed a peptide-based hydrogel system as an injectable extracellular matrix (ECM) with nanofibrous structures. They can incorporate bioactive peptide sequences and/or growth factors into the hydrogels. The 3D matrix system also allows for mammalian cell growth. The researchers measured the modulus of their hydrogels various pHs and concentrations using rheology. They studied cell morphology and proliferation on hydrogels of various moduli. They also imaged the hydrogel pore structure using scanning electron microscopy. They developed a 3D migration assay using commercial microchannel technology and studied migration as a function of hydrogel stiffness.

Key Words: Synthetic extracellular matrix, peptide amphiphile, nerve regeneration, tissue engineering, micelles, vesicles

Introduction

In this project, the researchers are developing synthetic 3D ECMs that are gel-like and designed to aid in the regenerative processes of peripheral nerve regrowth following traumatic injury. Using the Tirrell laboratory's platform material, peptide amphiphiles (PAs)—short peptides attached to fatty acid tails—are designed to self-assemble in solution into extended wormlike micelles. These micelles then entangle at a high concentration to form a fibrous hydrogel, which can be tuned to reflect the stiffness of the native tissue of interest.

During the first 3 years of this project, the researchers synthesized double-tailed PAs with controlled bioactive components and found that double-tailed PAs that incorporate arginine-glycine-aspartic acid units promote attachment, proliferation, and differentiation of human neural stem cells (hNSC). They also developed an alanine-rich peptide head group containing PAs that can have modulated physicochemical and biological properties based on electrostatics control, shear force modulation, and compositional changes. Additionally, they developed a biocompatible and pH-responsive PA hydrogel system that incorporates histidine and serine amino acid units in the head group.

Research Progress – Year 4

At the end of Year 3, the researchers redesigned their PA system with new branched head group peptide architecture. This new PA, termed "C16GSH," included a histidine arm, a glycine spacer, and a serine arm, all attached to a 16 carbon fatty acid tail (**Figure 1**). With this design, the group applied a new mode of peptide head group stabilization by controlling hydrogen bonding between imidazole groups on the histidine residues and primary alcohol side residues on the serines after self-assembly through the modulation of pH. Below pH 6, histidines are predominately acidic and form weak hydrogen bonds with serines as proton donors. Above pH 6.5, histidines are mostly basic and form strong hydrogen bonds as

proton acceptors. As a result, the PAs form weak fibers at low pH and strong fibers above pH 6.5. Weak fibers in solution resemble a low viscosity liquid and strong fibers form self-supporting hydrogels. Additionally, the researchers found that the C16GSH hydrogel system was biocompatible with NIH 3T3 cell line, supporting proliferation and growth.

The Tirrell group used rheology in Year 4 to study the mechanical properties of its C16GSH hydrogel system as affected by PA concentration and pH. The researchers loaded gel solutions onto the instrument at pH 4 and measured storage modulus (**Figure 2A**, Open Squares). They subsequently increased the pH by adding concentrated drops of base to the perimeter of the sample and measured the modulus again (Figure 2A, Closed Squares). The modulus was found to scale with PA concentration in the raised pH sample set. A stiff gel of 10 kPa (G′) is achieved at 1% by weight (10 mg/mL) of PAs. This corresponds to the stiffness of muscle tissue of the body. The increase in stiffness was found to be caused by an increase in fiber density that results from greater PA concentration; this can be observed in the scanning electron microscope (SEM) images (Figure 2B and 2C).

Moving toward the application of nerve regeneration, the Tirrell group studied the effect of gel modulus on in vitro cell behavior using Schwann cells. Schwann cells were sensitive to the stiffness of the material and spread most on the softest gel (G′=0.92 kPa) tested (**Figure 3**). Cell proliferation was measured after culture for 48 hours, and commercially available collagen gel and tissue culture plastic (TCP) were used as controls. After 48 hours, cell proliferation on the 0.92 kPa gel was statistically similar to that of TCP. Stiffer gels showed less proliferation but were statistically similar to the commercially available collagen gel (**Figure 4**).

To better mimic the cellular environment during the repair of peripheral nerve, the Tirrell group designed a 3D microchannel experiment in

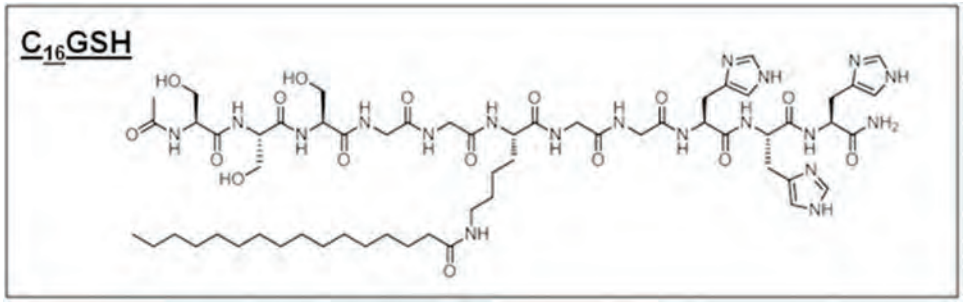

Figure 1. PAs were synthesized in a branched architecture with serine and histidine peptides conjugated to a fatty acid through a lysine residue, "C16GSH" (S3G2KC16G2H3).

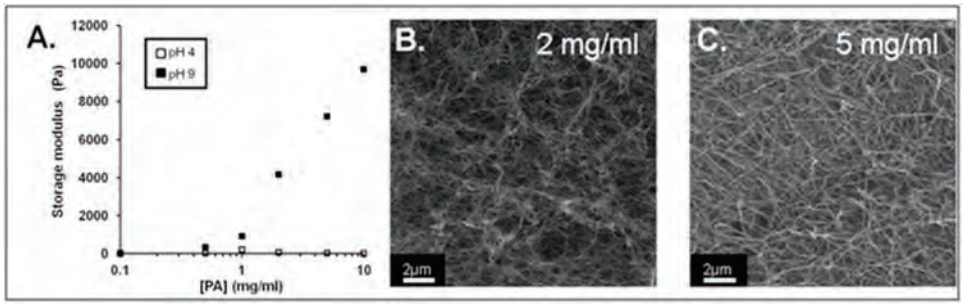

Figure 2. C16GSH hydrogels stiffened when the pH was raised. (A) At pH 4, the samples were viscoelastic liquids over the range of concentrations studied. At pH 9, the modulus increased with increasing concentration. (B–C) Representative SEM images of C16GSH depicting the increase in fiber density with increased PA concentration.

which the migration of Schwann cells were measured across the C16GSH hydrogels. Briefly, the researchers used passive pumping microchannel arrays developed by Bell Brooks Labs. C16GSH solution at low pH was added to the inlet port and allowed to wick across the channel (1 mm width x 0.14 mm height x 5 mm length). Next, basic solution was added to crosslink the matrix. A phosphate-buffered saline wash was used to bring the pH back down to 7.4. Finally, a suspension of Schwann cells in media was added to the outlet port and allowed to migrate through the 3D C16GSH hydrogel for 5 days.

Figure 5 shows a representative image from a longitudinal slice where cells have migrated from the inlet port (white arc) along the channel through a 1 mg/mL C16GSH hydrogel. The researchers used a range of gel concentrations, and they counted the number of cells that migrated into the channel for each gel concentration using ImageJ software. They found that the maximum number of cells that migrated into the channel occurred in 0.5 mg/mL gels.

Conclusions

This research shows that C16GSH hydrogels span a range of relevant stiffnesses and may be useful in many regenerative medicine applications due to their fibrous, ECM mimicking structure. The concentration of the C16GSH hydrogels, which is directly linked to stiffness, can be tuned to promote the spreading, proliferation, and migration of Schwann cells.

Research Plans for the Next Year

The researchers will choose the concentration of C16GSH hydrogel that performs best in their in vitro models and will use that concentration in in vivo studies.

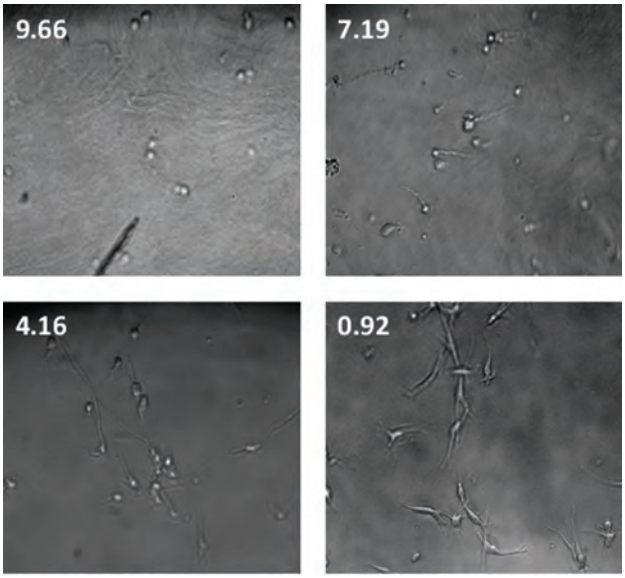

Figure 3. Cell spreading after 18 hours on C16GSH gels, images taken at 20X magnification.

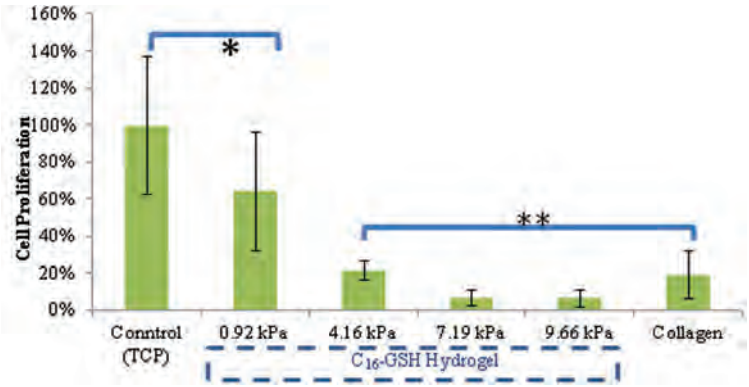

Figure 4. Cell proliferation measured after 48 hours using Alamar Blue viability assay. *0.92 kPa and control are not statistically different, Tukey Test ($p<.05$), **no statistical difference, Tukey Test ($p<.05$).

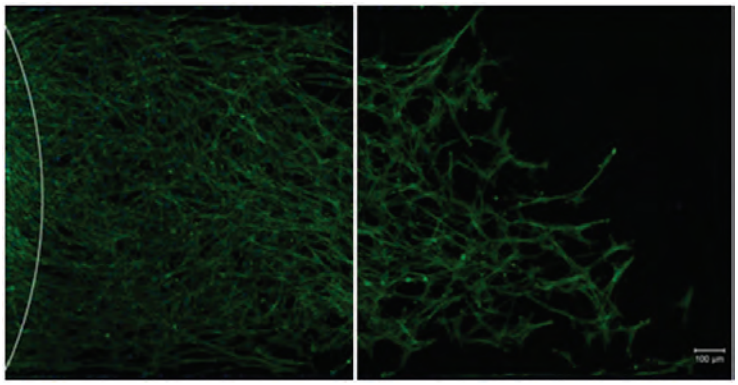

Figure 5. Migration through channels loaded with 1 mg/mL C16GSH. White arcs show outline of port where cells were added. Cells were stained with Hoescht (blue) and phalloidin (green).

Composite Tissue Injury Repair

Spatial and Temporal Control of Vascularization and Innervation of Composite Tissue Grafts

Project 4.4.3, WFPC

Team Leader(s): Robert Guldberg, PhD (Georgia Institute of Technology)

Project Team Member(s): Barbara Boyan, PhD, Ravi Bellamkonda, PhD, Isaac Clements, Yash Kolambkar, PhD, Angela Lin, Brent Uhrig and Nick Willett, PhD (Georgia Institute of Technology); Natalia Landazura, PhD and Robert Taylor, MD, PhD (Emory University)

Collaborator(s): Dietmar Hutmacher, PhD (Queensland University of Technology); Andres Garcia, PhD (Georgia Institute of Technology); David Kaplan, PhD (Tufts University); Benjamin Harrison, PhD (Wake Forest Institute for Regenerative Medicine); Shawn Gilbert, PhD (University of Alabama-Birmingham); Thomas Clemens, PhD (Johns Hopkins University); George Muschler, PhD (Cleveland Clinic); and Josh Wenke, PhD (USAISR)

Therapy: Functional limb regeneration following severe combined bone, nerve, and vascular injuries

Deliverable(s): (1) Develop composite injury animal models that simulate complex military wounds
(2) Establish and test spatiotemporal delivery strategies for regeneration of bone, nerve, and vascularity

TRL Progress: 2008, TRL 1; 2010, TRL 2; 2011, TRL 3; 2012, TRL 3

Key Accomplishments: The Georgia Tech team has established composite injury models in the rat that simulate bone/nerve, bone/vascular injuries, and bone/muscle injuries. These models have been used to test nanofiber biomaterials delivery systems (patents pending) that provide spatial and temporal cues to guide improved bone, vascular, and nerve regeneration. During the past year, the researchers established critical dose response relationships and direct clinical comparisons. They initiated a large animal (sheep) study with leveraged funding. The small animal models and imaging methods at Georgia Tech are also being used to assess strategies developed at other AFIRM laboratories.

Key Words: Bone, nerve, vascularization, composite injury, animal model

Introduction

Traumatic injury to the extremities in combat is a significant problem for reconstruction and restoration of function. Complicated fractures and fragmented bone can cause loss of limb function even if the limb is restored esthetically. One reason for this is traumatic injury to the nerve, with resulting loss of the musculature or bone tissue. Another reason is the lack of adequate vasculature needed to supply nutrients and connective tissue progenitor cells. There is a clear need for regenerative technologies that enable the restoration of limb function following composite tissue trauma. However, current preclinical testing models generally involve injury to only a single tissue type.

To address this limitation, a primary objective of this project was to establish animal models of composite tissue trauma that combine a massive segmental bone defect with peripheral nerve resection and/or femoral artery ligation. Importantly, quantitative evaluation methods such as 3D microCT imaging, electrophysiology, biomechanics, and gait analysis have been integrated into these models to compare competing regenerative strategies. The studies were conducted using the rat since it is amenable to highly quantitative assessment methods (e.g., microCT assessment of vascularization and bone formation). The researchers are using their models to quantitatively evaluate spatial and temporal delivery of biological cues that direct nerve, vascular, and bone growth in a synchronized

manner. These quantitative evaluation models are being used to test regenerative technologies developed at Georgia Tech and in several other AFIRM laboratories.

The specific aims of this project are to (1) develop composite injury rodent models of severe limb trauma and (2) quantitatively evaluate strategies for delivering spatial and temporal information to direct segmental bone regeneration, peripheral nerve repair, and vascular regrowth. During the first 3 years, the researchers established composite injury models in the rat that simulate bone/nerve, bone/vascular, and bone/muscle injuries. They have used these models to test nanofiber biomaterial delivery systems (patents pending) that provide spatial and temporal cues to guide improved bone and nerve regeneration. Notably, the researchers' rat segmental bone defect model has been adopted and used by other AFIRM investigators.

Research Progress – Year 4

Over the past year, the Guldberg team has made significant progress in developing models of composite limb injury and hybrid construct bone repair technology. The researchers published five papers on the development of the hybrid nanofiber mesh/hydrogel construct to restore function to large segmental bone defects. In these studies, the researchers defined in vitro and in vivo release kinetics, minimum effective dose, and degradation characteristics. They also determined effectiveness relative to the current clinical standard and attained the ability to overcome concomitant soft tissue injury and mechanical instability.

The researchers have completed additional studies on the effects of varying the hydrogel composition, volume, and degradation characteristics. They previously demonstrated that macro perforations around the periphery of the nanofiber meshes accelerated bone regeneration. Subsequently, they investigated the effects of macro-perforation size on vascular ingrowth and bone formation. All three sizes they tested accelerated bone healing equally well.

In March 2012, Dr. Guldberg travelled to Australia to initiate a large animal study in sheep. As part of this effort, Pfizer provided a gift of recombinant BMP-2, and FMC Biopolymer manufactured the alginate hydrogel. Before they started the sheep study, the research team verified in a rat model that the commercially produced hydrogel was functionally equivalent to the laboratory-produced hydrogel and assessed the potency of the Pfizer recombinant BMP-2 in the rat segmental defect model using an in vitro alkaline phosphatase assay (**Figure 1**). Because Pfizer uses a different reconstitution buffer than the research laboratory, the researchers tested that buffer as well. The results demonstrated a significant effect of reconstitution buffer and a small but significant reduction in Pfizer BMP potency. Accordingly, the researchers decided to use the HCl reconstitution buffer and a 25% increase in Pfizer BMP-2 dose for the sheep study.

Three composite injury models have now been fully established: bone defect/ischemia, bone defect/nerve defect, and bone defect/muscle defect. The bone/vascular composite injury studies revealed an unexpected and interesting outcome in that transient limb ischemia was found to accelerate BMP-2 mediated large bone defect regeneration. The researchers therefore repeated this study over the past 12 months and verified this intriguing

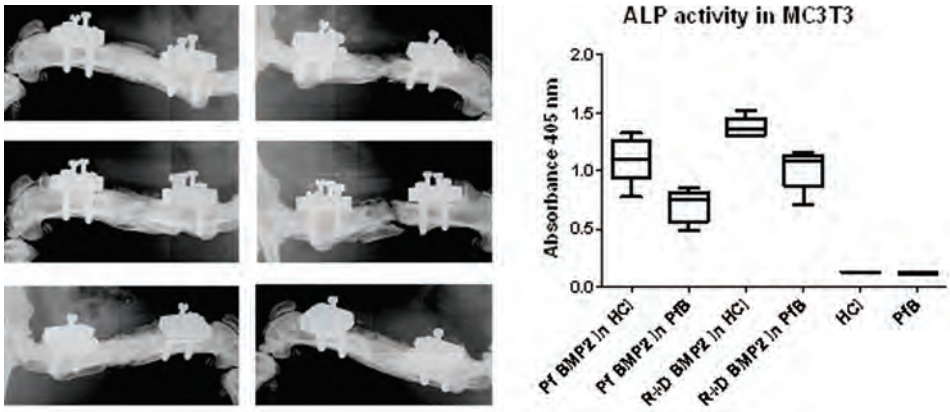

Figure 1. In vivo comparison of recombinant human BMP-2 source delivered using the hybrid nanofiber mesh/alginate BMP delivery system (left). Alkaline phosphatase in vitro assay showing supporting results.

result. They also initiated short-term endpoint (3, 7, and 14 day) studies to assess the mechanism of this stimulatory effect. These studies are specifically evaluating whether transient limb ischemia accelerates early invasion of blood vessels or progenitor cells expressing osteogenic genes within the bone defect. The research team also developed a method for assessing the spatial distribution of vascular ingrowth into muscle and bone and used this method to demonstrate a gradient reduction in vascular ingrowth from the proximal to the distal end of limb injuries.

The researchers' composite bone/nerve injury model has been established and study completed showing increased functional deficit associated with the composite injury. This study has now been accepted for publication. The researchers' composite bone/muscle injury model has been established and the study, completed with leveraged funds, shows that massive muscle loss significantly impairs BMP-mediated bone repair. Two manuscripts are in preparation. Also, the researchers have published a collaborative study with David Kaplan of Tufts University that involved testing of his silk-based hydrogels for delivery of BMP in the standardized 8 mm bone defect model.

The researchers have filed patents for their contact nerve guidance scaffold and their nanofiber mesh/hydrogel spatiotemporal growth factor delivery system.

Conclusions

The research team has established promising, patent-pending, regenerative strategies for bone and nerve using nanofiber mesh spatial guidance and sustained delivery of clinically approved BMP-2. Composite multitissue injury models have been developed to simulate complex combat injuries and test spatial and temporal guidance strategies that take advantage of synergistic interactions among the tissues observed during development and repair. Variations of the composite injury model included bone/nerve, bone/vascular, and bone/muscle injuries. These models are available for testing regenerative strategies developed by other AFIRM investigators.

Research Plans for Year 5

The researchers plan to complete the testing of their nanofiber mesh/hydrogel BMP delivery technology in sheep. This work is being funded by the Australian Research Council and is being conducted at Queensland University of Technology. Once the patent has been issued and the sheep study is completed, companies will be approached to license the technology. Companies with potential interest in this technology include: Pfizer; Medtronic-Sofamor Danek; MiMedx; Zimmer; Smith & Nephew; Stryker; and Synthes. The researchers will also complete optimization studies of hydrogel composition and degradation characteristics. Having completed development of an improved approach to treating acute segmental bone injuries, they will now turn their attention to overcoming the challenges of treating bone defects that fail to heal, with and without adjacent concomitant soft tissue injury or mechanical instability.

Planned Clinical Transitions

A Material Transfer Agreement with Pfizer to provide BMP for the sheep study has been completed. The addition of the sheep study is a revision to the original plan and improves the chances of successful transition to a human pilot study. The intellectual property will be marketed to members of the Georgia Tech industry partners program. Once proof-of-concept has been demonstrated in the sheep model, the researchers' goal is to initiate a human clinical trial pilot study.

Corrections/Changes Planned in Year 5

Large animal studies have been added to the project plan to accelerate progression toward clinical translation of the spatiotemporal delivery systems.

Epimorphic Regeneration (and associated methods)

Epimorphic, Non-Blastemal Approach to Digit Reconstruction

Project 4.4.1, WFPC

Team Leader(s): Stephen F. Badylak, DVM, PhD, MD (University of Pittsburgh)

Project Team Member(s): Lisa E. Carey, BS, Vineet Agrawal, PhD, Scott A. Johnson, MS, Neill Turner, PhD, Li Zhang, MD, MS, and Janet Reing, MS (McGowan Institute for Regenerative Medicine, University of Pittsburgh)

Collaborator(s): Ron Stewart, PhD and Jamie Thomson, PhD, VMD (University of Wisconsin); Susan Braunhut, PhD (University of Massachusetts, Lowell); David Kaplan, PhD (Tufts University); Eileen Moss, PhD and Muthu Wijesundara, PhD (The University of Texas at Arlington)

Therapy: Treatment of digit loss with epimorphic regeneration strategies

Deliverable(s): 1. A biologic scaffold based strategy for inducing epimorphic regeneration in limb and digit soft tissues. 2. A biomaterial that can facilitate epimorphic regeneration in soft tissues (multiple forms, solid sheet, gel, powder, etc.)

TRL Progress: 2008, TRL 3; 2009, TRL 4; 2010, TRL 5; 2011, TRL 5; 2012, TRL 5

Key Accomplishments: The researchers established a consistent model of digit amputation in the C57Bl/6 mouse (mid P2 amputation). They established a method for recruiting multipotential stem cells to the site of amputation by regional injection. They isolated, sequenced, and synthesized a potent ECM fraction with chemotactic properties for multiple progenitor cells in vitro. They characterized the innate immune response to ECM treatment, in vitro and in vivo. Preliminary results showed that the ECM cultured macrophages took on a predominantly M2 phenotype when cultured in the presence of ECM degradation products. The researchers refined a prototype BIODOME device for controlling the microenvironment of the site of amputation. They also designed a new prototype BIODOME for controlling the microenvironment of a soft tissue injury site in a large animal model.

Key Words: Limb regeneration, extracellular matrix (ECM), epimorphosis, innate immune response, multipotent cell cluster (MCC), M2 Macrophage

Introduction

Improved survival rates for soldiers following severe injury have resulted in an increase in the number of soldiers afflicted with life-altering extremity injuries, including amputations. Conventional treatment methods are inadequate to restore functional tissue in most patients, and it is therefore attractive to investigate unconventional treatment methods. This work investigates regeneration of lost limbs/digits following acute trauma via a non-blastemal epimorphic regeneration approach. Certain non-mammalian species, such as the amphibian urodele, are capable of full regeneration of limbs through accumulation of pre-programmed stem cells at the site of amputation, forming a blastema. In adult mammals, the liver, skin, bone marrow, and intestinal lining of epithelial cells are examples of tissues that exhibit non-blastemal epimorphic regeneration. However, virtually every other mammalian tissue does not have this capacity for wound healing. In this project, the researchers are focused on inducing this non-blastemal regenerative capacity in alternative tissues. The signals to facilitate non-blastemal regeneration reside within the ECM. Developing therapeutic strategies that can take advantage of this matrix-based approach is the fundamental objective of the present work.

During the first 3 years of the project, the researchers demonstrated in a mouse model of mid-second phalanx digit amputation (**Figure 1**) that treatment with bioactive molecules derived from ECM can recruit endogenous multipotent stem cells to the

site of injury. These multipotent cells have the ability to differentiate into tissues from all three germ layers (i.e., ectoderm, mesoderm, and endoderm) and cause a significant shift in the wound-healing potential of mammals. The researchers also partially characterized the source of the previously identified Sox2 cells recruited to the site of digit amputation following ECM administration, and they characterized one of two isolated fractions of bioactive ECM molecules that can also recruit multipotent Sox2+, Sca1+, and Lin cells to a site of amputation. Finally, they demonstrated that treatment with bioactive ECM molecules resulted in functional tissue formation, such as bone, at the site of amputation.

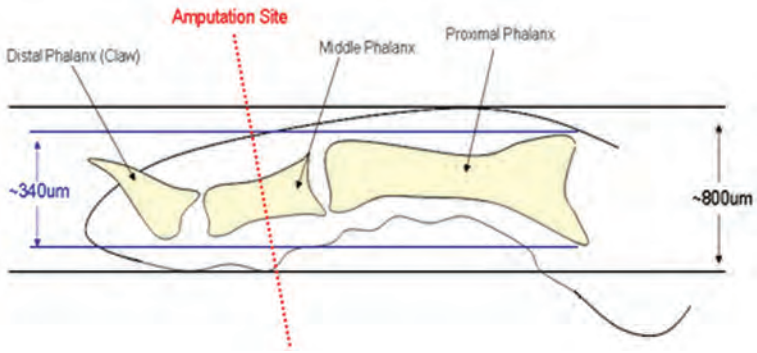

Figure 1. Site of P2 amputation in mouse model.

Research Progress – Year 4

Specific Aim 1: To identify a refined "genetic signature" for cells that participate in the formation of a blastema-like structure, as opposed to the gene expression profile of cells that participate in default wound healing and scar tissue formation.

Work from the Thomson laboratory (publication pending) has identified through deep RNA sequencing specific transcription factors, oncogenes, and blastemal genes that peak throughout the healing and regeneration of the salamander limb. These newly identified genes are distinct from those that are up-regulated in response to mouse digit amputation without treatment. This work helps identify the unique genetic signature of blastema formation as well as the local cues that may be targeted to generate a similar response in mammals. There is a manuscript in preparation that compares the genetic profile of regenerating newts and nonregenerating mice as part of this collaboration.

Specific Aim 2: To identify in vitro bioactive molecules that can instruct, facilitate, or promote the formation of a blastema-like structure following injury.

Earlier in this project, the Badylak team demonstrated the capability of bioactive matrix peptides to recruit multipotent cells to the site of injury after acute trauma. An additional aspect of evaluating the effect of these therapeutic molecules is to characterize the innate immune response. Recent studies from the Badylak team and other labs have indicated the importance of the innate immune response in tissue remodeling. To investigate the effect that ECM has on the immune system, the Badylak team characterized mouse and human macrophage polarization in vitro. In one study, monocytes harvested from human donors were cultured with different concentrations of decellularized urinary bladder matrix (UBM) that was digested in pepsin. The monocytes were subsequently labeled with immunofluorescent antibodies for markers of proinflammatory macrophages (M1) and regulatory macrophages (M2). The markers were CCR7 and CD206, respectively.

Flow cytometry results demonstrated that at UBM concentrations from 100 to 1,000 µg/mL, monocytes were predominantly polarized to an M2 phenotype, as compared to a pepsin control (**Figure 2**). Mouse macrophages were harvested from bone marrow and cultured with three different types of ECM and stained with F4/80 (a mouse-specific macrophage marker), FIZZ1 (a mouse-specific M2 marker) and iNOS (an M1 marker). Preliminary results show that the ECM-cultured macrophages take on a predominantly M2 phenotype when cultured in the presence of ECM degradation products.

Specific Aim 3: To evaluate potentially therapeutic molecules for digit reconstruction in vivo.

The potential of bioactive molecules to constructively stimulate tissue remodeling in a mouse digit amputation model has been shown in previous work. As a consequence of this evaluation, the

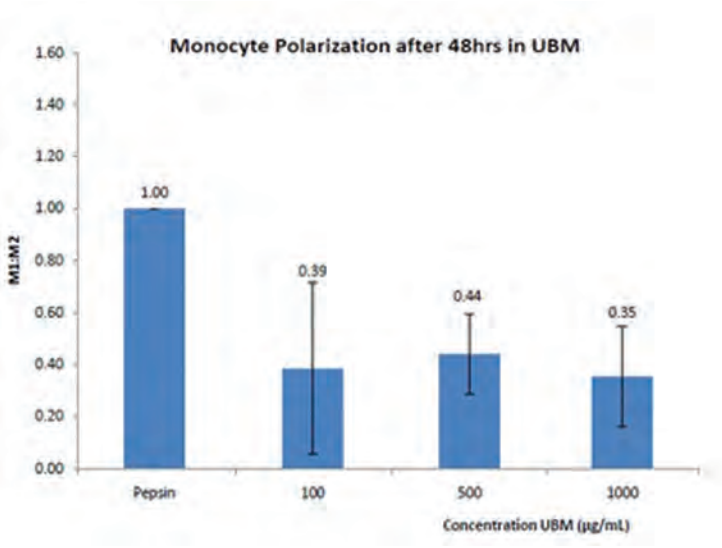

Figure 2. Human monocyte polarization response. M1:M2 ratio greater than 1 is predominantly an M1 response, lower than 1 is a predominantly M2 response.

Badylak team is now developing strategies to characterize changes in the innate immune response to ECM degradation product treatment. Using immunofluorescent staining, results indicated that mice treated with UBM in a digit amputation model showed an increase in M2 phenotype macrophages over time, compared to digit amputation without treatment (**Figure 3**).

Specific Aim 4: To evaluate digit reconstruction in a human pilot study, to be conducted in Years 7–10 of this project, pending funding. A collaboration with the Automation & Robotics Research Institute (ARRI) at the University of Texas Arlington has yielded a novel prototype device designated as the Biomechanical Interface for Optimized Delivery of MEMS Orchestrated Mammalian Epimorphosis (BIODOME), which was developed for an adult mouse model of digit amputation. Development and testing of the BIODOME device continue through small amounts of leveraged funding. The researchers have implemented a number of design improvements in the device, including better flexibility to allow for toe swelling, a smaller profile for greater mouse mobility, and a design that is easier to remove for reuse and better preservation of the healing digit (**Figure 4**).

The researchers are testing the new prototype in the mouse model. The ARRI group is working on concurrent development of a device for a large animal study in canines. Optimization of both mouse and large animal designs is ongoing and will inform future designs for a BIODOME device to control digit reconstruction in a human pilot study. The proposed work will focus on utilization of the findings of aims 1–3 and the mouse and canine BIODOMEs to refine a prototype for a human BIODOME.

Conclusions

The researchers have shown the ability to recruit endogenous multipotent cells to the site of injury in a nonregenerating mammalian system (i.e., a step toward non-blastemal epimorphic regeneration). They are continuing to characterize the proteins and peptides of the ECM that are involved in the recruitment of the MCC to the site of injury. They are also continuing to further define the population of cells involved in the formation of the MCC and to examine the ability of those cells to differentiate into different functional tissues. The ability to specifically direct the differentiation of the MCC into functional tissue is one of the next major hurdles. The researchers believe that control of the "microenvironmental niche" will be required and to that end they have developed a conceptual prototype for a BIODOME device. The device will eventually

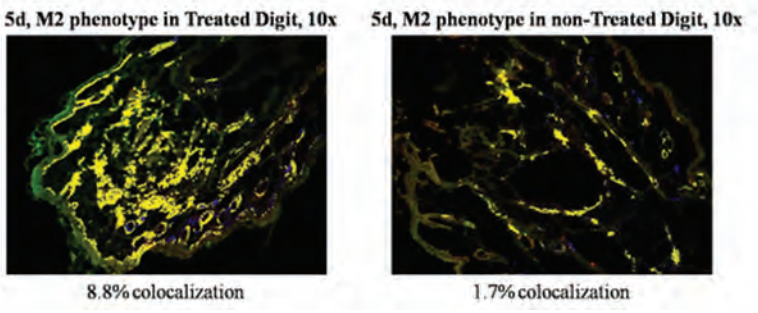

Figure 3. Frozen mouse digit sections immunofluorescently labeled with markers for macrophages (F4/80 in green), M2 phenotype (FIZZ1 in red), and nuclei (DAPI in blue) show a greater M2 macrophage presence at the digit amputation injury site 5 days after treatment (A) compared to 5 days after no treatment (B). Colocalization of F4/80+, FIZZ1+, and DAPI+ cells is indicated in yellow and expressed as a percentage of total pixels.

be used to control microenvironmental conditions including hydration state, pH, oxygen tension, electrical potential, and other factors known to affect stem cell fate.

Research Plans for Year 5

Research in upcoming years will focus on the testing and utilization of the BIODOME functional delivery device, with an objective of eventual use in human trials in specific aim 4. Studies in mice and canines will be ongoing as different bioactive molecules are introduced in a controlled fashion to the injury site microenvironment. Further work will be done to fractionate the ECM into constituent peptides, which will be screened to test their ability to induce or differentiate the MCC.

Planned Clinical Transitions

The Badylak team continues to collaborate with Dr. Peter Rubin at the University of Pittsburgh to evaluate a powder form of ECM for the treatment of distal digit amputations. The product being used is a commercially available FDA-approved form of powdered ECM. The patients who present at the University of Pittsburgh with this particular problem are evaluated, and selected individuals are treated based upon the findings of the work conducted during the past several years of research using the digit amputation model.

In collaboration with ARRI, the researchers are developing the prototype for a canine BIODOME treatment delivery device to be used in a preclinical trial for tissue regeneration using control of the injury microenvironmental niche.

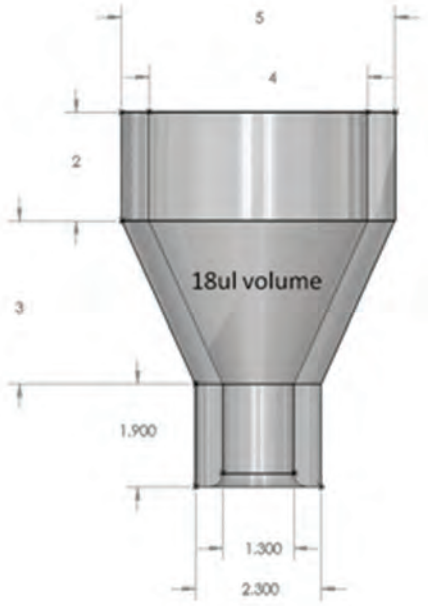

Figure 4. BIODOME prototype schematic, measurements in millimeters.

Clinical Trials

Hand Transplantation for Reconstruction of Disabling Upper Limb Battlefield Trauma – Translational and Clinical Trials

Project 4.4.2, WFPC

Team Leader(s): W.P. Andrew Lee, MD (Johns Hopkins University School of Medicine)

Project Team Member(s): Gerald Brandacher, MD, Damon S. Cooney, MD, PhD, Justin M. Sacks, MD, Stefan Schneeberger, MD, Eric Wimmers, MD and Zuhaib Ibrahim, MD (Johns Hopkins University School of Medicine); Vijay S. Gorantla, MD, PhD and Joseph E. Losee, MD (University of Pittsburgh)

Collaborator(s): None

Therapy: Reconstructive transplantation of upper extremity under a novel bone marrow/stem cell-based immunomodulatory protocol

Deliverable(s): Phase 1 (Translational/Preclinical Trials): Novel immunosuppressive protocol that combines systemic stem cell-based therapy with local immunomodulation in a swine heterotopic hind limb model of composite tissue allotransplantation. Phase 2 (Clinical Trial): Reconstructive transplantation as treatment for hand or forearm loss under a novel cell-based immunomodulatory protocol.

TRL Progress: 2008, TRL 4; 2009, TRL 4; 2010, TRL 5; 2011, TRL 5; 2012, TRL 5

Key Accomplishments: In Phase 1, the research team determined that 60 x 10^6 bone marrow (BM) cells result in significantly higher levels of micro-chimerism. The researchers optimized their novel immunomodulatory protocol using BM infusion in combination with costimulatory blockade (CTLA4/Ig) in a complete MHC mismatched MGH miniature swine model. This novel immunomodulatory protocol resulted in indefinite graft survival in four out of six animals to date. In Phase 2, eight successful hand/forearm transplants have been performed in five patients including the first bilateral and first above elbow arm transplant in the United States. No new transplants have been performed since September 2010. Four out of five patients transplanted to date are maintained on a single immunosuppressive drug at low levels and continue to have increased motor and sensory function of their transplanted hands, which correlates with their level of amputation, time after transplant, and participation in hand therapy.

Key Words: Hand transplantation, immunosuppression, immunomodulation, swine

Introduction

Extremity trauma accounts for the majority of battlefield injuries sustained by troops during Operations Iraqi Freedom and Enduring Freedom. Composite tissue allotransplantation (e.g., hand/face transplants) is an innovative reconstructive modality for such complex injuries. Despite excellent and highly encouraging functional results, composite tissue allotransplantation has not reached widespread clinical use because recipients require lifelong high-dose multidrug immunosuppression to prevent graft rejection. The Lee group aims to minimize and possibly eliminate the requirement for maintenance immunosuppression through targeted immunomodulation.

This project has two phases:

- Phase 1 (Translational Trials): A preclinical model of targeted immunomodulation in heterotopic hind limb transplantation utilizing complete MHC mismatched miniature swine.
- Phase 2 (Human/Clinical Trial): The overall goal is to establish hand transplantation as a treatment strategy for reconstruction of disabling combat injuries involving hand or forearm loss using a novel bone marrow/stem cell-based protocol.

During the first 3 years of the project, the researchers in Phase 1 demonstrated a prolonged allograft

survival using a three-part immunosuppressive regimen: (1) pre-transplant induction with whole-body and thymic irradiation, (2) tacrolimus monotherapy, and (3) donor bone marrow cell infusion. They showed that CTLA4/Ig fusion protein prolonged allograft survival in a swine model. In Phase 2, the research team performed five hand transplants. All five patients who underwent transplants were maintained on a single immunosuppressive drug at low levels, and they had increased motor and sensory function of their transplanted hands.

Research Progress – Year 4

Phase 1

The optimal dose of BM infusion (60 million cells/kg) was applied to subsequent experiments evaluating the addition of CTLA4/Ig fusion protein (20 mg/kg IV on post-operative days 0, 2, 4, and 6) to replace the need for induction treatment with total body and thymic irradiation (XRT). Group 5 (CTLA4/Ig and tacrolimus) animals demonstrated significantly prolonged muscle survival beyond 150 days post transplant; the skin component of the allograft survived past 150 days in three out of five animals (**Table 1**).

Skin and muscle histology in all long-term surviving animals showed no evidence of rejection (**Figure 1**). Two animals in Group 5 had diarrhea and acute weight loss due to parasitic infestation and were euthanized at post-operative day 45. There was no clinical or histologic evidence of rejection at the time of euthanasia. Group 6 (CTLA4/Ig, BM, and tacrolimus) is currently in progress.

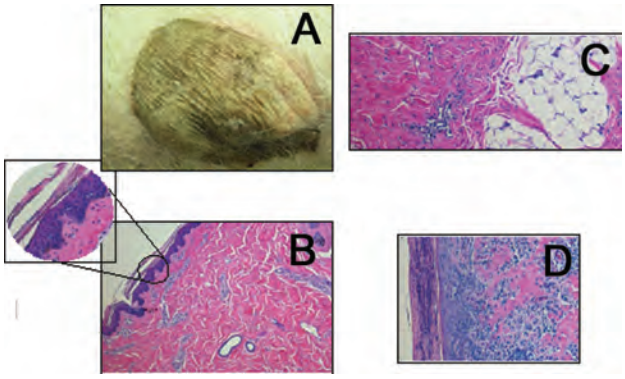

Figure 1. (A) No clinical evidence of rejection at post-operative day 173 in a long-term survivor. (B) Allograft skin biopsy at post-operative day 173 showing intact epithelium (H&E stain). (C) Allograft subcutaneous tissue and muscle biopsy at post-operative day 173 with no evidence of rejection. (D) Skin biopsy from control group showing dermal and intraepithelial lymphocytic infiltrates with epithelial necrosis at early post-operative days.

The combination of CTLA4/Ig and donor BM infusion has provided promising results to date. FK spacing was not necessary since the majority of animals receiving costimulatory blockade had indefinite graft survival with short-term tacrolimus treatment alone. However, some animals still rejected the skin component of the allograft after prolonged rejection-free survival. In the remaining experiments, a local immunomodulatory strategy will be evaluated in combination with BM infusion and costimulatory blockade to achieve indefinite survival without systemic immunosuppression.

Table 1. Rejection-free survival of skin component of composite tissue allotransplantation (*Group 6 is in progress; BM = bone marrow cell infusion at 60 million cells/kg IV on post-operative day 0, CTLA4/Ig given at 20 mg/kg IV on post-operative days 0, 2, 4, and 6).

Group	Immunosuppressive Protocol	Rejection-Free Survival of Skin Component (Days)
1	No treatment	5, 6, 8
2	Tacrolimus (FK) only (30 days)	30, 31, 32
3	XRT + FK (30 days)	35, 37
4	XRT + BM + FK (30 days)	50, 52, 53
5	CTLA4/Ig + FK (30 days)	100, 127, >150, >150, >150
6*	CTLA4/Ig + BM + FK (30 days)	>150, >45

Phase 2

Candidates for hand transplantation continue to be screened and accrued via an approved IRB protocol; however, no new transplants have been performed since September 2010. Four out of the five patients[1] transplanted to date are maintained on a single immunosuppressive drug at low levels and continue to have increased motor and sensory function of their transplanted hands. Patients demonstrated sustained improvements in motor function (range of motion, intrinsic return, grip, and pinch strength) and sensory return correlating with the time after transplantation, level of amputation and participation in hand therapy. Four out of five patients have regained function, allowing resumption of independent living, and they have been highly satisfied with their results. Side effects were few and included a transient increase in serum creatinine, hyperglycemia that was managed with oral hypoglycemics, minor wound infection, an episode of hyperuricemia, and bony non-union in two cases. No systemic bacterial or viral infectious complications occurred.

Conclusions

This project features the development of a preclinical heterotopic hind limb transplant model for composite tissue allotransplantation using a novel immunomodulatory protocol. Stable levels of microchimerism were achieved in all groups after bone marrow cell infusion. The addition of costimulatory blockade (CTLA4/Ig) enabled the researchers to optimize induction therapy, further reduce maintenance immunosuppression, and indefinitely prolong graft survival. Such targeted immunomodulatory protocols that combine BM cell-based strategies and biologics might facilitate immune tolerance and eliminate the need for multidrug immunosuppression to maintain graft survival after composite tissue allotransplantation. Such immunomodulatory concepts have been applied in parallel in performing human hand transplantation using a novel BM cell-based strategy that aims to reduce maintenance immunosuppression necessary for successful composite tissue allotransplantation. Five patients have been transplanted and monitored for 19–39 months. The success of this experimental protocol will allow for greater clinical application of hand transplantation for the reconstruction of upper extremity amputations.

Research Plans for Year 5

Based on the data obtained in Years 1–4, CTLA/Ig represents a potential paradigm shift in the immunosuppression protocol in composite tissue allotransplantation. Additional experiments will be performed using donor BM infusion with costimulation blockade in conjunction with topical application of the skin component of the allograft.

Planned Clinical Transitions

The project goal is to promote long-term hand transplant acceptance while minimizing the need for immunosuppressive drug therapy. The large animal protocol will be further augmented with topical application of the skin component of the allograft. Once their regimen has been successfully implemented in the translational large animal model, the researchers will obtain FDA approval to utilize it in their ongoing clinical trial of human upper extremity transplantation. This regimen might enable tolerance induction and widespread clinical application of hand transplantation for the reconstruction of upper extremity amputations.

Corrections/Changes Planned for Year 5

Transition of the team and laboratory from the University of Pittsburgh to Johns Hopkins University School of Medicine delayed the translational trials for a total of 14 months (see detailed explanation outlined in the 2011 AFIRM annual report). Therefore, remaining large animal experiments involving topical application of the skin component will have to be completed during Year 5 prior to the adaption of this regimen to a human clinical trial for hand transplantation.

[1] In addition to the AFIRM, the Orthopedic Extremity Trauma Research Program and the University of Pittsburgh Medical Center provided support for these transplants.

Clinical Trials

Clinical Trial – Safety Assessment of a Novel Scaffold Biomaterial

Project 4.4.1a, RCCC

Team Leader(s): Anthony Windebank, MD and Michael Yaszemski, MD, PhD (Mayo Clinic)

Project Team: Robert Spinner, MD, Huan Wang, MD, PhD, Mahrokh Dadsetan, PhD, Brett Runge, PhD, Andrew Knight, Suzanne Segovis, and Julia Lewis (Mayo Clinic)

Collaborators/Secondary Sites: Ralph Carmichael, JD, Daniel Pollmann, JD, Erengul Carmichael, and Justin Hughes (BonWrx™)

Therapy: Treatment of peripheral nerve injuries

Deliverable(s): Neuralum, a tissue-engineered scaffold suitable to repair nerve defects up to 6 cm

Clinical Trial Title: Safety Assessment of a Novel Scaffold Biomaterial

TRL Progress: 2011, TRL 4; 2012, TRL 5; Target at end of AFIRM 1, TRL 6

Key Accomplishments: The researchers confirmed the final formulation and sterilization methods for PCLF tubes to be used in the clinical trial. They finalized labeling/packaging materials and product design and submitted an IDE to the FDA.

Key Words: Peripheral nerve, conduit, biodegradable polymer, GMP, FDA, clinical trial

Introduction

Peripheral nerve lesions occur through a variety of injuries including battlefield injuries. The resulting disabilities greatly affect the quality of life and also have a significant socioeconomic impact. With an estimated 300,000 nerve injuries annually, the socioeconomic burden is huge. Nerve injuries occurring in the battlefield often involve loss of entire segments of major nerves spanning 5–20 cm. A limb salvaged without nerve function is useless and, in most cases, painful.

The current clinical standard of care for repairing nerve defects is autologous nerve graft, which has major limitations. Alternatives to nerve autografts are needed. A number of FDA-approved, commercially available nerve tubes can be used to aid repair of nerve defects ranging from 15–30 mm. These tubes have mainly shown effectiveness in repairing sensory nerves in clinical studies. Application of these nerve tubes in repairing motor nerves has been sporadic and inconclusive. The nerve tubes have shown little to no efficacy for the repair of longer defects in either civilian or military applications.

The Mayo group is developing novel biodegradable polymer nerve conduits that are suitable for the repair of nerve defects longer than 3 cm. To this end, the research team has proposed a new balanced risk/benefit parallel process in developing and translating into practice novel materials for nerve repair, using a carefully defined clinical model: sural nerve biopsy that leaves a 6 cm nerve gap. The safety and efficacy of PCLF tubes will be studied in nerve gaps reconstructed with 6 cm PCLF tubes.

Prior to AFIRM Year 4, the researchers had completed IRB and HRPO pre-review of their clinical trial protocol. They converted the clinical protocol, consent form, and other relevant materials from IRBe to PDF files and submitted them to the HRPO for pre-review. They implemented a conflict of interest management plan. They received the approval of their Department of Neurology research committee for the clinical trial protocol. They also initiated GMP scale-up and optimization of sterilization methods of the PCLF tube.

Clinical Trial Status

Product Refinement

PCLF has been reformulated with 1,2 propane as a polymerization initiator. This change eliminates the diethylene glycol end product, which was previously shown to be toxic. The newly formulated PCLF has similar mechanical properties and a comparable capacity to support nerve regrowth as the old PCLF.

Validation of Sterilization

The researchers autoclaved PCLF tubes at 121°C for 20 minutes and 10 minutes of exhaust time. The PCLF tube tolerated the autoclave process and stayed intact with the lumen open and patent. There was only a slight change in mechanical properties of the autoclaved PCLF tubes. However, the autoclaved PCLF did not pass the cytotoxicity test. The score of agar overlay test was 3, indicating moderate cytotoxicity, in which the zone of cell destruction extended 1.0 cm beyond the test sample.

The researchers tried another FDA-approved sterilization method. They sterilized PCLF tubes using ethylene oxide (EO) with a 12-hour cycle and 11-hour purge. They subsequently tested EO-sterilized PCLF materials for cytotoxicity. The scores for agar overlay test and MEM elution test were both 0, indicating no toxicity. Therefore, they will use EO as the sterilization method for the Neuralum PCLF conduits.

Other Accomplishments

The researchers completed design review meetings with members of the research, clinical, and manufacturing communities. They completed the selection of clinical study administrative support staff at Mayo Clinic. They updated the design history file. They completed and reviewed a risk analysis. They finalized labeling/packaging materials and product design. Finally, they submitted an IDE, which is currently under review at the FDA.

Conclusions

Initiation of the clinical trial is pending.

Clinical Plans in Year 5

Once the FDA approves the IDE, the Mayo group will obtain IRB and HRPO approval of the clinical protocol and begin patient enrollment.

Planned Commercialization Transitions

The clinical trial is a Phase 1 safety study. The team has submitted a proposal to study the efficacy of PCLF conduits to reduce neuroma formation after nerve transection injury to the AFIRM Program Management Office and the Office of the Congressionally Directed Medical Research Programs. If funded, the team will conduct a Phase 2 trial. The Mayo group will partner with BonWrx to file a 510(k) and move toward commercialization using the infrastructure and resources of the industrial partner.

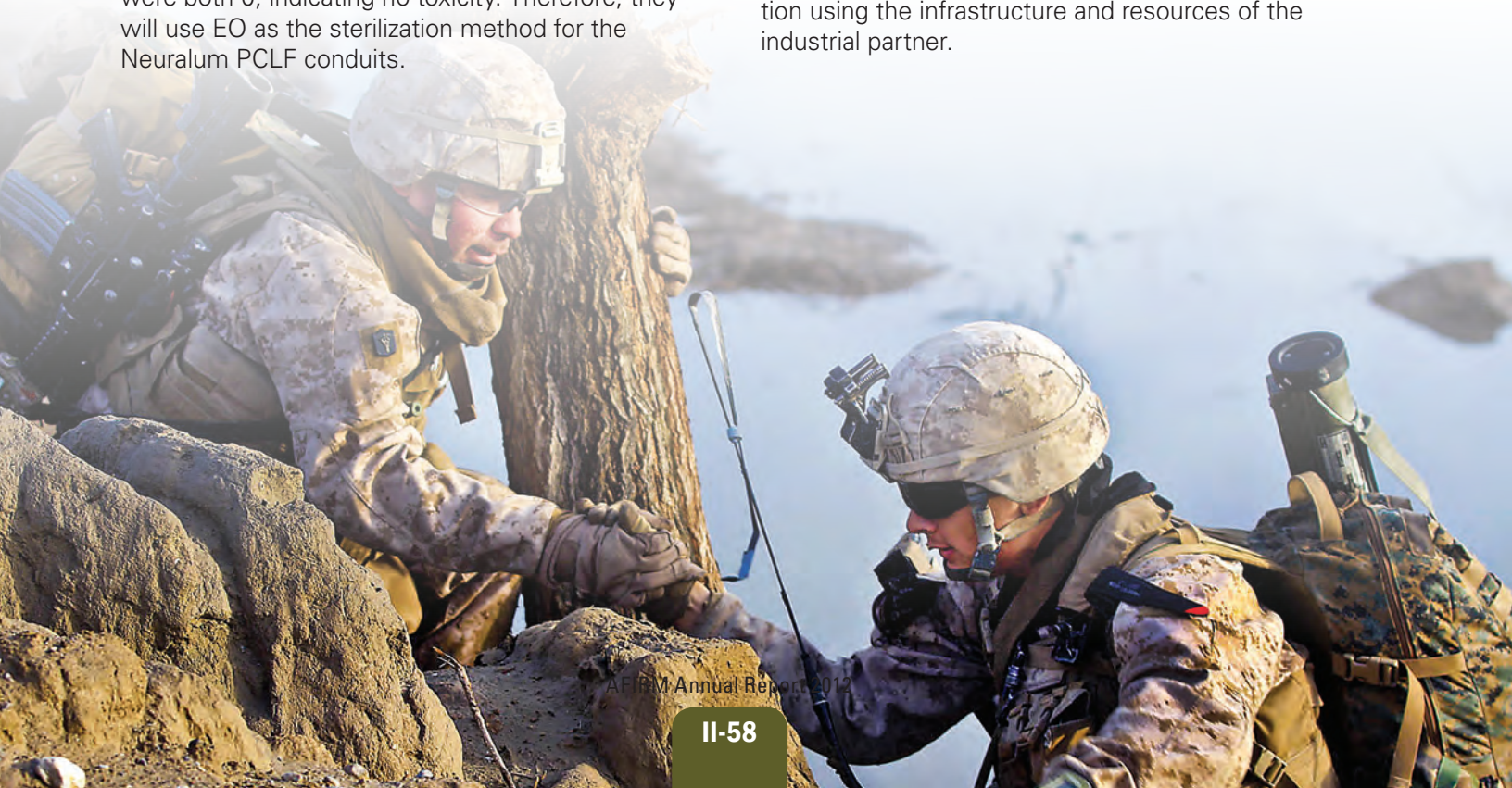

III: Craniofacial Reconstruction

Bone Regeneration

Space Maintenance, Wound Optimization, Osseous Regeneration, and Reconstruction for Craniomaxillofacial Defects

Project 4.1.2, WFPC

Team Leader(s): Antonios G. Mikos, PhD (Rice University); Mark E. Wong, DDS (University of Texas Health Science Center at Houston); and F. Kurtis Kasper, PhD (Rice University)

Project Team Member(s): Allan M. Henslee, BS, Lucas Kinard, BS, James D. Kretlow, MD, PhD, Sarita R. Shah, BS, Patrick Spicer, BS, Limin Wang, PhD (Rice University); and Nagi Demian, DDS, MD and Simon Young, DDS, MD, PhD (University of Texas Health Science Center at Houston)

Collaborator(s): Shanghai 9th People's Hospital, Shanghai, China and Radboud University of Nijmegen Medical Centre, Nijmegen, The Netherlands

Therapy: Staged reconstruction of large osseous defects in the craniofacial region restoring function and esthetics

Deliverable(s): (1) Biocompatible, antibiotic-releasing implants to maintain bony wound spaces; (2) "in vivo bioreactor" that will allow for the generation of vascularized bone; (3) injectable system for delivery of growth factors necessary for bone regeneration and wound healing

TRL Progress: 2008 (Start), TRL 2; 2009, TRL 4; 2010, TRL 4; 2011, TRL 5 ; 2012 (Current), TRL 5

Key Accomplishments: The researchers have completed in vitro studies characterizing the physicochemical properties of their porous poly(methyl methacrylate) (PMMA)-based space maintainers. They have received Institutional Review Board (IRB) approval for a randomized prospective clinical study of porous space maintainers versus the clinical standard in continuity defects resulting from resection of benign pathology. They completed an in vivo study evaluating the efficacy of colistin-releasing PMMA-based space maintainers in mitigating an *Acinetobacter baumannii* infection in an inoculated rabbit composite tissue mandibular defect model. They completed an in vitro study evaluating the controlled release of several antibiotics from polymeric microparticles for inclusion into antibiotic releasing porous PMMA-based space maintainers. The researchers have also completed an in vitro study evaluating the controlled release of a growth factor from an injectable hydrogel for bone augmentation and contouring and initiated an in vivo study of the same hydrogel in a rat cranial augmentation model.

Key Words: Craniofacial bone reconstruction, space maintenance, bone flap, controlled drug delivery, in vivo bioreactor

Introduction

Immediate reconstruction has been shown to produce better functional as well as aesthetic outcomes due to the minimization of wound contracture and maintenance of bone structure; however, immediate reconstruction with grafts or flaps fail up to 54% of the time due to infection.[1] Alloplastic materials have been used during immediate reconstruction, but commonly result in wound dehiscence or infection. Porous materials have been shown to decrease wound dehiscence through increased tissue-material interactions. The researchers of this project are focused on applying materials currently approved for clinical use, such as PMMA in combination with a gel porogen, to produce porous space maintainers for the dual purpose of maintaining the bony defect space without dehiscence and releasing antibiotics in a controlled manner to mitigate wound infection.

The researchers are seeking to apply a technique pioneered in their laboratory.[2] Their overall strategy

[1] Lawson W, et al. *Laryngoscope*. 1982 Jan;92(1):5-10.
[2] Thomson RC, et al. *Biomaterials*. 1999 Nov;20(21):2007-18.

involves the placement of an antibiotic-releasing space maintainer into a bone defect at the time of injury. Simultaneously, a chamber composed of PMMA filled with clinically available bone fillers is placed at an alternative site on the body, generating a vascularized bone flap. After wound healing, the bone flap can be harvested from the chamber and placed into the defect upon removal of the space maintainer.

The purpose of this research is to improve outcomes, decrease the complications and infections, and reduce the number of procedures associated with large bony reconstructions in this particular patient population through three mechanisms: (1) by the initial implantation of a biocompatible, antibiotic-releasing space maintainer within a large osseous defect during the early phases of treatment; (2) through the implantation of an "in vivo bioreactor" construct away from the site of injury that will allow for the generation of a vascularized bone flap, to be used as donor tissue for second-stage reconstructive surgeries; and (3) by augmentation of the implanted vascularized bone flap within the recipient defect site by using an injectable system tailored for both the delivery of growth factors needed to promote bone regeneration and wound healing until sufficient integration of the bone flap has occurred.

During the first 3 years of the project, the researchers fabricated and characterized a variety of porous space maintainer formulations in vitro that represented a range of porosities and mechanical properties. They evaluated the implants for efficacy in maintaining a bony defect space while supporting soft tissue healing in a rabbit mandibular defect model in vivo. Additional in vitro studies revealed that antibiotics could be incorporated into space-maintaining implants and released in a controlled fashion by varying specific properties of the implant (e.g., degree of porosity and pore interconnectivity). Initial results from an ongoing in vivo study in a sheep model suggested the feasibility of the in vivo bioreactor approach for the generation of vascularized autologous bone flaps and the transfer of the flaps to fill mandibular defects.

Research Progress – Year 4

Several important steps were made on the regulatory pathway for clearance of a porous PMMA-based space maintainer product. Toward this end, a study was completed to characterize the physicochemical properties of various formulations of porous PMMA as well as a nonporous PMMA-based bone cement formulation according to American Society for Testing and Materials (ASTM) and International Organization for Standardization (ISO) standards set forth in the U.S. Food and Drug Administration (FDA) Guidance Document for PMMA Bone Cement.[3,4,5] This study found that while mechanical properties stipulated by ISO 5833, specifically the compressive strength and bending modulus and strength, were decreased in porous materials over nonporous materials, the properties maintained are sufficient for their intended use in space maintenance applications. Moreover, the porous materials performed equal to or better than nonporous materials in other tests, such as residual monomer release and setting temperature. The University of Texas Health Science Center at Houston IRB approved a protocol to initiate a randomized, prospective clinical study of the porous PMMA-based space maintainer technology compared to clinical standards evaluating safety and efficacy. The study will commence once the U.S. Army Medical Research and Materiel Command's (USAMRMC's) Human Research Protection Office (HRPO) approves the protocol.

A number of laboratory studies were completed or continued in the past year to investigate and optimize the antibiotic-releasing technologies envisioned for application in the space maintenance approach. First, an in vitro study characterized the activity of the antibiotic colistin upon release from gelatin or poly(lactic-*co*-glycolic acid) (PLGA) microsphere carriers incorporated into porous

[3] ASTM Standard F451, 2008, "Standard Specification for Acrylic Bone Cement," ASTM International: West Conshohocken, Pennsylvania.

[4] ISO 5833, 2002, Implants for surgery – Acrylic resin cements, International Organization for Standardization, Geneva, Switzerland.

[5] Class II Special Controls Guidance Document: Polymethylmethacrylate (PMMA) Bone Cement; Guidance for Industry and FDA. 2002 Jul; Center for Devices and Radiologic Health. FDA. Silver Spring, Maryland.

PMMA-based space maintainers. Specifically, it was found that colistin released from either delivery vehicle (gelatin or PLGA) remained active against the target species *A. baumannii*. An in vivo study was performed to evaluate colistin-releasing porous PMMA space maintainers in a rabbit mandibular composite tissue defect model inoculated with *A. baumannii.* This study evaluated soft tissue healing of the mucosal defect in addition to histological and safety measures, which included analysis of kidney function as reflected by plasma concentration of blood urea nitrogen (BUN) and creatinine. Representative images of healed and nonhealed mucosal defects are shown in **Figure 1**. The formulation that delivered a high dose of antibiotics over an extended period of time resulted in a significantly greater number of healed mucosal defects compared to a high dose delivered with a burst-release profile. Also, cultures of swabs obtained from within and around the defect showed no detectable *A. baumannii* at the end of the study, indicating an eradication of the bacteria from the defect. Nephrotoxicity, a known adverse side effect of systemic use of colistin, was not observed in any group. To expand the applicability of this technology, an in vitro study was completed to characterize the release of several common antibiotics from PLGA-based particulate delivery systems, including vancomycin, clindamycin, cefazolin, ciprofloxacin, doxycycline, and tobramycin. The delivery system was shown to be capable of releasing antibiotics in a sustained manner at levels sufficient to inhibit the growth of target bacteria.

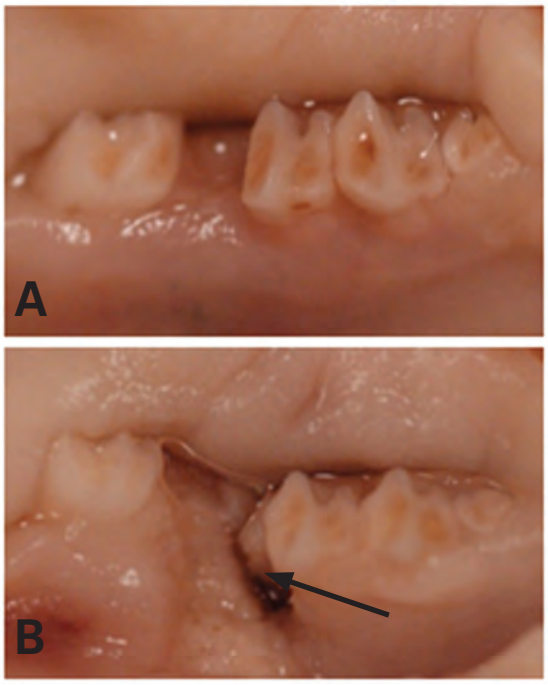

Figure 1. Photographs of (A) healed and (B) nonhealed mucosal defects. Black arrow indicates exposed space maintainer.

Finally, studies regarding degradable materials for bone augmentation were initiated. Specifically, an in vitro study characterizing the release of bone morphogenetic protein-2 (BMP-2) from an injectable degradable hydrogel carrier, oligo(poly(ethylene glycol) fumarate) (OPF) was completed, showing controlled release of BMP-2 from the hydrogel. An in vivo study was initiated evaluating the release of BMP-2 from these OPF hydrogels for bone augmentation in a rat cranial augmentation model.

Conclusions

Considerable progress has been made over the course of the past year toward the clinical translation of porous PMMA-based space maintainers. Additional progress has been made toward the development of antibiotic-releasing implants for bony space maintenance. Specifically, an extended high-dose release of antibiotics led to more soft tissue healing and coverage in an inoculated composite tissue defect model than a burst release of antibiotics. Further, in vitro studies demonstrated that the antibiotic colistin remains active against *A. baumannii* upon release from PMMA-based space maintainers.

Research Plans for Year 5

To expand the potential application of antibiotic-releasing porous space maintainers, several commonly used antibiotics have been incorporated into degradable microsphere carriers for extended release, which will be continued through the application into an infected bone defect in vivo. The researchers will also complete the recently initiated in vivo study involving the controlled delivery of BMP-2 from injectable hydrogels for bone augmentation.

Planned Clinical Transitions

The researchers plan to initiate a randomized, prospective clinical trial upon USAMRMC HRPO approval.

Bone Regeneration

Regeneration of Bone in the Cranio-Mandibulo-Maxillofacial Complex Using Allograft Bone/Polymer Composites (4.5.1a), and Expedited Commercialization of an Injectable Allograft Bone/Polymer Composite for Open Fractures (4.5.7)

Projects 4.5.1a/4.5.7, RCCC

Team Leader(s): Scott A. Guelcher, PhD (Vanderbilt University)

Project Team Member(s): Kasia Zienkiewicz and Anne Talley (Vanderbilt University)

Collaborator(s): Pamela Brown-Baer, DDS, COL Robert Hale, DDS, and Joseph C. Wenke, PhD (USAISR); Kerem Kalpakci, PhD and Susan Drapeau, PhD (Medtronic, Inc.)

Therapy: Bone graft therapy

Deliverable(s): Injectable, settable LV® bone graft (+/-recombinant human bone morphogenetic protein-2 [rhBMP-2])

TRL Progress: 4.5.1a: 2010, TRL 2; 2011, TRL 3; 2012 (Current), TRL 3; 2013 (Target), TRL 4

4.5.7: 2010, TRL 3; 2011, TRL 4; 2012 (Current), TRL 5; 2013 (Target), TRL 6

Key Accomplishments: The researchers made significant progress in animal studies on allograft bone/polymer composites in Year 4. They demonstrated that flowable and moldable LV formulations supported bone remodeling and healing in rabbit femoral plug defect model. They also found that delivery of rhBMP-2 from flowable LV enhanced new bone formation in a rat critical-sized calvarial defect model.

Key Words: Injectable, settable, bone graft, rhBMP-2, rabbit

Introduction

The high incidence of head and neck injuries experienced by soldiers in Operation Iraqi Freedom and Operation Enduring Freedom has resulted in a large patient population that requires improved treatments. The researchers at Vanderbilt University are pursuing two projects in collaboration with USAISR and Medtronic. The first project is the development of injectable, settable LV bone grafts for the repair of metaphyseal bone defects. The second project is the development of injectable, settable LV bone grafts augmented with rhBMP-2 for the regeneration of (a) alveolar bone that supports dentition and (b) load-bearing bone that supports an articulating process.

Proof-of-concept experiments have shown that allograft/polyurethane (PUR) composite grafts regenerate new bone in rat and rabbit femoral plug defects and in rabbit critical-size calvarial defects. Addition of rhBMP-2 as a powder prior to mixing enhances bone healing. There is currently no commercially available injectable load-bearing bone graft for delivery of recombinant growth factors such as rhBMP-2.

LV augmented with growth factors is being developed to meet this compelling clinical need, which presents several advantages: (1) administration using minimally invasive surgical techniques; (2) mechanical strength approximating that of host mandibular bone to provide space maintenance and prevent soft tissue prolapse; and (3) sustained release of rhBMP-2 that is anticipated to lower the required dose. Considering that no product with all these attributes is currently available, LV augmented with growth factors is anticipated to be a

disruptive technology that positively impacts the clinical management of open fractures in the face.

Research Progress – Year 4

Commercialization of Flowable and Moldable LV Bone Grafts

Flowable and moldable LV bone grafts were evaluated in a rabbit femoral condyle plug defect model at 6 and 12 weeks. The flowable formulation initially had allograft bone particles (ABP) 45% by weight (36% by volume) and expanded to ~45% porosity. The moldable formulation had ABP 70% by weight (57% volume) and <10% porosity.

Flowable LV grafts injected into rabbit femoral condyle plug defects supported new bone formation and remodeling at 6 and 12 weeks (funded by Medtronic). Representative microcomputed tomography (microCT) scans and histological sections are presented in **Figures 1** and **2**, respectively. At 6 weeks, bone fill was incomplete and bone marrow was largely cellular. Bone and bone marrow infiltrated the majority of the residual implant material with incorporation of implant material into bone throughout the defect in those sections with complete fill. Predominantly lamellar modeling, with some intramembranous and endochondral, bone formation was ongoing in all sections. Some residual implant material that was not infiltrated with cells was found in the central portion of the defects. A very small amount of organized fibrous tissue was seen within the defects in some sections. Giant cells present were associated with residual implant material and contained some intracellular material. Aggregates of red blood cells (RBC) were seen at the periphery of the residual bulk material located at the central portion of the defects. No acute inflammation was seen in any of the sections.

There was more implant material present and little bone fill at 6 weeks in grafts fabricated from small ABP (< 100 µm), compared to grafts fabricated from large ABP (100–500 µm). Bone formation occurred predominantly at the periphery of the defects while the central portion of the implants was largely acellular. New bone and bone marrow incorporated within the implant was immature. A small amount of lamellar and intramembranous bone formation was occurring. Bone fill was largely incomplete in three of four instances and largely complete in one of the four sections. Bone marrow filling the defect was a combination of fatty and cellular bone marrow. Residual implant material was incorporated throughout the new bone and, like other groups, had less carrier material compared to the 6-week time point. Lamellar bone formation was primarily occurring, but

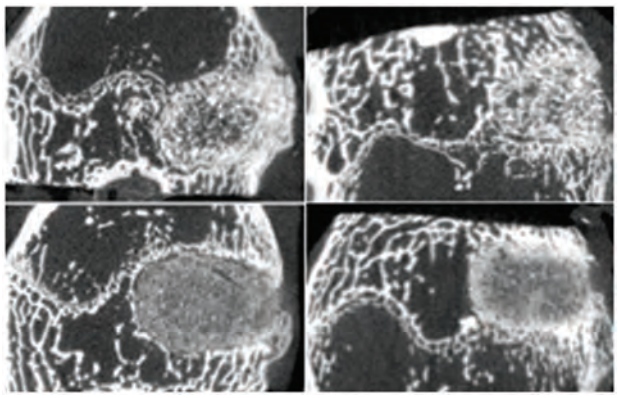

Figure 1. Representative microCT images of LV flowable grafts in rabbit femoral condyle plug defects at 6 weeks. Composites prepared from large ABP (180 µm; top) supported extensive new bone formation while composites prepared from small ABP (<100 µm; bottom) were infiltrated by fewer cells due to the smaller pore size (< 50 µm).

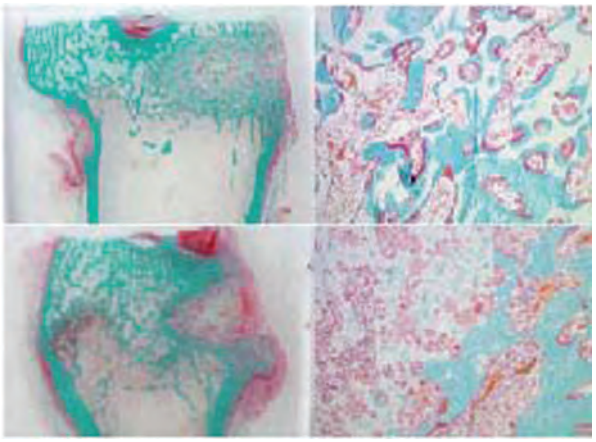

Figure 2. Remodeling of LV flowable grafts in rabbit femoral condyle plug defects at 6 weeks. Grafts with large ABP (top, 1.25X (left) and 20X (right)) supported cellular infiltration (red) and new bone formation (blue) while grafts prepared from <100 µm ABP (bottom) were infiltrated by fewer cells due to the lower pore size (< 50 µm).

some intramembranous bone formation was also ongoing in areas where residual implant material was present. No endochondral bone formation was observed.

A total of 5 kg of current Good Manufacturing Practice (cGMP) material has been manufactured for testing of the injectable bone void filler. The raw materials are stable for 2 years, and the product meets specifications as well as reactivity and applications tests established at Vanderbilt University. These analyses show that the stored material is comparable to historical controls. Thus, the stored cGMP material will proceed to ISO 10993 biocompatibility testing.

Remodeling of Flowable LV Synthetic Grafts Augmented with rhBMP-2 in a Critical-Size Rat Calvarial Defect Model

Flowable and moldable LV grafts incorporating allograft bone particles and augmented with rhBMP-2 enhance new bone formation in a critical-size rabbit calvarial defect model. However, due to the regulatory complexity of product that incorporates both allograft bone and a recombinant human growth factor, work in Year 4 focused on the development of fully synthetic LV grafts. To prepare synthetic biocomposites, the allograft bone component was replaced with beta-tricalcium phosphate (β-TCP). Materials were injected into 8 mm critical-size rat calvarial defects (Dr. Pamela Brown Baer funded and performed the surgeries at USAISR). The outcomes were assessed by radiographs, microCT, and histology at 4 and 8 weeks. As shown in the histological sections in **Figure 3**, LV grafts incorporating β-TCP supported new bone formation as early as 4 weeks in the rat calvarial defect model. Addition of rhBMP-2 increased new bone formation by 30%.

Conclusions

LV grafts remodel when injected into rabbit femoral condyle plug defects. Sterilized cGMP raw materials used to prepare the grafts are stable for up to 2 years. When augmented with recombinant human growth factors, LV grafts enhance new bone formation in a rat calvarial defect model.

Research Plans for Year 5

During the upcoming year, the researchers will perform a pivotal study in sheep, with flowable and moldable LV grafts, to support a 510(k) regulatory filing. They will repeat rat calvarial defect experiments using faster degrading matrices and porogens to accelerate cellular infiltration and new bone formation.

Planned Clinical Transitions

Medtronic will complete cGMP-compliant manufacturing and ISO 10993 biocompatibility testing activities (funded by AFIRM) and pivotal studies in a preclinical model acceptable to the FDA (funded by Medtronic). A 510(k) application will be submitted based on these data.

Corrections/Changes Planned for Year 5

LV augmented with rhBMP-2 successfully healed critical-size calvarial defects in rats. However, new bone formation was somewhat hindered by slow cellular infiltration that resulted from the small size of the β-TCP particles. In Year 5, the researchers will investigate the effects of alternative matrices and porogens.

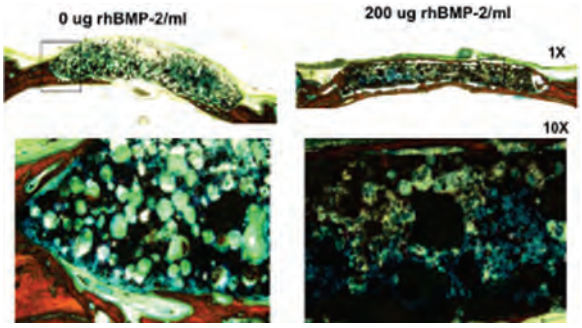

Figure 3. Injectable LV with β-TCP and rhBMP-2 induces new bone formation at 4 weeks in a rat calvarial defect model. Left: With no rhBMP-2, there is new bone formation near the host bone interface (red), as well as cellular infiltration (blue) throughout the defect. Right: With 200 µg rhBMP-2/mL, there is bridging of the upper and lower surfaces with new bone (red), as well as cellular infiltration into the interior of the defect.

Bone Regeneration

Regeneration of Bone in the Cranio-Mandibulo-Maxillofacial Complex

Project 4.5.1b, RCCC

Team Leader(s): Jeffrey Hollinger, DDS, PhD (Carnegie Mellon University [CMU]) and Sonja Lobo, DDS (Rutgers University)

Project Team Member(s): Jinku Kim, PhD, Sean McBride, BS, Pedro Alvarez, BS (CMU); Joachim Kohn, PhD, Pallassana Narayanan, PhD, Hanshella Magno, Ophir Ortiz, PhD, Aniq Darr, PhD, and Das Bolikal, PhD (Rutgers University)

Collaborator(s): Amit Vasanji, PhD, Rick Rozik, Brett Hoover, MBA, MS (ImageIQ) and Pam Brown Baer, PhD (USAISR)

Therapy: Bone regenerative therapies for the cranio-mandibulo-maxillofacial (CMF) complex

Deliverable(s): Tyrosine-derived polycarbonate (TyrPC) scaffolds for bone regeneration, fabricated by salt leaching, and supplemented with either rhBMP-2, other growth peptides, or combinations of the two

TRL Progress: 2010, TRL 3; 2011, TRL 4; 2012 (Current), TRL 4; 2013 (Target), TRL 5

Key Accomplishments: The researchers developed and optimized a fabrication method that incorporates different calcium phosphate (CaP) minerals into TyrPC bone regeneration scaffolds for the rabbit calvaria and radius critical-size defect (CSD) models. They prepared biologically enhanced bone regeneration scaffolds for evaluation in vivo. They completed surgeries and necropsies and performed microCT and histology analyses. Their data suggested that the synthetic TyrPC+CaP scaffolds were biocompatible, biodegradable, and osteoconductive. They demonstrated that TyrPC+CaP bone regeneration scaffolds enhanced with rhBMP-2 significantly promoted new bone formation in the rabbit calvaria CSD model at 16 weeks post implantation.

Key Words: Bone regeneration, cranio-mandibulo-maxillofacial, tyrosine-derived polycarbonates, bone marrow aspirate

Introduction

Current therapies for the reconstruction of massive bone loss in the CMF complex include (1) PMMA, (2) hard tissue replacement (HTR) with poly(ethyl/methyl methacrylate), (3) metallic devices (e.g., titanium), and (4) allogeneic and autologous grafts. Additional clinically available cranioplasty materials are based on calcium-phosphate cement (Norian CRS, HydroSet, BoneSource HAC, BoneSource Classic) or β-TCP (chronOS). All of these current treatment options are inadequate in restoring anatomical form and function in the CMF complex. Autogenous and allogeneic tissues are inadequate in terms of supply and donor site morbidity to treat the unique and massive craniofacial deficits incurred in combat. Currently available synthetic materials do not remodel and integrate with host tissues; can become infected; and may require extensive, multiple revision surgeries. Moreover, PMMA, HTR, and metallic devices lack the capability to deliver antibiotics and growth factors in a controlled manner. Consequently, patients suffer from significant functional tissue deficits that cause both challenges in healing and rehabilitation, as well as psychological distress, including a negative self-image that can make it hard to face the public.

TyrPC plus CaP can serve as a biomaterial platform that may provide a compelling therapeutic solution to regenerate bone. This design will overcome the technical barrier to regenerate osseous-bone form and function in the CMF complex.

The research team began this project by prefabricating tyrosine-based copolymer scaffolds to fit into a rabbit calvarial CSD. Their preliminary results showed that 3D tyrosine-based scaffolds induced significant osteogenic differentiation and

mineralization of preosteoblasts compared to two-dimensional (2D) tissue culture surfaces. Both injectable and implantable compositions based on two types of polyester copolymers were identified for craniofacial applications. During the second year of the project, the researchers demonstrated the in vitro and in vivo biocompatibility of TyrPC and poly(ε-caprolactone fumarate) scaffolds and efficacy of the scaffolds containing rhBMP-2 for bone regeneration using the rabbit CSD calvarial model. During Year 3, the researchers added a CaP surface coating to TyrPC scaffolds with the goal of increasing bone formation. They found that the addition of rhBMP-2 to the TyrPC+CaP scaffolds led to substantially increased bone formation in a rabbit CSD calvarial model in 6 weeks.

Research Progress – Year 4

Scaffold Fabrication

Scaffolds were provided to CMU and USAISR for four different animal studies aimed at evaluating the safety and efficacy of biologically enhanced TyrPC bone regeneration scaffolds in the rabbit calvarial CSD model. These studies evaluated the effect of different CaP mineral compositions and doses of rhBMP-2 on the enhancement of bone regeneration.

In Year 4, the Rutgers team also performed several tasks aimed at better defining the scaffold manufacturing process. In particular, the effect of each step of the fabrication process on the polymer's molecular weight was characterized so that appropriate controls could be specified for the commercial manufacture of the scaffold. The researchers developed a method to determine the amount of CaP lost during shipping and handling. They elucidated the effect of the polymer's molecular weight on scaffold pore morphology and architecture. Finally, they completed preliminary work in designing and fabricating a larger mold for creating a scaffold block. The block can then be sliced, from which scaffold discs can be punched.

Evaluation of Biologically Enhanced TyrPC Bone Regeneration Scaffolds in the Rabbit Calvarial CSD Model

Coronal histological sections were stained with Sanderson's Rapid Bone Stain and counterstained with van Gieson's picrofuchsin. In all studies, there appeared to be no adverse tissue responses, such as inflammatory reactions (e.g., macrophages or foreign body giant cells) or osteolysis in the defect area. The histology analysis verified biocompatibility, biodegradation, and osteoconductivity of the TyrPC+CaP scaffolds. The histology and histomorphometric data (new bone area) verified microCT data (new bone volume) and suggest that new bone formation in rabbit calvarial CSDs was rhBMP-2 dose-dependent and time-dependent. It was determined that 25 µg/scaffold of rhBMP-2 significantly promoted new bone formation in the rabbit calvarial CSD model at 16 weeks post implantation. Please refer to RCCC's Project 4.2.1a (Chapter II) for information on the performance of TyrPC+CaP bone regeneration scaffolds in the rabbit radius CSD model.

Conclusions

The researchers have developed a method for coating the surface of TyrPC scaffolds by solution precipitation of minerals, both for CaP and synthetic bone mineral mix. The microCT, histology, and histomorphometry data suggested that the synthetic TyrPC+CaP scaffolds were biocompatible, biodegradable, and osteoconductive at a level similar to commercially available bone graft substitutes in the rabbit calvarial and radius CSD models. The incorporation of 25 µg/scaffold of rhBMP-2 into TyrPC+CaP increased new bone formation in the calvarial model at 16 weeks compared to TyrPC+CaP alone, suggesting the effectiveness of rhBMP-2.

Research Plans for Year 5

The researchers plan to complete the necropsies and analyses for rabbit calvarial and radius CSD models. They will also develop TyrPC-based therapeutics that will regenerate bone in a goat calvarial CSD model.

Planned Clinical Transitions

The researchers designed a Phase 1 clinical trial to evaluate the safety of their TyrPC bone regeneration scaffold in humans. They may deliver the bone regeneration scaffold for a Phase 1 clinical trial after Year 5 and will prepare a regulatory strategy with both their industry partner, Trident Biomedical, Inc., and a regulatory consultant.

Bone Regeneration

Vascular Tissue Engineering

Project 4.5.6, RCCC

Team Leader(s): Daniel G. Anderson, PhD and Robert S. Langer, ScD (Massachusetts Institute of Technology [MIT])

Project Team Member(s): Omar Z. Fisher, PhD and Omar F. Khan, PhD (MIT)

Collaborator(s): Michael Longaker, PhD (Stanford)

Therapy: Bioactive scaffolds for vascular tissue engineering

Deliverable(s): (1) Fabricate bioactive microparticles that induce vasculogenesis, (2) engineer vascularized tissue constructs using novel hydrogel materials, and (3) analyze integration of vascularized bone constructs in vivo

TRL Progress: 2010, TRL 3; 2011, TRL 3; 2012 (Current), TRL 3; 2013 (Target), TRL 4

Key Accomplishments: The researchers have developed a biodegradable scaffold that can support the differentiation of endothelial and osteoblastic progenitor cells. They created melanic hydrogels and successfully integrated mesenchymal stem cells (MSC) into the hydrogels. They also developed methods for achieving spatially controlled zeolite deposition onto hydrogel thin films.

Key Words: Microparticles, vascularization, tissue engineering, vascular endothelial growth factor (VEGF), hydrogels, mesenchymal stem cells

Introduction

The clinical application of engineered large bone constructs is hampered by a limited blood supply. Thus, blood vessel recruitment into engineered tissues is the pivotal step toward long-term engraftment and survival. The treatment of large segmental defects requires large scaffolds, and the long-term viability of these engineered tissues in patients is highly dependent on the anastomoses between engineered and host blood vessels (i.e., formation of an integrated vascular network). The MIT group's strategy is to create synthetic growth factor-releasing and/or growth factor-immobilized microenvironments within the scaffold system to generate an interpenetrating vascular network. This addresses the unmet clinical need of providing a sustained blood supply within the implanted engineered tissues. Furthermore, the MIT group is working to design a scaffold capable of supporting bony tissue deposition and the differentiation of osteoblasts from human stem cells.

The clinical application of tissue-engineered bone constructs is also hampered by cell-sourcing issues. There are a limited number of suitable cell types that can give rise to bone cells in sufficient quantities. Previous work has shown that adipose-derived stem cells (ASC) can be isolated and grown in culture. MIT has demonstrated that these cells can differentiate into osteoblasts in vitro and subsequently form bone tissues in preclinical animal experiments. Moreover, recent evidence indicates that supplementation of MSC with endothelial progenitor cells can augment the osteogenic differentiation of the MSC.

MSC also secrete growth factors and cytokines whose effects can enhance the survival and performance of tissue-engineered constructs. The positive effects of MSC in different contexts include the inhibition of apoptosis and fibrosis, the stimulation of angiogenesis, the stimulation of tissue-specific and tissue-intrinsic progenitors, and the ability to turn off T-cell surveillance and chronic inflammatory processes in allogeneic implants. For example, in the context of producing vascular grafts in severe combined immunodeficient (SCID) mice, MSC stabilized the nascent human umbilical vein endothelial cells (EC) within an engineered blood vessel, which remained stable and functional for more than 130 days in vivo. The soluble factors platelet-derived growth factor (PDGF-β), transforming growth factor (TGF-β) and fibroblast growth factor (FGF9) have been implicated in the function

of MSC in blood vessel maturation. Furthermore, embedding MSC within EC-seeded constructs accelerated vessel formation and maturation in vivo, with the MSC appearing to differentiate into smooth muscle actin-positive pericyte-like cells that integrated with the new vasculature.

Therefore, the MIT group is using a coculture system and functionalized bioactive scaffolds to engineer vascularized bone grafts. Specifically, they have been utilizing microparticle-based controlled release and/or chemical immobilization of growth factors to promote a vascular network within the biodegradable scaffold and a hydrogel-based scaffold capable of supporting the mineralization of an inorganic bony matrix. They anticipate that the vascular network created in vitro via functionalized scaffolds will promote the integration and calcification of these bone tissues in vivo.

During the first year of the project, the researchers optimized a scaffold system of enhanced vascular engraftment. They identified an optimal biomaterial for effective bone tissue engineering. They also optimized human (h)VEGF-release microparticles for effective use in vasculogenesis.

Research Progress – Year 2 (This project was funded in 2010.)

Endothelial Differentiation of Stem Cells on Bioactive Scaffolds

Toward the goal of engineering vascularized tissues with stem cells, the MIT group has developed a system to monitor vascular differentiation utilizing induced pluripotent stem cells (iPSC) on bioactive scaffolds with VEGF. iPSC were seeded onto the scaffolds at 3 million cells/construct and grown for 10 days in culture media. Polymerase chain reaction (PCR) array was performed and data were normalized to a control gene (β-actin). The researchers analyzed cells on bioactive scaffolds by comparing the data to control scaffolds.

The results demonstrate that immobilization of hVEGF on the scaffolds resulted in efficient endothelial differentiation of iPSC, as indicated by the marked increase in genes related to endothelial differentiation. To support the fact that hVEGF immobilization induced efficient differentiation of iPSC, the group also looked at genes related to the "stemness" of embryonic stem cells. Poly(L-lactide)/poly(ε-caprolactone) (PLLA/PLCL) scaffolds coated with dopamine resulted in the highest expression of stemness genes while hVEGF coating resulted in the marked down-regulation of these genes.

In addition to endothelial differentiation, hVEGF coating resulted in the marked upregulation of the myogenic markers MYOD1 and MYF5. Utilizing iPSC, the researchers showed that PLLA/PLCL immobilized with hVEGF could induce biological activities related to endothelial differentiation. However, expressions of other lineage markers indicate that hVEGF is not sufficient to induce controlled differentiation into homogenous cell types. Further studies, utilizing combinations of bioactive molecules, are desirable for the controlled differentiation of stem cells.

Vascularized Bone Graft

A bioactive scaffold with the capacity for enhanced blood vessel recruitment would be desirable in a clinical setting. As a proof-of-concept, the MIT team immobilized hydroxyapatite on the PLLA/PLCL scaffold using a polydopamine coating method. They demonstrated that hydroxyapatite enhanced mineralization during bone development. They also demonstrated that hVEGF induced the vascular formation of stem cells and elicited vascular development. The team's strategy is to combine hydroxyapatite and hVEGF for vascularized bone tissue engineering.

The researchers demonstrated that these bioactive components can be immobilized onto the biodegradable scaffolds and that they elicit bone-specific differentiation of stem cells in vitro. To immobilize hydroxyapatite on the surface of the scaffold system, dopamine (5 mg) and hydroxyapatite (50 mg) were dissolved in a Tris buffer solution (pH 8.5), and the PLLA/PLCL scaffold was immersed in the solution. After overnight coating at room temperature, the substrate was rinsed with deionized water and dried under a stream of argon. Similar to hVEGF coating, substrate coating and functionalization were achieved via a one-pot procedure in a reaction vessel; dopamine and the target molecule were used together for surface coating and functionalization.

Dopamine can self-polymerize under alkaline conditions, and the polymerized-dopamine (polydopamine) acts as a surface coating agent due to its surface-adherent property. The immobilization of hydroxyapatite significantly enhanced MSC attachment and resulted in dose-dependent activation of the osteogenic gene marker Runx2. Compared to the plain PLLA/PLCL scaffold, scaffolds immobilized with hydroxyapatite demonstrated rougher topology. Furthermore, immobilization of hVEGF via the polydopamine coating method resulted in upregulation of Runx2 after 2 weeks of MSC seeding. The MIT team's results demonstrate that surface modification with hydroxyapatite and hVEGF may provide an efficient way to generate vascularized bone tissues.

Melanic Hydrogels

The researchers developed a composite hydrogel with interpenetrating CaP inclusions and created a method for CaP deposition within the hydrogels via the hydrolysis of phosphate esters. They subsequently developed methods for grafting biomolecules into a melanic hydrogel during and/or post gelation, followed by integration of MSC into melanic hydrogels. Melanic hydrogels were coated with zeolites (somewhat porous minerals that are commonly used as adsorbents), and methods were developed for achieving spatially controlled zeolite deposition onto hydrogel thin films. The team made initial progress toward the layered patterning of mammalian cells onto hydrogel thin films.

Conclusions

The researchers developed a biodegradable scaffold that can support the differentiation of endothelial and osteoblastic progenitor cells. The future challenge will be to incorporate this technology into a device, such as a hydrogel, that possesses the mechanical and chemical characteristics that will allow it to integrate optimally with host tissue. The ultimate goal is a vascularized bone graft.

Research Plans for the Next Year

The MIT group will integrate the vasculogenic and osteogenic properties of the system described previously into a biodegradable hydrogel system capable of supporting bony matrix deposition and the coculturing of both endothelial and osteoblastic progenitor cells.

Bone Regeneration

Accelerating the Development of Bone Regeneration Scaffolds by 510(k) Application to FDA for Tyrosine-Derived Polycarbonate Fracture Fixation Device

Project 4.5.8, RCCC

Team Leader(s): Carmine P. Iovine, PhD (Rutgers University) and Deborah Schmalz (Trident Biomedical, Inc.)

Project Team Member(s): Das Bolikal, PhD, Aniq Darr, PhD, Veena Bolikal, Lulu Wang, Marius Costache, PhD, and Ganesan Subramanian (Rutgers University); Bob Marcus and Hoddy Klein (Trident Biomedical, Inc.); and Howard Schrayer (Regulatory Affairs Consultant)

Collaborator(s): None

Therapy: Small bone fracture repair

Deliverable(s): 510(k) submission for a TyrPC bone fixation pin

TRL Progress: 2010, TRL 4; 2011, TRL 4; 2012 (Current), TRL 4; 2013 (Target), TRL 8

Key Accomplishments: The researchers developed a polymer synthesis process and produced more than 2 kg of non-GMP polymer. They validated both monomer and polymer synthesis processes through a third-party subcontractor. They developed a bone pin fabrication process using injection molding and incorporated a processing aid (zinc stearate). They manufactured bone pins through a third-party subcontractor.

Key Words: 510(k), bone pin, tyrosine derived polycarbonate, fracture repair

Introduction

There is an unmet clinical need for osteoconductive orthopedic devices—those that promote the attachment and growth of bone at the bone-implant interface. The objective of this project is to familiarize the FDA with the use of a tyrosine-derived polymer in an orthopedic implant. To accomplish this goal, the team selected a relatively simple device with a well-established clinical use, for which there exists a successful "predicate" device—a synthetic, resorbable bone pin used in fracture fixation. The researchers have been focused on the completion of tasks required to submit a 510(k) application to gain regulatory approval for the device. Importantly, approval of the tyrosine-derived polymeric, resorbable bone pin is envisioned as an intermediate step toward the team's overall AFIRM goals—to develop bone regeneration scaffolds for CMF reconstructions and for large segmental long bone defects.

Degradable biomaterials are used regularly in orthopedics as internal fracture fixation devices, bone void fillers, bone regenerations scaffolds, and in the management of osteotomies (i.e., surgeries in which bone has been cut to foster healing). All currently used small-bone fixation devices and degradable orthopedic implants are made of non-osteoconductive materials, which have yielded limited clinical results. The development of a polymer based on TyrPC that is both osteoconductive and tissue integrative would significantly improve the clinical performance of degradable orthopedic devices.

During the first year of the project, the researchers developed and documented a robust polymer synthesis process. They completed vendor selection for fabrication, sterilization, preclinical safety, toxicity, and efficacy testing. They identified an efficacy model and created a quality system to oversee development efforts. They also finalized a pin design as well as a kit and packaging design.

Research Progress – Year 2 (This project was funded in 2010.)

Monomer and Polymer Material Synthesis

Monomer: The synthesis procedure for either 500 or 1,000 g scale of N-dithiocarbonyl ethoxycarbonyl (DTE) monomer was validated at Rutgers University, and the quality of the monomer produced was confirmed through a combination of internal and external analyses. The individual batches of 500–1,000 g DTE monomer were prepared by combining several of the 500 and 1,000 g batches of previously prepared DTE monomer. The team confirmed that both the individual batches of 500–1,000 g each and the combined batch of 2.5 kg met the acceptance criteria for monomer.

Polymer: Through a series of experiments, the process for synthesis, isolation, and purification of the polymer (named E1001(1K)-CT) was optimized for production of a 200 g batch. Following this protocol, 21 batches of polymer were separately prepared. The yield of polymer that met the acceptance criteria ranged from 85%–90%, and consequently, more than 2 kg of E1001(1K)-CT was produced to support the needs for this program.

A synthesis package was then transferred to a third-party GMP-compliant production subcontractor, Cyalume (West Springfield, Massachusetts). The package consisted of a written standard operating procedure (SOP) for polymer synthesis at a 200 g batch, a batch record template, an Excel spreadsheet to calculate batch-related information, a polymer specification sheet, raw-material specifications, and a training video. In addition, a team of Cyalume scientists and engineers met with the laboratory personnel at Rutgers for a 2-day on-site visit to get firsthand experience with the synthesis of E1001(1K)-CT. To date, one 200 g batch of medical-grade polymer has been synthesized at Cyalume. Manufacture of a second 200 g batch is currently in progress.

A laboratory procedure for the preparation of injection molding grade E1001(1K)-CT was developed and documented. The injection molding grade is prepared by wet blending the solid E1001(1K)-CT with 1% zinc stearate powder in hexane. The blended solids are recovered from the hexane by solid-liquid and solvent evaporation techniques.

Optimization of Device Fabrication Process

Medical-grade polymer was sent to a contract vendor, Medical Murray (North Barrington, Illinois), for evaluation of the polymer's molecular weight loss post processing via injection molding. Preliminary analysis indicated that the molecular weight loss was greater than the minimum amount required to produce mechanically robust pins. To reduce the effect of processing on the polymer's molecular weight, modifications to the mold design and the injection-molding parameters were implemented, to minimize the polymer's exposure to oxygen, minimize the shear force that the polymer experiences during the molding process, and shorten the residence time and heat exposure of the polymer during processing. These changes in combination with the use of a processing aid, zinc stearate, improved the outcome of the overall fabrication process.

On April 5, 2012, a small batch of zinc stearate (0.5%)-treated E1001(1K)-CT polymer was processed into about 50 pins, according to the process optimized in this project. Analysis of the pins indicated that polymer molecular weight was retained. The performance of the pins is under evaluation by a third-party collaborator (at no cost to the Department of Defense [DoD]). A second and larger production run of pins fabricated with E1001(1K)-CT polymer treated with 1% zinc stearate will be conducted in the near future.

Biocompatibility and Efficacy Studies

Trident Biomedical (Bridgewater, New Jersey) engaged with Applied Biological Concepts, Inc. (Los Alamitos, California) and has finalized an Animal Care and Use Review Office (ACURO)-approved protocol (USAMRMC 08288003.54) for the purpose of determining the efficacy of a bioresorbable pin compared to a predicate device when used for the repair of an osteochondral bone fracture in the femoral condyle of a goat. The vendor contract and time line for efficacy studies are under development. Trident Biomedical has also engaged with Nelson Laboratories (Salt Lake City, Utah) to obtain biocompatibility protocols and pricing. Submissions for ACURO approval will follow.

Conclusions

In conjunction with Trident Biomedical, Inc., the Rutgers team has made significant progress toward the submission of a 510(k) application for the TyrPC bone pin, which is made from the same polymer used in the TyrPC bone regeneration scaffolds. Third-party vendors have validated the synthesis procedures for both monomer and polymer. Specifically, 2 kg of medical-grade polymer has been synthesized for the activities to be included in the 510(k) package. The manufacture of bone pins by a third-party contract vendor has been initiated, and the optimization of the process is ongoing. In addition, the activities required to complete GMP validation of polymer synthesis are under way.

Research Plans for the Next Year

In Year 5, the team will complete all activities required for the submission of a 510(k) application. These activities include the finalization of the manufacturing process, in vitro performance testing, and in vivo biocompatibility and efficacy studies.

Planned Clinical Transitions

Trident Biomedical, Inc. (the commercial partner of this technology) is pursuing a 510(k) regulatory pathway for the TyrPC bone pin.

Bone Regeneration

Preclinical Animal Model Development for Bone Regeneration Studies

Project 4.5.1c, USAISR

Team Leader(s): Pamela R. Brown Baer, DDS, COL Robert Hale, DDS, and LTC Wen Lien, DDS (Dental and Trauma Research Detachment, USAISR)

Project Team Member(s): COL Phillip DeNicolo, DMD, MS and David T. Silliman, BS (USAISR)

Collaborator(s): Joseph C. Wenke, PhD (USAISR) and Teja Guda, PhD (University of Texas at San Antonio)

Deliverable(s): Translational animal models for evaluating technologies for clinical mandible reconstruction

TRL Progress: 2010, TRL 3; 2011, TRL 3/4; 2012 (Current), TRL 3/4; 2013 (Target), TRL 5

Key Accomplishments: The researchers characterized the rabbit mandible notch defect model and verified it as a nonchallenging bone regenerative model. They also completed the animal portion of a pig mandible notch defect study and initiated analysis to characterize the bone regeneration and healing potential of this model. In addition, they worked closely with AFIRM collaborators to evaluate potential bone regenerative materials in various animal models.

Key Words: Animal models, mandibular defects, bone regeneration, clinical modeling

Introduction

Craniomaxillofacial battle injuries caused by explosive devices are characterized as open wounds and comminuted fractures. In combat casualties, the majority of the facial fractures are to the mandible (36%).[1] Currently, no satisfactory treatments are available to aid in reconstructing the face ravaged by explosive devices to an acceptable level, much less to natural form and function. The frequency and complexity of these injuries require novel approaches to improve the outcome for mandibular battle wounds.

Though autologous bone grafts are considered the standard of care, novel biomaterials for bone regeneration are being developed to address the clinical challenges by combining the structural strength of biocompatible, biodegradable scaffolds with the ability to deliver growth factors and/or stem cells.[2,3] Prior to using these materials to restore severe mandibular battle injuries, they need to be evaluated in clinically relevant and progressively challenging animal models. The purpose of the research was to select and validate a medium and large animal model to be used to screen regenerative bone technologies prior to clinical trials.

Medium Preclinical Animal Model (Rabbit)

Among medium animal maxillofacial preclinical models, the CSD model in the rabbit mandible in particular has not been sufficiently standardized with multiple defect sizes reported in the literature. The objective of this study was to establish a CSD model in the rabbit mandible that does not mechanically compromise the loading environment to allow for standardized evaluation of bone regeneration therapies.

An osseous defect was created in the inferior border of the rabbit mandible (measuring 5 mm in height x 12 mm in length x 5 mm in width = volume 300 mm^3), and the edge of the defect was cauterized to decrease bone healing (**Figure 1A**). Investigation showed that the 300 mm^3 defect did not significantly compromise the mechanical integrity of the mandible when compared to the

[1] Lew TA, et al. 2009. *J Oral Maxillofac Surg*. 68: 3-7
[2] Chim H, Gosain AK. 2009. *J Craniofac Surg*. 20:29-33.
[3] Torroni A. 2009. *J Oral Maxillofac Surg*. 67:1121-1127.

intact contralateral side (**Figure 1B**), eliminating the need to plate the defect. An extraoral approach was used to eliminate the chance of infection from intraoral flora.

The endpoints of the study were 6 weeks and 12 weeks post surgery (n=10). No significant differences were found in mineral density, bone volume, and overall regenerated tissue volume (**Figure 1C**) between 6 and 12 weeks. In addition, the defects were 87% healed at 6 weeks and 88% healed at 12 weeks. The presence of stem cells from the pulp and periodontal ligament associated with the remaining teeth in the region of surgery may be an explanation for the robust healing response in this region.

These data suggest the need for having an appropriate defect size to study bone regeneration in a relevant rabbit mandibular defect model. The 300 mm^3 size allowed for simulation of a physiologically stabilized defect. However, contrary to other reports, a significant bone-healing response at 6 weeks post surgery was observed with this defect size even with cauterization of the bone at the defect margins. This finding indicates that this model does not sufficiently challenge bone healing, which prevents discrimination between bone regenerative treatment options.

Large Preclinical Animal Model (Pig)

Goats and pigs have traditionally been used as large animal mandible regenerative preclinical research models. A comparison of previous anatomical investigations in pigs and goats revealed that the pig is the better choice of the two species for mandibular regenerative studies (**Figure 2**).

Though pigs have been used for these studies, a standardized experimental investigation of a mandibular defect is lacking.[4] Based on previous research, it was hypothesized that a mandibular defect with a volume greater than 5 cm^3 with

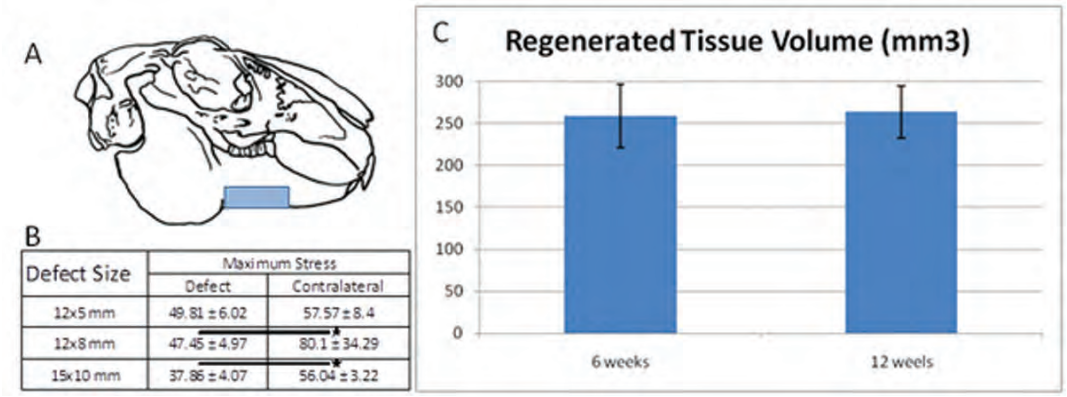

Defect Size	Maximum Stress	
	Defect	Contralateral
12x5 mm	49.81 ± 6.02	57.57 ± 8.4
12x8 mm	47.45 ± 4.97	80.1 ± 34.29
15x10 mm	37.86 ± 4.07	56.04 ± 3.22

Figure 1. Rabbit mandible study. (A) Defect site. (B) Strength of the hemi-mandible with different defect sizes, compared to intact contralaterals. (C) Regenerated tissue volume as determined by microCT analysis.

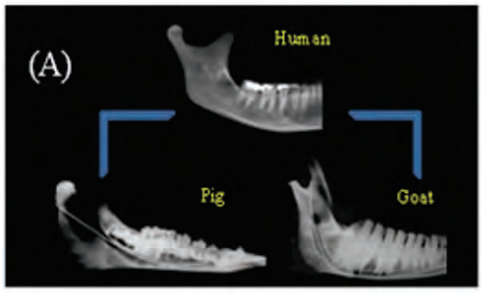

Selection Criteria	Goat	Pig	Favorable Model
Soft Tissue Dissection	< 1.0 cm	> 1.5 cm	Goat
Surgical Site	Ramus	Body	Pig
Nerve Proximity to Defect	Definitely Encountered	Not Encountered	Pig
Fixation	Probably necessary	Probably not necessary	Pig
Dentition Lengths	Elongated Roots	Human-Like	Pig
Chewing Pattern	Herbivorous Chewing	Human-Like	Pig
Post Op Diet	Cannot change	Soft Diet	Pig
Source of Animal	Known	TBD	Goat
Costs	$$	$$$+	Goat

Figure 2. Anatomical comparisons of large animals. A: Clinical CT comparisons among human, pig, and goat mandibles. Table on right: Selection criteria used to determine the more favorable large preclinical animal model.

[4] Ruehe B, et al. 2009. *Oral Surg Oral Med Oral Pathol Oral Radiol Endod.* 108:699–706.

bordering periosteal stripping would not heal without intervention, creating a challenging preclinical large animal bone regenerative model.

The researchers created subtotal osseous mandible defects bilaterally in five dentally mature pigs to evaluate post-operative complications, jaw stability, and the surgical site's healing potential with and without the clinical gold standard, autologous bone graft (**Figure 3**).

Post-operative observations and CT exams demonstrated that the plated defects were stable and the animals tolerated the surgery and healing period well. The initial results from the microCT scans showed that a significant amount of healing occurred in both treated and untreated defects (**Figure 4**). Though the defect treated with the autologous bone graft showed a higher percentage of bone fill, the difference between the two treatment groups was not significant (**Figure 4B**).

Despite the fact that the defects were larger in volume (~6 cm^3) than defects previously reported as CSDs (5 cm^3), substantial bone healing was observed at 16 weeks, even without any treatment. A systematic way of defining the defect at the 16-week time point is under way to validate CT, microCT, and histological analysis. The researchers note that quantification of healing using CT, microCT scans, and histology will aid in determining whether this can be considered a challenging bone regeneration model. From the initial results, it appears that this model cannot be recommended as a CSD large animal model for testing the healing potential of candidate biomaterials in the mandible prior to human clinical trials.

Conclusions

Ultimately, validating challenging mandible injury models in medium and large animals will aid in progressing preclinical studies of bone-regenerating biomaterials necessary to better restore mandibular battle wounds.

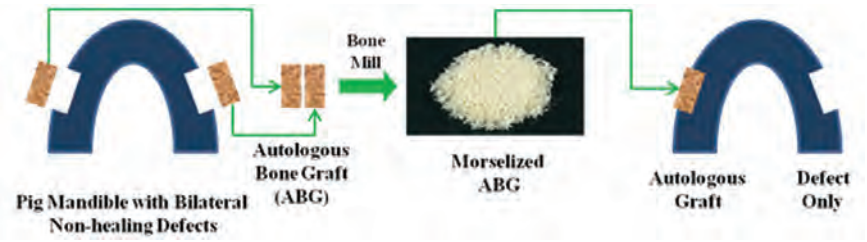

Figure 3. Pig mandible study design. Autograft was the combination of morselized bone removed during the defect creation. For each of the five pigs, the left side was treated with autograft (positive control), and the right side was left untreated (negative control).

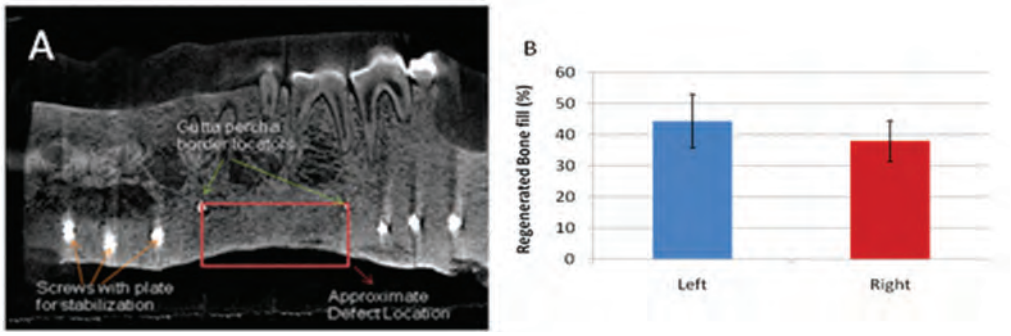

Figure 4. (A) MicroCT images highlighting bone regeneration in the defect without treatment. (B) Initial microCT analysis showing no significant difference between the treatment (autograft; left) and no treatment (right) sides.

Research Plans for the Next Year

The researchers will create and characterize a segmental defect in the pig mandible with the goal of creating a challenging preclinical animal model that mimics the battle injuries of our wounded warriors to allow for accurate testing of bone regenerative technologies. In addition, they will continue to develop novel ways to quantify bone regeneration using clinical computer tomography studies in large animal bone regenerative models.

Soft Tissue Regeneration

Soft Tissue Reconstruction (4.1.4)/Injectable and Implantable Engineered Soft Tissue for Trauma Reconstruction (4.1.5)

Projects 4.1.4 and 4.1.5, WFPC

Team Leader(s): Peter Rubin, MD, Kacey Marra, PhD (University of Pittsburgh); David Kaplan, PhD (Tufts); James Yoo, PhD and Sang Jin Lee, PhD (Wake Forest University)

Project Team Member(s): Evangelia Bellas, PhD, Bruce Paniliatis, PhD, and Jodie Moreau, PhD (Tufts); Rachel Hoyer, Jolene Valentin, PhD, Nurul Aini, MD, and Donna Ward, PhD (University of Pittsburgh); Chang Mo Hwang, PhD, Sang-Hyug Park, PhD and Young Min Ju, PhD (Wake Forest University)

Collaborator(s): Jeff Gimble, MD, PhD (Louisiana State University, Pennington Research Center) and Steve Badylak, DVM, PhD, MD (University of Pittsburgh)

Therapy: Long-term soft tissue restoration of traumatic defects with cell-based degradable scaffolds, resulting in sustained shape and volume over time

Deliverable(s): (1) Engineering of vascularized connective tissue and fat pad; (2) development of implantable and injectable vascularized soft tissue composed of connective tissue and fat; (3) demonstration of the applicability of using implantable and injectable soft tissue composites for limb, burn, and craniofacial applications in a large animal model; and (4) initiation of clinical testing of soft tissue replacement for small defects

TRL Progress: 2008 (Start), TRL 2; 2009, TRL 3; 2010, TRL 4; 2011, TRL 4; 2012, TRL 5

Key Accomplishments: The researchers have completed numerous preclinical studies using silk biomaterials and ASC. They found that the volumes of implanted silk scaffolds were maintained for 18 months in a rat model. Mature adipose tissue was found in groups pre-seeded with lipoaspirate or differentiated ASC. Silk implants, with or without autologous lipoaspirate, maintained their volumes through a 6-month period in a horse model. The researchers developed injectable silk foams and tested them in the small animal model. Preliminary 2-week in vitro studies demonstrated that stem cells survived and migrated through the foams, and the foams readily absorbed lipoaspirate. The researchers completed in vivo silk gel studies, which indicated that fat grafts containing lipoaspirate, silk, and ASC showed retention of the graft over time and a favorable tissue response. They also found that alginate particles embedded in a fibrin hydrogel improved volume retention over time while the transplanted cells produced extracellular matrix (ECM) proteins in vivo.

Key Words: Adipose, adipose-derived stem cells, lipoaspirate, volume stable, silk scaffold, regeneration, connective tissue, fibrin-based hydrogel

Introduction

The retention of implanted fat and/or connective tissue grafts over time remains a challenge for soft tissue reconstruction procedures such as the repair of craniofacial defects. The restoration of traumatic soft tissue defects must start with a strategy that will restore tissue size and shape to near normal dimensions for at least 1 year while the body gradually remodels and regenerates the tissue with seminormal or normal structure and function. Silk biomaterials have been employed for soft tissue reconstruction because of their controllable degradation rates and biocompatibility, suitability for processing into various formats (e.g., sponges, gels, and foams), ability to deliver bioactive agents, and robust mechanical properties.

The specific aims of this project are as follows.

Aim 1: Biomaterial-Based Scaffolds for Adipose Tissue Regeneration – An injectable scaffold will be designed to provide sustained morphology and structure for at least 1 year while supporting

cellular and vascular ingrowth to restore functional tissue.

1.1 Development of an injectable sustainable silk protein biomaterial scaffold that can be combined with lipoaspirate to serve as a template for soft tissue regeneration.

Aim 2: Cell-Based Scaffolds for Adipose Tissue Regeneration – The second-generation scaffolds will include adipose stem/progenitor cells (ASC, with or without transfection with VEGF/fibroblast growth factor genes) in combination with the scaffolds from Aim 1, to accelerate adipose tissue regeneration.

2.1 Development of quantitative analytical methods for cell characterization.

2.2 Development of an implantable sustainable silk biomaterial scaffold that can be cultured with ASC, adipocytes, or lipoaspirate to serve as a template for soft tissue regeneration.

Aim 3: Injectable Fibrin-Based Hydrogel System for Soft Tissue Regeneration

3.1 Development of an injectable hybrid hydrogel system composed of alginate particles and a fibrin hydrogel

3.2 Development of a porous injectable hydrogel system composed of rapid degradable gelatin microfibers

3.3 In vivo evaluation of an injectable hydrogel system with dermal fibroblasts

During the first 3 years of this project, the researchers successfully combined silk-based scaffolds, lipoaspirate, and stem cells to form stable injectable and implantable soft tissue constructs in a small animal model. Overall, they have maintained a pathway for developing clinically useful injectable and implantable soft tissue therapies that can improve facial deformities with greater precision than current techniques.

Research Progress – Year 4

Silk Sponge and Foam in Vivo Studies

The researchers have completed their long-term silk sponge in vivo study. They implanted silk sponges as is, with stem cells cultured ex vivo, or with lipoaspirate into a rat for up to 18 months. Volume was maintained in all groups (**Figure 1a,c**) for 18 months. Tissue was regenerated as the sponge degraded (Figure 1a,b). Adipose tissue was found only in seeded groups. This study demonstrated volume retention greater than 6 months. The silk sponge, alone or with autologous lipoaspirate, was then implanted into the back of a horse

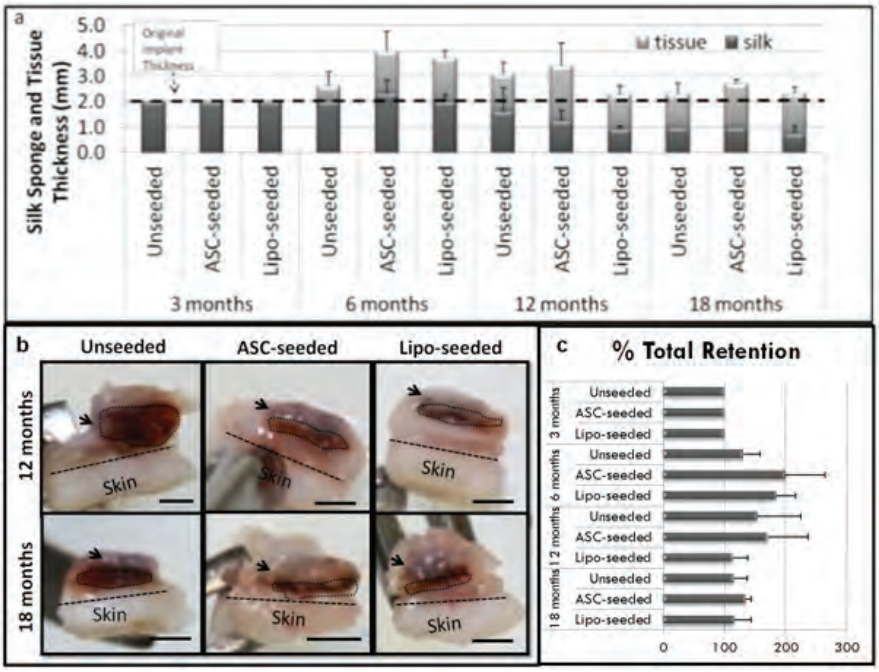

Figure 1. (a) Silk sponge volume was calculated by measuring sponge thickness and diameter upon explantation. Complete volume retention in all groups was seen. (b) Cross-sections of 12 (top row) and 18-month explants (bottom row) are shown for unseeded (left), ASC-seeded (middle), and lipo-seeded (right) groups. Square dotted lines outline the silk sponge while rectangular dotted lines demarcate skin from subcutaneous tissue. Arrows point to regions of subcutaneous fat. Subcutaneous fat formation was greatest in lipo-seeded group (right column) and least in the unseeded group (left column). Scale bar- 2 mm. (c) Total retention (silk plus regenerated tissue). Scale bar- 100 µm, inset- 200 µm.

for 6 months. As with the small animal study, the sponges maintained their volume for 6 months. In both unseeded and seeded groups, the regenerated tissue was well-organized collagenous connective tissue (**Figure 2**). Injectable silk foam was conducive to cell spreading, attachment, and survival in vitro. The foam was easily injected through the skin via a custom injection gun and remained palpable after 90 days in vivo. The foams became well integrated with surrounding host tissue, and vasculature was seen leading to the foams at early time points (**Figure 3**).

Silk Gel in Vivo Studies

Injectable silk gel was fabricated and tested in vivo in an athymic mouse model to study volume maintenance and biologic response over time. Silk gel (8%) was combined with lipoaspirate at gel:lipoaspirate ratios of 0:1, 1:0, 1:3, and half of the gel-lipoaspirate preparations were combined with 4 million ASC/mL. Macroscopically, all explants showed normal fat appearance and were encapsulated (**Figure 4**). No decrease in volume retention was noted for the lipoaspirate/silk gel/ASC group. Grafts composed of lipoaspirate contained blood vessels and normal fat tissue (**Figure 5**). Cellularity increased in groups containing ASC. When blended with lipoaspirate, the

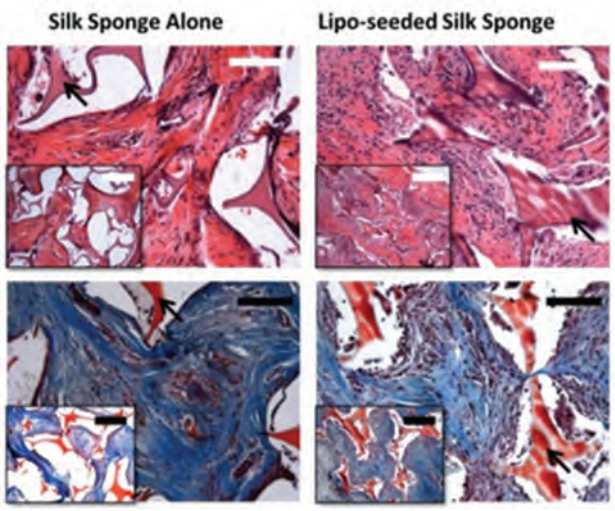

Figure 2. Masson's Trichrome images of silk sponges after 6 months following implantation in a horse. Silk is visible (black arrows). Tissue is well organized and volume was retained. No mature adipocytes were present at 6 months. Scale bar- 100 µm, inset- 200 µm.

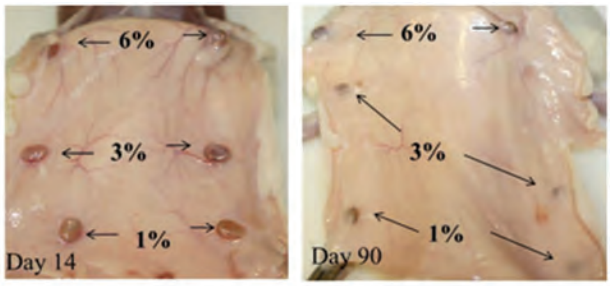

Figure 3. Injectable silk foams (1%, 3%, 6% silk w/v) after 14 and 90 days post injection. Vasculature leading to foams was evident at early time points. Foams are well integrated with surrounding host tissue. After 90 days, 50% of silk foam was retained.

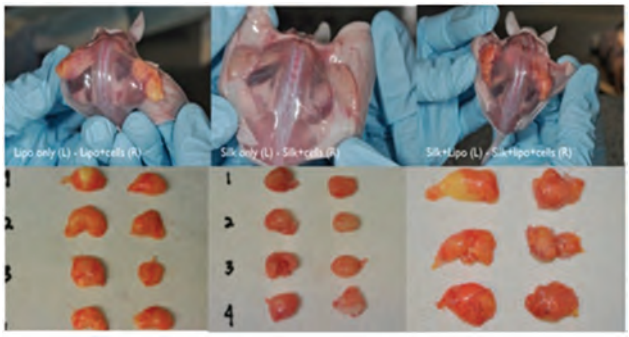

Figure 4. Macroscopic images of fat grafts explanted at 6 weeks.

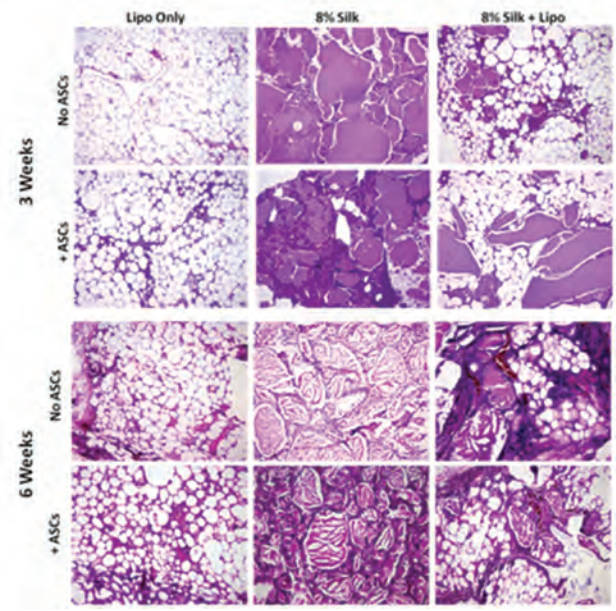

Figure 5. Hematoxylin and eosin (H&E) images of explanted silk fat grafts at 3 and 6 weeks (10X).

silk gel did not appear to inhibit vascularization of the implants.

In Vivo Evaluation of Injectable Alginate Particle-Embedded Fibrin Hydrogels

The researchers developed a novel hybrid hydrogel system that consisted of alginate particles and fibrin matrix that maintained tissue volume over the long term. They fabricated alginate particles by mixing 5% alginate with a 20 mM calcium solution. Dermal fibroblasts and alginate particles were embedded in fibrin hydrogels using a dual syringe mixer. To determine the in vivo dimensional stability of the alginate–fibrin constructs as well as in vivo ECM production, the cell-encapsulated hydrogel constructs were implanted subcutaneously under the dorsal skin of athymic mice (nu/nu, Charles River Laboratories Inc.). In vivo explants showed that cells contained within fibrin-only hydrogels did not contribute to neo-tissue formation, and the fibrin was fully degraded within a 12-week period (**Figure 6**). In the alginate-fibrin system, higher cellularity and vascular ingrowth were observed in vivo (**Figure 7**). This resulted in neo-tissue formation in the alginate-fibrin hydrogels. These results demonstrate that fibrin may enhance cell proliferation and accelerate formation of ECM proteins in the alginate-fibrin system while the alginate particles could contribute to volume retention.

Conclusions

This project has demonstrated the feasibility of using stem cell-seeded silk scaffolds for long-term soft tissue restoration. Notably, the 18-month study in a small animal model using silk sponge implants with lipoaspirate is the first study to show long-term volume-stable adipose tissue regeneration.

Research Plans for Year 5

Small animal studies are under way to test various formats of silk injectables (e.g., hydrogel, sponges, and foams) in physiologically relevant models (subcutaneous, submuscular, and intramuscular sites). The researchers have initiated discussions with the FDA for a pre-IDE meeting.

Planned Clinical Transitions

Initial clinical trials are under way at the University of Pittsburgh, supported by the competitive AFIRM clinical trials funding program.

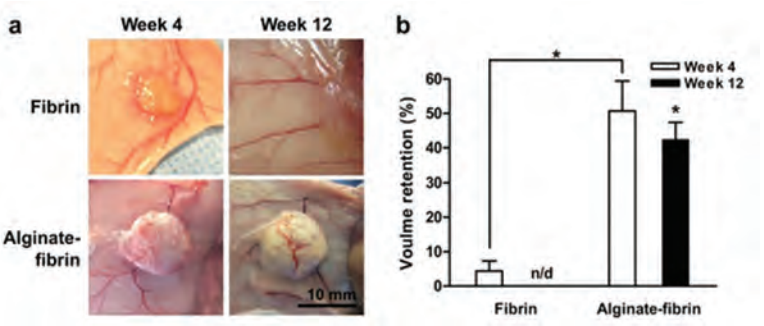

Figure 6. (a) Gross appearance and (b) volume retention (%) of cell hydrogel constructs at 4 and 12 weeks post implantation. At 12 weeks post implantation, the cell-fibrin constructs were completely absorbed and no tissue remnant was observed while the alginate-fibrin hydrogels maintained approximately 42.4% of original volume (n/d: not detectable).

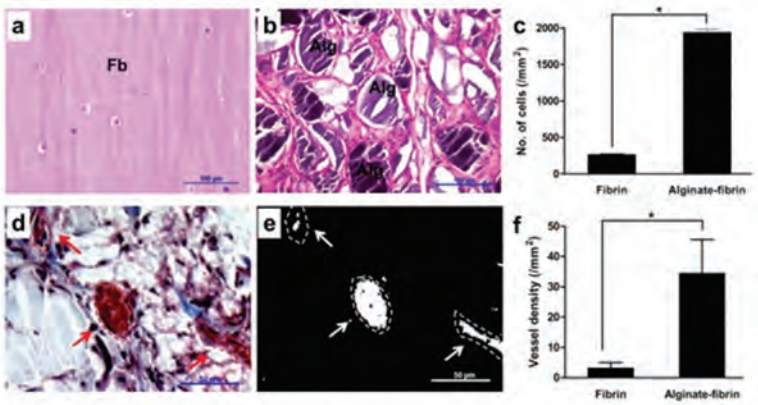

Figure 7. H&E staining of the cell hydrogel constructs at 4 weeks of implantation: (a) Fibrin and (b) fibrin/alginate. (c) The alginate-fibrin constructs showed higher cellularity when compared with the fibrin-only constructs (*p<0.01). (d–f) Vessel density (vessels/area) in the cell hydrogel constructs was analyzed by the autofluorescence of RBC. (f) The degree of vascularization in the alginate-fibrin constructs was significantly higher than that in the fibrin-only constructs (*p<0.01).

Soft Tissue Regeneration

Bioreactors and Biomaterials for Tissue Engineering of Skeletal Muscle

Project 4.1.6, WFPC

Team Leader(s): George J. Christ, PhD (Wake Forest University)

Project Team Member(s): James Yoo, MD, PhD, Sang Jin Lee, PhD, Benjamin T. Corona, PhD, Masood A. Machingal, PhD, Venu Kesireddy, PhD, and Catherine Ward, PhD (Wake Forest Institute for Regenerative Medicine [WFIRM])

Collaborator(s): Tom Walters, PhD (USAISR) and David Kaplan, PhD (Tufts)

Therapy: Autologous bioengineered skeletal muscle implant for functional reconstruction/repair of complex craniofacial injuries

Deliverable(s): An implantable tissue-engineered muscle repair (TEMR) construct capable of restoring clinically relevant force/tension following a volumetric muscle loss (VML) injury

TRL Progress: 2008 (Start), TRL 2; 2009, TRL 3; 2010, TRL 3; 2011, TRL 4; 2012 (Current), TRL 4; 2013 (Target), TRL 4

Key Accomplishments: The researchers completed the physiological and histological analyses, which documented that the rat tibialis anterior (TA) VML injury model is an appropriate model for the evaluation of the TEMR technology. They completed in vivo pilot studies on first and second generations of controllable silk scaffolds for TA VML injury that showed ~47% and ~65% functional recovery at 2 months post implantation, respectively. They conducted histological analyses of the two generations of silk construct–tissue explants to decipher mechanisms of regeneration and integration with surrounding tissue and to further guide the manufacture of the novel scaffolds. They also completed further characterization of human muscle progenitor cells (MPC) for derivation of a clinically applicable population of cells at up to the fourth passage.

Key Words: Tissue engineering, skeletal muscle repair, volumetric muscle loss, bioreactor, muscle progenitor cells, myoblasts, myotubes

Introduction

Current management of tissue coverage and augmentation involves the use of existing host tissue to construct muscular flaps or grafts. In many instances, this approach is not feasible, delaying the rehabilitation process as well as restoration of tissue function. In fact, the inability to engineer clinically relevant functional muscle tissues remains a major hurdle to the successful skeletal muscle reconstructive procedures required to repair the complex facial injuries suffered by warfighters. The research team's long-term goal is creation of a skeletal muscle tissue implant capable of generating clinically relevant force/tension. Engineering skeletal muscle tissues de novo with the patient's own cells would accelerate wound healing and cosmetically augment the tissue defect, thus enhancing restoration of tissue function. The researchers are developing a technology to further probe the feasibility and applicability of creating contractile skeletal muscle tissues through the use of a bioreactor system in conjunction with novel biomaterials/scaffolds and optimized bioreactor protocols. The initial clinical application will be repair and restoration of craniofacial battlefield wounds.

The specific aims of this project are to:

1. Demonstrate proof-of-concept for engineering functional (i.e., contractile) skeletal muscle tissue for craniofacial defects.
2. Conduct a feasibility study involving the implantation of engineered skeletal muscle in a rat skeletal muscle replacement model.

3. Conduct an applicability study involving the implantation of engineered skeletal muscle in a large animal (dog) model of craniofacial defects.

4. Determine the feasibility of using biopsies from human patients for the engineering of functional skeletal muscle.

During the first year of the project, the researchers generated a set of SOPs to successfully generate an organized muscle tissue in vitro. They also optimized the scaffold and bioreactor preconditioning in comparison to their previously reported methods for engineering contractile skeletal muscle. In addition, they established a surgically created latissimus dorsi (LD) muscle defect in which tissue-engineered skeletal muscle constructs could be implanted to replace up to 50% of excised LD muscle.

During the second year of this project, the researchers focused on characterizing their first-generation TEMR constructs to restore tissue function in the rodent LD model of VML. The results of these studies indicated that 2 months after implantation, TEMR constructs promoted functional recovery to 70%–75% of the force generated by uninjured muscle while untreated, VML-injured LD muscle produced only approximately 50% of uninjured force values. Histological analysis revealed the presence of myotubes and mature muscle fibers within the implanted scaffolding material as well as vascular and neural structures necessary to support functional tissue formation.

During Year 3, the researchers developed a rodent TA VML injury model for proof-of-concept studies. Once again, implantation of the TEMR construct led to robust functional recovery of dorsiflexion of the foot following stimulation of the peroneal nerve in vivo, which indicated functional reinnervation of the leg implanted with the TEMR construct.

Research Progress – Year 4

TEMR Treatment for TA VML Injury Study: Additional Histological Analyses

The researchers completed the preliminary physiological and histological analyses of the initial TA VML injury model at 3 months post implantation. Comparison of functional recovery data for the TEMR-treated TA VML injuries with the bladder acellular matrix (BAM)-scaffold-only treated injuries showed significant variability in recovery for the TEMR-treated constructs, ranging from nearly complete functional recovery in six of the animals, to little or no recovery in the other seven. The research team is still determining the most physiologically relevant method to compare the extent of recovery and expect these analyses to be completed during the first quarter of Year 5.

Nonetheless, the observed variability in the extent of functional recovery prompted further histological investigation. The researchers performed a pan-macrophage stain, which showed the presence of a significant inflammatory response in the TEMR-treated TA VML injuries that also displayed poor recovery. Myosin heavy chain staining showed that thicker fibers had formed within the construct beyond the native tissue interface of the TEMR-treated TA VML injuries that displayed near complete recovery. An experiment is under way to determine if diminished cellular coverage during implantation of the sheet-like TEMR constructs (due to excessive handling during implantation relative to the ease of implantation in the LD VML injury model) is responsible for the observed inflammatory response and poor degree of recovery observed with some constructs implanted in this animal model.

These initial observations suggest that a largely 2D sheet-based scaffold design may be suboptimal for more complex 3D VML injuries, such as that represented in the TA model (where the TA VML injury is more canoe-shaped and created in the belly of the muscle, in contrast to the planar sheet VML injury that is created in the LD muscle), especially when compared to the more consistent functional recovery observed for the planar sheet-type of injury characteristic of the LD VML injury model. Hence, the researchers continued to focus on the development of alternative scaffolds for the treatment of the full spectrum of craniofacial VML injuries.

Completion of Initial Investigations of Controllable Silk Constructs for VML Injury Repair

The researchers have focused on silk as a potential alternative source for the TEMR construct. The team tested two iterations of the novel controllable 3D silk scaffold made by the Kaplan team at Tufts University in both in vitro and in vivo studies. They completed morphological and histological analyses begun in Year 3 (**Figure 1**). While some modest degree of functional recovery was observed in rats implanted with the silk-based TEMR construct in the TA VML injury, upon retrieval of the implanted tissues, the silk constructs showed a lack of integration with the surrounding native tissue. Furthermore, the histology revealed a lack of integration and new muscle formation within or surrounding the constructs (Figure 1; n =2). Although not shown, cell-seeded first-generation silk scaffolds showed little or no functional improvement (n=3).

These initial findings guided the design and implementation of a second-generation silk scaffold. Researchers on the Kaplan team sought to increase the integration of the silk with the host tissue by increasing both the porosity and the degradation rate of the scaffold. These second-generation scaffolds were manufactured with and without the arginine-glycine-aspartic acid (RGD) cell attachment sequences. At the Christ laboratory, preliminary in vitro studies illustrated that both RGD and non-RGD coupled constructs were capable of promoting cellular infiltration throughout the scaffold. An in vivo pilot study was conducted using non-RGD, non-cell-seeded constructs. In contrast to the first-generation, second-generation scaffolds were more precisely fashioned to fit the contour of the surgically created VML injury, reducing the bulk and thickness of the implanted construct. Initial functional testing indicated an average of approximately 65% functional recovery at 8 weeks (n=2; in the absence of cell seeding).

Tissues were retrieved for morphological and histological assessment at 9 weeks post implantation. In stark contrast to observations with the first-generation silk scaffold, there was a dramatic improvement in degradation of the second-generation scaffold, as revealed by explant and histological analysis at 9 weeks post implantation (compare Figure 1 and **Figure 2**). As illustrated in Figure 2, there appeared to be excellent integration of the second-generation silk scaffold with the host tissue even in the absence of cellular seeding at implantation. These preliminary results are favorable for this second-generation scaffold and will be used to guide the continued creation and implementation of future silk constructs. In summary, these constructs show promise as a scalable and translatable treatment for VML injuries.

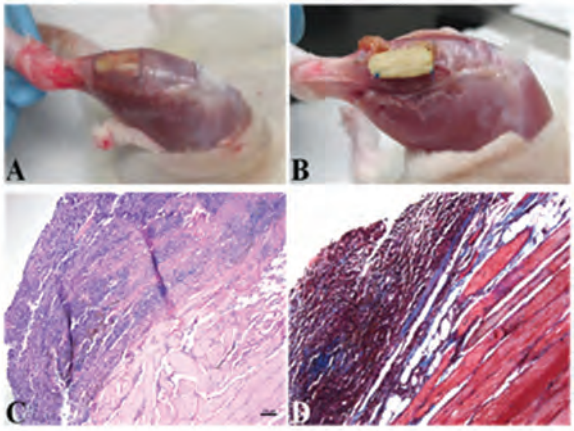

Figure 1. First-generation silk scaffold morphology and histology 3 months after implant. External tissue morphology at the fascicular layer (A) and below the fascia at the muscular layer (B). H&E stain at 100X (C) and Masson's trichrome at 100X (D).

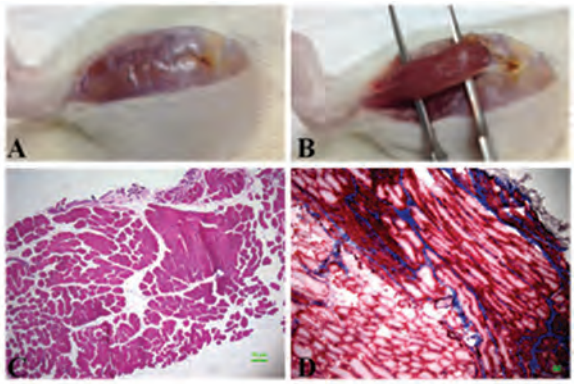

Figure 2. Second-generation silk scaffold morphology and histology 2 months after implant. External tissue morphology at the fascicular layer (A) and below the fascia at the muscular layer (B). H&E stain at 100X (C) and Masson's trichrome at 100X (D).

Evaluation of Phenotype and Scalability of Human Muscle Precursor Cells

In collaboration with the Regenerative Medicine Clinical Center team at WFIRM, the researchers characterized the expansion, proliferation, and phenotype of human MPC out to the fourth cell passage. Characterization of human muscle MPC on BAM scaffolds and after preconditioning is presently under way.

Conclusions

The most important accomplishment of this past year has been demonstration that silk is a potential scaffold for treatment of a spectrum of VML injuries.

Research Plans for Year 5

The researchers will use the guidance from a pre-Investigational New Drug (IND) teleconference with the FDA to determine the definitive toxicology and final preclinical studies required for the filing of an IND for the use of the TEMR BAM scaffold scalable sheet-based technology for the revision of primary cleft lip. They will continue to develop and optimize the controllable silk scaffold for pre-implantation cell seeding as well as improved host tissue integration and functional recovery of the rat TA VML injury model.

Planned Clinical Transitions

Two key development events are planned for Year 5. First, the researchers will hold a pre-IND teleconference with the FDA. Second, they will prepare a briefing document for submission to the FDA. Based on that conversation, their goal is to submit an IND application at end of Year 5.

The researchers anticipate proceeding with second-generation technology that increases cellular density/phenotype during bioreactor conditioning and prior to implantation. Details of this approach can be found in a recent publication supported by leveraged funding from the Telemedicine and Advanced Technology Research Center.[1]

Contingent on the FDA's acceptance of the rat TA VML injury model as the definitive preclinical study required prior to human trials, the researchers could eliminate the canine studies planned for Year 5 and accelerate the remaining toxicology, manufacturing, and second-generation studies.

Corrections/Changes Planned for Year 5

The researchers have decided to pursue a first-in-man study for cleft lip rather than Bell's palsy, as they believe this indication better suits their initial technology in the VML patient population.[2] They will continue to discuss and refine the clinical development plan internally at WFIRM, as well as consult with their colleagues at USAISR and within the craniofacial program consortium (Drs. Wong and Freeman at the University of Texas Health Science Center at Houston).

[1] Corona et al., 2012. Further development of a tissue engineered muscle repair construct in vitro for enhanced functional recovery following implantation in vivo in a murine model of volumetric muscle loss injury. *Tissue Eng Part A.* 18(11-12):1213–28.

[2] Grogan BF, Hsu JR, and Skeletal Trauma Research Consortium. 2011. Volumetric muscle loss. *J Am Acad Orthop Surg.* 2011;19 Suppl 1:S35-7.

Soft Tissue Regeneration

Develop Innervated, Vascularized Skeletal Muscle

Project 4.1.2, RCCC

Team Leader(s): Cathryn Sundback, ScD and Joseph Vacanti, MD (Massachusetts General Hospital [MGH])

Project Team Member(s): Craig Neville, PhD, Olive Mwizerwa, BS, Tom Cervantes, BS, Irina Pomerantseva, MD, PhD, and Nina Joshi, BS (MGH); Tessa Hadlock, MD and Marc Hohman, MD (Massachusetts Eye and Ear Infirmary [MEEI]); N. Sanjeeva Murthy, PhD and Joachim Kohn, PhD (Rutgers University)

Collaborator(s): Keith Baar, PhD (UCD); Jeffrey Widrick, PhD (Spaulding Rehabilitation Hospital, Boston); and Steve Stecyk, BS (Intrinsix Corp.)

Therapy: Replacement of severely injured facial skeletal muscles

Deliverable(s): Innervated, vascularized skeletal muscle

TRL Progress: 2010, TRL 3; 2011, TRL 3; 2012 (Current), TRL 3; 2013 (Target), TRL 3

Key Accomplishments: The researchers showed that prevascular networks within engineered muscle were perfused with blood by the host within 1 day of implantation and acquired native-like morphology within 14 days of implantation. They found that engineered muscle can form effective neuromuscular junctions (NMJs) and respond to neural-like electrical stimulation, inducing muscle hypertrophy and increasing the isometric contraction force. They also showed that the three tested compositions for braided polymeric sleeves had varying degradation times and showed sufficient biocompatibility in vivo.

Key Words: Tissue-engineered skeletal muscle, vascularization, innervations, orbicularis oculi

Introduction

Traumatic injuries to the head, neck, and particularly the face have been major contributors to the mortality and morbidity of military personnel in the current conflicts in Iraq and Afghanistan. A severely damaged eyelid muscle (orbicularis oculi) prevents eyelid closure, potentially resulting in blindness. Autologous tissue transfer is the standard of care, but the outcome is suboptimal. Engineered replacement orbicularis oculi muscles can restore functionality of the eyelid, prevent blindness, and restore aesthetics of the face. This therapy would improve the wounded warrior's quality of life and maximize eyelid function to allow for return to duty. In civilian populations, eyelid reconstruction with replacement muscle would significantly benefit patients with extensive eyelid skin cancers, major facial trauma, and long-standing facial paralysis with both neural and muscular deficits.

The MGH–Rutgers team is developing a muscle construct with native muscle morphology. Myotubes, differentiated from a coculture of myoblasts and fibroblasts, self-assemble to form a 3D muscle on the scale of a fascicle (500–1,000 μm in diameter). The resulting construct has the complex multinucleated muscle architecture of native neonatal skeletal muscle. The project team designed the muscle constructs to be rapidly perfused with blood and scaled to a muscle the size of the orbicularis oculi. The researchers used vasculogenesis to establish a prevascular network within the engineered muscles. To scale the muscle size, the researchers developed a highly porous sleeve scaffold from TyrPC, a bioresorbable, biocompatible material. Leveraged funding from the Congressionally Directed Medical Research Programs supported the scaffold development work.

The hypothesis of this project is that the scaled-up, 3D, engineered, innervated, and prevascularized muscle will develop sufficient muscle contractility to replace orbicularis oris function. During the first 3 years, the researchers engineered 3D vascularized skeletal muscle with morphology and

maturation metrics similar to those of immature skeletal muscle. Upon implantation, the engineered vascular networks in the muscle constructs connected with the host vasculature in less than 2 days. The researchers also began innervation studies in vitro with spinal cord (SC) explants in first 2D and then 3D differentiated muscle. They further refined prototype scaffolding to support scale-up of the MGH-engineered muscle to the size of the human orbicularis oculi muscle and confirmed biocompatibility of the scaffold.

Research Progress – Year 4

Immature skeletal muscles were produced in vitro using a coculture of primary myoblasts and fibroblasts seeded onto a fibrin gel for proliferation and differentiation. Fibrin was an appropriate scaffold material as it supported cellular proliferation and differentiation and was readily degraded during muscle construct self-assembly. Differentiation induced alignment and fusion of myoblasts to form long multinucleated myotubes. Contraction of the fibrin gel induced the cell sheet to roll and ultimately form an immature muscle 10 days after differentiation.

Vascularization

A prevascular network was established within the engineered immature muscle prior to implantation to induce rapid perfusion of the muscle construct. A coculture of endothelial cells and human MSC formed an endothelial network, supported and maintained by the MSC. Prevascularized self-assembled muscles were implanted into nude mice and harvested at 1 to 21 days post implantation. Blood vessels made from human cells were observed throughout the muscle and contained RBC. Connection of the host and engineered vasculatures occurred in less than 1 day post implantation. The permeability of the engineered vessels was assessed by Evans blue leakage. Engineered blood vessels acquired native-like morphology and were leak tight to Evans blue by day 14 post implantation.

Demonstrate Innervation of Muscle Tissue

Slices of embryonic day 12 (E12) rat SCs formed functional NMJs engineered muscle fibers in vitro. As proof-of-concept, SCs were added to 2D myoblast and fibroblast cocultures. After 7 days of coculture, neurite outgrowth from the SCs formed NMJs with 2D myotubes, which coincided with coordinated myotube contraction. Sections of SCs were incorporated into 3D self-assembling muscle. Extensive neurite outgrowth and mature NMJs were observed in 3D muscles.

Characterize Muscle Function

3D-engineered muscle was electrically stimulated with a neuronal-like stimulation pattern to improve muscle function. Muscle contractility was measured with standard in vitro muscle mechanics instrumentation following 24- or 48-hour stimulation. The engineered muscle was responsive to extended electrical stimulation and approached fused tetanus in the 48-hour stimulated muscle; a muscle recruits all motor units in a fused tetanus state, generating maximum contraction force. The specific isometric contraction force for a muscle, calculated as the maximum isometric contraction force normalized by the muscle cross-section area, increased more than 200% as a result of pulsed electrical stimulation. This contractility increase correlated with significant myofiber hypertrophy, suggesting muscle maturation.

Scale-Up of Engineered Muscle

The engineered muscle will be scaled up to the size of the human orbicularis oculi by bundling self-assembled muscles. The engineered muscle may ultimately be enclosed within a TyrPC braided sleeve, designed and fabricated by the Kohn laboratory. Alternate scaffold approaches are also being pursued.

E1002(1K) polymeric sleeves were implanted subcutaneously into rats. E1002(1K) polymer lost approximately 80% molecular weight in 4 weeks. At 3 weeks post implantation, tissue had infiltrated the sleeves, but little inflammation was found on histologic processing; only several giant cells were detected within and outside of the sleeves. A second set of scaffolds was implanted and harvested at 1, 2, 3, and 4 weeks post implantation. At the latter time points, a fibrous capsule and a moderate inflammatory infiltrate were observed along with a few giant cells.

A third set of sleeves was implanted, which contained four sleeves of E0000 polymer and five sleeves of E1001 polymer. E0000 polymers degraded in approximately 16 weeks without significant erosion while E1001 degraded in 16 weeks with some erosion. The researchers produced sleeves of varying weave tightness and implanted them into rats. Histologic analysis is ongoing.

Conclusions

The main focus in Year 4 was vascularization and in vitro innervation of the engineered muscle. Engineered endothelial networks within 3D muscle permit early perfusion of the implanted engineered muscle. This perfusion will maintain viability as the construct is scaled up. Engineered muscle was effectively innervated in vitro and responded to chronic pulsed electrical stimulation. A significant increase in specific contraction force was demonstrated after stimulation for 48 hours. Multiple scale-up approaches are being developed. The braided sleeve concept appears to be a viable concept for supporting multiple 3D-engineered muscles during implantation.

Research Plans for Year 5

Innervation of muscle tissue. The researchers will demonstrate how the host innervates 3D-engineered muscle in immunocompromised rodents. They will characterize the contractility of 3D innervated engineered muscle.

Muscle construct scale-up. The research team will assess the scaffold's impact on innervation and vascularization of engineered muscle.

Engineer human muscle on scale of orbicularis oculi. The researchers will engineer muscle tissue in vitro using human cell sources and will demonstrate innervation and vascularization of human muscle construct in an animal model. They will scale up muscle toward the size of orbicularis oculi and will assess muscle function.

Planned Clinical Transitions

Given the complexity of this product, a Request for Designation will be submitted to the FDA Office of Combination Products to determine an appropriate regulatory path. Based on this review, an IND or IDE will be filed with the Center for Biologics Evaluation and Research or the Center for Devices and Radiological Health, respectively. Preclinical (animal) studies will be performed in immunocompromised rats (contractile human muscle on the scale of a human orbicularis oculi) and in an immunocompetent rabbit model (autologous sphincter muscle with architecture similar to the orbicularis oculi).

Soft Tissue Regeneration

Composite Tissue Allograft Transplantation Without Lifelong Immunosuppression

Project 4.3.1c, RCCC

Team Leader(s): Maria Siemionow, MD, PhD, DSc (Cleveland Clinic)

Project Team Member(s): Joanna Cwykiel, MSc, Miroslaw Lukaszuk, MD, Halil Uygur, MD, Can Ozturk, MD and Maria Madajka, PhD (Cleveland Clinic)

Collaborator(s): Jim Herrman, PhD (Tolera Therapeutics)

Therapy: Fused human chimeric cell therapy for composite tissue allograft (CTA) and solid organ tolerance induction

Deliverable(s): Ex vivo created donor-recipient chimeric cell therapy for prolonged vascularized skin allograft survival

TRL Progress: 2010, TRL 3; 2011, TRL 3; 2012 (Current), TRL 3/4; 2013 (Target), TRL 4

Key Accomplishments: The researchers have proven that the fusion of cord blood cells from two unrelated donors is feasible. They established an experimental protocol for ex vivo fused human chimeric cells and the optimization of chimeric cell-culturing conditions.

They characterized the phenotype and assessed the viability of fused human chimeric cells after the fusion procedure.

In vivo experiments showed the presence of fused human chimeric cells in the athymic nude rat model.

Key Words: Ex vivo human chimeric cells, vascularized skin allograft, cell fusion, tolerance induction, cellular therapy

Introduction

Modern battlefield injuries pose a serious challenge for the medical community due to high-energy explosive materials and fragmentation weapons, which inflict tremendous destruction and multiple traumatic injuries. Blast trauma can cause severe limb and craniofacial injuries as well as large area burns. Additionally, it can cause significant foreign body loading and bacterial infection. Massive tissue loss can occur either at the time of the initial trauma or during subsequent surgical wound debridement. A great need for efficient medical treatment to cover large tissue loss due to severe variable traumas also exists in the civilian population.

The only treatment option for patients with severe extremity and craniofacial tissue loss is vascularized composite allograft (VCA) transplantation from an unrelated deceased donor. VCA transplantation is an established surgical procedure. However, the immunological aspect of it is still a challenge. Skin, lymphoid tissue, and bone marrow may generate a high immunologic response. Stem cell-based therapies are being investigated as a supportive treatment for solid organs and VCA transplantation. However, aggressive preconditioning of the recipient can diminish the success rate of graft survival and is detrimental for the recipient. In such cases, supportive therapy with donor-recipient chimeric cells may serve as an alternative method. Ex vivo created donor-recipient chimeric cells are capable of eliminating the necessity of lifelong immunosuppression in patients with non-life-threatening conditions. Reduction of severe side effects of immunosuppression will allow surgeons to improve protocols for solid organ transplantation and introduce VCA in routine clinical applications.

During the first 2 years of this project, the research team confirmed that ex vivo creation of donor–recipient chimeric cells by cellular fusion was a feasible method in a rat model. They determined

the chimeric cells' proliferative potential by colony-forming unit assays. In a rat VCA transplant model, the researchers confirmed the therapeutic potential of ex vivo fused chimeric cells as a supportive therapy combined with a selective, short-term immunosuppressive protocol of anti-αβ T-cell receptor (TCR) monoclonal antibody and cyclosporine A. In Year 3, the researchers established optimal conditions for fusion cell proliferation and improved their bone marrow preparation and isolation procedure. They performed a phenotypic characterization of their donor–recipient chimeric cells, tested the therapeutic potential of an adherent subpopulation of chimeric cells, and evaluated the cells' migratory potential.

Research Progress – Year 4

Establishing Protocol for Human Umbilical Cord Blood Fusion

The Siemionow laboratory determined that fusion of human umbilical cord blood (UCB) cells derived from two different cord blood donors is feasible. The procedure was performed as follows: After isolation of mononuclear cells from human UCB, cells were stained with fluorescent tracking dyes. Fusion was performed using polyethylene glycol (PEG). Cell fusion was determined using confocal microscopy and flow cytometry.

Evaluation of Phenotype, Genotype, and Viability of Fused Human Chimeric Cells

Phenotypic evaluation of fused human chimeric cells. The researchers performed low cytometry analysis of the fused human chimeric cells, looking for the presence of cellular surface markers. They found that the chimeric cells showed the same distribution of hematopoietic cell surface markers as cord blood cells used for the fusion procedure.

Assessment of fused human chimeric cell viability. The research team performed Annexin V staining, TUNEL assays, and viability staining to evaluate fused human chimeric cell viability and apoptosis. They demonstrated that the fusion procedure did not have a significant effect on the viability of the fused human chimeric cells.

Verification of Chimeric Cell Generation

Serological valuation of human leukocyte antigen (HLA) class I and II antigens. Phenotypic evaluation of fused human chimeric cells for the presence of HLA class I and class II antigens was performed. The human-fused chimeric cells maintained a mix of phenotypic HLA class I and II molecules on their cell surfaces that were characteristic of each donor's cord blood cells. This indicates that cells from two donors were successfully fused to form a chimeric cell.

Genetic characterization of fused cells. By determination of HLA class I and II genes specific for each of the UCB donors, the Siemionow laboratory was able to prove the presence of genetic material from both cord blood donors in the fused chimeric cells and confirm the results of the serological evaluation of the chimeric cells.

Genetic contribution of the UCB cells from each donor to the fused cells. Genetic content of fused chimeric cells was analyzed by evaluation of specific short-tandem repeat genetic markers. The presence of DNA from each of the UCB donors in the fused chimeric cells was confirmed.

Evaluation of the Effect of ex Vivo Fused Human Chimeric Cells in an Immunodeficient Rat Model

The Siemionow laboratory is currently collecting data from in vivo experiments in which fused human chimeric cells are injected into the bone of immunodeficient (athymic nude) rats. The presence of human chimeric cells was detected in the bone compartment, as well as in lymphoid tissues in the liver, skin, and lungs.

Conclusions

The Siemionow laboratory has proven that fusion of cord blood cells from two unrelated donors is feasible. Phenotypic and genotypic assessment of fused chimeric cells showed that chimeric cells maintain a mix of characteristics from both donors. High viability of fused chimeric cells was confirmed. In vivo experiments showed the presence of fused human chimeric cells in an immunodeficient (athymic nude) rat model.

Research Plans for Year 5

In Year 5, the Siemionow laboratory will continue the evaluation of human chimeric cells in vivo in the immunodeficient rat model. Different delivery routes (intravenously or intraosseously) and doses of fused chimeric cells will be used to test the viability and migratory sites of the cells. Flow cytometry, fluorescent in situ hybridization, and PCR analysis will be performed to assess the level of chimerism in peripheral blood and in the bone marrow compartment. Lymphoid tissues will be immunostained to evaluate the presence of ex vivo fused human chimeric cells and the role of these cells in lymphoid tissues in the liver, spleen, lungs, thymus, and lymph nodes. Immunofluorescent staining for the presence of multiple cell lineages including stem and progenitor cells will be performed to characterize the phenotypic profile of the chimeric cells in vivo.

Planned Clinical Transitions

At the end of Year 5, the Siemionow laboratory is planning to apply for IRB approval for the application of bone marrow-derived human-fused chimeric cells as a supportive therapy for living kidney and liver donor transplantation. Tolera Therapeutics will support the chimeric cell therapy transition to a clinical trial.

Soft Tissue Regeneration

Clinical Trial – Composite Tissue Allograft Transplantation (Face)

Project 4.3.1a, RCCC

Team Leader(s): Maria Siemionow, MD, PhD, DSc (Cleveland Clinic)

Project Team Member(s): Cheryl Smith (Cleveland Clinic)

Collaborator(s)/Secondary Sites: COL Robert Hale, DDS (USAISR)

Therapy/Deliverable(s): Composite Tissue Allograft Transplantation (Face)

TRL Progress: 2011, TRL 7; 2012 (Current), TRL 7; 2013 (Target), TRL 7

Key Accomplishments: The research team has screened 13 subjects for this study. They enrolled 5 patients in the study and completed in-depth transplant evaluations on 3 of them.

Key Words: Transplant, composite tissue allograft, immunosuppression

Introduction

Current military conflicts in Iraq and Afghanistan have created a patient cohort (approximately 400 identified patients) who could benefit from a CTA of face, upper extremity, or other tissue. In addition, 150 facial trauma or burn patients may benefit from this type of procedure.

An unmet clinical need exists for a single surgical procedure (treatment) that is capable of restoring the function and aesthetic appearance of the face. The human scalp and face define two important body units, both functionally and aesthetically. Traumatic deformities of the head and neck region resulting from burn injuries, gunshot wounds, or ablative tumor surgeries may involve a defect of a single component such as the skin, subcutaneous tissue, or muscle, or the combination of all these elements. An ideal reconstructive procedure should replace the missing tissues and restore motor and sensory function. Traditional reconstructive procedures of facial deformities involve skin grafting, local flap applications, tissue expansion, and prefabrication as well as free tissue transfers. In this clinical trial, the entire injured/absent area of the face can be replaced in one surgical procedure. Bone, skin, and vessels from other areas of the body do not need to be used for grafting. Repeated, lengthy surgeries are not required. Pain is reduced and the functional results are superior. At this time, face transplant is the only competitive technology to traditional reconstructive procedures in patients with severe facial deformities.

Clinical Trial Status

To date, 13 patients have completed prescreening for face transplantation. The enrollment continues to be open for potential candidates.

Transplant Process for Currently Enrolled Subjects

A multidisciplinary transplant team is currently evaluating three subjects to determine the best surgical approach for each patient. Transplantation evaluation is comprehensive of all body systems, and each patient receives a consult with transplant infectious disease, psychiatry, social work, and anesthesia. All subjects undergo extensive laboratory, diagnostic, and radiologic testing during evaluation. The principal investigator and the multidisciplinary transplant team analyze and discuss all results and consults with the goal of optimal patient reconstruction. Due to the complexity and need for lifelong immunosuppression, a Participant Protection Liaison is assigned to all potential face transplant recipients with reporting requirements to the Cleveland Clinic IRB.

Clinical Plans for Year 5

The researchers will continue to screen subjects for this study based upon IRB-approved inclusion/exclusion criteria. Extensive evaluation will occur for those subjects who meet inclusion/exclusion criteria and consent to enrollment in the study. The goal for Year 5 will be to list one to two subjects for face transplantation and perform this procedure according to the surgical protocol outlined for each subject. Patient safety and monitoring regulations will be followed according to IRB and the USAMRMC's HRPO regulations. All IRB and HRPO reporting and accreditation requirements will be met.

Corrections/Changes Planned for Year 5

To increase subject screening and potential enrollment, an information sheet was created for distribution to referring physicians. IRB and HRPO approval was obtained prior to distribution. Every effort is made to provide a seamless referral process from military hospitals to Cleveland Clinic.

Soft Tissue Regeneration

Clinical Trial – Anti-TCR Monoclonal Antibody (TOL-101), for Prophylaxis of Acute Organ Rejection in Patients Receiving Renal Transplantation

Project 4.3.1b, RCCC

Team Leader(s): Maria Siemionow, MD, PhD, DSc (Cleveland Clinic)

Project Team Member(s): Stuart Flechner, MD, David Goldfarb, MD, Titte Srinivas, MD, Richard Fatica, MD, Jon Myles, MD and Andres Chiesa-Vottero, MD (Cleveland Clinic)

Collaborator(s)/Secondary Sites: University of Colorado, Denver, Baylor University Medical Center, Medical University of South Carolina, St. Barnabas Medical Center, University of Michigan, University of Utah, University of Kentucky, Baylor All Saints, Buffalo General Hospital, University of Virginia, Montefiore Medical Center

Therapy/Deliverable(s): TOL-101, which is an anti-αβ-T-cell receptor murine IgMK monoclonal antibody

TRL Progress: 2011, TRL 6; 2012 (Current), TRL 7; 2013 (Target), TRL 7

Key Accomplishments: The researchers have completed all operational requirements to facilitate the setup and operations of the Core Laboratory at the Cleveland Clinic. They received 29 biopsies from participating centers and have evaluated 19 of the biopsies to date. They completed 7 cases, with a completed case being defined as all expected biopsies having been received and reported on.

Key Words: TOL-101, anti- T-cell receptor monoclonal antibody, renal transplantation

Introduction

An unmet clinical need exists for both the military and civilian transplant populations for an agent that is capable of selectively depleting specific T cells in a nonmitogenic manner, without unnecessarily exposing the transplant recipient to nonspecific or open-ended immune suppression, which may exacerbate the risks of infections and malignancies. A more specific approach to the prevention of acute organ rejection is by selectively targeting the αβ-TCR and sparing T cells, which may provide similar or better efficacy than the currently used T-cell depleting antibodies.

The main hypothesis of this Phase 1/2 clinical trial is that use of the selectively blocking αβ-TCR antibody, TOL-101, will result in a lower incidence of opportunistic infections, faster recovery of the immune system of kidney allograft recipients, and a better functional outcome, which will be confirmed by kidney function assays and kidney biopsies. The research team hopes that this clinical trial, which is specifically focused on studying the safety, pharmacokinetics, pharmacodynamics evaluation, and preliminary efficacy (of ascending doses) of TOL-101 in subjects undergoing their first renal transplantation, may greatly decrease or eliminate the need for a lifelong immunosuppressive drug regimen.

The Cleveland Clinic Pathology and Laboratory Medicine Core Laboratory is contributing to this clinical trial through its analysis of the kidney biopsy samples. The project team expects to continue through all phases of the clinical trial, and if results are positive, then TOL-101 would be applied as an induction therapy for various kinds of transplants, including composite face/bone allografts. TOL-101 could help surgeons to reconstruct complex craniofacial defects for both military service members and civilians, by providing a safer antibody that would potentially reduce side effects such as

opportunistic infections, cytokine release syndrome (a type of inflammatory response), and the development of myeloproliferative diseases (i.e., diseases that cause abnormal growth of blood cells in the bone marrow).

The nonclinical studies that have been conducted with TOL-101 support the potential efficacy and safety of this novel antibody in renal transplant patients. Tolera Therapeutics, Inc. has shown that TOL-101 is biochemically and functionally similar to its predecessor antibodies, MEDI-500 and T10B9, in a number of assays and that the clinical safety and efficacy data obtained with the predecessor antibodies may be relevant to the clinical evaluation of TOL-101. T10B9 and MEDI-500 were administered to 135 subjects in 13 studies from 1986 to 2000 by Dr. John Thompson at University of Kentucky and by MedImmune, Inc., with 100 subjects being recipients of solid organ transplants. Clinical studies have demonstrated the safety and effectiveness of these predecessor antibodies in minimizing adverse cytokine release and in preserving γδ T cells while specifically inhibiting αβ T cells.

TOL-101 is being evaluated in this clinical trial as part of an immunosuppression regimen that includes steroids, mycophenolate mofetil, and tacrolimus, an immunosuppressive drug used to lower the risk of rejection, in first-time kidney transplant recipients. The researchers are testing to see if TOL-101 demonstrates a lower incidence of side effects such as opportunistic infections, cytokine release syndrome, and development of myeloproliferative diseases, compared to standard immunosuppressive regimens.

Clinical Trial Status

Enrollment

To date, 28 subjects have been enrolled in 7 cohorts, including 6 cohorts of a fixed dose and 1 dose-escalation cohort. The dose-escalation cohort enrolled 2 subjects who received living donor kidneys and 4 subjects that received deceased donor kidneys.

Data were sent to the Data Monitoring Committee (DMC) on April 30, 2012, for its review and recommendations. The DMC declared the first dose-escalation cohort (DE 1) to be the Potentially Therapeutic Dose-A (PTD-A). The DMC recommended opening a cohort of 6 subjects to receive deceased donor kidneys to test a 5- to 12-dose regimen for a possible PTD-B. Enrollment is on hold pending a protocol amendment.

Adverse Events

In the DE 1 cohort, drug-related adverse events (AEs) were limited to a transient rash (2 subjects) and pruritis (2 subjects). There have been no other significant drug-related AEs reported. In total, 23 serious adverse events (SAEs) have been reported. One SAE was possibly related to the study drug (pneumonia).

Other Activities

The researchers completed all operational requirements to facilitate the setup and operations of the Core Laboratory for biopsy evaluation, which includes programming of the OnCore database to record biopsy results, training of key laboratory personnel, and receipt and processing of all biopsy slides from clinical sites. They received 29 biopsies from participating centers and have evaluated 19 of the biopsies to date. They completed 7 cases, with a completed case being defined as all expected biopsies having been received and reported on.

Conclusions

This open-label, two-part, multicenter, first-in-human study is investigating the safety, preliminary efficacy, and immunogenicity of TOL-101 administered to first-time kidney transplant recipients. It has a modified adaptive design including an initial dose-escalation component followed by a randomized active control component. Study goals for collaborating centers and study participants are being met. The first part of the study (Part A), with the goal of identifying two potentially therapeutic dose levels (PTD-A and PTD-B), is in process with limited AEs related to the study drug.

Clinical Plans for Year 5

Tolera Therapeutics, Inc. and Cleveland Clinic Pathology and Laboratory Medicine Institute will continue to monitor and complete biopsy reports on participants in this study. Results will continue to be transmitted to Tolera Therapeutics, Inc. as required.

Cartilage Regeneration (Focus: Ear)

Engineered Cartilage Covered Ear Implants for Auricular Reconstruction

Project 4.1.1, WFPC

Team Leader(s): James J. Yoo, MD, PhD (Wake Forest University)

Project Team Member(s): Sang Jin Lee, PhD, John Jackson, PhD, Chang Mo Hwang, PhD, Young Min Ju, PhD, Cheil Kim, MD, PhD, Idris El-Amin, DVM and Denethia Green, BS (Wake Forest University)

Collaborator(s): Greg Sword (Porex Surgical, Stryker)

Therapy: Reconstruction of the external ear

Deliverable(s): Engineered cartilage tissue covering the commercially available alloplastic implant

TRL Progress: 2008 (Start), TRL 3; 2009, TRL 3; 2010, TRL 4; 2011, TRL 4; 2012 (Current), TRL 4; 2013 (Target), TRL 4

Key Accomplishments: The researchers have fabricated a flexible ear scaffold using an integrated organ printing technology. During the past year, they characterized the isolation and growth of chondrocytes from ear, nose, and rib cartilage of humans and rabbits. They also continued to evaluate the structural and functional integrity of engineered cartilage-covered ear constructs for clinical application by implanting autologous chondrocyte-coated ear constructs in rabbits. Post implantation, the ear constructs showed no evidence of skin necrosis, implant exposure, or extrusion. In addition, they exhibited similar mechanical characteristics to natural ear cartilage.

Key Words: Auricular cartilage, chondrocytes, alloplastic ear implant, reconstruction, tissue engineering

Introduction

Traumatic injuries constitute a major cause of morbidity and mortality for the armed forces. The incidence of craniofacial injuries has been rapidly increasing due to the frequent ballistic and explosive injuries on the battlefield. Protruding tissues such as ear and nose are frequently affected in these injuries. Although the loss of ear tissue does not pose life-threatening danger, it is functionally and cosmetically debilitating and hinders injured soldiers from returning to society.

The standard treatment method for auricular reconstruction uses autologous costal cartilage as a graft material. However, autologous costal cartilage is limited in supply, provides inadequate dimensions, and is progressively absorbed after implantation. A current alternative approach involves the use of alloplastic ear implant devices composed of silicone or polyethylene. These implants are approved by the FDA, and they are nontoxic, cause minimal foreign body reactions, and possess adequate mechanical properties for use in non-load-bearing tissues of the craniofacial region. Although alloplastic ear implants are able to effectively eliminate the morbidity associated with the costal cartilage graft, the use of these implants is often related to complications including inflammation, infection, erosion, and dislodgement. Also, implant extrusion occurs frequently due to the limited vascularization and constant abrasion against the surrounding tissues. A common practice to overcome these complications includes the use of a temporo-parietal tissue flap from the side of the head to cover the implant, which provides a vascularized tissue cushion against the abrasive implant.

In this project, the researchers have developed an engineered cartilage that entirely covers the ear implant, which prevents implant exposure and extrusion while maintaining the appropriate mechanical properties. Creation of cartilage tissue using a soldier's own cells is beneficial since it minimizes the morbidity associated with implant

dislodgement. The research team plans to further refine and optimize the processing system for a smooth translation into soldiers who require auricular reconstruction.

During the first 3 years of the project, the researchers prepared fibrin hydrogels with various concentrations of fibrinogen and thrombin, mixed cultured chondrocytes with the hydrogels, and implanted the constructs subcutaneously into athymic mice. They harvested the mice at various times post implantation. While nontreated ear implants resulted in severe skin necrosis at 2 weeks post implantation, cartilage-covered ear implants were able to maintain device contour and placement without causing skin necrosis. The researchers fabricated a flexible ear scaffold using an integrated organ bioprinting technology. They optimized cell isolation and culture procedures by characterizing auricular chondrocytes from fresh ear cartilage tissue biopsies from rabbits in terms of cell growth, maintenance of phenotypic and functional characteristics, and the quality of neocartilage formation.

Research Progress – Year 4

During the past year, the researchers continued cell isolation and expansion using different cell sources, including ear, nose, and rib cartilages of human and rabbit origins. They optimized cell isolation efficiency and cell growth, as well as the maintenance of phenotypic and functional expression, and ECM production. They continued to develop SOPs for autologous cell sourcing, the expansion system, and the cell delivery system (human origins). The researchers also developed and fabricated a novel flexible ear scaffold that mimics ear cartilage using an integrated organ printer system and evaluated the flexible ear implants both in vitro and in vivo (described in the following paragraphs).

Customized Ear-Shaped Scaffold Construction Using Integrated Organ Printer System

The research team developed a computerized bioprinting system that is composed of a three-axis stage, a high-precision pressure and temperature controller, and four cartridges. A flexible ear-shaped scaffold is fabricated by the bioprinting system. **Figure 1** shows the process used to obtain a motion program for scaffold fabrication using a 3D CAD (computer-aided design) model. This motion program (a command list for operating the bioprinting system) is transferred to the bioprinting system, and then a scaffold with a desired 3D shape can be fabricated. The researchers used poly(ε-caprolactone) (PCL) as a scaffold material for ear construction. They performed PCL printing with a nozzle of 300 μm inner diameter under temperature and pressure ranges of 80°C–90°C and 750–800 kPa, respectively.

The researchers were able to use the integrated organ printing system to fabricate ear implants with primary chondrocytes (40 M cells/mL) in a controlled manner. After being implanted in rabbits, the ear constructs showed no evidence of skin necrosis, implant exposure, or extrusion. In addition, the ear constructs exhibited similar mechanical characteristics (elasticity) to those of natural ear cartilage (**Figure 2A**). Notably, ear implants without cells (controls) resulted in the severe exposure of the PCL scaffold.

Histomorphological evaluation revealed the formation of neocartilage in the implants (Figures 2B and C). The researchers demonstrated the consistent presence of evenly dispersed triangular and ovoid-shaped chondrocytes with lacunae, surrounded by perichondrium. Safranin-O staining confirmed the presence of sulfated glycosaminoglycans (GAG), indicating that a mature neocartilage framework had formed. These results demonstrate that bioprinting of PCL ear scaffolds has the potential for

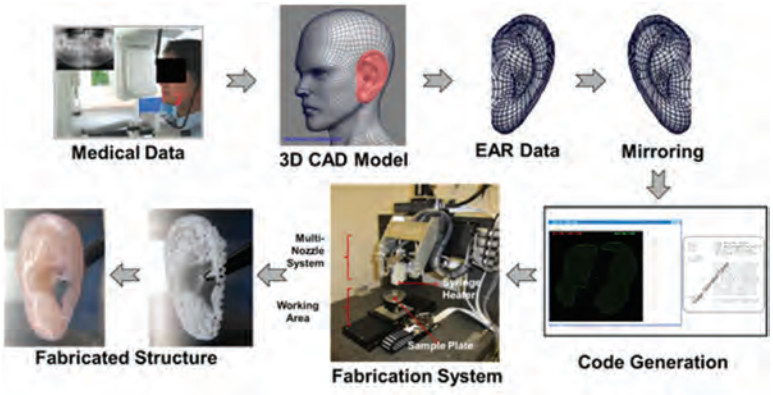

Figure 1. Customized ear-shaped scaffold construction using an integrated organ printer system.

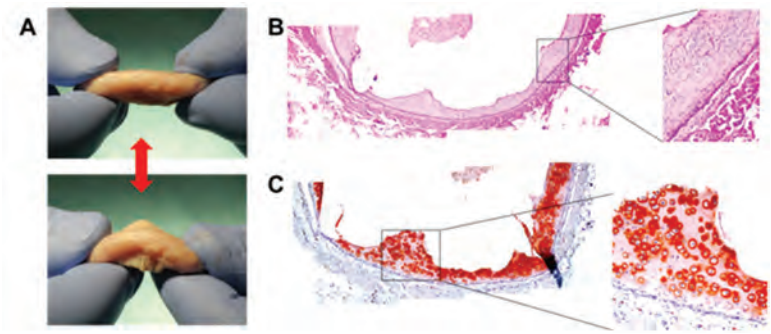

Figure 2. (A) The flexible ear scaffold can be customized for the patient's unique size and shape. (B) H&E staining and (C) Safranin-O staining of a bioprinted ear scaffold 2 months post implantation in vivo.

patient-specific complex ear shape fabrication with reproducible cartilage formation in vivo.

The final goal of ear reconstruction is aesthetic recovery to the satisfaction of the patients. To achieve this goal, the fabricated ear should be symmetrical with the ear on the other side of the head. 3D reconstruction and replication after mirroring of the existing ear can provide a high level of symmetry between the two ears of patients. 3D bioprinting can provide patient-specific 3D scaffolds with high symmetry in a short amount of time and can be used for optimized cartilage regeneration. The researchers demonstrated that their computerized bioprinting technology could be applied for the fabrication of a clinically relevant scaffolding system for auricular reconstruction. Their results demonstrated that bioprinting of PCL ear scaffolds has the potential to fabricate patient-specific complex ear shapes with reproducible cartilage formation in vivo.

Conclusions

The researchers isolated and grew human chondrocytes from several sources. Notably, the identification of the optimal tissue source for covering an implant will be important for future clinical trials. The research team also fabricated a flexible 3D engineered ear implant using a bioprinter. In addition, the researchers initiated a transplant study in a rabbit model using ear implants coated with autologous chondrocytes.

Research Plans for Year 5

The researchers will complete the autologous rabbit transplant study. They will also complete SOPs for autologous cell sourcing, the expansion system, and the cell delivery system of human chondrocytes. They will refine the cell delivery system for clinical use.

Planned Clinical Transitions

The researchers plan to prepare documents and initiate communications with the FDA for a clinical trial.

Cartilage Regeneration (Focus: Ear)

Engineering a Replacement Autologous Outer Ear Using a Collagen/Titanium Platform

Project 4.5.4, RCCC

Team Leader(s): Cathryn Sundback, ScD and Joseph P. Vacanti, MD (MGH)

Project Team Member(s): Mack Cheney, MD, Tessa Hadlock, MD, Marc Hohman, MD (MEEI, Facial Plastic Surgery); Irina Pomerantseva, MD, PhD, Craig Neville, PhD, Nina Joshi, Tom Cervantes, Alan Tseng, and Danai Chagwedera (MGH Tissue Engineering); Mark A. Randolph and Matt Johnson (MGH Plastic Surgery Research Laboratory)

Collaborator(s): Nicholas Roscioli (Kensey Nash Corp.)

Therapy: Tissue-engineered cartilage constructs for ear replacement

Deliverable(s): A permanent implantable engineered living external ear replacement for the wounded warfighter

TRL Progress: 2010, TRL 3; 2011, TRL 3; 2012 (Current), TRL 4; 2013 (Target), TRL 5

Key Accomplishments: The researchers finalized in vitro protocols and achieved high-quality stable auricular cartilage in a large immunocompetent animal (sheep) model. Specifically, they confirmed that the shape and size of the engineered auricle were preserved by the embedded titanium wire coil for up to 20 weeks in the sheep. In addition, high-quality stable autologous elastic cartilage was engineered in sheep using extensively expanded chondrocytes.

Key Words: Tissue-engineered ear, cartilage, porous collagen, chondrocytes

Introduction

Following blast injuries to the head and neck, limited options exist for reconstructing the external ear. Current clinical approaches include implantation of a cartilage framework that is hand-carved in the operating room from patient's own (autologous) rib cartilage or a synthetic ear-shaped implantation made of porous polyethylene (Medpor®). Both reconstructive options are prone to complications, require multiple surgeries, and have unpredictable and often poor cosmetic outcomes. The MGH team found initial success in engineering ear-shaped cartilage using biodegradable scaffolds and chondrocytes. Tissue-engineered autologous ear replacements would combine the best of both current clinical approaches. Because of the precisely defined architecture of Medpor implants and the autologous properties of carved cartilage, the required number of surgeries could be reduced from four to two. The greatest challenge is to maintain the complex 3D structure of largely unsupported ear cartilage, especially when it is subjected to the mechanical forces of the surrounding tissues during cartilage maturation and wound healing after implantation. The second challenge, occurring specifically in the military population, is the difficulty in obtaining a sufficient number of autologous chondrocytes from a very limited source of undamaged cartilage. In this project, the researchers seek to develop a permanent, implantable, living external ear for the injured service member, and to achieve cosmetic outcomes that meet patient expectations.

During the first 3 years of the project, the research team developed an ovine model for subcutaneous implantation of ear-shaped constructs. The researchers engineered cartilage from both ovine and human cartilage cells and MSC in immunocompromised mice. They also designed ear-shaped scaffolds using CAD principles and tested the scaffolds with numerous materials. The researchers demonstrated robust autologous cartilage formation on porous fibrillar collagen scaffolds in an immunocompetent sheep model. They also

demonstrated the effectiveness of internal support in maintaining the size and shape of human-ear-shaped neocartilage constructs in a proof-of-concept study in nude mice. In a pilot study, they found that mixing culture-expanded P3 chrondrocytes with freshly isolated P0 chondrocytes, followed by expansion in bFGF-supplemented medium, led to robust neocartilage formation in nude mice. The size and shape of neocartilage were maintained using a new-generation, adult-size human ear-shaped scaffold in a nude rat model.

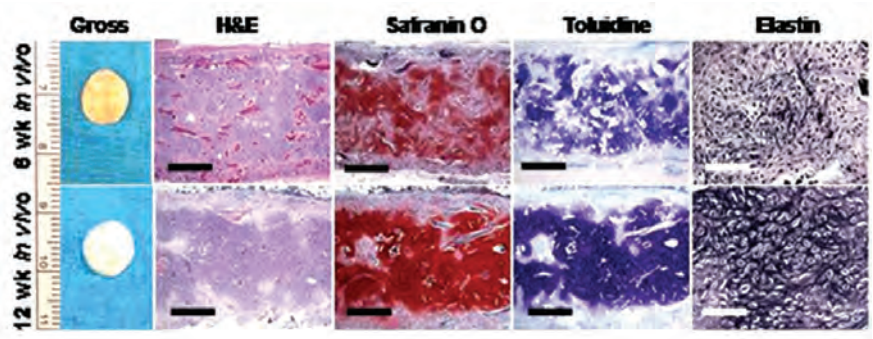

Figure 1. Gross and histological appearance of cartilage engineered in sheep using extensively expanded chondrocytes mixed with freshly isolated chondrocytes. Neocartilage was stable and its quality improved with longer implantation times as evidenced by an increase in elastin expression. Scale bars, 500 µm, except 100 µm for elastin.

Research Progress – Year 4

Develop Reliable Cell Source

In human patients, the cartilage biopsy size is limited by its availability and/or quality, aesthetic considerations, or donor-site morbidity. A sufficient number of cells can be achieved by extensive chondrocyte proliferation in vitro. However, with repeated passaging, cartilage cells "de-differentiate" and lose their potential to form neocartilage.

Demonstrate neocartilage formation and stability in immunocompromised animals (animal and human cells) using re-differentiated chondrocytes expanded beyond 300-fold. The results obtained during the past year confirmed the earlier proof-of-concept findings and demonstrated, for the first time, the ability to form high-quality neocartilage using extensively expanded chondrocytes in an immunocompromised nude mouse model.

Demonstrate neocartilage formation and stability in autologous sheep model using re-differentiated chondrocytes expanded beyond 300-fold. Formation of neocartilage engineered from extensively expanded chondrocytes was followed for 6 and 12 weeks in sheep. The size of neocartilage was largely maintained during the experiment (**Figure 1**). Histologically, high-quality neocartilage was present throughout the implants after both 6 and 12 weeks in sheep as evidenced by staining for sulfated GAG with safranin O and toluidine blue. The quality of the stable neocartilage improved with longer implantation times, as seen by increased elastin staining (Figure 1). The MGH pilot studies validated the ability of extensively expanded chondrocytes to form neocartilage in sheep. Additional studies in large immunocompetent animals will be needed to further develop the methodologies and evaluate the quality and long-term stability of auricular neocartilage engineered from extensively expanded chondrocytes. These studies will be critical for translation of the developed methodologies to human trials.

Assess Shape and Size Retention and Formation of Neocartilage in the Adult Human Ear-Shaped Scaffolds in vivo

Evaluate retention of original ear size and shape in sheep, achieving TRL 4 upon completion. Human ear-shaped constructs with internal wire support retained a characteristic ear shape both at 12 and 20 weeks in a sheep model (**Figure 2**). Histologically, neocartilage formed throughout ear-shaped constructs at 20 weeks post implantation (**Figure 3**). These data confirm earlier findings in immunocompromised rodent models and demonstrate the efficacy of embedded titanium wire scaffolds in the preservation of size and shape. The embedded wire had no negative effect on neocartilage formation in a large immunocompetent animal model over the period of 20 weeks. High-quality neocartilage was demonstrated in sheep for up to 20 weeks (**Figure 4**). Neocartilage ECM stained intensely with safranin

O and toluidine blue, indicating the presence of abundant GAG. Cartilage-specific collagen type II staining was positive at all time points. Moreover, the elastic nature of neocartilage was confirmed; the intensity and distribution of elastin fibers gradually increased from very scant at 6 weeks to that similar to native auricular cartilage at 20 weeks.

Successful demonstration of the high-quality stable neocartilage and retention of original ear size and shape in a subcutaneous sheep model over an extended period of time are important milestones in the development of the MGH-engineered replacement ear, advancing the research to TRL 4.

Modify ear scaffold design. Based on the results of in vivo testing of the ear-shaped scaffolds in nude rats, it became evident that the latest ear scaffold design had progressively suboptimal coverage of the metal skeleton as in vivo incubation time increased. Shrinkage of excessively thin collagen scaffold material during neocartilage maturation is believed to happen after progressive exposure to the wire skeleton. To address this coverage problem, the molds used for fabricating the scaffolds were modified to enlarge the space surrounding the metal skeleton. This enlargement allows for an increase of collagen scaffold material, which should translate to an improvement in cartilage coverage of the metal skeleton.

Conclusions

Embedded titanium wire coil helped preserve the engineered auricle shape and size for up to 20 weeks in a large immunocompetent host. Autologous neocartilage was stable and its quality improved with longer implantation time. High-quality stable autologous elastic cartilage was engineered in sheep using extensively expanded chondrocytes. Successful engineering of stable human ear-shaped cartilage in a large immunocompetent host represents an important milestone in the MGH translational program to develop a replacement living auricle for patients with external ear defects.

Research Plans for Year 5

In Year 5, the MGH team will continue developing clinically relevant cell sources for the engineered ear. Stability of neocartilage engineered from extensively expanded chondrocytes and retention of the size and shape of ear-shaped scaffolds will be assessed in immunocompromised rats using sheep and human cells. The next generation of full-size human ear-shaped constructs will be tested to assess size and shape retention in an immunocompetent animal model. In preparation for clinical trials, the researchers will perform a Good Laboratory Practice (GLP) preclinical trial in sheep to demonstrate the safety and efficacy of the engineered ear.

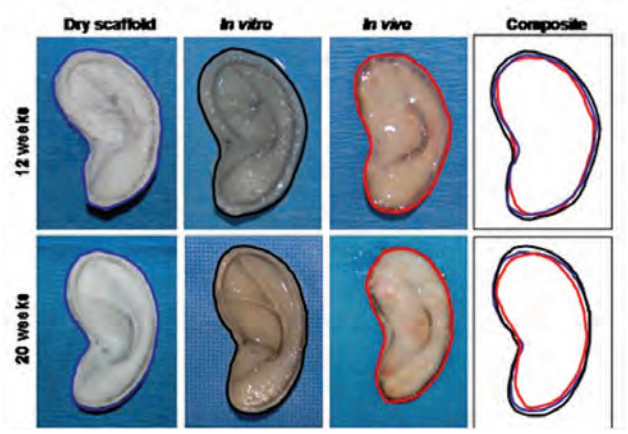

Figure 2. Gross images of ear-shaped constructs tested in sheep. The dimensional changes were minimal at both time points: 5.3% in length and 3.4% in width after 12 weeks and 4.9% in length and 2.9% in width after 20 weeks in vivo.

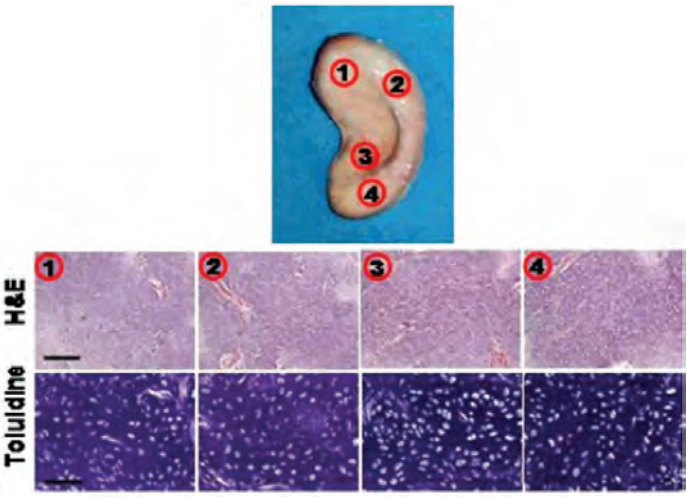

Figure 3. Histological appearance of ear-shaped cartilage in sheep at 20 weeks. Quality cartilage was demonstrated in biopsies obtained from four locations in engineered ear. Scale bars, 200 μm for H&E and 100 μm for toluidine.

Planned Clinical Transitions

The engineered ear is a combination product, and therefore the MGH team will submit a Request of Designation to the Office of Combination Products of the FDA to determine the regulatory path. Subsequently, the MGH team will hold a pre-IND or IDE meeting with the appropriate FDA agency and will prepare and file the required documentation. The MGH team representatives will audit Kensey Nash Corp., the manufacturer of the scaffolds, and the Harvard Medical School GMP facility, where cells and seeded scaffolds will be cultured. The MGH team will develop a clinical trial protocol, which will include preclinical data from small and large animal studies and submit it to the local IRB. After the approval from the local IRB is obtained, the MGH team will submit the clinical protocol to the USAMRMC HRPO for review.

Corrections/Changes Planned for Year 5

The MGH researchers will further validate the methodologies for acquiring sufficient cell population for the engineered ear. Originally, MGH collaborators at MIT supplemented primary chondrocytes with MSC. Their results are encouraging; however, the scale-up studies were not performed and the possibility of using stem cells for auricular cartilage repair in a clinical trial within the next year remains unclear. The MGH team has refocused its attention on using extensively expanded primary chondrocytes. The project team will assess the neocartilage stability and retention of the size and shape of ear-shaped scaffolds in sheep in long-term sheep studies. A preclinical GLP sheep study will be initiated depending on the level of funding.

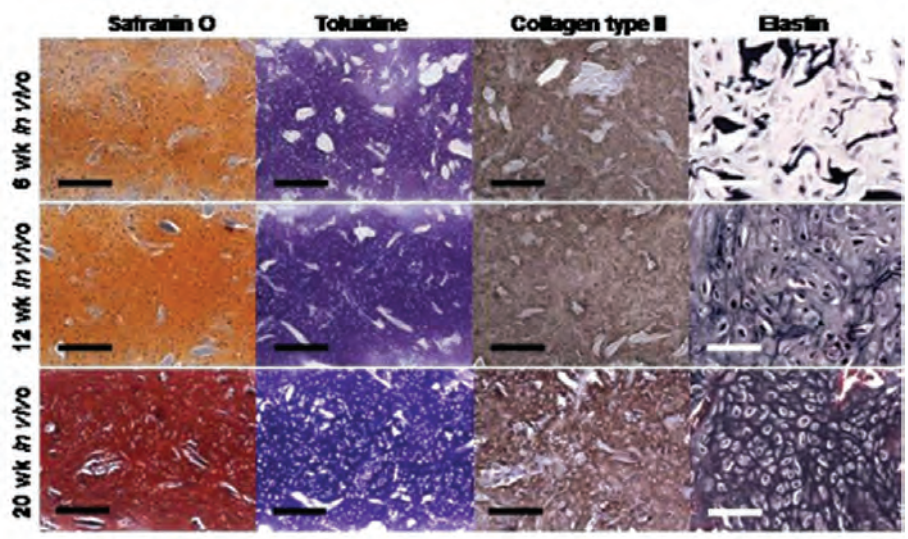

Figure 4. Histological evaluation of cartilage engineered in sheep in long-term studies. Neocartilage was stable and its quality improved with longer implantation time, as evidenced by increase in elastin expression. Scale bars, 200 μm, except 100 μm for elastin.

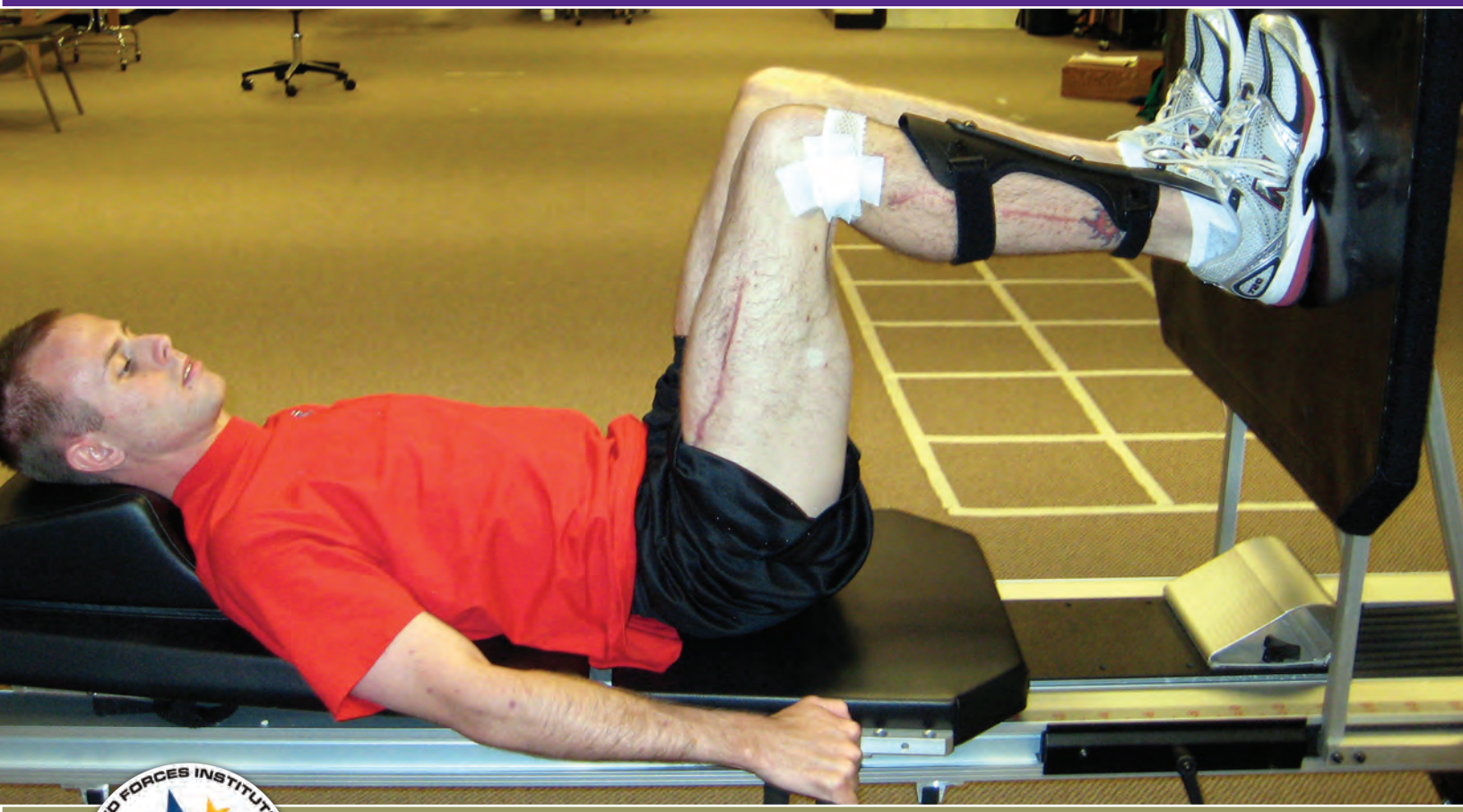

IV: Scarless Wound Healing

Control of Wound Environment and Mechanics

Mechanical Manipulation of the Wound Environment to Reduce Manifestation of Scar

Project 4.5.1, WFPC

Team Leader(s): Geoffrey C. Gurtner, MD (Stanford University)

Project Team Member(s): Michael T. Longaker, MD, MBA (Stanford University) and Reinhold Dauskardt, PhD (Stanford University)

Collaborator(s): Neodyne Biosciences and Biomaterials and Advanced Drug Delivery Center at Stanford University

Therapy: Control of wound environment to minimize scarring

Deliverable(s): *Baseline:* Battlefield-ready, region-specific devices capable of stress-shielding mechanical forces to minimize scar formation

Revised: Novel molecular targets in scar mechanotransduction and drug-eluting mechanomodulatory scaffolds capable of mitigating fibrosis

TRL Progress: 2008, TRL 4; 2010, TRL 6; 2011, TRL 7; 2012 (Current), TRL 7

Key Accomplishment(s): The Stanford group has identified a key role for the molecular target focal adhesion kinase (FAK) in the regulation of inflammatory pathways contributing to skin fibrosis. They found that FAK knockdown results in a decrease in transcriptional levels of inflammatory cytokines including monocyte chemoattractant protein-1 (MCP1), both in vitro and in vivo. Exogenous administration of MCP1 to incisional wounds was found to recapitulate features of hypertrophic scars. The researchers identified the mitogen-activated protein kinase ERK as a critical downstream effector of FAK signaling. They also demonstrated molecular evidence of inflammation in wild-type scars, including activated fibroblasts, macrophage infiltrates, and inflammatory cytokines, all of which were reduced in scars in FAK knockout mice. Finally, they demonstrated that topical application of a small molecule FAK inhibitor reduced hypertrophic scarring of mechanically loaded wounds.

Key Words: Hypertrophic scarring, wound device, mechanotransduction, fibrosis

Introduction

Scar formation following trauma and burn injury leads to severe functional disability and disfigurement. Multiple factors are known to influence wound repair (such as inflammation, oxygen tension, and ischemia) but therapeutic modalities aimed at these targets have been largely unsuccessful. Mechanical force has long been recognized to influence cellular behavior in vitro, and clinical observations based on Langer's lines and hypertrophic scarring corroborate this phenomenon in vivo.[1] The Gurtner group recently published the first murine model of hypertrophic scarring based on increasing the skin stress of healing wounds.[2] They found that intrinsic skin mechanics correlated with scarring phenotype following wounding, as low mechanical stress fetal wounds exhibited minimal fibrosis and stiffer human skin displayed robust scarring. These findings prompted the research team to examine the role of mechanical stress in scar formation and to develop a novel device to actively control wound environment mechanics to mitigate fibrosis. Ultimately, the Stanford group aims to create battlefield-ready, region-specific devices for different wounded areas of the body, capable of precision stress-shielding of mechanical forces to minimize scar formation.

[1] Edlich, RF, and Carl, BA. 1998. *The Journal of Emergency Medicine* 16:759-760.
[2] Aarabi, S. et al. 2007. *FASEB J* 21:3250-3261

There are no commercially available wound care products that specifically address the mechanical stress state of healing wounds to reduce scarring. Elastic bandages and pressure dressings provide a widely variable range of compressive forces and are generally used for hemostatic purposes but not directly for scar attenuation. Negative pressure wound sponge devices (WoundVac) are used on large, open exudative wounds but require elaborate components and an electrical energy source. In addition, their mechanism of action is in part based on increasing mechanical stimulation. In contrast to existing wound care options, the Stanford group's technology enables precision stress-shielding of area-specific wound forces through a portable, ready-to-use, simple pressure adhesive dressing that can be readily employed on the battlefield immediately following injury.

Additionally, current mechanotransduction literature implicates a central role for cell-matrix interactions in scar mechanotransduction. Specifically, FAK has been identified as a potential target in the mechanical activation of inflammation and fibrosis.[3] This molecular target may be a driving force in the formation of human hypertrophic scarring. As such, the Stanford group modified its project approach to consider developing drug-eluting devices targeting FAK in combination with mechanical control of wound forces.

During the first year of the project, the researchers determined that the Duroc pig is an ideal choice for biomechanical skin studies. They developed the first generation of safe, durable, and modifiable simple pressure adhesive dressings that could modify mechanical forces and alter scarring and fibrosis after injury. They determined that the dressings could be used on incisional swine wounds to effectively and reliably regulate wound stress and fibrosis following injury. During Year 2, the researchers completed a Phase 1/2 first-in-human study, which demonstrated that mechanical forces can be effectively off-loaded with a polymer device to prevent hypertrophic scar formation. They found a significant reduction in scar formation in wounds treated with the stress-shielding device compared to untreated wounds. A Phase 3 study, outside of this AFIRM project, was subsequently initiated with DoD support. In Year 3, the Stanford group validated its excisional wound model, showing that their novel stress-shielding polymer device could be effective for wounds more complex than linear incisions. Preliminary studies using a fibroblast-specific FAK knockout (KO) mice strain developed by the researchers indicated that FAK is a key mediator of load-induced fibrosis.

Research Progress – Year 4

In Year 4, the Stanford group verified that the FAK KO mice had decreased collagen deposition and scar tissue compared to wild-type mice (**Figure 1**). Further transcriptional analyses of FAK KO wounds demonstrated a decrease in expression of the inflammatory cytokine MCP1, which was verified by western blot analysis. Immunolocalization of

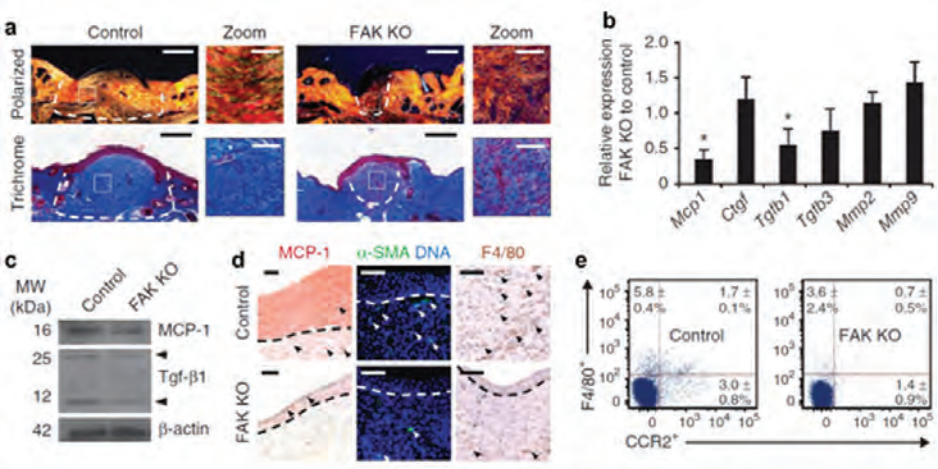

Figure 1. (a) Polarized light and trichrome-stained tissue sections demonstrate a reduction in collagen deposition in FAK KO scars. (b) Real-time polymerase chain reaction reveals a quantitative decrease in MCP1 and TGFb1 transcription in FAK KO wounds, (c) with validation by immunoblot. (d) Decreased immunolocalization of MCP1, alpha-smooth muscle actin (α-SMA)+ cells, and F4/80+ cells (e) is followed by flow cytometry demonstrating a reduction in F4/80+ and CCR2+ cells in FAK KO tissue.

[3] Parsons, J.T. 2003. *J Cell Sci* 116:1409-16.

histologic sections confirmed a reduction in MCP1 in FAK KO wounds as well as a reduction in macrophages and activated fibroblasts. MCP1 injection into wild-type wounds exacerbated scarring and resulted in increased macrophage recruitment into wounds (**Figure 2**), further demonstrating the relevance of a FAK-MCP1 pathway to hypertrophic scar formation. Topical treatment of mechanically loaded murine wounds with a FAK inhibitor reduced gross scar area and histologic evidence of scarring (**Figure 3**). These studies suggest the importance of fibroblast FAK in mechanosensation and inflammatory signaling through MCP1 in effecting hypertrophic scarring. Preclinical studies demonstrated that pharmacologic inhibition of FAK is therefore a promising therapeutic strategy for reducing wound inflammation and scarring (**Figure 4**).

Conclusions

The Stanford group has successfully demonstrated that fibroblast FAK plays a critical mechanosensory role in the skin. Activation of FAK in high tension wound environments precipitates an inflammatory cascade of events, including MCP1 secretion, that results in collagen deposition and scarring. Pharmacologic inhibition of FAK reduces wound inflammation and scarring and holds great potential for treatment and prevention of scarring.

Research Plans for Year 5

The Stanford group is planning to further investigate the role of FAK in cutaneous wound healing by exploring the function of keratinocyte FAK in wound healing and scarring. A keratinocyte-specific FAK KO mouse is currently in development and will be used to investigate the effects

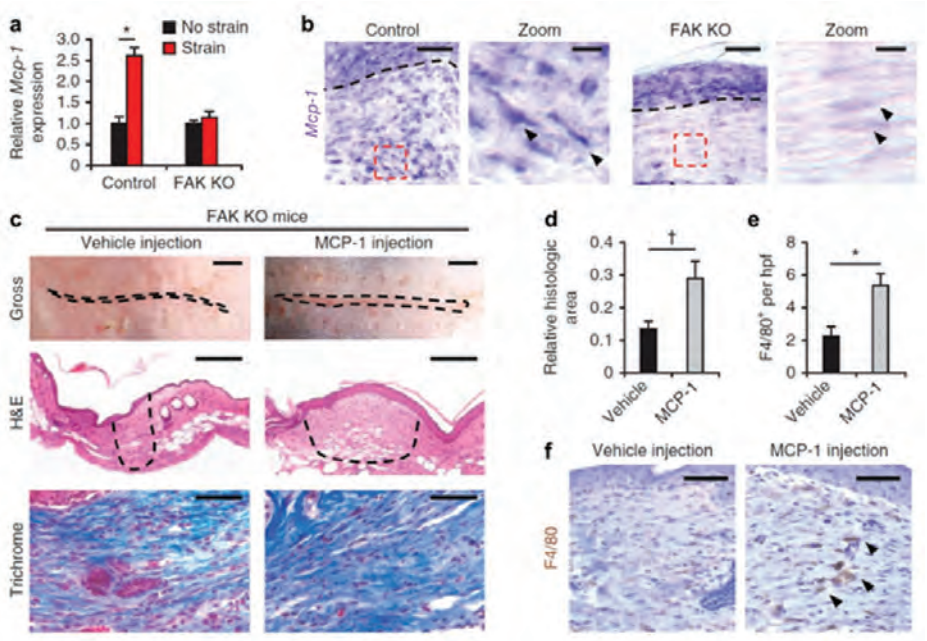

Figure 2. (a) MCP1 transcription in strained FAK KO fibroblasts is reduced. (b) In situ hybridization reveals decreased dermal MCP1 in FAK KO mice at day 10 following injury. (c) Injection of MCP1 into mechanically loaded FAK KO wounds restores scar hypertrophy, with a significant increase in (d) scar area and (e–f) macrophage infiltration into the wound bed.

of this keratinocyte protein on scarring and wound remodeling. A more rigorous understanding of how keratinocyte FAK signaling contributes to wound healing will help frame the research team's previous findings on fibroblast FAK and ultimately enable them to develop targeted, cell-specific strategies toward improving tissue regeneration and reducing scarring.

Planned Clinical Transitions

Neodyne Biosciences Inc. is in the process of conducting Phase 3 trials, which will recruit a larger patient population. In conjunction with the Materials Science and Engineering Department at Stanford University, they will further refine the polymeric device to custom-design treatments for various size wounds and tension states. This will allow for body-specific regional stress-shielding to address a wide variety of surgical wounds.

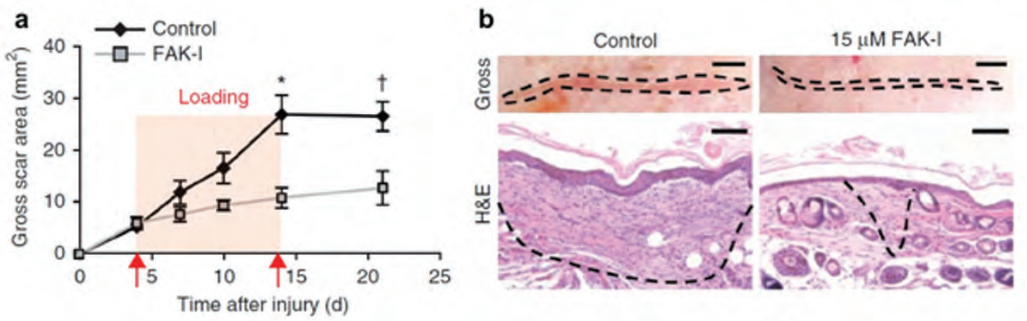

Figure 3. Wounded mice subjected to mechanical loading undergo treatment with a small molecule FAK inhibitor, PF573228 (Tocris), resulting in (a) a significant reduction in gross scar area and (b) a decrease in cross-sectional scar area as demonstrated by hematoxylin and eosin (H&E) staining. Not shown: Reduction in dermal MCP1 immunolocalization to wounds treated with PF573228.

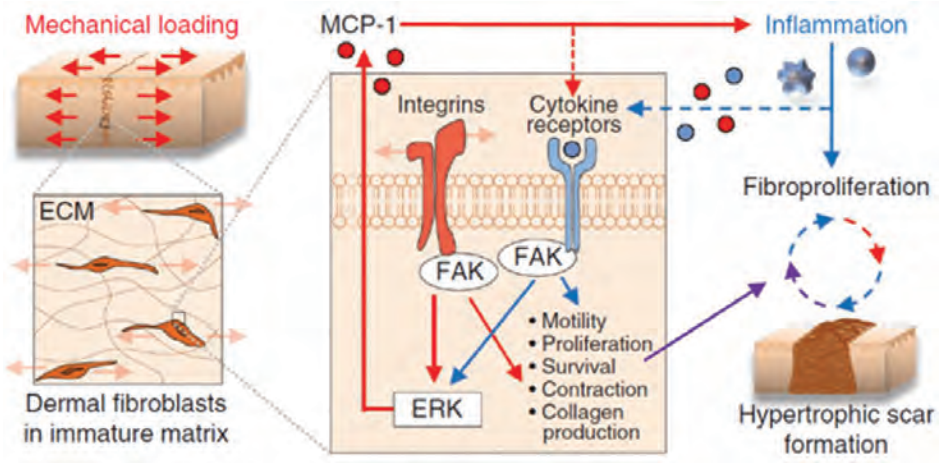

Figure 4. Schematic demonstrating the activation of fibroblast FAK by local and systemic mechanical and inflammatory stimuli, resulting in the activation of extracellular signal-regulated kinase (ERK) and upregulation of MCP1, which further incites fibroproliferative pathways and hypertrophic scar deposition.

Therapeutic Delivery to Wounds

Therapy to Limit Injury (TLI) and Promote Non-Scar Healing After Burns and Severe Battle Trauma

Project 4.6.3, RCCC

Team Leader(s): Thomas Mustoe, MD (Northwestern University)

Project Team Member(s): Seok Jong Hong, PhD, Sheng-Xian Jia, MD, PhD, Ping Xie, PhD, and Marina Vracar-Grabar, MSc (Northwestern University)

Collaborator(s): Richard Clark, MD (Stony Brook University)

Therapy: Curcumin to enhance healing and attenuate scarring

Deliverable(s): Intravenous (IV) treatment with curcumin

TRL Progress: 2010, TRL 3; 2011, TRL 4; 2012 (Current), TRL 4; 2013 (Target), TRL 4

Key Accomplishments: The Mustoe group developed a porcine skin flap model to evaluate therapies to reduce ischemic injury and promote wound healing. They initiated a study to evaluate the efficacy of IV curcumin in the pig model. The results suggest that treatment at the time of surgery with 1 µM curcumin can effectively reduce the area of necrotic skin. Studies in a rabbit ear ischemic-reperfusion (I/R) model demonstrated that delayed curcumin treatment (4 days post wounding, which coincided with I/R injury) had a similar effect on wound healing compared to treatment with a preventive dose given prior to I/R injury (evaluated at 7 days post injury).

Key Words: Burn, scar, curcumin, rabbit ear model, pig skin flap

Introduction

There is no effective therapy to limit I/R injury in marginally viable tissue following major trauma. Curcumin, administered as a single IV injection, can potentially fulfill that role. During the first 3 years of this project, evidence of efficacy was obtained in a rabbit I/R model where curcumin supported wound healing. Additional proof-of-concept of curcumin's efficacy in a nonischemic rabbit ear wound model was obtained using timed-release nanosphere technology. Given the positive results of curcumin in the rabbit wound-healing models, the study has been translated into large animals—a pig skin flap model that simulates the clinical application.

Research Progress – Year 4

IV Curcumin Efficacy in the Pig Flap I/R Model

In Year 4, the research team developed a large animal model—pig skin flap—to determine if IV curcumin could reduce ischemic injury progression and promote survival of the marginally viable flap tissue after surgery. The surgical procedure to create dorsal pig skin flaps was developed as shown in **Figure 1**. Two animals were used as controls—one treated with a blank control and the other with the vehicle (1% Et-OH) only . Eleven animals received a single IV injection of curcumin at the time of surgery at one of three doses.

Representative images of the flaps 7 days after treatment are presented in **Figure 2**. The necrotic area (black colored) of each flap was analyzed, and results are reported as a ratio of the necrotic area to the full skin flap area. Preliminary results indicate that the 1 µM of systemically administered curcumin had a statistically significant effect in reducing necrosis after dorsal skin flap surgery, therefore supporting survival of the marginally viable tissue.

Evaluation of Post-Injury IV Curcumin Treatment in the I/R Rabbit Ear Model

One of the main goals of Year 4 was to explore the effect of curcumin on wound healing when administered post injury, rather than at the time of injury. This effect was assessed 10 days after wound creation in the I/R rabbit ear model. Animals were

Figure 1. Pig skin flap surgery. To create dorsal skin flaps, incisions were made along both sides (4 x 14 cm) to ensure distal zone of necrosis. The flaps were elevated in its base and sutured back in place. Survival length or percentage of necrosis was evaluated 7 days later.

treated with 2 µM curcumin IV via the peripheral ear vein on days 4 and 6 post wounding to coincide with I/R cycles. The results showed that most of the wounds were completely re-epithelialized by day 10. No significant difference was observed between control and I/R ears in any of the histologic parameters. In conclusion, 10 days after wounding is not the optimal time point to determine if curcumin enhanced wound healing since most of the 6 mm wounds were completely re-epithelialized by day 10.

To address the limitations described previously, the evaluation of IV curcumin in the I/R rabbit ear model was done at 7 days post wounding, rather than 10 days. In this study, 2 µM curcumin IV was administered as a single dose via the cephalic vein on day 4 post wounding in two rabbits. The control ear underwent sham surgery, whereas the ears that received the experimental treatments received I/R cycles on days 4, 5, and 6 post wounding. The re-epithelialization results are consistent with previously reported data in the I/R model (single IV curcumin at 2 µM administered at day 0). The I/R wounds showed slightly delayed healing in comparison to non-I/R control ear wounds. Granulation tissue formation was not significantly different between control non-I/R and I/R wounds.

Conclusions

The Mustoe group developed a porcine skin flap model. They initiated a study using seven animals to evaluate the efficacy of IV curcumin in the pig model. The results suggest that treatment at the time of surgery with 1 µM curcumin can effectively reduce the necrotic area. Efficacy of delayed IV curcumin treatment on I/R wound healing was evaluated 7 and 10 days after wound creation in the rabbit ear model. Data on wound re-epithelialization at 7 days suggest that curcumin supports wound healing and/or limits I/R injury progression.

Research Plans for Year 5

In Year 5, the project will investigate the effect of dose, timing of IV curcumin infusion, and number of infusions on the reduction of ischemic injury progression and the survival of marginally viable skin flap tissue.

Planned Clinical Transitions

The transition to clinical studies and further planning is dependent on the Year 5 results obtained from the curcumin efficacy studies in large animals. If IV curcumin treatment is successful in the porcine flap model, NeoMatrix Formulations, Inc. will negotiate an option to license the technology from Stony Brook University, who has filed a patent on the IV use of curcumin.

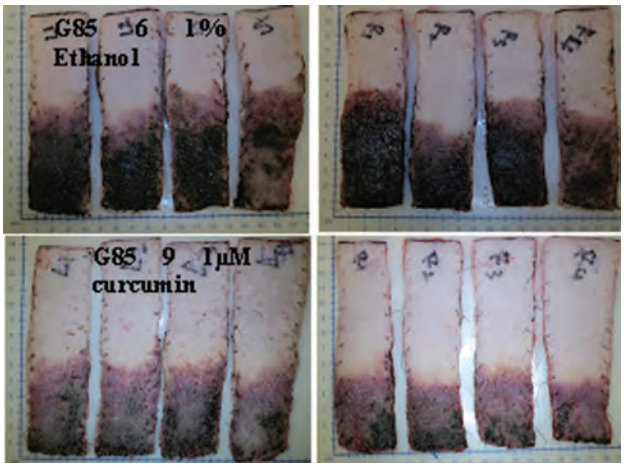

Figure 2. Positive effect of IV curcumin (1 µM) on dorsal skin flap survival and reduction of tissue necrosis. Tissue was harvested 7 and 10 days after surgery. Single IV curcumin treatment (1 µM) reduced the size of the necrotic (black) area in comparison to vehicle control treatment.

Therapeutic Delivery to Wounds

Adipose-Derived Therapies for Wound Healing, Tissue Repair, and Scar Management

Project 4.7.1, RCCC

Team Leader(s): Adam J. Katz, MD (University of Florida but formerly University of Virginia)

Project Team Member(s): Ning Yang, PhD (University of Virginia) and Hulan Shang, MS (University of Virginia)

Collaborator(s): Glycosan/BioSystems, Inc. and The GID Group, Inc.

Therapy: Autologous wound paste (AWP) using adipose-derived cells for tissue repair and wound healing

Deliverable(s): A novel and flexible AWP platform for the treatment of full-thickness cutaneous wounds due to blast injury, amenable to a "point-of-care" treatment paradigm

TRL Progress: 2010, TRL 3; 2011, TRL 4; 2012 (Current), TRL 4; 2013 (Target), TRL 5

Key Accomplishments: The research team conducted studies to characterize the effects of AWP, including its angiogenic/vasculogenic properties, its growth factor profile, and its paracrine effect on the migration of target cells such as keratinocytes and endothelial cells. They obtained evidence to support the use of a more simplified buffer-based cell stabilization solution (CSS) in the AWP formulation.

Key Words: Adipose stromal cells, autologous cell therapies, stromal vascular fraction (SVF), wound healing, wound contraction

Introduction

Essentially all battlefield wounds involve some component of skin and/or soft-tissue injury, and in many cases the tissue loss/damage can be quite extensive. Regardless of etiology, extensive full-thickness wounds are associated with significant cutaneous scar formation, even with the implementation of the most advanced reconstructive techniques. Such scarring can result in significant deformity and/or functional loss. In all cases, reconstruction/repair requires some degree of donor morbidity associated with the harvest of skin grafts or flaps—sometimes resulting in significant "donor disease" that is itself disfiguring and/or disabling. New treatment options that minimize donor-site harvest and morbidity are technically simple and yet provide equal or better functional and aesthetic outcomes to current standards of care are readily needed.

The research team is developing a novel and flexible AWP platform for the treatment of full-thickness cutaneous wounds. During the first 2 years of the project, the researchers made substantial progress in developing a point-of-care therapy whereby adipose-derived stem cells (ASC) are isolated, seeded onto/combined with a dermal scaffold, and applied to an open wound all within the context of a single operative session. They determined that multicell spheroids could undergo spontaneous, self-directed migration into a bilaminar-like orientation when placed onto dermal scaffold. They also demonstrated the ability to seed and subsequently proliferate suspensions of ASC and/or spheroids onto intact and/or microperforated acellular dermal scaffolds and the ability of such constructs to assist in wound healing in vivo while also decreasing wound contraction. Finally, they developed AWP, which is composed of ASC and particulated acellular dermal scaffolds, and demonstrated the feasibility and proof-of-concept of its delivery to open wounds and its ability to incorporate into and close wounds while minimizing wound contraction. Progress in Year 3 focused on refining and evaluating the AWP formulation. The research team determined that cell-enhanced wound paste reduced wound contraction in a mouse model with full-thickness wounds more

effectively than acellular wound paste. Finally, they found no gross or systemic evidence of detrimental effects related to a high dose of ASC in immunocompromised mice in a long-term tumorigenesis and migration study.

Research Progress – Year 4

Regulatory: Pre-IND Meeting

A pre-IND meeting was held with the FDA for the novel AWP platform. The meeting helped to clarify specific requirements and objectives related to the details of preclinical safety and efficacy studies (such as the duration/extent of time points, etc.). The meeting also provided valuable feedback regarding the design of Phase 1 clinical studies.

AWP Formulation and Potency: Effect of CSS

AWP consists of adipose-derived SVF cells and extracellular matrix components mixed together in a CSS. The team's initial CSS formulation was media-based but with a goal of simplifying manufacturing and regulatory objectives, they experimented with the use of a more practical, buffer-based CSS formulation. Subsequent experiments were performed to evaluate the impact of a buffer-based CSS on AWP, with outcome metrics including routine histology, CD31+ staining, cell viability, Luminex quantification of secreted growth factors and cytokines, and paracrine signaling of wound cell migration.

Interestingly, the results of these studies revealed that both media-based and buffer-based CSS maintained cell viability and proliferation in AWP for up to 14 days. Cell numbers in buffer-based CSS increased to 124% at day 14 compared with day 0. Staining with H&E indicated that cells were distributed evenly within AWP, and staining with CD31 showed that endothelial cells formed lumen-like structures suggestive of neo-capillaries (**Figure 1**). Transwell migration assays demonstrated that AWP conditioned-media facilitated endothelial cell and keratinocyte migration compared to an acellular paste control. Furthermore, conditioned media from buffer-based AWP effected equal or greater cell migration compared to media-based AWP (**Figure 2**). Luminex evaluation demonstrated that AWP secretes a number of growth factors implicated in wound healing, with significantly higher

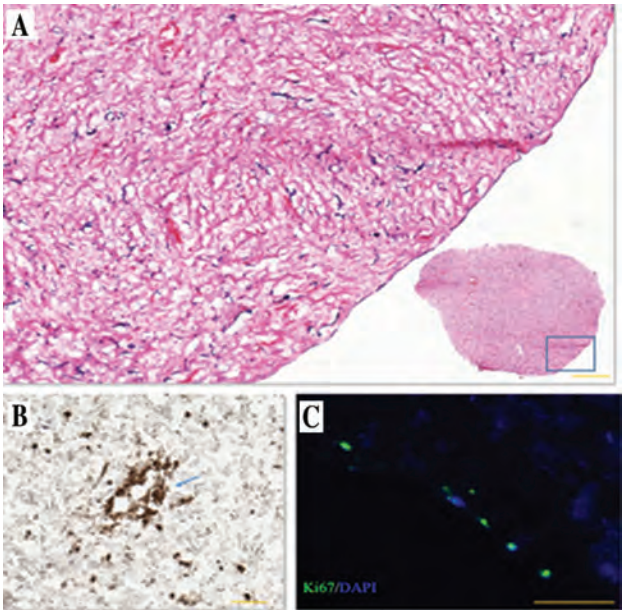

Figure 1. H&E histology (A), CD31 staining (B), and Ki67 fluorescent staining (C) of AWP with human SVF cells formulated with buffer-based CSS.

amounts secreted by AWP formulations with ASC, as compared to AWP formulations without cells (controls).

Together, these studies suggest that using buffer-based solutions does not negatively impact the biological properties of AWP but likely does simplify manufacturing and regulatory objectives. In addition, the inclusion of adipose-derived SVF cells within the paste provides significant biological benefit as demonstrated by quantitative and functional assays.

Conclusions

The team continues to make progress in the development of mechanistic and potency assays that will support an Investigational New Drug (IND) filing. A major milestone was achieved with the completion of a pre-IND meeting with Center for Biologics Evaluation and Research (CBER)/U.S. Food and Drug Administration (FDA).

Research Plans for Year 5

During the next year, the team will focus on completing studies necessary for supporting an IND filing, as determined by the recently completed pre-IND meeting. These will include CMC (chemistry, manufacturing, and control) studies to accrue

data that pertain to the manufacture of AWP components and AWP final formulation. More specifically, a novel cell isolation device will be tested and validated for the reproducible isolation of SVF cells, and the cells will be characterized for identity, purity, and potency. Identity and purity will be determined by flow cytometry and related metrics, and potency will be assayed using protein methods and paracrine-related assays (e.g., cell migration). If time and funding permit, the team will proceed with definitive preclinical animal testing to support the safety and efficacy of the AWP paradigm. During these studies, Dr. Katz will maintain dialogue with appropriate FDA/CBER representatives, with an aim of incorporating continued feedback into preclinical and clinical trial design. In the best of circumstances, the completion of all of these studies will yield sufficient data to support an IND filing.

Planned Clinical Transitions

The research team intends to submit an IND filing with the FDA for approval to begin Phase 1 clinical testing. Funding for such clinical studies would need to be obtained. Dr. Katz continues to foster relationships with potential commercial partners.

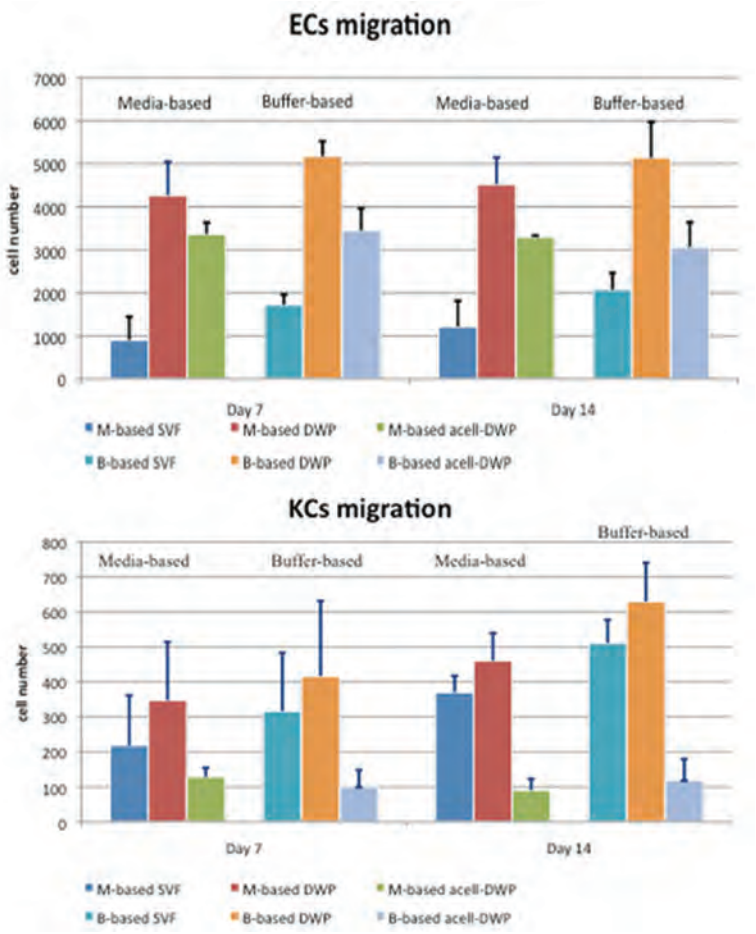

Figure 2. AWP-conditioned-media facilitates endothelial cell (EC; top) and keratinocyte (KC; bottom) migration using transwell migration assays.

Therapeutic Delivery to Wounds

Regenerative Bandage for Battlefield Wounds

Project 4.5.2, WFPC

Team Leader(s): Geoffrey C. Gurtner, MD and Michael T. Longaker MD, MBA (Stanford University)

Project Team Member(s): Anthony Oro, MD, PhD (Stanford University)

Therapy: Improved wound healing and reduced scarring

Deliverable(s): Regenerative bandage that promotes fetal-like wound healing instead of scarring

TRL Progress: 2008, TRL 1; 2010, TRL 3; 2011, TRL 4; 2012 (Current), TRL 5

Key Accomplishments: The researchers have developed a novel biomaterial scaffold that is highly biocompatible with numerous cell types important for wound repair. They developed and tested a capillary seeding method for rapid and efficient distribution of stem cells throughout the hydrogel substrate. They initiated characterization of the dermal architecture of fetal murine skin and unwounded murine skin using various cell stains and advanced microscopic techniques. They found an increase in expression of stemness genes among hydrogel-seeded cells compared to plated cells. They applied hydrogels seeded with bone marrow-derived mesenchymal stem cells (MSC) to stented excisional wounds in mice and found an improvement in wound closure and vascularity with evidence of restoration of dermal architecture and cell differentiation into stromal subtypes (fibroblasts, pericytes, and endothelial cells).

Key Words: Dermal matrix, wound healing, fetal skin

Introduction

Wounded soldiers returning from the present conflicts have sustained significant trauma to the head, neck, face, and limbs. Timing is critical to optimize salvage of traumatic wounds; once wounds are surgically debrided, coverage is important to reduce a prolonged inflammatory state, infection with subsequent contraction, and disability. A novel approach is needed to minimize this inflammatory and fibrotic cascade in the initial days following injury while promoting tissue regeneration. The research team's technical approach begins immediately post injury with a regenerative bandage consisting of a fetal biomimetic matrix and human progenitor cells to maintain an acute wound in a pro-regenerative state of "suspended animation" and prevent the onset of scarring, fibrosis, and infection. Utilizing their knowledge of fetal skin development, scarless repair, and burn therapy, the researchers hope to preserve wounds in a "fresh state" by recreating a fetal-like wound-healing milieu to promote regeneration and optimize the results of definitive therapy.

During the first 3 years of this project, the Stanford group developed a hygroscopic dressing mimicking unwounded dermal micropatterning. The material is a biocompatible dermal scaffold based on the architecture of fetal murine skin and is highly modifiable with predictable swelling, degradation, and rheologic properties. This engineered construct significantly improved cutaneous wound healing in a mouse model and demonstrated potent immunomodulatory properties that enhanced wound vascularization. The researchers are now focused on using this regenerative template to maintain progenitor cells in suspended animation for delivery into wounds and to develop a battlefield-ready, rapidly expanding hydrogel that can be used as a regenerative bandage and vehicle for autologous stem cell delivery.

Research Progress – Year 4

The Stanford group has made significant progress in further developing its carbohydrate-based collagen hydrogel for wound healing by performing both in vitro and in vivo experiments, demonstrating the potential therapeutic efficacy of this technology.

They developed a new, efficient method of seeding hydrogels with stem cells using capillary force (**Figure 1**).

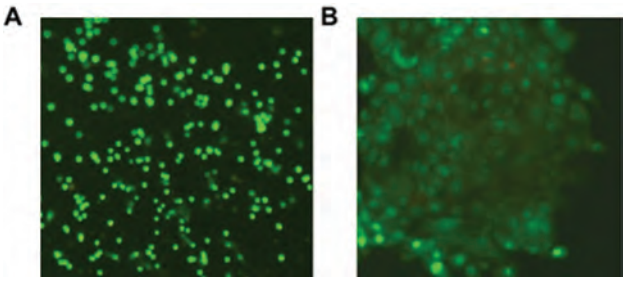

Figure 1. Cell viability using new seeding method of capillary force. A. Live/dead assay results at day 3. B. Cluster of cells using live/dead assay at day 14.

MSC that were plated or seeded in hydrogels were evaluated for expression of transcription factors associated with self-renewal and pluripotency, including *Oct4*, *Sox2*, and *Klf4*. Transcriptional levels of these stemness markers were increased in the hydrogel group, and this observation was confirmed by immunoblot analysis (**Figure 2**).

The research team subsequently performed in vivo experiments using a stented excisional wound model and found that wounds treated with the MSC-seeded hydrogel were significantly more vascular than wounds that were untreated or injected with MSC (**Figure 3**). Histologic wound analyses revealed evidence of MSC differentiation into fibroblasts, pericytes, and endothelial cells (**Figure 4**). Cross-sectional H&E staining demonstrated evidence of dermal architecture regeneration in wounds treated with MSC-seeded hydrogels (**Figure 5**).

Conclusions

The Stanford group has successfully demonstrated the therapeutic potential of a regenerative bandage composed of stem cells seeded on a biocompatible hydrogel scaffold. In vitro studies revealed that the hydrogel creates an environment for MSC that increases stemness factor expression, and in vivo studies revealed an improvement in wound closure and vascularity with evidence of dermal architecture restoration and cell differentiation into stromal subtypes.

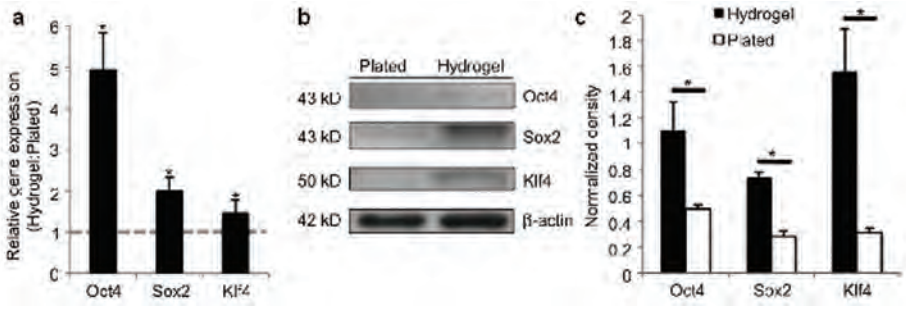

Figure 2. MSC expression of stemness genes. A. qRT-PCR analysis of *Oct4*, *Sox2*, and *Klf4* gene expression in hydrogel culture versus standard plating (dotted grey line, n=7). B. Western blotting of stemness genes. C. Quantification of western blotting (n=4).

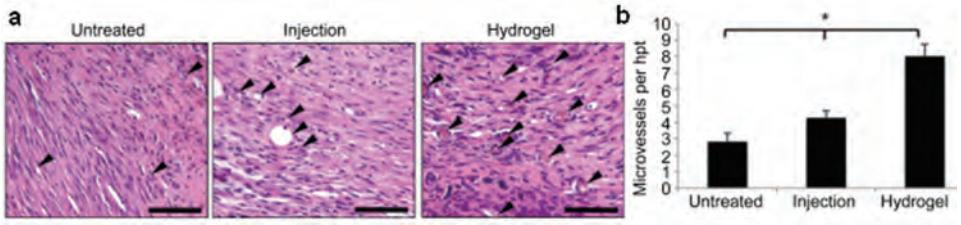

Figure 3. Effect of MSC delivery method on wound vascularization. A. H&E-stained sections of day 14 wounds. Arrowheads indicate microvessels. Scale bar = 20 μm. B. Microvessel counts.

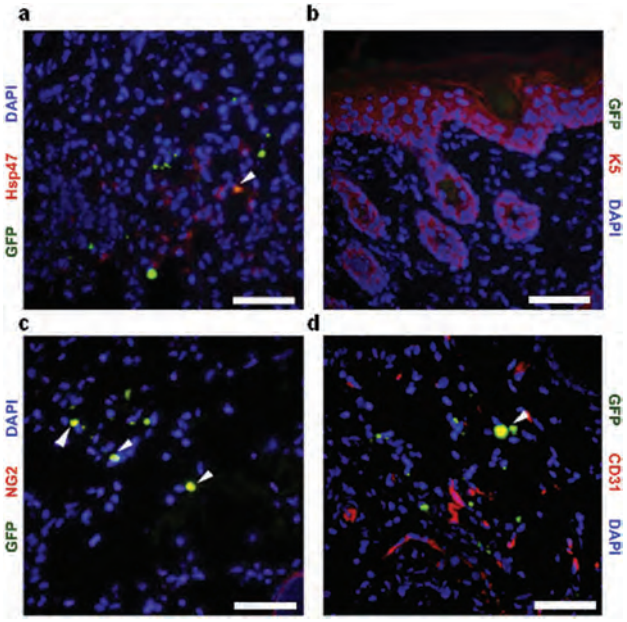

Figure 4. Colocalization of green fluorescent protein (GFP)-positive MSC with cell-specific markers to determine MSC fate within wounds. MSC colocalized (arrowheads) with fibroblast marker Hsp47 (a), pericyte marker NG2 (c), and endothelial marker CD31 (d). No GFP+/K5+ cells were observed (b). Scale bar = 20 µm. DAPI = 4',6-diamidino-2-phenylindole.

Research Plans for Year 5

The researchers will continue to optimize their regenerative bandage by investigating the therapeutic potential of ASC implantation into the hydrogel. ASC are a promising group of MSC that are easy to isolate from human patients and therefore a practical cell type to investigate for clinical use. The research team will initially perform in vitro studies on ASC-seeded hydrogels to determine cell viability and stemness factor transcription and to characterize the transcriptional profile of wound-healing cytokines. The researchers will then conduct in vivo studies using an excisional wound model that resembles human wound healing to determine whether ASC-seeded hydrogels can augment wound closure, improve wound growth factor expression and vascularity, and promote dermal architecture restoration. Initial studies using murine cells will be performed prior to using human cells.

Planned Clinical Transitions

The Stanford group plans to continue in vivo small animal studies using murine and human ASC to further characterize the observed improvement in early wound healing. The team plans to file a 510(k) application for a cell-free matrix if they continue to obtain positive results. This could set the path for clinical trials using this dressing on open wounds to enhance granulation tissue formation.

Corrections/Changes Planned in Year 5

The researchers are expanding the types of progenitor cells they are seeding in the biomatrices to include adipose- and bone marrow-derived stem cells. These cells have greater clinical applicability compared to embryonic stem cells (as initially proposed) and their use bypasses ethical concerns regarding the use of embryonic tissues. Autologous cells can potentially be harvested from injured patients and used to seed biomatrices in vitro for subsequent use as a regenerative wound bandage.

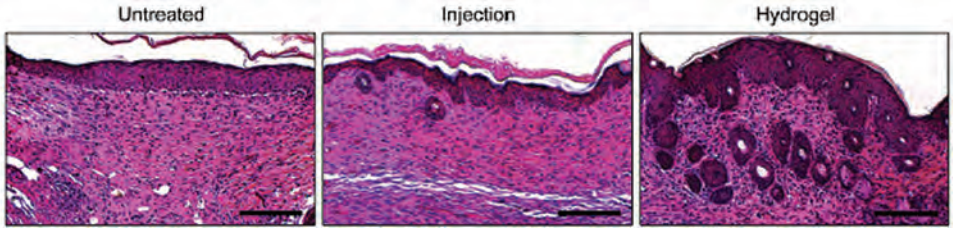

Figure 5. Effects of MSC delivery method on wound closure. H&E staining of wounds at day 14. Scale bar = 100 µm.

Therapeutic Delivery to Wounds

Scarless Wound Healing Through Nanoparticle-Mediated Molecular Therapies

Project 4.5.5, WFPC

Team Leader(s): Sandeep Kathju, MD, PhD (University of Pittsburgh)

Project Team Member(s): Latha Satish, MSc, MPhil, PhD (University of Pittsburgh)

Therapy: Small interfering RNA (siRNA)-based formulation for mitigation of scar formation in healing wounds and a probiotic therapy to inhibit pathogenic infection and reduce scar formation in burn wounds.

Deliverable(s): (1) Formulation of molecular agents that can be applied to healing wounds so that they repair with diminished or absent scar formation using nanoparticulate technology. (2) A probiotic therapy to reduce infection and scar in a burn wound scenario.

TRL Progress: 2008, TRL 1; 2009, TRL 1; 2010, TRL 3; 2011, TRL 3; 2012 (Current), TRL 4

Key Accomplishments: The researchers are using siRNA in novel nanoparticulate formulations to mitigate scar formation in healing wounds. They applied siRNA constructs that deplete chaperonin containing T-complex polypeptide subunit eta (CCT-eta) to healing incisional wounds and found reduced α-smooth muscle actin in the wounds, suggesting an inhibition of myofibroblast activity. The researchers also established a new mouse model of burn wound infection and determined that septic translocation leading to death occurs in this animal model. They applied a novel probiotic therapy for infected burn wounds using *Lactobacillus* to their new mouse model and found that it could rescue the animal from burn wound-induced sepsis and death.

Key Words: Scarless wound healing, nanoparticles, siRNA, probiotics, burns

Introduction

The purpose of this project is to arrive at technologies that will enable the reduction of scar formation after injury. Scar, while useful in sealing an injured area, is also the source of significant morbidity, including restriction of movement (e.g., in tendons and muscle), narrowing of viscera, entrapment of nerves, etc. Burn injuries are particularly prone to extensive and crippling hypertrophic scarring. Mammalian fetal wound healing proceeds without scar formation and has served as a model for the investigations.

Past effort under this project has determined that CCT-eta is specifically reduced in fetal wounds but is increased in scar-forming adult wounds. CCT-eta is permissive for the accumulation of α-SMA and therefore the function of myofibroblasts. The researchers are using siRNA constructs that deplete CCT-eta to attempt to reconstitute a more fetal pattern of wound healing in adult wounds and thereby mitigate scar formation. The researchers designed and validated a siRNA-expressing plasmid vector that can be used to manipulate CCT-eta in wounds. The team has reported that siRNA versus CCT-eta can reduce deposited collagen in a healing wound while actually improving its tensile strength.

A second focus of the research team has been on the use of probiotic intervention using *Lactobacillus* to reduce scar from burn wound infection. They have tested bacteriotherapy with *Lactobacillus* in a rabbit model of *Pseudomonas* infected burn injury as a countermeasure to the hypertrophic scarring that can typically ensue. Their results to date indicate that probiotic therapy of infected burn wounds leads to attenuation of the infection and resulting scar deposition.

Research Progress – Year 4

siRNA Versus CCT-eta as an Antifibrotic Agent

The research team continued to analyze various molecular and biochemical parameters in their rabbit model of adult incisional wound healing. They examined whether in vivo siRNA therapy using the nanoparticulate formulation results not only in reduction of target mRNA but also of target protein species. They previously showed that siRNA against CCT-eta effectively depleted CCT-eta protein in vitro. Western blot analysis of healing wounds was therefore carried out to determine if the same could be achieved in vivo (**Figure 1**).

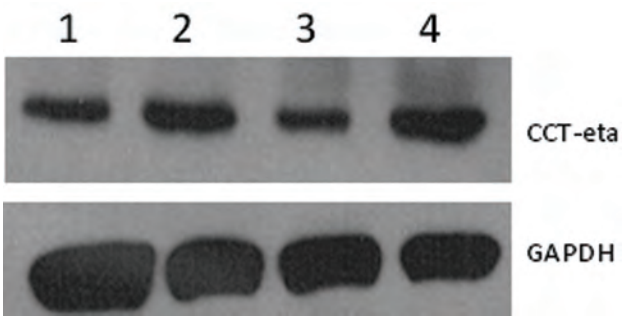

Figure 1. Expression of CCT-eta protein in healing wounds. 1 = control unwounded skin. 2 = control wound with vehicle only. 3 = wound treated with CCT-eta siRNA. 4 = wound treated with scrambled siRNA. A representative image of five replicate experiments is shown. Glyceraldehyde 3-phosphate dehydrogenase (GAPDH) was used as the loading control.

Animals were wounded on their dorsums and wounds were treated with either vehicle only, CCT-eta siRNA, or a scrambled control siRNA. After 4 weeks, wounds were re-excised and assayed for both CCT-eta and the downstream target protein α-SMA. An increase in CCT-eta protein was seen in wounded specimens compared to control unwounded skin, consistent with the researchers' previous results. CCT-eta siRNA significantly decreased CCT-eta protein expression, whereas the nonspecific control siRNA had no such effect (Figure 1).

Similar results were noted with α-SMA; treatment of wounds with CCT-eta siRNA significantly diminished α-SMA expression, but control scrambled siRNA had no such effect (**Figure 2**). These results reinforce previous observations that siRNA against CCT-eta can meaningfully and beneficially modulate the physiology of a healing adult wound.

Suppression of Scar in Infected Burn Wounds by Probiotics

The researchers previously observed that a single administration of prophylactic probiotic therapy with *Lactobacillus* is sufficient to attenuate the length and severity of a pseudomonal infection of the burn wound and that this therapy also significantly reduced the amount of deposited collagen in the wound, amounting to a reduction in the scar burden. Over this past year, additional samples were processed to confirm observations so that conclusive data could be obtained. The expanded data set is being readied for publication. Because no new conclusions were reached, the data are not shown here.

Concomitant with that effort, the researchers established a new model of probiotic therapy that demonstrates that this approach can rescue an animal from burn wound-induced sepsis and death.

Conclusions

The University of Pittsburgh team concludes that siRNA versus CCT-eta, delivered as a complexed nanoparticle in an agarose matrix, can effectively deplete its cognate protein, and inhibit scar formation without any deleterious effects on wound healing. The team also concludes that probiotic

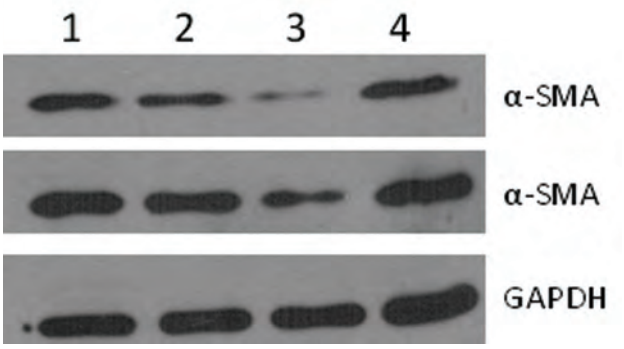

Figure 2. Expression of α-SMA protein in healing wounds. 1 = control unwounded skin. 2 = control wound with vehicle only. 3 = wound treated with CCT-eta siRNA. 4 = wound treated with scrambled siRNA. Two images from three replicate experiments are shown. GAPDH was used as the loading control.

therapy with *L. plantarum* can effectively abrogate pseudomonal (and possibly other) infections and significantly mitigate the scarring that can ensue after such infected burn injuries. Additionally, such probiotic therapy can rescue a burn-infected organism from sepsis and death.

Research Plans for Year 5

With regard to the siRNA-mediated antifibrotic therapy, the researchers plan to recapitulate the system in a porcine model (which more closely mimics human skin) and examine whether their agents are effective in burn wounds as well as incisional wounds. In addition, the team will investigate if an injectable formulation of the siRNA is practical or effective.

With regard to burn injury and probiotics, the team will continue to define the utility of probiotics in reducing the local and systemic inflammation elicited by an infected burn wound and attempt to delineate the mechanisms involved. They will try to determine if whole bacteria are required or some secreted product might be sufficient. Investigations are also planned to test the ability of probiotics to treat already infected burn wounds and determine how to counteract other burn wound pathogens with probiotics.

Planned Clinical Transitions

At this point, both interventional strategies have essentially demonstrated proof-of-concept benefit in animal models although some minor clarifying work still needs to be finished. The siRNA formulation is ready to proceed to a porcine model as the final step before considering Phase 1 studies in human to evaluate for safety, toxicity, immunogenicity, etc.

The probiotic therapy has several possible routes to clinical use. Probiotics already have a much more extensive history of clinical use in other scenarios (e.g., gastrointestinal and genitourinary infections), and direct application of live bacteria onto burn wounds may be one avenue. Another possibility is to construct dressing materials for burn wounds that incorporate dehydrated (and rehydratable) probiotic agents as an off-the-shelf therapy. The team will explore the best pathways forward in this regard.

Therapeutic Delivery to Wounds

Peptide-Mediated Delivery of Therapeutic Compounds into Injured Tissues During Secondary Intervention

Project 4.5.6, WFPC

Team Leader(s): Erkki Ruoslahti, MD, PhD (Sanford-Burnham Medical Research Institute at University of California, Santa Barbara [UCSB])

Project Team Member(s): Tero Järvinen, MD, PhD (Sanford-Burnham Medical Research Institute at UCSB and University of Tampere, Finland); Eunhye Lee, PhD, Sajid Hussain, PhD, Shweta Sharma, PhD, Gary Braun, PhD, Chris Brunquell (Sanford-Burnham Medical Research Institute at UCSB and Institute for Collaborative Biotechnologies); and Olivia Yu, (Undergraduate student UCSB).

Therapy: Systemic drug targeting to injured tissues/preventing scarring/enhancing tissue regeneration

Deliverable(s): Systemic and local wound targeting with peptides that penetrate into wound and scar tissue

TRL Progress: 2008, TRL 1; 2009, TRL 1; 2010, TRL 3; 2011, TRL 5; 2012 (Current), TRL 5 (targeted decorin), TRL 3 (CAR peptide as a therapeutic)

Key Accomplishments: The research team developed tCAR, which is a truncated, linear form of the CAR peptide (CARSKNK), and found that it demonstrated superior performance in wound-homing in vivo. The researchers found that tCAR requires the free sulfhydryl group for its enhanced activity. They determined that prolonged blood half-life was a major reason for the enhanced activity of tCAR. The researchers completed studies of the enhanced wound-healing activity of the CAR peptide to allow filing of a patent application. They provided evidence that systemically administered CAR enhanced the penetration of bloodborne substances into wounds. They produced a glycosaminoglycan-free decorin.

Key Words: Wound angiogenesis, homing peptides, antiscarring, transforming growth factor-beta (TGF-β)

Introduction

The research team previously published data focused on two wound-homing peptides that recognize wound blood vessels at different stages of healing. One of these peptides (CAR) appears to recognize a wound-specific form of heparin sulfate. The target molecule for the other is not known.

In the first 3 years of this project, the researchers used the CAR peptide to selectively deliver decorin, a natural inhibitor of TGF-β, into skin wounds. They obtained significant reductions in several markers of scarring. They found that CAR homes to injured tissue in pulmonary fibrosis and pulmonary hypertension and that the peptide can promote tissue-specific accumulation of compounds that are coadministered with the peptide and not chemically coupled to it in injuries. The researchers discovered an inherent wound-healing promoting activity of the CAR peptide (unpublished results). They determined that wound-targeted version of the antifibrotic protein decorin was more effective in suppressing various indicators of subsequent scarring than nontargeted decorin. They completed and published the scar suppression study. One of the key pieces of data in that publication is the unique selectivity of CAR-decorin against the different TGF-βs. The researchers found that CAR-decorin was significantly more active than decorin against TGF-β1 and TGF-β2 but, remarkably, it had no effect on TGF-β3.

Research Progress – Year 4

During the past year, the research team focused on optimizing the CAR-decorin conjugate for completion of the preclinical work and introduction of the compound into the clinic. Another focus has been

to confirm and extend the results on the healing-promoting activity of the CAR peptide.

Specific Aim 1

As reported last year, the research team generated a truncated form of their wound-targeting peptide CAR (tCAR; CARSKNK) by truncating the peptide at the second lysine, the C-terminal residue, and showing that tCAR phage binds more avidly to Chinese hamster ovary-K (CHO-K) cells than CAR. Like CAR, tCAR depends on heparin sulfate for cell binding as tCAR binds much less to the glycosaminoglycan (GAG)-deficient CHO mutant pgsA-745 cells than the parental CHO cells. tCAR also homed more strongly to skin wounds that CAR and penetrated deeper into the wound tissue.

The latest results provide a partial explanation for the superior performance of tCAR in wound homing in vivo. The researchers deleted the N-terminal cysteine and found that this peptide showed poor homing efficiency (shown for tumor homing in **Figure 1**). The researchers also made peptides in which the cysteine was converted into an alanine, serine, or methionine and found them to be inactive. Therefore, the free sulfhydryl group of the cysteine residue is needed for the homing.

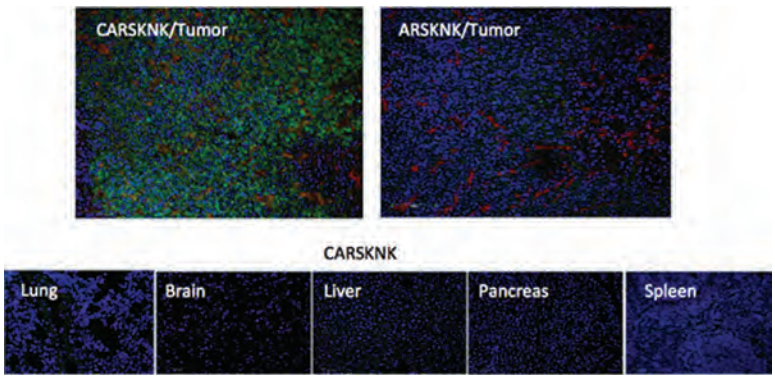

Figure 1. In vivo homing of tCAR peptide. Confocal images of sections of a 4T1 tumor and normal organs from mice injected with the 200 µL of 1 mM FAM-tCAR peptide. The circulation time was 2 hours. The tCAR peptide shows extensive homing and spreading within tumor tissue, whereas tCAR that lacks the cysteine residue (ARSKNK) shows no detectable tumor homing. There was no detectable accumulation of either peptide in normal tissues (shown for tCAR), except in the kidney (peptides are excreted into the urine). Red, CD31; green, peptides; blue, nuclei. Representative fields from multiple sections of tissues from 3 tumor mice are shown. Scale bars, 100 mm.

Preliminary data indicate that the reason for the sulfhydryl requirement in tCAR is that it links the peptide to the free sulfhydryl in albumin (and likely in other plasma proteins), which prolongs the half-life of the peptide in the circulation and results in stronger homing. However, this may not be the only reason for the strong homing activity, as nanoparticles coated with tCAR through the sulfhydryl group also showed efficient and specific homing (**Figure 2**) although the nanoparticle coupling also prolonged the half-life of the peptide in the blood.

Another new discovery reported by the research team last year is that systemic injections of the CAR peptide alone to mice with skin wounds accelerates wound healing. CAR penetrates into cells and tissues in a manner similar to the recently identified CendR peptides (Sugahara KN et al. 2010. *Science* 328:1031-35). Based on these results, the researchers hypothesize that CAR might enhance wound healing by improving the availability of natural growth factors from the blood and serum to the regenerating tissue and that because of the wound specificity of CAR, this effect would be specific to wounds. In essence, one would be pharmacologically manipulating a previously described plasma
that led to serum that led to plasma transition that takes place during normal tissue repair and controls tissue regeneration.

The research team has obtained evidence to support the plasma protein hypothesis. Mice with full-thickness skin wounds received an intravenous injection of CAR or the inactive *m*CAR control peptide together with the albumin-binding dye Evans Blue on day 7 after creation of a skin wound. After 30 minutes, the mice were perfused, the wounds and the control organs harvested, and Evans Blue was extracted with formamide. The researchers found that Evans Blue accumulated more strongly in wound tissue when it was injected together with CAR versus *m*CAR (**Figure 3**).

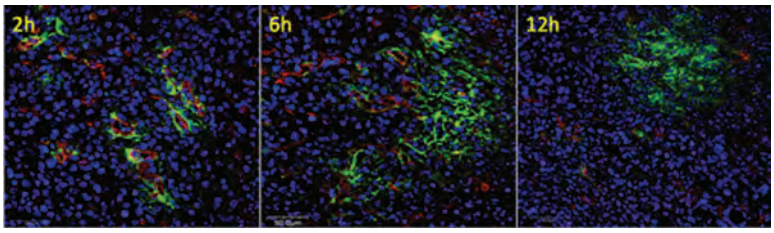

Figure 2. In vivo homing of nanoparticles coated with the tCAR peptide. Confocal images of 4T1 tumors from mice injected with tCAR iron oxide nanoworms (spherical nanoparticles linked together like the segments of an earthworm) in 130 µL were intravenously injected into the tumor-bearing mice. The circulation times were as shown. The tCAR nanoworms were initially found in and around the blood vessels, but over time extravasated and spread in the tumor tissue. Red, CD31; green, nanoworms; blue, nuclei. Representative fields from multiple sections of 3 tumors are shown. Scale bars, 50 mm.

Specific Aim 2

Wound-Targeted Decorin

The differential inhibitory activity of CAR-decorin against the TGF-β isoforms, noted earlier, could have important implications. TGF-β1 is the isoform responsible for scar formation, and TGF-β2 augments the profibrotic activity of TGF-β1. In contrast, TGF-β3 inhibits scarring. The researchers propose that CAR-decorin inhibits scar formation induced by TGF-β1 and TGF-β2 but does not affect the benefits of TGF-β3. An in vitro assay for measuring TGF-β inhibition, developed by the research team, should provide the researchers with an important tool for evaluating the clinical potential of their various CAR-decorin compounds.

The heterogeneity of recombinant decorin produced in mammalian cells stems from the single GAG chain and presents regulatory challenges in the commercialization of the product. Previous data indicate that the protein core is responsible for the binding of decorin to TGF-β and that the chondroitin sulfate side chain can actually hinder this interaction. Thus, the chondroitin sulfate chain may not be needed for the inhibition of TGF-β1 activity by decorin, and it may be possible to use homogeneous, GAG-free CAR-decorin that is more active than the native decorin as an antiscarring agent.

The researchers have now produced chondroitin sulfate-free CAR-decorin in mammalian and baculovirus systems and are in the process of testing these preparations for TGF-β inhibition, circulation half-life, wound homing, and antiscarring activity. In addition, they have made CAR-mouse decorin for immunogenicity studies in mice.

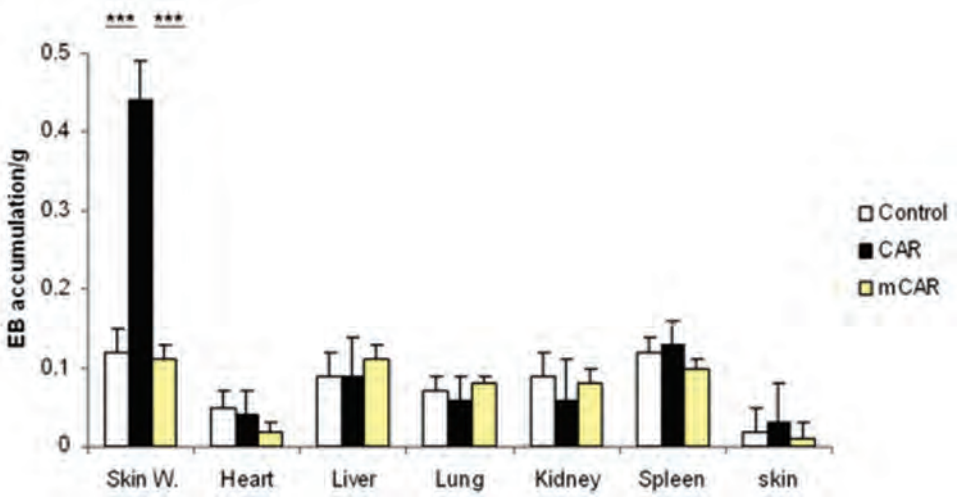

Figure 3. CAR peptide drives accumulation of blood-derived proteins in skin wounds. Systemically injected CAR peptide induces a "bystander effect" (i.e., drives blood-derived proteins into the wound bed), whereas the inactive *m*CAR control peptide does not. The "bystander effect" is specific to injured tissues as no accumulation is seen in uninjured organs. N=20, the statistical significance was examined with analysis of variance (ANOVA), (***) $p < 0.001$. Mean ± SD.

Conclusions

The development of systemic delivery of therapeutic agents to injured tissues is progressing as planned. The new tissue-penetration technology offers particular promise, most notably the potential of enhancing drug delivery to wound tissue of bloodborne compounds that are not chemically coupled to the tissue-penetrating peptide. The inherent activity of the peptide in wound healing is another potentially important new lead. The activity of the antiscarring agent decorin can be greatly enhanced by fusing this protein with a homing peptide.

Overall, these studies may result in new systemic treatments that cannot only accelerate the tissue regeneration in major trauma, but also limit the permanent damage caused by fibrosis in injured, operated, and inflamed tissues. The CAR peptide may provide a new way of enhancing wound healing, and perhaps tissue regeneration in general, that is systemic, yet target-specific, and nontoxic. In addition, CAR co-injection may enable injury-selective delivery of other compounds with beneficial effects on tissue healing.

Research Plans for Year 5

The work on the peptide delivery systems will focus on the cell and tissue-penetrating properties of the CAR peptide and its use in enhancing wound and scar penetration of coadministered compounds. Characterization of the CAR variant tCAR, which appears to be more potent in wound homing than the original CAR, will be another focus area. The decorin project will focus on improving the properties of CAR-decorin to facilitate commercial production and regulatory approvals. CAR-decorin and tCAR-decorin will also be compared in wound homing and scar prevention experiments. The inherent biological activity of CAR in promoting wound healing will be confirmed. Possible synergies of the CAR-decorin and CAR peptide treatments will also be studied. Finally, the molecular basis of the wound-healing promoting activity of the CAR peptide will be studied to facilitate the transition of this treatment into the clinic. The researchers will compare wounds from CAR-treated and control-treated mice by using proteomics analyses and mRNA microarrays.

Attenuation of Wound Inflammatory Response

Multifunctional Bioscaffolds for Promoting Scarless Wound Healing

Project 4.5.3, WFPC

Team Leader(s): Newell Washburn, PhD (Carnegie Mellon University [CMU])

Project Team Member(s): Allison Elder, Emily Friedrich, and Mohamed Ramadan (CMU)

Collaborator(s): Robert Christy, PhD (USAISR)

Therapy: Burn treatment

Deliverable(s): Gels that control inflammation and promote healing

TRL Progress: 2008, TRL 3; 2009, TRL 3; 2010, TRL 4; 2011, TRL 5; 2012 (Current), TRL 5

Key Accomplishments: The researchers produced conjugates consisting of the proinflammatory cytokine tumor necrosis factor-α (TNF-α) linked to hyaluronic acid (HA). They found that (anti-TNF)-HA conjugates are highly effective at inhibiting burn progression in a rat burn model. They are investigating the mechanism by which the conjugates inhibit burn progression in the rat model. Additionally, the researchers developed a new analogue formulation that does not require covalent conjugation, which will facilitate clinical translation.

Key Words: Burns, cytokines, inflammation, antibodies, gels

Introduction

The trajectory of burn wound healing is a complex process starting with necrosis due to the thermal injury, followed by a two-stage inflammatory process, delayed cell death, formation of granulation tissue, and remodeling. The complications from partial- or full-thickness burns are broad ranging, including compromised protection by the epidermis and loss of resident leukocytes and lymphocytes, edema, reduced host defenses to bacterial colonization, multiple organ failure, and loss of connective tissue cells that would normally contribute to the repair response. Burned tissue has been modeled as having three concentric zones: (1) irreversibly damaged tissue in the zone of coagulation; (2) hypoperfused tissue in a zone of stasis; and (3) edematous tissue in a zone of hyperemia. The central necrotic zone often progresses into surrounding zones, which increases the likelihood of hypertrophic scarring and patient morbidity. Deleterious physiological responses following thermal injuries are driven by inflammatory responses.

The goal of this research project is to determine whether it is possible to use antibodies against the proinflammatory cytokine TNF-α conjugated to HA to inhibit burn progression.

During the first 3 years of this project, the Washburn group, in collaboration with Dr. Robert Christy at USAISR, created uncrosslinked HA gels by coupling monoclonal antibodies to HA. They identified and validated cytokine-neutralizing gel formulations that control inflammation and inhibit burn progression at burn sites. Validated means that FDA indicated in a pre-IND meeting that these studies in rats would be sufficient for proving efficacy. They demonstrated that neutralization of TNF-α alone may provide a significant reduction of inflammatory signaling. Maximum reduction of inflammatory responses occurred when both TNF-α and IL-1β were neutralized. The researchers also identified material design parameters that optimized the activities of covalently attached monoclonal antibodies. They demonstrated that application of (anti-TNF-α)-HA conjugates to partial-thickness burns reduced burn progression,

rescuing 70% of viable tissue from inflammation-induced necrosis in the rat burn model.

Research Progress – Year 4

The researchers expanded their program in immunostaining tissue sections during the past year to determine how the conjugates affect the inflammatory microenvironment at the burn site. These fundamental studies will be important to facilitate regulatory approval and adoption by leaders in the burn treatment community. They quantified macrophages in the treated and control sites using CD68 immunostaining, with representative images and results shown in **Figure 1**.

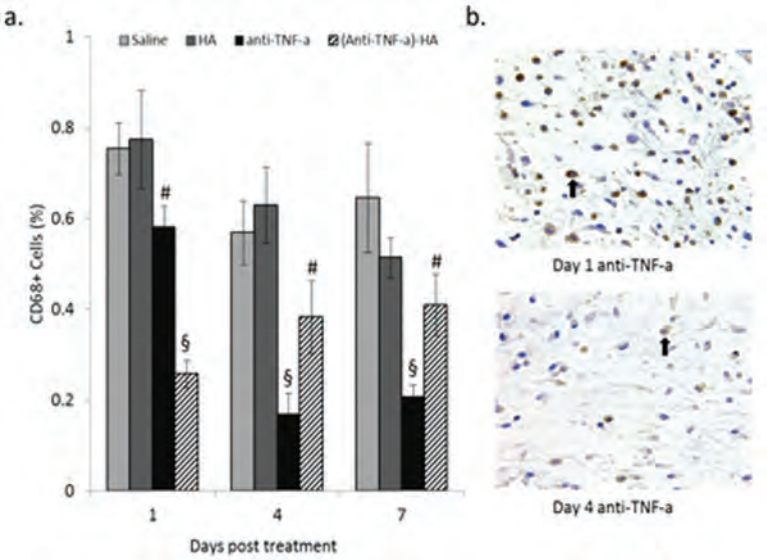

Figure 1. Results from macrophage immunostaining. (a) Quantification of results. (b) Sample data.

It is interesting to note that while there was a 40% reduction in macrophage levels at sites treated with (anti-TNF)-HA conjugates, the lowest macrophage levels were observed in sites treated with anti-TNF alone. It is hypothesized that nonconjugated antibody may have diffused from the burn site into the bloodstream and inhibited recruitment of circulating monocytes. Work has also been done in measuring healing responses, such as the formation of granulation tissue at the site and will continue in Year 5.

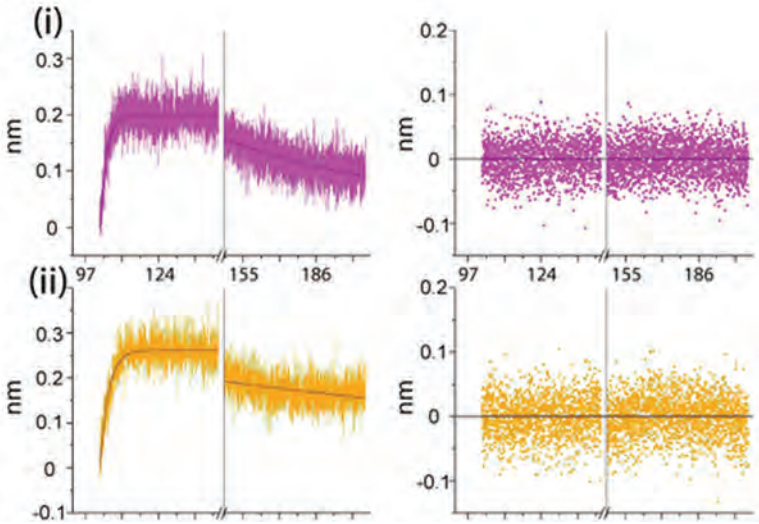

Figure 2. Binding of anti-TNF alone (top set of curves) and new formulation of anti-TNF (bottom set of curves) followed by binding of TNF along with associated fitting residuals. Association curves were fit to y = A[1 – exp(-kont)] and dissociation curves were fit to y = Aexp(-kofft) where kon and koff are kinetic parameters and t is the time during association or dissociation, respectively.

To facilitate translating this technology into the clinic, an analogue has been developed that does not require covalent conjugation of the antibody. The Washburn laboratory used a biolayer interferometer from ForteBio to investigate physical properties of the new formulation. Representative plots are shown in **Figure 2**. The abscissa shows the time during adsorption or desorption, and the ordinate shows the computed change in thickness of the sensor surface. The bottom family of curves is TNF antibody alone, with a characteristic maximum thickness change of approximately 1 nm. The top family of curves is the new formulation including TNF antibody at the same concentration. There is a significant increase in thickness, indicating that the antibody interacts strongly with the carrier. These stronger interactions could serve a similar function in vivo, increasing antibody residence time at the site of inflammation. CMU is applying for a provisional patent on this approach, which will be validated in Year 5 of this grant in the rat burn model.

Conclusions

The results indicate that (anti-TNF)-HA conjugates are highly effective at inhibiting burn progression in a rat model. Due to fundamental similarities in early inflammatory responses across species, the Washburn group expects a similar response in humans.

Research Plans for Year 5

During the upcoming year, the researchers will focus on performing more fundamental studies to understand the mechanism of the effect of the conjugates. They will test the nonconjugated analogue in the rat burn model in preparation for a potential clinical trial. This version, in which all the components have established records of safety and efficacy in treating inflammatory conditions, would have a much lower regulatory barrier for proceeding to early phase clinical trials. The researchers will also develop strategies for the long-term storage of these materials.

Planned Clinical Transitions

The researchers' planned clinical transition will involve the CMU spin-off company, Washburn Therapeutics. This company has an exclusive license for patents filed by CMU and has formed a partnership with a manufacturer of anti-TNF that can be used in humans. The company will begin clinical trials of the new formulation in late 2012 or early 2013.

Attenuation of Wound Inflammatory Response

Regulation of Inflammation, Fibroblast Recruitment, and Activity for Regeneration

Project 4.5.4, WFPC

Team Leader(s): Patricia A. Hebda, PhD (McGowan Institute for Regenerative Medicine)

Project Team Member(s): Joseph E. Dohar, MD and Tianbing Yang, PhD (McGowan Institute for Regenerative Medicine)

Therapy: Attenuate local inflammatory responses to reduce scarring and promote healing

Deliverable(s): Combinatorial anti-inflammatory topical therapy to reduce scar formation

TRL Progress: 2008, TRL 3; 2009, TRL 3; 2010, TRL 3; 2011, TRL 3; 2012 (Current), TRL 4

Key Accomplishments: The researchers had previously found that one-time topical treatment with isogenic adipose-derived stem cells (ASC) and fetal skin fibroblasts (embryonic day 15 [E15]) led to reduced scarring and increased healing. They explored the mechanism of regenerative healing by ASC and E15 cells in the adult wound-healing environment. They found that wound healing induced by ASC and E15 cells shared some key similarities compared to adult or E18 fibroblasts, including improved survival in the wound environment, faster restoration of wound tissue tensile strength, expression of higher levels of cell surface vimentin, production of higher levels of intracellular collagen type III and fibronectin, greater levels of collagen secretion, and comparable NFkBp65/IkBα ratios.

Key Words: Scarless healing, inflammation, fibrosis, cell therapy

Introduction

The Hebda group is focusing on two related processes highly relevant to scar formation: inflammation and fibroblast activity. The overriding hypothesis is that the development of fibrosis can be prevented by blunting early wound-healing processes that lead to fibroblast recruitment and activation of synthetic properties. To achieve regeneration, it is first essential to regulate the inflammatory response and the influx of host fibroblasts. Control of these two fibrogenic processes will serve to establish an optimal foundation for therapies and interventions leading to regenerative healing. The early inflammatory phase of tissue repair has been shown to be important for the long-term outcome of wound healing.

The Hebda group proposes to use a novel method, transplantation of fetal fibroblasts into an adult dermal wound bed, to precisely characterize the impact of inflammatory and other soluble mediators on the fibroblast phenotype. This approach will allow them to determine if the fibroblast phenotype is a dynamic one, largely influenced by the wound environment. Should this be the case, then prevention of fibrosis/scarring could be primarily a matter of reducing profibrotic signals in the wound bed. Alternatively, if the donor fibroblast phenotype persists within the wound after transplantation, therapeutic efforts will be directed toward enhancing the wound-healing contribution of fibroblasts with a regenerative phenotype.

This project has three specific aims:

- To determine the potential of combinatorial anti-inflammatory therapy in decreasing subsequent fibroblast activity in the wound bed.
- To precisely characterize the contribution of the fibroblast phenotype to the overall degree of tissue fibrosis.

- To design interventions, based on the results of the first two aims that provide a wound environment for rapid, regenerative healing.

During the first year of the project, the researchers demonstrated that early, short-term topical treatment with the anti-inflammatory agents nimesulide and prostaglandin E2 (PGE2) attenuated the wound inflammatory response following skin incisional wounds in the rat, leading to a reduced amount of scarring and the promotion of healing. This determination was based on clinical assessment of healing, wound histology, tissue levels of ECM components, tissue biomechanics, and collagen organization. During Year 2, the researchers characterized the effects of therapeutic treatment on collagen production and organization in the healing wounds. They also established donor cell strains of different phenotypes, including cell strains with regenerative healing capability, for continuing work with cell therapy. The results from Year 3 show that early, one-time topical treatment with isogenic ASC, fetal skin fibroblasts (E15), and even adult skin fibroblasts, leads to reduced scarring and increased healing.

Research Progress – Year 4

Aim 2: To Precisely Characterize the Contribution of the Fibroblast Phenotype to the Overall Degree of Tissue Fibrosis

Since isogenic fibroblast transplants had been traced successfully at the wound beds of day 14 by histology, an animal experiment was performed to detect the population balance between host (endogenous) fibroblasts and the isogenic transplants. GFP-positive isogenic cells were applied at $5x10^5$ cells per incisional wound and $2x10^5$ cells per excisional wound. On day 6 post wounding and cell treatment, wound beds were harvested, and cells were processed for flow cytometry. After intracellular staining with an antibody to vimentim, endogenous fibroblasts were identified as vimentin single positive while donor cells were vimentin and GFP double-positive. The results indicated that donor cells consisted of 7% to 11% (**Figure 1**) of the total fibroblast population at the wound beds; this ratio was also observed for both incisional and excisional wounds, and among the four cell types investigated (fetal skin fibroblasts at E15 and E18, adult skin fibroblasts, and ASC).

Based on their previous observations that treatment with ASC and E15 fetal skin fibroblasts significantly increased the restoration of tensile strength ($p<0.001$ and $p=0.007$, respectively), the researchers have been exploring the molecular mechanisms underlying this phenomenon.

As shown in **Figure 2**, the cell surface vimentin-positive population was found to be significantly

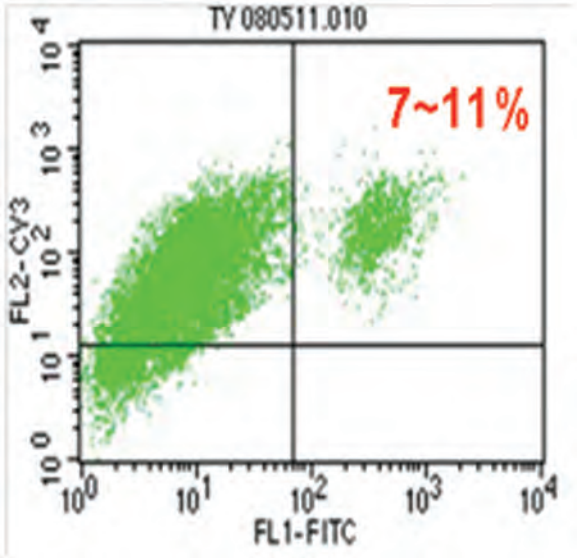

Figure 1. Two-parameter histogram Dot Plot displays the distribution of endogenous (left) and exogenous (right) cells in day 6 wounds. Sample size = 10^4 cells.

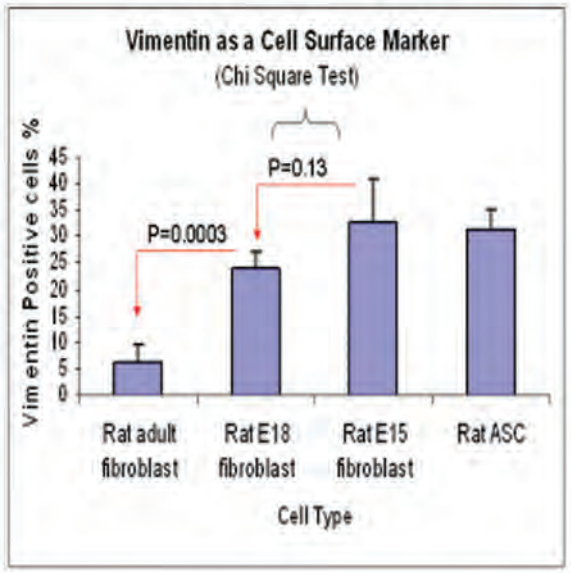

Figure 2. Surface vimentin-positive cell portion in the four cell types (10^4 total cells), mean fluorescence intensity (MFI) showing no differences.

lower in adult fibroblasts compared with the other three cell types (6% for adult fibroblasts, 24% for E18 fibroblasts, 32% for E15 fibroblasts, and 31% for ASC). Scientists have indicated a role for cell surface vimentin in wound healing since it is a receptor for soluble CD44, a hyaluronan binding domain, and recruitment of hyaluronan is beneficial at wound beds.

Cell intermediate collagen type I, collagen type III, and fibronectin were detected by flow cytometry after intracellular staining. No differences were found in intracellular collagen type I among the four cell types, but collagen type III and fibronectin shared a similar pattern, with a higher intracellular expression in ASC and E15 fibroblasts compared to adult fibroblasts (data shown for collagen type III, **Figure 3**). This pattern shows a positive correlation between tissue tensile strength and intracellular collagen type III level and fibronectin levels.

Collagen secretion was detected in fetal cell supernatant but not in adult cell supernatant by western blotting, indicating that both collagen type I and collagen type III play an important role in fetal wound healing compared to adult wound healing (**Figure 4**). It has been well documented that fetal cells produce more collagen than adult cells, especially collagen type III, and a higher ratio of type III to type I collagen reduces scarring. The researchers believe their E15 fetal cells and ASC

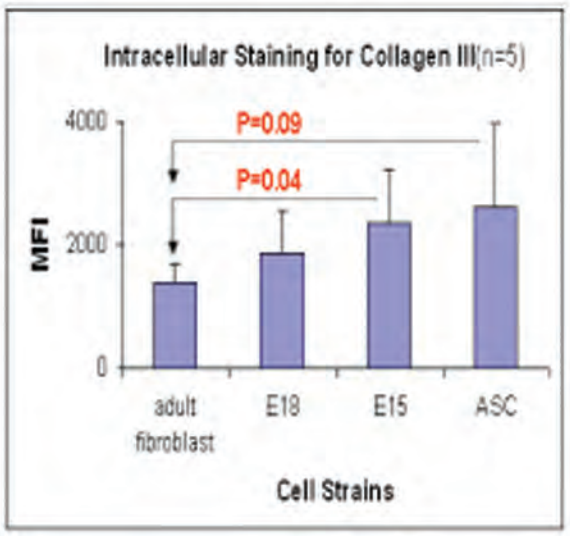

Figure 3. MFI shows differences in intracellular collagen type III (fetal type) level among the four cell types (10^4 total cells).

are beneficial for wound healing, due at least partially to their collagen production.

The researchers also detected, by western blotting, NFkBp65 and its inhibitor, IkBα, in whole cell lysate following stimulation with IL-1β stimulation. They found an interesting lower NFkBp65/IkBα ratio in E18 cells, implying that an immunological change is occurring at the developmental switch point of E18, when scarless regeneration changes to reparative (adult-type) wound healing (**Figure 5**).

Conclusions

The current results demonstrate that early, one-time topical treatment with isogenic ASC and fetal skin fibroblasts (E15) leads to reduced scarring and increased healing. ASC and E15 cells shared some key similarities compared to adult or E18 fibroblasts, such as improved survival in the wound environment, faster restoration of wound tissue tensile strength, expression of higher levels of cell surface vimentin, production of higher levels of intracellular collagen type III and fibronectin, and comparable NFkBp65/IkBα ratios. ASC and E15 cells also had similar multipotency and collagen synthetic capacity, and they contribute to collagen fiber organization in a comparable manner. Based on their benefits in the healing process, both ASC and E15 cells are ideal candidates to combine with the anti-inflammation agent nimesulide and the antifibrotic agent PGE2 for either novel therapeutic strategy development or molecular mechanism exploration.

Research Plans for Year 5

The research team will focus in Year 5 on using the results of the studies to date to design interventions that provide a wound environment for rapid, regenerative healing.

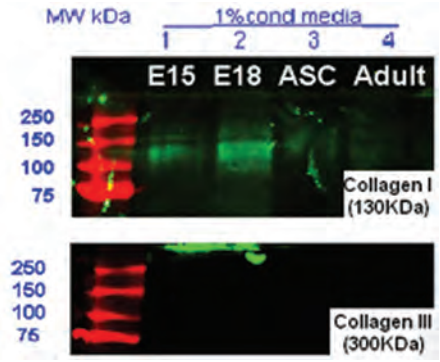

Figure 4a. Western blot detection of collagen types I and III in cell culture supernatant: 5x10^5 cells were cultured in 5 mL low serum medium (1% fetal bovine serum) in 6-well plates, and the supernatant was collected after 24 hours.

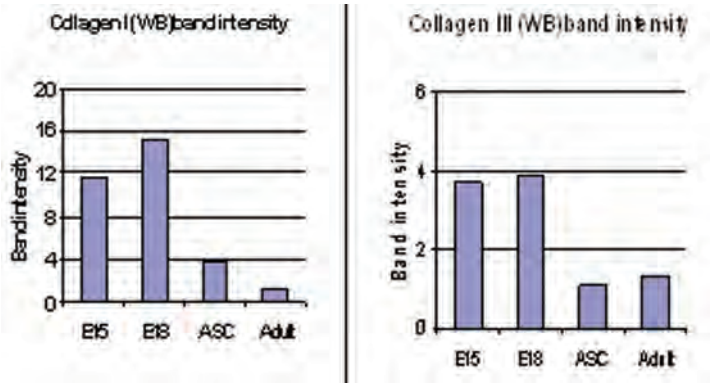

Figure 4b. Quantitative analysis of Odyssey western blots: Band intensity measured by the Odyssey Imaging System indicated a much higher collagen secretion in fetal cells than adult cells. The collagen type III/type I ratio was 0.32 in E15 cells while 0.26 in E18 cells.

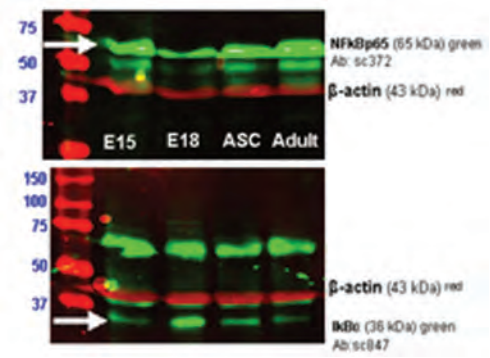

Figure 5a. Western blot detection of NFkBp65 and IkBα: SDS-PAGE (50 µg protein per well) was followed by blotting analysis with two independent channels (green for target protein and red for β-actin) scanning using the Odyssey Imaging System.

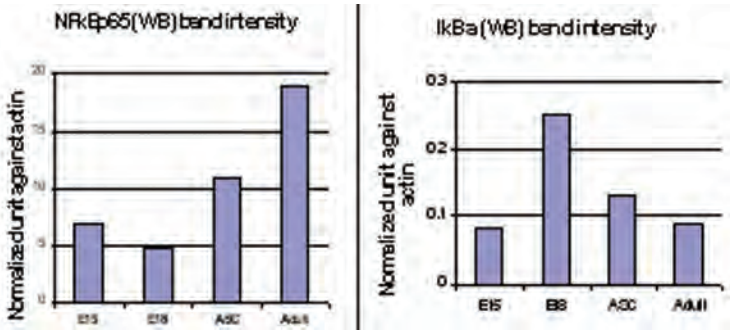

Figure 5b. Quantitative analysis of Odyssey western blots: Band intensity was measured and normalized against β-actin, indicating NFkBp65 expression is higher in adult cells, lower in fetal cells. The NFkBp65/IkBa ratio was 207 in adult fibroblasts, 19 in E18 fibroblasts, 82 in E15 fibroblasts, and 80 in ASC.

Clinical Trials

Neodyne's Device to Actively Control the Mechanobiology During Wound Healing and Prevent Scar Formation

Project 4.5.9, WFPC

Team Leader(s): Bill Beasley, BS (Neodyne Biosciences) and Geoffrey C. Gurtner, MD (Stanford University)

Project Team Member(s): John Zepeda, BS, Jasper Jackson, BS, Rich Caligaris, ABA, Peggy McLaughlin, BS, and Christy Cowley, MPH (Neodyne)

Collaborator(s): Michael T. Longaker, MD, MBA, Reinhold Dauskardt, PhD, Paul Yock, MD (Stanford University); Dr. Rodney Chan, COL Robert G Hale, Michael G. Chambers, MPAS, and Gale Mankoff, RN (USAISR)

Therapy: Control of wound environment to minimize scarring

Deliverable(s): Commercially available devices capable of stress-shielding mechanical forces to minimize scar formation

TRL Progress: 2009, TRL 5; 2010, TRL 6; 2011, TRL 7; 2012 (Current), TRL 8

Key Accomplishments: Neodyne has enrolled and treated more than 60 patients in a clinical trial designed to test its commercial-ready third-generation (Gen 3) device capable of stress-shielding wounds and off-loading pathologic mechanical forces to prevent fibrosis. The researchers finalized the manufacturing process flow for the commercial product. They initiated and completed design improvements for improved manufacturing efficiency. They conducted clinical product manufacturing to support the clinical trial and completed an evaluation of contract manufacturers for commercial product manufacturing.

Key Words: Hypertrophic scarring, mechanobiology, wound device

Introduction

Scar formation following trauma and burn injury leads to severe functional disability and disfigurement. Multiple factors are known to influence wound repair but therapeutic modalities aimed at these targets have been largely unsuccessful. Mechanical force has long been recognized to influence cellular behavior in vitro, and clinical observations based on Langer's lines and hypertrophic scarring corroborate this phenomenon in vivo. Recently, the Gurtner laboratory published the first murine model of hypertrophic scarring induced by increasing the skin stress of healing wounds. They found that intrinsic skin mechanics correlated with scarring phenotype following wounding, as low mechanical stress fetal wounds exhibit minimal fibrosis and stiffer human skin displays robust scarring. These findings prompted the initial studies to examine the role of mechanical stress in scar formation and to develop a novel device to actively control wound environment mechanics to mitigate fibrosis.

Today, there are no commercially available products that specifically address the mechanical stress state of healing wounds to reduce scarring. In contrast to existing wound care options, Neodyne's technology enables precision stress-shielding of area-specific wound forces through a portable, ready-to-use, pressure-sensitive adhesive dressing that can be readily applied after surgery. The Neodyne technology consists of a load-bearing biopolymer that is stretched by means of an applicator and then applied to the skin with a goal of optimizing a regenerative wound environment for minimal scar formation.

In this project, Neodyne is utilizing a novel stress-shielding device developed by researchers at Stanford University to safely and effectively modulate the mechanical wound environment in

post-surgical human subjects to markedly reduce cutaneous scarring. They completed a Phase 1 first-in-man clinical trial with the device and found a dramatic reduction in hypertrophic scar formation in treated wounds compared to untreated wounds within patient controls. A pilot trial of 61 subjects with a second-generation device further supported the need for precise control of skin strain and a design that is intuitive to the user and suggested that there is a narrow range of stress levels that provide optimal scar reduction. The second-generation device was designed to deliver precise stress-shielding at several strain levels to determine efficacy and patient tolerance. Trial results indicated a clear correlation between delivery of higher strains and skin irritation. Data collected on strain measurement indicated that the device delivered precise strain that was maintained for the full wearing period. **Figure 1** shows treated and control incisions from the pilot trial.

With these understandings, Neodyne has developed a Gen 3 device and initiated a clinical trial. Using digital imaging correlation (DIC) technology, Neodyne has the capability to accurately measure the compressive and tensile forces in the skin within the treated area and surrounding tissue. This information will enable Neodyne to further improve the precision and efficacy of its incisional wound treatment. Notably, Neodyne has received 510(k) clearance from the FDA for its first family of products and has released the product for commercial use. The researchers have also developed and released a second size dressing for smaller incisions.

Clinical Trial Status and Results

Neodyne has completed work in the past year in two primary areas: (1) Clinical trial execution and (2) manufacturing readiness to prepare for larger scale production and commercialization.

Gen 3 Clinical Trial Execution

The Gen 3 trial to test market readiness of the product design and build additional clinical evidence has been enrolling and treating patients following de novo abdominoplasty procedures since the summer of 2011. The Gen 3 trial is a prospective, open-label, randomized study of up to 100 subjects to measure scar formation as a primary endpoint in surgical abdominoplasty

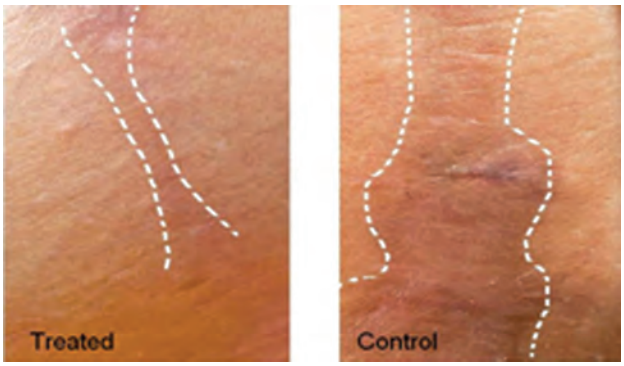

Figure 1. Pilot study treated and nontreated incisions (same patient) after 6 months.

procedures where patients will serve as their own control. Up to one-half of the incision is treated by the Neodyne device, and the contralateral half is treated with the physician's preferred standard of care. Ease of use, pain amelioration, comfort, and scar smoothness are among the outcome measurements. Follow-up will occur at 6 months and 1 year post surgery.

Neodyne has enrolled patients at 15 sites as well as the USAISR in San Antonio and has received approval at David Grant Hospital at Travis Air Force Base. The company has plans to treat military injuries and reconstructive surgeries at these and other military hospitals. More than 60 patients have been enrolled in the clinical trial, with approximately 15–20 who will have reached the 6-month post-surgery endpoint of the trial by June 2012. Since December 2011, the USAISR has enrolled 4 subjects, with 2 subjects expected to complete the study by June 2013. Neodyne stopped accrual at all sites in June 2012 after meeting target enrollment.

In addition to the AFIRM-sponsored trial, Neodyne is conducting a scar revision trial with a similar design to the abdominoplasty trial, enrolling 10 patients since October 2011. Results of this trial show dramatic improvements in scar reduction on the treated side of scar revision incisions (**Figure 2**).

Manufacturing Readiness

In the summer of 2011 Neodyne completed the evaluation of current and potential vendors and suppliers to provide the raw materials, subassemblies, and infrastructure to support the

Figure 2. Scar revision – 6-month post procedure (treated side on left).

manufacturing required to deliver clinical product for the current clinical trial. In support of its 2011–2012 clinical trials, the Neodyne manufacturing team has built more than 1,000 clinical devices.

Subsequently, Neodyne has focused on developing the final specifications for their Gen 3 device in preparation to outsource commercial manufacturing in the United States. Several contract manufacturers have been evaluated, and the selection of the manufacturers for the adhesive, dressing, and final product assembly has been completed. The manufacturing process flow has been finalized for the commercial product (**Figure 3**). Neodyne will be responsible for the final packaging and delivery of devices to the customer.

Conclusions

In summary, Neodyne has utilized a novel stress-shielding device to safely and effectively modulate the mechanical wound environment in human subjects post surgery to markedly reduce cutaneous scarring. This innovative device demonstrates the capability to precisely regulate skin fibrosis post injury and is a promising translational approach to minimize the biomedical burden of hypertrophic scar formation. The first-in-man study set a strong foundation for the promise of the Neodyne technology. The pilot trial with a second-generation device further supported the need for precise control of skin strain and an intuitive user design and suggested that there is a narrow range of strain levels that provide optimal scar reduction. With these understandings, Neodyne has nearly completed testing the latest design in clinical trials and will soon launch the product commercially.

The current Neodyne devices are able to create an optimal mechanical environment for linear incisions. With the use of DIC technology, the company has the capability to accurately measure the compressive and tensile forces in the skin within the treated area and surrounding tissue. This information will enable Neodyne to further improve the precision and efficacy of its incisional wound treatment. The most recent product design has dramatically improved the usability and intuitiveness of the treatment and has potential uses beyond the application of Neodyne's stress-shielding device. Additional clinical trials to test the expanded capabilities of the technology are desired.

Clinical Trial Plans for Year 5

Neodyne plans to continue with clinical studies in both military and civilian populations to validate the full range of potential uses for the product and to test hypotheses for use on incisional wounds as well as scar revision procedures. Neodyne will continue to collaborate with Stanford University to conduct human trials with advanced versions of the technology that are further developed in the Gurtner laboratory.

Neodyne is in the late stages of enrolling its third device trial, which is recruiting a larger and ethnically broader patient population to test the efficacy and market readiness of its latest product design. In addition to the AFIRM-funded trial, Neodyne plans to continue to enroll patients in a scar revision study to evaluate the efficacy of its product on lower tension incisions. In conjunction with the Department of Materials Science and Engineering at Stanford University, Neodyne will further refine the polymeric device to custom-design treatments for various size wounds and tension states. This will allow for body-specific regional stress-shielding to address a wide variety of surgical wounds.

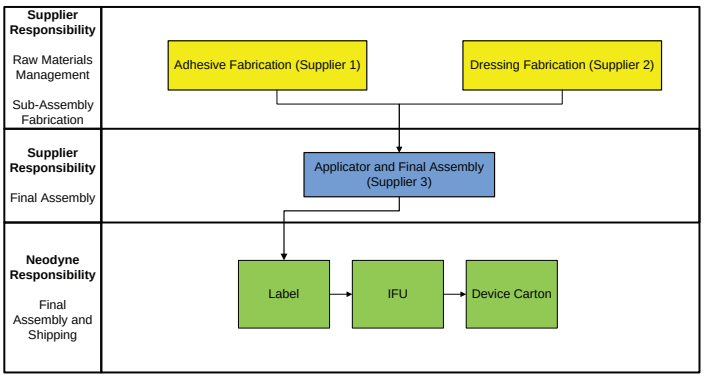

Figure 3. Manufacturing flow for Neodyne's commercial product.

Clinical Trials

Clinical Trial – Autologous Fat Transfer for Scar Prevention and Remodeling (AFT-SPAR)

Project 4.7.3, RCCC

Team Leader(s): Adam J. Katz, MD (University of Florida, formerly the University of Virginia)

Project Team Member(s): David Drake, MD, Catherine Ratliff, PhD (University of Virginia); Lauren Macri, PhD (Rutgers University); Jane Reese, MBA, MS and Emily Collins, MS (CWRU)

Collaborator(s): Rodney Chan, MD , Colonel Robert Hale, DDS, Michael G. Chambers, MPAS, LtCol Michael R. Davis, James A. Chambers, MD, and Gale Mankoff, RN (USAISR/BAMC)

Therapy: Scar Prevention and Management

Product: Autologous fat transfer for scar prevention and remodeling (AFT-SPAR): A new indication for an existing surgical procedure

TRL Progress: 2011, TRL 6; 2012 (Current), TRL 6; 2013 (Target), TRL 7

Key Accomplishments: The research team has continued to screen, enroll, and treat study patients with autologous fat transfer (AFT). To date, they have enrolled and treated a total of 10 patients, with 7 in the late treatment cohort and 3 in the early treatment cohort. The late treatment cohort has now enrolled enough subjects to advance to the Phase 2 portion of the study. No adverse events have been encountered to date.

Key Words: Adipose tissue, fat grafting, scar, autologous fat transfer

Introduction

Severe blast and burn injuries are associated with extensive cutaneous scar formation, even with the implementation of the most advanced reconstructive techniques. Such scarring can result in significant deformity or functional loss. At the tissue level, many scar beds are devoid of a subcutaneous layer (hypodermis). This deficit is often overlooked or minimized as part of a patient's reconstruction and recovery, yet it presents a significant and important challenge and therapeutic target. The "creation" of a hypodermis (subcutaneous) layer beneath a tight, immobile scar bed (whether through AFT or by the de novo regeneration/engineered replacement of such tissue) has the potential to affect both the appearance and quality of scar and therefore to improve the patient's quality of life.

Currently available therapies, such as semiocclusive dressings (e.g., silicone), pressure (garment) therapy, and local steroid injections, are limited in their use. Recent reports suggest that adipose tissue, and the mesenchymal stem cells it contains, may not only enhance the healing of difficult wounds but beneficially affect the scarring process as well. AFT represents the simplest and most fundamental approach to exploring this concept, with the potential to provide immediate positive impact. AFT is a single-stage procedure that involves the removal of adipose tissue from one site of a patient, followed by the immediate and autologous transplantation or infiltration of this tissue into a different site of the same patient. AFT is a routine surgical procedure, albeit with the clinical intent of bulking or filling contour deformities, and has been proven to be safe. More than 50,000 AFT procedures were performed last year in the United States alone.

AFT-SPAR could emerge as a simple yet effective approach to improving the lives of wounded soldiers. The results of this trial may change the manner in which burned, and otherwise scarred, patients are routinely cared for, supporting the use of a relatively simple procedure to decrease

the cosmetic, functional, and psychological consequences patients experience in association with scarring. However, this approach has yet to be evaluated within the setting of controlled studies; evidence-based treatment parameters need to be established.

Clinical Trial Status and Results

This past year, the research team screened approximately 30 new subjects for the study. Only 3 chose to enroll in the study although most of the potential subjects were qualified to participate. This low rate of enrollment remains the major limiting factor to the expedient completion of the study. Primary reasons given for not to enrolling relate to concerns associated with time commitment and missing more work, "surgical fatigue," and concern that the treatment site would look abnormally different than control (sham) site at the conclusion of the study.

To date, the team has enrolled and treated a total of 10 patients, 7 in the late-treatment cohort, 3 in the early-treatment cohort. The late-treatment cohort has advanced to the highest treatment dose per protocol; the early-treatment protocol will begin the second-level treatment dose with the next enrolled subject. All data acquisition has proceeded smoothly to this point, and there have been no adverse events, but it is still too early to draw any conclusions from the data. The team has only recently begun preliminary analysis of data obtained to date to confirm the adequacy and consistency of the data being accrued. USAISR/BAMC continues to prepare for initiation of the AFT trial at a second site. The protocol was approved (for implementation at USAISR) with stipulations during the 27 June 2012 USAMRMC Institutional Review Board (IRB) meeting; study initiation is pending final approval.

As mentioned earlier, active challenges relate primarily to continued efforts to enhance the enrollment of patients into the study. In addition, Dr. Katz has decided to accept a new faculty position at the University of Florida (UF). His transition to Florida has led to revision of research plans. The University of Virginia (UVA) will remain as an open clinical trial site, with Dr. David Drake serving as the new Principal Investigator and Dr. Ratliff continuing as the study coordinator. The Virginia IRB has approved the amendment to the protocol that changed the Principal Investigator, and review at the HRPO has been initiated. In parallel, Dr. Katz is working to open UF as a clinical trial site, where he will be the lead Principal Investigator. The clinical protocol for submission to UF's IRB is currently under preparation.

Conclusions

Conclusions on the clinical trial outcome cannot be drawn until more data are collected.

Clinical Trial Plans for Year 5

Future efforts will focus on improving the recruitment and enrollment of study subjects. The team is considering providing a financial incentive to subjects who enroll, and Dr. Drake is planning to pursue a direct recruitment strategy (personal mailings to his patients). The team will continue to support the USAISR/BAMC team to obtain USAMRMC IRB and HRPO approvals as soon as possible. Dr. Katz will be hiring a full-time clinical nurse coordinator at UF, and efforts to obtain Florida IRB approval of the clinical protocol are under way. There is full and eager support for this study at UF. Of note, UF will have nearly four times the number of burn patient admissions as UVA. UF is also associated with one of the busiest VA Medical Centers in the country. Dr. Katz anticipates that these factors will help accelerate the accrual of enrolled subjects. In addition, by the end of summer, the team expects to have three active trial sites for the study: UVA, UF, and USAISR/BAMC.

Commercialization Plans

There are multiple companies that currently market fat tissue transplantation devices and systems. If the evidence from this trial supports the use of AFT for scar remodeling, then commercialization will be likely.

V: Burn Repair

Intravenous Treatment of Burn Injury

Therapy to Limit Injury Progression, Attenuate Inflammation, Prevent Infection, and Promote Non-Scar Healing After Burns and Battle Trauma

Project 4.6.1, RCCC

Team Leader(s): Fubao Lin, PhD and Richard Clark, MD (Stony Brook University)

Project Team Member(s): Adam J. Singer, MD (Stony Brook University)

Collaborator(s): Molly Frame, PhD and Marcia Tonnesen, MD (Stony Brook University)

Therapy: Burn injury progression inhibitor

Deliverable(s): Intravenous (IV) P12

TRL Progress: 2010, TRL 3; 2011, TRL 4; 2012 (Current), TRL 4; 2013 (Target), TRL 5

Key Accomplishments: The researchers developed a porcine vertical burn injury progression model and demonstrated that P12 infusion limits burn injury progression in this model. They found that P12-enhanced endothelial cell survival under hypoxic conditions. They evaluated burn injury progression quantitatively at early stages of burn injury using a noninvasive system with infrared contrast imaging.

Key Words: Burn, injury progression, curcumin, peptide P12

Introduction

Battlefield polytrauma secondary to blasts and explosions is increasingly common, affects multiple sites, and is complex. Many of these injuries, particularly burns, are subject to progressive tissue damage over subsequent days and can have a devastating effect on the wounded warrior. Over the course of a few days to 1 week, deep partial-thickness burns can progress to full thickness and lead in the short term to increased tissue loss, longer healing time, and excess morbidity and mortality. In the long term, increased scarring, wound contractures, and poor quality of life become major issues. Therapies to improve blood flow, such as nonsteroidal anti-inflammatory drugs (NSAIDs) and anticoagulants (heparin), have not shown substantial benefit in preventing burn injury progression. A therapy to limit burn injury progression remains an unmet need.

During Year 1, the researchers tested five therapeutic agents, with low-risk profiles, that target three of the major sequelae of reperfusion injury in a rat hot comb model: (1) cytokine release, (2) generation of reactive oxygen species (ROS), and (3) markedly increased programmed cell death (apoptosis). The five therapeutics agents were: (1) human bone marrow-derived mesenchymal stem cells (BM-MSC); (2) pentoxifylline, which inhibits tumor necrosis factor-alpha (TNF-α) production; (3) curcumin, a potent antioxidant; (4) desferrioxamine (DFO), a potent iron cheater that blocks free radical chain reactions; and (5) P12, a peptide derived from fibronectin with remarkable antiapoptotic properties. BM-MSC, pentoxifylline, and DFO showed little effects in the studies while curcumin and P12 significantly inhibited burn injury progression. In Years 2 and 3, the researchers developed a porcine hot comb model to evaluate these candidate inhibitors. Curcumin showed no protective effect against burn progression in this model. The results demonstrated that a single 0.01–3.0 mg/kg P12 infusion significantly limited burn injury progression, with the maximum effect observed at 1.0 mg/kg. In addition, MicroConstants, Inc. (San Diego, CA) validated a method to detect P12 in biologic fluids, including blood, and studied P12's stability in vitro.

Research Progress – Year 4

Preclinical safety and efficacy studies must be performed prior to starting clinical trials, in accordance with U.S. Food and Drug Administration (FDA) guidance. Focusing on P12 using a porcine vertical burn injury progression model, the Clark laboratory was able to determine the compound's safety and efficacy and establish systemic dosing details and treatment validation to prevent burn injury progression, reduce inflammation, induce healing, and inhibit scarring with IV infusion. Notably, the FDA granted P12 Orphan Drug Designation on June 29, 2011.

Evaluation of P12 Effect on Burn Injury Progression in a Porcine Burn Injury Model

Female Yorkshire swine (~20 kg) were used in these studies. The researchers removed hair and then created 20 burns on the back of each animal with an aluminum block preheated in a water bath to 70°C or 80°C and applied to the skin surface for either 20 or 30 seconds. P12 or buffer was infused 1 hour post burn. Full-thickness 4 mm punch biopsies were taken from selected sites at 1, 24, and 48 hours , and 7 days (**Figure 1**). On day 28, following a macro-evaluation of the wounds for necrosis and scarring and photographs, a full-thickness 8 mm punch biopsy was taken from the center of each wound and bisected (Figure 1). All biopsy samples were placed in labeled cassettes and fixed in formalin.

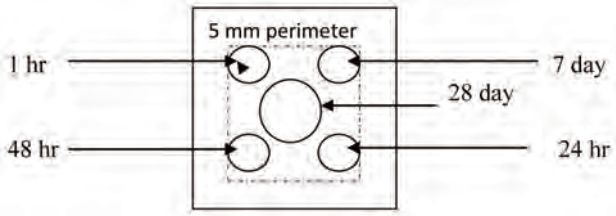

Figure 1. 2.5 x 2.5 cm burn with indicated perimeter area and biopsy locations in porcine vertical burn injury progression model.

To study the effect of P12 on vertical burn injury progression, two swine were infused with buffer as controls, and two others were infused with 1 mg/kg P12. As shown in **Figure 2**, the burn scar depth was decreased in both P12 infused swine, as compared with control, at all three burn conditions (70°C/30 sec, 80°C/20 sec, 80°C/30 sec). These results demonstrated that P12 limits burn injury progression in the porcine vertical burn model. The P12 safety studies have been performed with a 70° burn for 30 minutes, and the P12 efficacy studies have used 80° burns for 20 and 30 minutes, in accordance with FDA guidance obtained during a pre-Investigational New Drug (IND) meeting.

Noninvasive Quantitative Measurement of Burn Injury with Infrared Contrast Imaging

An early, noninvasive quantitative measurement of tissue injury that predicts depth of tissue necrosis and scarring at a later time would greatly assist evaluation of potential therapies for inhibition of burn injury progression in clinical trials. Most currently accepted methods of diagnoses are suboptimal. Forward Looking Infrared (FLIR) is a noninvasive method, operating in the far infrared (IR) region that instantaneously measures IR emission from tissue.

Pilot studies were carried out in a validated porcine vertical burn injury progression model to differentiate superficial from deep-dermal burns on the basis of a temperature scale. FLIR images show zones within burns that appear similar to the Jackson model of burn injury. Significantly, more than three zones were observed with differences in temperature between and within burns

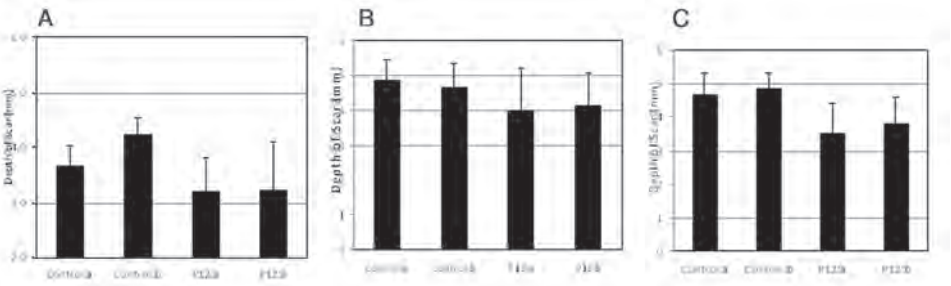

Figure 2. P12 infusion decreases the depth of scar in the porcine vertical burn injury progression model at all three burn conditions: (A) 70°C for 30 seconds, (B) 80°C for 30 seconds, and (C) 80°C for 20 seconds. The burns were evaluated histologically at 28 days post burn.

(**Figure 3**). Preliminary data suggest that superficial burns correspond to zones of greater core temperature and deeper burns to zones of lower core temperatures. The team hypothesizes that wounds with higher core temperature and periphery (as seen by FLIR) indicate less tissue damage while those with lower temperature indicate higher tissue damage. Superficial burns had warmer cores whereas deep dermal burns have colder cores. In addition, differences in burn severity can be quantified using ExaminIR© software.

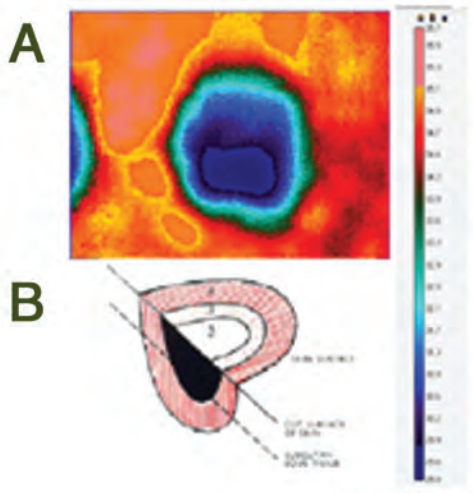

Figure 3. Comparison of FLIR image (A) with Jackson's model (1953) of burn injury (B). Both can distinguish between burns of varying severity.

P12 Enhanced Human Dermal Microvascular Endothelial Cell (HDMEC) Survival Under Nutrition Deprivation and Hypoxia Conditions

Burn injury induces early erythrocyte occlusion of surrounding cutaneous microvasculature and endothelial cell necrosis. Hypoxia and nutrition deprivation may be the major factors that induce endothelial cell death. To study whether P12 supports HDMEC survival under stress, HDMEC were cultured under hypoxic conditions (1% O_2) or nutrition deprivation conditions. Results showed that HDMEC survival was significantly decreased under hypoxic conditions, as compared to controls. However, in the presence of P12, HDMEC survival was increased (**Figure 4A**). HDMEC showed a low level of metabolic activity under nutrition deprivation. In the presence of P12, HDMEC metabolic activity was remarkably increased compared to vascular endothelial growth factor (VEGF) alone (Figure 4B).

Finally, the researchers demonstrated that P12, in the presence of platelet-derived growth factor-BB (PDGF-BB), modulates cell signal transduction pathways to favor survival under stress conditions (data not shown). They also performed stability studies for P12 in minipig and rat blood (data not shown).

Conclusions

One P12 infusion effectively limits burn injury progression in a porcine vertical burn injury progression model. These results are consistent with the effects of P12 previously reported in the porcine hot comb model. A noninvasive system with

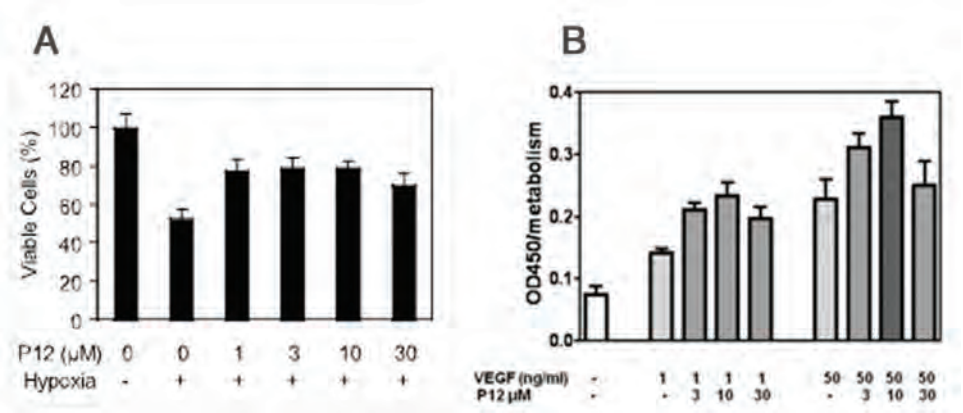

Figure 4. P12 enhanced HDMEC survival under hypoxia and nutrition deprivation conditions. HDMEC stressed by (A) hypoxia for 4 days or (B) serum/supplement withdrawal for 2 days ± P12 ± VEGF. Cell viability was determined by XTT assay. Values are means ± SD (n = 4).

infrared contrast imaging may be used to evaluate burn injury progression quantitatively. In vitro studies further demonstrated that P12 enhances endothelial cell survival under stress condition and upregulates the cell survival signal. These findings support the development of P12 infusion as a novel therapy to limit burn injury progression using a single dose.

Research Plans for Year 5

The research team will evaluate second-generation P12-like peptides for their ability to promote fibroblast and endothelial cell survival under stress conditions and angiogenesis both in vitro and in vivo. They will conduct safety studies for P12 in a porcine superficial burn model. P12 efficacy studies for inhibition of burn injury progression, promotion of healing, and reduction of scarring will be conducted in a porcine partial-thickness burn model.

Planned Clinical Transitions

In Year 5, the team will continue to transition peptide P12 toward the clinic. Specifically, the team will contract pharmacotoxicology studies and drug manufacturing, conduct safety and efficacy studies, design a Phase 1/2 clinical trial, and submit an IND to the FDA.

Topical Treatment of Burn Injury

Polymeric, Antimicrobial, Absorbent Wound Dressing Providing Sustained Release of Iodine

Project 4.6.4, RCCC

Team Leader(s): Carmine P. Iovine, PhD (Rutgers University)

Project Team Member(s): Richard Clark, MD and Adam Singer, MD (Stony Brook University); Joachim Kohn,PhD and Ganesan Subramanian (Rutgers University)

Therapy: Iodine-releasing dressing for treatment of infected traumatic or thermal heavily exuding wounds

Deliverable(s): Absorbent, conformable, nonadherent, self-supporting foam-based wound dressing containing 2%–15% by weight of bound molecular iodine that is released in contact with the wound in an on-demand, sustained manner over a period of several days

TRL Progress: 2010, TRL 3; 2011, TRL 3; 2012 (Current), TRL 4; 2013 (Target), TRL 4

Key Accomplishments: The research team finalized the prototype design (composition of matter, iodine content, physical properties) of their iodine-releasing wound dressing. The researchers developed a laboratory-scale process to manufacture their polymer. They demonstrated excellent reproducibility of the pre-polymer through a series of 10–12 laboratory preparations. They established preliminary specifications for the base foam, including water extractables, stress/strain characteristics, foam pore/cell size structure, and density. They demonstrated a broad bacterial kill spectrum versus standard antibiotics and silver-based dressings. They developed in vitro antimicrobial efficacy methods and their data confirmed the sustained delivery functionality of their novel starch polyurethane copolymer foam device, as compared to commercially available iodine containing dressings. Finally, they filed a provisional patent.

Key Words: Iodine, polymeric iodophor, wound dressing, antimicrobial, starch

Introduction

Although water-soluble polymeric iodophors have several advantages over tincture-based iodine, they have been shown to uncontrollably release iodine to the wound site due to high solubility. This quick release characteristic often provides a much higher dose of iodine than required for the intended antimicrobial action. As a result, the unused iodine is consumed by side reactions with body fluids; thus, the reservoir is prematurely depleted and may result in recolonization of the wound site by microorganisms. From a clinical point of view, wound dressings composed of water soluble polymeric iodophors should contain low concentrations of iodine and be clinically applied with frequent dressing changes.

The premature, burst-like release kinetics from water-soluble, polymeric iodophors can be avoided through the use of water-insoluble, polymeric iodophors. Attempted approaches have included nylon fibers, acetalized polyvinyl alcohol (PVA), and insoluble polyurethanes. Identification of an ideal dressing material has been hampered by issues with stability, iodine loading, and rapid release characteristics. The ideal dressing material would be an insoluble antimicrobial polymeric iodophor that is stable, highly adsorbent, and can release iodine in a controlled and sustained manner over several days.

Dr. Iovine's research team has focused on identifying an acceptable wound dressing material for further development. During Year 1, they identified the I-Plex Absorbent Antimicrobial Wound Dressing, which is a nonadherent, moist, formalin-treated PVA sponge that releases molecular iodine into wounds as exudates are absorbed by the polymer. However, this approach was terminated

when the PVA-based system failed due to concerns with toxicity. The basic foam is an acetyl of PVA and formaldehyde; it continually releases formaldehyde, a known carcinogen, during dressing. The wound environment presents optimum conditions for formaldehyde release. In Years 2 and 3, they identified a novel polymer system and used it to create a tunable iodine delivery system. They incorporated molecular iodine at very high-loading levels into an absorbent and wound-conformable, unsupported wound dressing material. This material contains a chemically linked novel iodophor and a biodegradable synthetic polymer in a flexible, nontoxic insoluble polymer network. The level of bound iodine in the network structure can be controlled by varying the ratio of the novel iodophor and the biodegradable synthetic polymer used to constitute the network. The rate, sustainability, and release time of the iodine antimicrobial can be controlled by varying the type of novel iodophor used in the structure. The researchers found that their iodine delivery system had significantly longer on-demand release of iodine compared to any known or tested iodophor system. The novel dressing showed promising results in a preliminary porcine infected burn model.

Research Progress – Year 4

Development of Reproducible and Validated Laboratory Process

In 2010, the researchers demonstrated proof-of-principle in vivo of their original prototype. This prototype was made using a "one shot" base foam process, in which the unmodified diisocyanate is combined with separate streams of water-soluble polyols (starch and glycerin) and water-insoluble polyols (polycaprolactone and polyethylene glycol [PEG] adipate). During this mixing phase of the copolymerization step, the reaction mixture is very exothermic and hard to control. The lack of process controls made it difficult to reproduce the key base foam properties from batch to batch. To address these shortcomings, a significant portion of the team's effort in Year 4 was devoted to the development of a reproducible, laboratory-scale (50 g) process using the pre-polymer process.

In the pre-polymer process, the diisocyanate component is pre-reacted with the water insoluble polyols. The resulting pre-polymer is less reactive and combines with the water-soluble polyols in a reproducible manner. The team produced reproducible foams by controlling mixing rate, shear input, and contact time, in combination with molding, curing, and cutting. They developed standard operating procedures (SOPs) for all of the base foam property measurements. The iodination step in the process involves the treatment of the cured foam with aqueous KI_3 solution. The standard, reproducible prototype contains 35% by weight of copolymerized starch, resulting in 8%–9% by weight of iodine bound per batch. By adjusting the concentration of iodine in the treating bath, targeted concentrations of iodine can be loaded into the wound dressings. In addition, both cumulative release profiles and daily release rates can be fine-tuned for the specific clinical application.

In Vitro Antimicrobial Testing and Efficacy

Kirby-Bauer disk diffusion is the standard method for evaluating the potency of antimicrobial agents against discrete bacterial strains. The Kirby-Bauer test was performed against the following gram-positive (G+) and gram-negative (G–) bacterial species using standard aseptic technique:

- *Staphylococcus aureus sub aureus* Rosenbach (ATCC 25923) (G+)
- *Staphylococcus saprophyticus sub saprophyticus* (ATCC 35552) (G+)
- *Bacillus cereus* (ATCC 2) (G+)
- *Pseudomonas aeruginosa* Schroeter (ATCC 10145) (G–)
- *Enterobacter cloacae* sub *cloacae* Jordan (ATCC 13047) (G–)

Efficacy of the prototype-iodinated foam scaffold against these species was measured in comparison to two commercially available wound dressings: Iodoflex® Cadexomer Iodine pads, 0.9% iodine w/w (Smith & Nephew), and the Silverlon® antimicrobial silver burn contact dressing (Argentum Medical). Diluted cultures were streaked onto agar plates, and the plates were spotted with the aforementioned 6 mm sample disks and one each of 10 U penicillin G, 10 µg streptomycin, and 30 µg tetracycline standardized antibiotic disks.

The prototype-iodinated foam scaffold was effective against all five bacterial species, with greater potency against the three gram-positive species . The iodinated foam scaffold disks appeared to have released only approximately half of their iodine load after 24 hours in contact with the agar. From these results, it was concluded that the prototype iodinated foam scaffold showed comparable functionality to the two commercially available products after 24 hours.

Due to the foam scaffold's extended release characteristic, the researchers also conducted Kirby-Bauer experiments with "preleached" sample disks. The initial experiments using this preleaching method demonstrated that the iodinated scaffold maintains its antibacterial properties against four of the five tested species of bacteria for at least 72 hours. The Iodoflex pad released its entire iodine load after 24 hours of preleaching and demonstrated no subsequent antibacterial activity. The Silverlon dressing showed minimal antibacterial capability only against *S. saprophyticus* after preleaching; it was no longer effective against the other four bacterial species after preleaching.

Conclusions

In Year 4, the researchers standardized their prototype design and laboratory-scale manufacturing process. In vitro antimicrobial efficacy data validated the sustained delivery functionality of the novel starch polyurethane copolymer foam device, as compared to commercially available iodine-containing dressings. This product is now ready for scale-up of the manufacturing process.

Research Plans for Year 5

The team will continue to develop the in vitro antimicrobial efficacy data to support the effort to generate third-party interest in the product concept and technology. They will perform in vivo safety and biocompatibility testing. They will explore stability and packaging of the device. In addition, they will transfer the laboratory process to a third party for manufacturing scale-up.

Topical Treatment of Burn Injury

Topical P12 Therapy to Limit Burn Injury Progression and Improve Healing

Project 4.6.5, RCCC

Team Leader(s): Lauren Macri, PhD (Rutgers University) and Richard Clark, MD (Stony Brook University)

Project Team Member(s): Atulya Prasad, MS, Adam Singer, MD, Laurie Crawford (Stony Brook University); Tom Morrow, PhD and Joachim Kohn, PhD (Rutgers University)

Therapy: Topical therapy to limit burn injury progression

Deliverable(s): A controlled release formulation of fibronectin-derived peptide P12 and a tissue-engineered construct with tethered P12

TRL Progress: 2010, TRL 3; 2011, TRL 3; 2012 (Current), TRL 4; 2013 (Target), TRL 4

Key Accomplishments: The research team validated a porcine excised hot comb burn model suitable for evaluating topical therapies that may limit burn injury progression. They determined that the P12 molecule must be modified to increase stability for topical applications. Exploratory research demonstrated the motogenic potential of P12 in response to various cell-binding peptides.

Key Words: Burns, burn progression, biodegradable polymers, drug delivery, peptide, electrospinning, wound healing

Introduction

Burn injuries can be extremely painful, debilitating, and complex to treat. One reason for this is that burn injuries are not localized to the initial site of trauma; rather, they progress (or extend) in size, in horizontal and/or vertical directions. Often, the tissue surrounding the burn, which initially looks like a healing partial-thickness burn, will convert into a nonhealing, full-thickness burn. Although burn wound care has advanced over the years (via resuscitation, emergency care, and transportation), there is still a critical need to develop treatments that limit burn injury progression, and specifically: (1) minimize tissue loss and need for grafting, (2) shorten healing and hospitalization time, (3) lower rates of morbidity and mortality, and (4) decrease scarring and contracture. Although many therapeutic agents have shown promise in small animal models, these beneficial effects have not been translated into FDA-approved therapies. Thus, a major clinical challenge exists to develop novel therapies that can reduce or prevent burn progression.

P12, a peptide derived from fibronectin, has recently been identified by the Clark laboratory at Stony Brook University and shows significant promise in the treatment of burns. This peptide enhanced the survival of adult human dermal fibroblasts, provided protection against oxidative and cytokine stress, and reduced burn injury progression in both rat and porcine hot comb burn models. The researchers chose tyrosine-derived polycarbonates (TyrPC) as their biodegradable polymer because they are biocompatible and readily processable, they undergo hydrolytic degradation, and they resorb benignly in a predetermined period of time. Carboxylic acid groups formed by degradation of the TyrPCs are not free to diffuse from the matrix or cause the rapid release of acid; thus, they decrease the possibility of excess inflammation. The goal of this research project is to develop biodegradable TyrPC fiber mats that produce topical, localized, controlled, and sustained P12 delivery, which would address the requirements of an efficient treatment to limit progression of localized burn injuries.

In Years 1 and 2, the researchers developed two TyrPCs as ultrafast- and fast-releasing, fiber-based drug delivery matrices for P12. The in vitro results from Years 1 and 2 indicated that these polymers satisfy the need for a class of biomaterials that can degrade and deliver a therapeutic agent in a rapid manner. The in vivo data confirmed the biocompatibility of both chosen polymer compositions. In Year 3, the team demonstrated that P12-loaded fiber mats were stable during storage and sterilization processes.

Research Progress – Year 4

Validation of Porcine Excised Hot Comb Model

The Clark and Singer laboratory at Stony Brook University uses the validated porcine hot comb burn model to evaluate the effects of intravenous administration of P12 on the limitation of burn injury progression. However, a modification to the protocol was required to evaluate topical administration of P12 and determine the effects of immediate burn excision on injury progression. The project team used immediate burn excision to allow direct contact between the P12-loaded fiber mats and the uninjured interspaces. Two types of wounds were created on one Yorkshire pig (comb burns and excisional wounds) using a preheated brass comb (**Figure 1A**). Each comb burn is composed of four full-thickness burn sites (the zone of coagulation) separated by three uninjured interspaces (the zone of stasis). Half of the comb burns were left nonexcised (Figure 1B) and the other half were immediately excised (Figure 1C). Similarly, excisional wounds of identical dimensions to the excised comb burns were also studied as controls.

For outcomes analysis, scar depth in the interspaces was measured to determine burn injury progression. The interspaces corresponding to the comb burns and excised comb burns progressed into full-thickness burns, resulting in a scar depth of 3.4 ± 1.5 mm and 3.9 ± 1.4 mm, respectively ($p>0.05$). Conversely, interspaces of the control excisional wounds showed no scar formation, i.e., complete viability.

These results confirm the histological results reported in Year 3. Thus, the agreement between the histological evidence of necrosis at day 7 and scar depth at day 28 confirms that surgical excision of the zone of coagulative necrosis in pigs is likely not sufficient to effectively reduce or prevent burn injury progression. Furthermore, excisional wounds with dimensions identical to the comb burn did not result in necrosis of the interspaces. The porcine excised hot comb burn model is a fully validated model for the evaluation of topical therapies on limiting burn injury progression.

Evaluation of In Vivo Efficacy of P12-Loaded Fiber Mats in Porcine-Excised Hot Comb Burn Model

The researchers believe that electrospun tyrosine-derived fiber mats offer the potential for topical clinical therapies requiring ultrafast or fast delivery of the therapeutic agent P12. They performed an exploratory study in pigs to evaluate the effects of topical P12 on reducing burn injury progression. Burn wounds were divided into subgroups where the excised comb burns were either left untreated or were treated with fiber mats + P12 ± platelet-derived growth factor-BB (PDGF-BB). Nonexcised, untreated comb burns were used as a control.

The data collected and analyzed under current study conditions suggest that topical treatment with P12-loaded fiber mats does not reduce burn injury progression. One possible reason is that the doses used were suboptimal. Second, it is likely

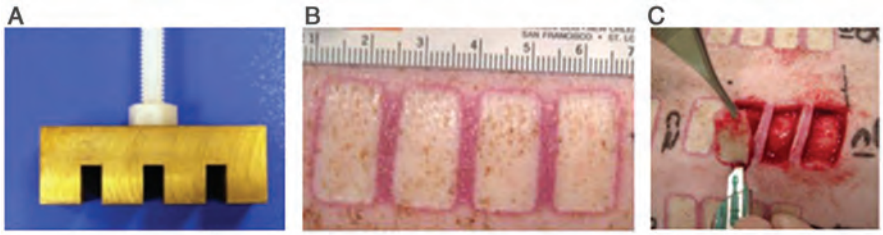

Figure 1. Porcine hot comb burn model. (A) Brass comb used to induce thermal injury. (B) Four burn sites with three unburned interspaces immediately after comb contact. The burns represent the zones of coagulation and the interspaces represent the zones of stasis. (C) Excision of comb burn immediately after its creation to allow direct contact between the P12-loaded fiber mats and the uninjured interspaces.

that P12 is susceptible to proteolytic degradation. Therefore, P12 may require modification at the amino and/or carboxy termini (e.g., by blocking or PEGylation) to prevent degradation in the burn wound. Third, it is possible that P12 nonspecifically adsorbs to various molecules, cells, or structures in the wound that may prevent its therapeutic effects. For example, in a collaborative study, P12 has been shown to absorb to red blood cells.

Conclusions

The goal of this research was to develop biodegradable, P12-releasing TyrPC fiber mats to limit injury progression of localized burns. In Year 4, the project team validated a porcine burn model that was suitable for evaluating topical therapies that may limit burn injury progression. They used this animal model to evaluate the efficacy of P12-loaded fiber mats in reducing the progression of burn injuries. The in vivo results of a pilot study suggest that further work is required to optimize the topical delivery of P12-loaded fiber mats to limit burn injury progression. In conclusion, electrospun tyrosine-derived fiber mats offer the potential for topical clinical therapies that require ultrafast or fast delivery of the therapeutic agent P12.

Research Plans for Year 5

In Year 5, the research team will fabricate fiber mats loaded with modified P12, determine the loading efficiency and release of modified P12, and demonstrate biocompatibility and efficacy in a porcine burn model.

Planned Clinical Transitions

Beyond Year 5, the project team will conduct safety and efficacy studies in accordance with Good Laboratory Practice (GLP) guidances, submit an IND to the FDA, and initiate the design of a clinical trial.

Topical Treatment of Burn Injury

Novel Keratin Biomaterials That Support the Survival of Damaged Cells and Tissues

Project 4.2.3, WFPC

Team Leader(s): Mark Van Dyke, PhD (Wake Forest School of Medicine [WFSM])

Project Team Member(s): Deepika Poranki, MS (WFSM); Carmen Gaines, PhD (WFIRM); and Olga Roberts, PhD (Wake Forest University)

Collaborator(s): Jimmy Holmes, MD, Joseph Molnar, MD, PhD, Justin Saul, PhD, Mark Lively, PhD, Roche de Guzman (WFSM); Luke Burnett, PhD (KeraNetics, LLC); and Michelle Merrill (Wake Forest University)

Therapy: Wound dressing for burn therapy

Deliverable(s): Keratin biomaterial-based burn treatment development and preclinical testing

TRL Progress: 2008, TRL 3; 2009, TRL 3; 2010, TRL 3; 2011, TRL 4; 2012, TRL 5

Key Accomplishments: The researchers completed a mechanistic study that demonstrates the effect of a specific fraction of keratin, gamma keratose, on cell death pathways following thermal injury. They found that heat treatment of mouse dermal fibroblasts upregulates genes related to the cell death pathway. A single gamma keratose treatment appeared to influence gene expression at 12 and 18 hours post injury, but this effect was diminished by 24 hours. Treating these thermally stressed cells with gamma keratose substantially diminished the upregulation of cell death genes compared to treatment with fresh fibroblast growth media.

Key Words: Burn, keratin, biomaterial, hydrogel, swine, pig, gel, dressing wound, skin, total body surface area (TBSA), tissue salvage

Introduction

In the United States, approximately 2.4 million burn injuries are reported each year. Burns also account for 5% to 20% of conventional war causalities. The cost of burn treatment products worldwide in 2008 was $2.1 billion dollars.[1] This number is for treatment products only and does not take into account other patient care costs, which reach into the tens of billions of dollars annually. For burns requiring hospitalization, the standard of care often involves a period of wound care and observation until wound demarcation is complete and the burn surgeon can make a determination as to the need for excision of dead skin and grafting. This "wait and see" period is based on the process of conversion, where damaged cells "convert" from thermally stressed to dead tissue. This is also referred to as burn wound progression. While the specific structures and cellular interactions remain to be fully understood, keratin biomaterials offer a platform for biomedical applications wherein materials can be tuned to elicit behaviors of interest (e.g., protection after thermal stress and wound healing).

The Van Dyke group at WFSM has spent the past 8 years developing and patenting methods to isolate and purify keratins to the level of subtypes that possess structural properties common to each. The group's recent work has shown that peptide by-products of the oxidation/extraction process, which have been identified using proteomic techniques, have the capacity to rescue cells from thermal damage by suppressing the upregulation of cell death signaling genes.

In collaboration with KeraNetics, LLC, the researchers have developed a keratin biomaterial hydrogel-based wound dressing, KeraStat Burn. Keratose, the base material of the KeraStat Burn product, has also been shown to be biocompatible by

[1] Wound Care Markets: Volume II Burns. Kalorama Information. New York, NY. April 2009.

ISO 10993 safety tests conducted at Toxikon Corporation. In addition, the Van Dyke group has demonstrated the feasibility of using keratin biomaterials for burn treatment in a mouse chemical burn model (**Figure 1**) and thermal burns in swine (**Figure 2**). These data demonstrate the feasibility of using a keratose hydrogel dressing to provide coverage to tissue and stabilize wound size (i.e., stop burn conversion and suppress an increase in TBSA).

The goal of this project is to translate and commercialize the KeraStat Burn product. To that end, the following aims are being pursued: (1) investigate the thermoprotective characteristics of keratin biomaterials in vitro, (2) test the thermoprotective characteristics of keratin biomaterials in a pig burn injury model, and (3) conduct the first clinical investigation of a keratin biomaterial treatment for burn injury.

During the first 2 years of the project, the research team developed a cell culture heat shock model that was used for mechanistic studies and to determine biomaterial dosing formulations for burn studies in swine. The researchers identified a key component of the keratin biomaterial, gamma-keratose, and developed new formulations using this material. In Year 3, the researchers developed and optimized a model of burn injury in swine; transferred the keratin biomaterial manufacturing technology to a partner company, KeraNetics, LLC, where it has been scaled-up and validated to be in compliance with the Quality System Regulation (QSR) standards (21 CFR Part 820). A pivotal animal study (second-degree burns in swine) was completed. A pre-IND meeting was held with the FDA to determine the regulatory pathway, and preliminary FDA and Institutional Review Board (IRB) approval was obtained for the proposed clinical trial design.

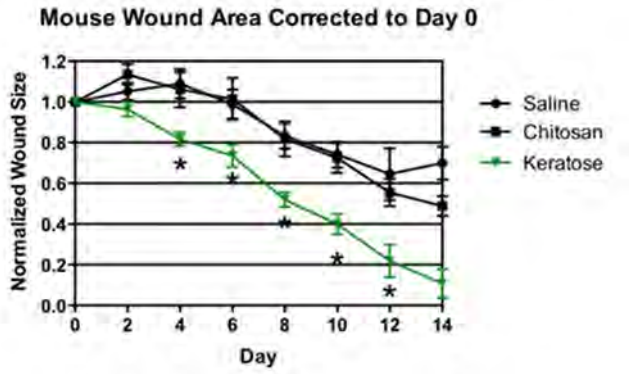

Figure 1. Mouse chemical burn wound area. Wound surface area for each treatment group was normalized to day 0 so as to express each subsequent day as a percentage of the day 0 wound area. Keratose-treated wounds did not grow in size and were completely healed by day 16. Other treatment groups showed an increase in initial wound size and required longer to heal. There was a statistically significant difference between keratose and both controls at all time points between day 4 and 16 (data are truncated for clarity; *p<0.05, repeated measures analysis of variance (ANOVA) was used).

Research Progress – Year 4

During the past year, the researchers utilized their previously developed swine burn model to conduct a pivotal, preclinical trial. They also continued mechanistic studies to help define the primary mode of action of the keratin biomaterial.

Pivotal Swine Burn Study

Twenty-eight female Yorkshire swine were used under a protocol approved by the Wake Forest Institutional Animal Care and Use Committee

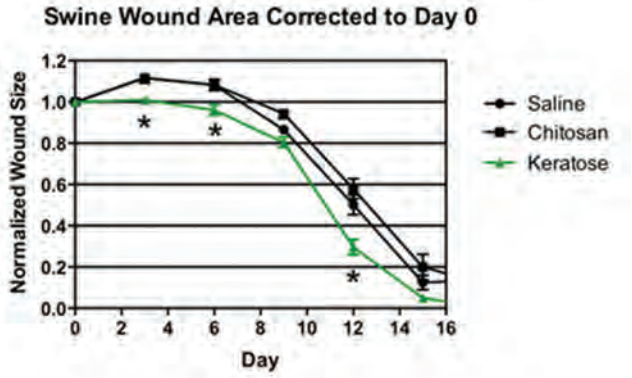

Figure 2. Swine thermal burn wound area. Wound surface area for each treatment group was normalized to day 0. Keratose-treated wounds did not grow in size and were completely healed by day 18. Other treatment groups showed an increase in initial wound size and required longer to heal. There was a statistically significant difference between keratose and both controls at days 3, 6, and 12 (data are truncated for clarity; *p<0.05, repeated measures ANOVA was used).

and the Animal Care and Use Review Office. The animals were randomly divided into the two arms of the study, one in which treatment would be administered within 60 minutes of burning and another in which treatment was delayed for 10 hours. In each arm, 14 animals were randomized and 12 burn wounds were created on each animal with heated cylindrical brass blocks, 6 on each side of the dorsal mid-line between the shoulder and hip under general anesthesia. The brass blocks were heated in an 80:20 (volume:volume) boiling PEG:water solution. Once the boiling liquid was heated to 105°C–115°C, the brass blocks were used to create burns on the pig by contact with the skin for 20 seconds. The wounds were randomized into one of four treatment groups: Saline-soaked gauze, Coloplast (a collagen-based wound gel), keratin treatment 1, and keratin treatment 2. Keratin treatment 1 represented the form of keratose hydrogel used in previous pilot studies, and keratin treatment 2 represented the KeraStat Burn formulation.

For each treatment, at each time point in both arms of the study, six replicate wounds were created using two animals. The researchers used 3 cc of keratin or Coloplast on each wound, and all wounds were covered with a Telfa pad, Ioban dressing, a protective plastic shield, and a nylon jacket. Every 3 days, the dressings were removed, and the wounds were cleaned and debrided with saline-soaked gauze. Digital photos were taken with a color wheel and ruler in view for digital image processing. On days 1, 3, 6, 9, 12, 15, and 30 post surgery, two animals were euthanized and tissue was collected. The skin tissue sections were analyzed histologically using Gomori trichrome, H&E, and von Willebrand factor (blood vessels) staining, and results were quantified using typical morphometric techniques. Digital photos taken at dressing changes were measured for wound area.

Wound area measurements showed that keratin-treated wounds were significantly smaller at days 9, 12, and 15 compared to silver sulfadiazine (SSD) cream (**Figure 3**). Wounds were also tattooed so that contracture could be measured. No appreciable wound contracture was noted in any of the treatment groups. Histomorphometric analysis showed two distinct phases of healing. In one phase, there was a modest rate of re-epithelialization due to the changing nature of the wound bed. A second, more rapid phase was marked by the appearance of granulation tissue. Re-epithelialization data for both phases appeared to show that keratin treatment provided benefit in the early phase of treatment whereas SSD did not, and all treatments appeared to provide benefit in the later phase of healing although SSD was discontinued after day 15. The average number of days to wound closure was the shortest in the KeraStat Burn treatment group. However, none of these data were statistically significant.

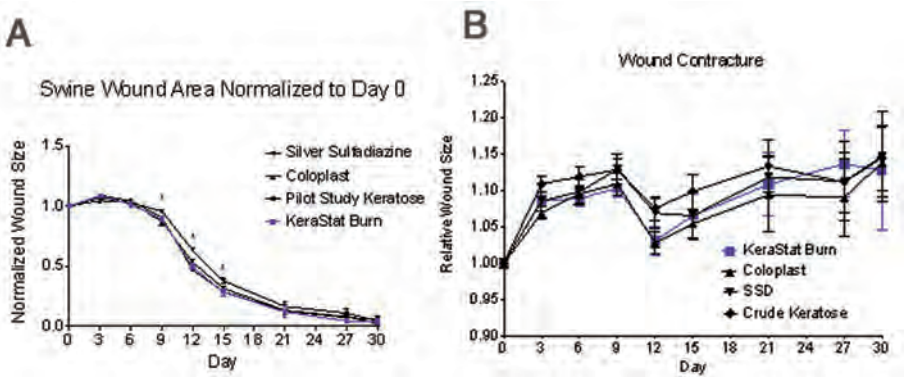

Figure 3. Morphometric analysis of digital images. Digital image analysis showed that wound area was lowest in the KeraStat Burn treatment group at days 9, 12, and 15 (*$p<0.05$ by repeated measure ANOVA).

Heat Shock Mechanism Study

Additional heat shock experiments have been conducted using the in vitro model, previously reported, in which gene microarray analysis was used to investigate the regulation of cell death pathways in keratin-treated mouse dermal fibroblasts. Briefly, mouse dermal fibroblasts were isolated from adult cd1 mouse ear pads and grown to near confluence. Cultures were treated at 44°C for 150 minutes to induce necrosis and stress. Following this "heat shock," cells were maintained for 6 hours under normal culture conditions, and then nonadherent cells were removed and treatments were applied to the remaining adherent cells. Cells were harvested at 12, 18, and 24 hours, and RNA extraction was performed for PCR microarray analysis. cDNA synthesis was performed and then a PCR microarray mouse cell death pathway finder was used to identify the expression of genes that are involved in cell death.

The researchers compared post-treatment (12 hr, 18 hr, and 24 hr) to the pre-treatment control (6 hr). They calculated the ratio of gene expression (fold change) for gamma keratose treatment to fibroblast media treatment (i.e., fold change value for keratose treatment divided by the fold change value for fibroblast media control treatment). Compared to the control group, the gamma keratose treatment at 12 hours showed a significant downregulation ($p<0.05$) in 29 out of 86 genes. In spite of the high differential gene expression (fold change) in the fibroblast media-treated cells, the difference was not statistically significant compared to the pre-treatment control. Among the 29 genes that showed significant difference with gamma keratose treatment compared to the pre-treatment control, 19 genes had higher expression in the fibroblast media-treated cells, four genes had a similar expression between both the treatment groups, and 6 genes (*Htt, Mcl1, Ulk1, Atg16l1, Irgm1, Casp3*) had higher expression in gamma keratose-treated cells. Out of these 6 genes that had higher expression in gamma keratose cells, 4 genes are involved in autophagy, 1 gene is involved in both autophagy and apoptosis, and 1 gene is antiapoptotic. There were more subtle changes in gene expression at 18 and 24 hours.

Conclusions

The AFIRM keratin biomaterials burn project is currently on budget and ahead of the original schedule. The researchers have completed the preclinical efficacy and safety testing required for an Investigational Device Exemption (IDE) application to the FDA.

Research Plans for Year 5

Other commercialization activities and preclinical testing includes preparation of clinical batches of KeraStat Burn and final quality control (i.e., lot release testing) and toxicity testing of these batches. These activities will be conducted by the research team's commercialization partner, KeraNetics, LLC, during Year 5 of the project.

Planned Clinical Transitions

An IDE application will be submitted to the FDA in the third quarter of 2012.

Wound Healing and Scar Prevention

Delivery of Stem Cells to a Burn Wound via a Clinically Tested Spray Device. Exploring Human Skin Progenitor Cells for Regenerative Medicine Cell-Based Therapy Using Cell Spray Deposition

Project 4.2.2, WFPC

Team Leader(s): Jörg C. Gerlach, MD, PhD (University of Pittsburgh)

Project Team Member(s): Patrick Over, Matthew Young, and Roger Esteban, PhD (University of Pittsburgh)

Collaborator(s): James Holmes, MD (Wake Forest) and Steven Wolf, MD (USAISR)

Therapy: Skin stem cell delivery for cell-based treatment of burn wounds

Deliverable(s): (1) Optimized cell isolation and spraying methodologies and (2) Next-generation skin gun FDA-approved spray device that can deposit fetal skin stem cells onto wound surfaces

TRL Progress: 2009, TRL 1; 2010, TRL 2; 2011, TRL 3; 2012, TRL 4

Key Accomplishments: The research group established an antibody marker characterization panel for fetal and adult epidermal cells and demonstrated the differentiation stage of various skin cells and stem cells. They initiated fetal epidermal and dermal progenitor isolation, in vitro culture, expansion and cell banking. The group also submitted an application to the FDA for 510(k) approval for their spray device.

Key Words: Skin stem cells, burn wounds, human fetal tissue, progenitor cells, cell spray method

Introduction

The survival of combat victims with large burns is often limited, since large burn areas reduce the availability of healthy donor skin for split-skin mesh grafting. The human body responds to skin burn injuries involving the basal epidermal layer with regeneration that often results in fibrosis and scarring. Current treatments for burns, other than mesh grafting, do not speed up epidermal re-epithelialization time and do not reduce complications, such as infections, which contribute to significant scarring, functional impairment, and undesirable aesthetic outcomes.

The therapy for burns depends on the size and depth of the wound and varies from conservative therapies in smaller second-degree burns to split-skin mesh-grafting, cadaveric, and artificial skin sheet coverage in third-degree burns. Mesh grafting is the gold standard, but donor area is limited, and it also generates an additional wound, both of which are problematic in larger combat-related burns. The ratio of the size of the donor area to the size of the treatable mesh-graft is typically 1:3 but may range to 1:8. The outcomes of grafting become worse with the increase of this ratio. Regenerative medicine research provides cell-based therapies that are designed to improve wound healing by offering viable cells that accelerate regeneration and reduce complications. The use of isolated single cells enables split ratios larger than 1:20. Cell grafting for partial-thickness second-degree burns requires epidermal stem cells from the basal layer of the epidermis to be successful. In full-thickness third-degree wounds, dermal MSC may be needed to compensate for the dermis loss.

The Gerlach group has developed skin cell isolation techniques for epidermal and dermal stem cells from adult and fetal tissues, along with methods and devices to improve single cell spray grafting.

Applications using autologous cells for partial-thickness burns were reported both in Europe and the United States. In addition, the research team is exploring cell-spray grafting of dermal cells to address third-degree burn therapy. They compared adult- and fetal-derived epidermal and dermal progenitor cells and initiated off-the-shelf product development. They moved forward with adult autologous cells rather than fetal cells because research indicated that inclusion of the MSC into the spray system would allow the project to extend from development of second-degree to third-degree burn therapy. The researchers initiated the 510(k) regulatory process for their skin gun device. Their long-term clinical goal is to refine and control the deposition of skin progenitor cells in a burn wound and to develop the ability to control their differentiation into basal keratinocytes and other terminally differentiated skin cells.

Research Progress – Year 4

Adult Skin Progenitor Cells

The Gerlach group focused on characterizing epidermal progenitors from autologous adult autologous cell isolations for cell spray deposition. They also investigated dermal cell isolation and performed progenitor characterization, cell culture behavior, and stemness studies, to address third-degree burn therapy development.

Adult epidermal keratinocytes. The group has defined a panel of markers for identifying different keratinocyte differentiation stages. This panel includes basal keratinocyte stem cell markers [CK15 and alpha6-integrin (α6-integrin)], early differentiation stages markers CK5 and CK13, and one late differentiation stage marker, LOR (loss of resistance). The researchers examined levels of CK15 and α6-integrin in skin biopsies using stacked layer confocal immunofluorescence microscopy, which confirmed an undulated basal layer and revealed an irregular distribution of basal keratinocytes over the inner surface of the epidermis (stratum basale) (**Figure 1A**).

Further studies that used the differentiation stage markers on cells in culture showed the effects of in vitro techniques on cell differentiation. The group compared isolated keratinocytes from biopsies with cultured cells during several passages. Using the differentiation stage markers in combination

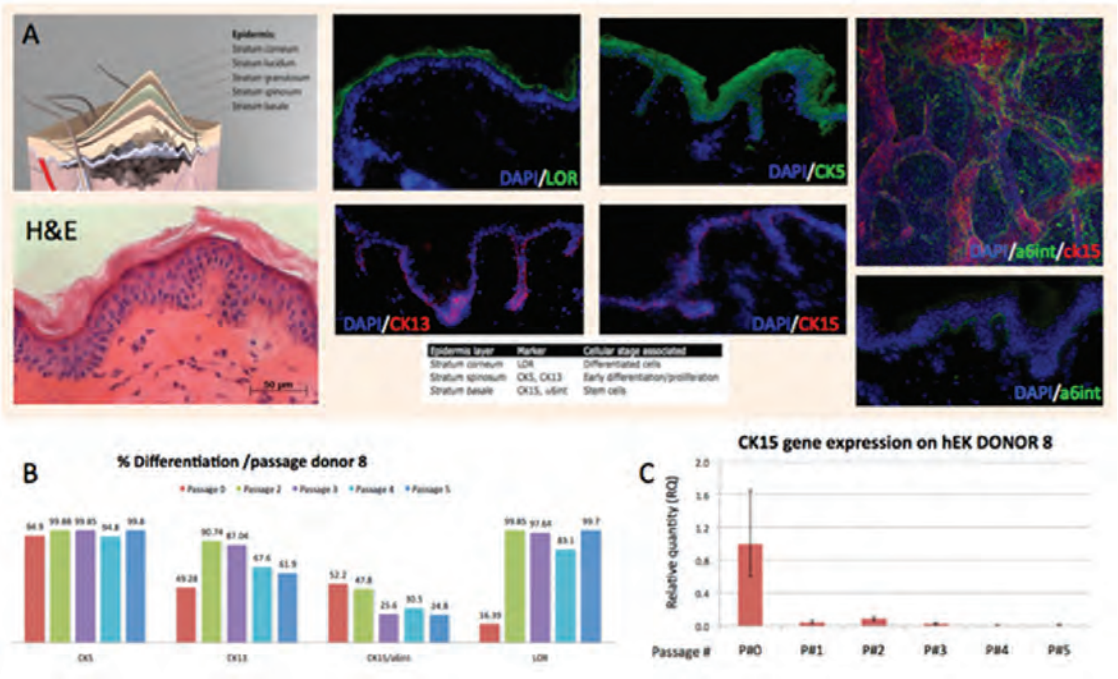

Figure 1. (A) Antibody markers for keratinocyte differentiation stage. (B) Flow cytometry results on differentiation markers for five passages on donor 8. (C) Donor 8 gene expression results for basal keratinocyte marker CK15 during five passages.

with flow cytometry (Figure 1B) and real-time PCR (Figure 1C), they observed a progressive differentiation along the passages with an increase of the differentiation markers CK5, CK13, and LOR. They also observed that in vitro culture led to decreased expression of stemness markers CK15 and α6-integrin and depended on culture passages and time. These results have implications for the cell-banking activities and the choice of adult- versus fetal-derived progenitors.

This analysis can also be used to establish a quality control database for predicting autologous cell isolation results in an on-site setting that are thought to depend on a patient's age, lifestyle, previous diseases, and medication.

Adult dermal fibroblasts. Previously, the group investigated properties of dermal fibroblasts for their potential clinical use on full-thickness burns. The group isolated progenitor cells from dermis during epidermal cell spray-grafting procedures at the Mercy Hospital Burn Center using previously developed techniques. They also studied dermal progenitor cell isolation from full-thickness skin obtained from aesthetic surgery donations in collaboration with Peter Rubin, MD.

The researchers found no significant differences in the amount of enzymatic digestion among Type I, Type II, or Type III collagenase. The amount of dermis to be digested in relation to the volume of enzyme used turned out to be important. The researchers found that higher amounts of dermis liberated lower amounts of cells in comparable amounts of solution. Thus, dermis thickness and enzyme volume will impact the cell isolation results.

To standardize the experiments according to the regular practices performed in the hospital, the researchers used a dermatome set at 8/1,000 of an inch to obtain the same thickness of skin from aesthetic specimen donations as being used for burn patients. The results confirmed previous work in Berlin, Germany , and could be used to advance autologous dermal reconstruction for third-degree burn wounds.

Fetal Skin Progenitor Cells

This year the group also focused on enhancing the cell growth of isolated epidermal and dermal progenitors in vitro. They also conducted regular analyses of cell culture behavior to characterize the cells' stemness during in vitro expansion.

Fetal epidermal keratinocytes. The group analyzed the stemness antibody markers α6-integrin and CK15 to determine the degree of differentiation of fetal keratinocytes (**Figure 2A**) in tissue biopsies before in vitro cell growth. This information was needed to implement isolated cell flow cytometry and gene expression analyses. Cells were seeded in Petri dishes for expansion to obtain sufficient cell numbers for analyses and cell banking. After three passages, the effect of in vitro culture on the fetal keratinocytes was analyzed. Approximately 60% of the cultured keratinocyte population was positive for the stemness markers α6-integrin and CK15 (Figure 2B). Interestingly, levels of the differentiation markers CK13, C5, and LOR were also elevated (Figure 2B).

Fetal dermal cells. The group collected additional data about the culture behavior of fetal dermal cells to get more information about their progenitor

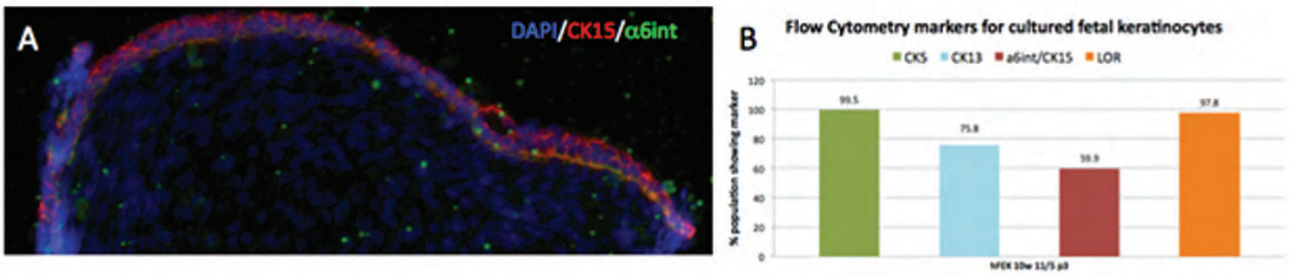

Figure 2. (A) Immunofluorescence staining on a 10-week fetal human biopsy for markers α6-integrin and CK15. (B) Flow cytometry results per differentiation stage to detect the effect of differentiation during in vitro culture cell expansion.

potential, which is of interest for wound healing in full-thickness burns. The results suggest that isolated fetal tissue-derived "fibroblasts" show some of the same markers (**Figure 3A**) as MSC, as published by the International Society for Cellular Therapy.[1]

The group isolated cells from different donors, expanded them in vitro, and cryopreserved them after several passages in liquid nitrogen tanks for dermal cell banking. These cells showed a reproducible and sufficient cell expansion rate (Figure 3B), making them suitable as an off-the-shelf product.

Skin Cell Spray Deposition Device for Grafting, "Skin Gun" Prototype

The research team has successfully tested the new prototype of Stem Cell Systems (Berlin, Germany) for experimental cell spray deposition. Parallel work in the framework of Innovative Practice in the Mercy Hospital Burn Unit demonstrated clinical feasibility, practicability, and reproducibility with superior results of the application over Avita Medical's ReCell sprayer. The group also initiated the FDA 510(k) process.

Conclusions

Primary adult keratinocytes that are isolated in an on-site setting exhibit a higher number of basal keratinocytes as well as colony-forming capability and thus provide a higher potential for wound healing over in vitro cultured/expanded keratinocytes. The research team also demonstrated a high content of epidermal progenitors, suggesting that its own method is competing well with the ReCell method. Additionally, the group also established an autologous dermal cell isolation technique for epidermal cells, which may address third-degree burn healing.

Research Plan for Year 5

The results on fetal tissue-derived cells suggest that fetal epidermal and dermal progenitor cells cultured in vitro do not represent pure stem cell populations. While the dermal progenitor expansion and cell banking results are very promising, the fetal epidermal progenitor expansion is not yet satisfying. Some further method refinement and studies are required to obtain sufficient data for a decision on using either fetal or adult cells for the anticipated final work on product development for cell-based wound-healing therapies.

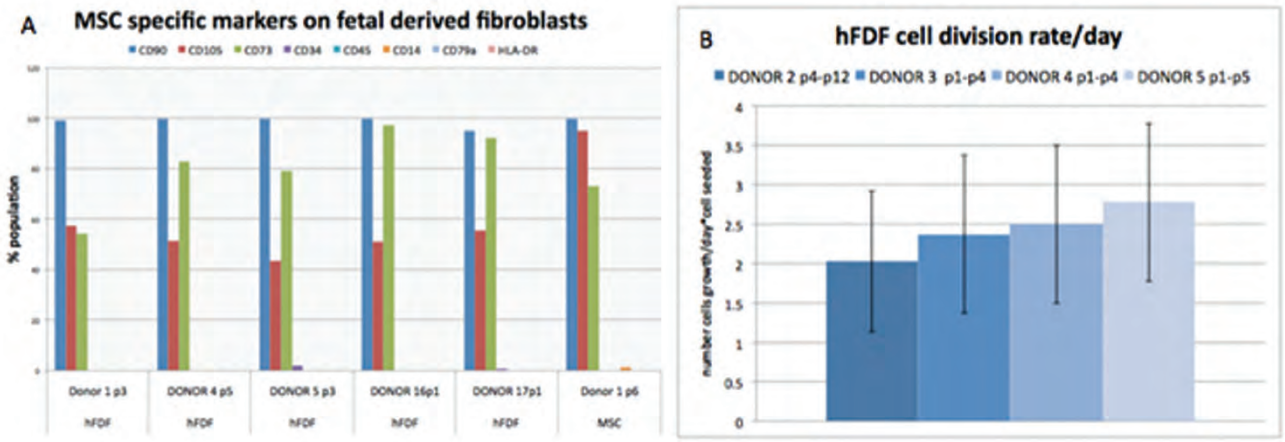

Figure 3. (A) Results of flow cytometry data showing MSC-specific markers on different populations of fetal-derived fibroblasts. (B) Cell division rates for different donors.

[1] Dominici M, et al. Minimal criteria for defining multipotent mesenchymal stromal cells. The International Society for Cellular Therapy position statement. *Cytotherapy* 2006; (8) 4:315-317).

Wound Healing and Scar Prevention

In Situ Bioprinting of Skin for Battlefield Burn Injuries

Project 4.2.5, WFPC

Team Leader(s): James J. Yoo, MD, PhD (Wake Forest University)

Project Team Member(s): Mohammad Albanna, PhD, Sean Murphy, PhD, Weixin Zhao, MD, Idris El-Amin, BS, Dennis Dice, BS, and Josh Tan, MS (Wake Forest University)

Therapy: Burn repair

Deliverable(s): Bioprinted skin

TRL Progress: 2009, TRL 2; 2010, TRL 3; 2011, TRL 3, 2012, TRL 4

Key Accomplishments: The bioprinting of keratinocytes and fibroblasts into a full-thickness incisional wound in a porcine model was successful and effectively covered the wound defect. The researchers found faster wound healing, smaller wound contracture, and a higher re-epithelialization rate with autologous treatments compared to other treatments. Formation of epidermis and dermis in wounds receiving bioprinted autologous cells was observed at 2 weeks post injury.

Key Words: Wound, burn, skin, bioprinting, autologous cell therapy, allogeneic cell therapy

Introduction

Severe burn injuries are a major cause of mortality and morbidity in civilians and military personnel. Conventional skin grafts are often limited in providing immediate wound coverage for large wounds. To overcome this limitation, the Yoo group developed a skin bioprinter that accurately delivers skin cells and biomaterials to rapidly cover large wounds.

In the first 2 years of the project, the researchers demonstrated the feasibility of in situ skin printing by bioprinting human fibroblasts and keratinocytes directly in a nude mouse wound model. Wounds treated with the bioprinter closed up to 3 weeks faster than controls. Printed skin cells required approximately 10–14 days to organize into skin, which is consistent with previous experiments using cell-spraying techniques. In the third year of studies, the researchers began to perform experiments in a porcine model using their skin bioprinting technology. They were successful in isolating and expanding dermal fibroblast and keratinocytes from porcine skin. The isolated and expanded cells remained viable when delivered through the printer nozzles. The printed cells participated in skin tissue formation and full-thickness wound repair.

Research Progress – Year 4

The researchers investigated whether their skin bioprinter could be used for the repair of large full-thickness wounds in a porcine model. Skin fibroblasts and keratinocytes were isolated from the dorsum of porcine skin through a partial-thickness (0.015 inch) skin biopsy. The researchers refined their fibroblast and keratinocyte cell isolation and culturing protocols to improve cell yield and viability in cultures. Both types of cells were cultured for 10 days until they reached confluence. Four full-thickness excisional wounds (10 x 10 cm each) were created on the back of a pig (n=6). Autologous and allogenic fibroblasts and keratinocytes, suspended in a fibrinogen-collagen solution, were printed directly on two wounds. Fibroblasts were printed first and crosslinked with thrombin to form a gel layer, and then keratinocytes were layered over the fibroblast. The remaining two wound groups received fibrinogen-collagen gel without cells and were left untreated as controls. The animals were followed for up to 5 weeks and analyzed for wound healing, re-epithelialization, and contracture.

Wounds treated with autologous cells showed complete healing by 3 weeks, whereas the other treatment groups showed healing in 6 weeks

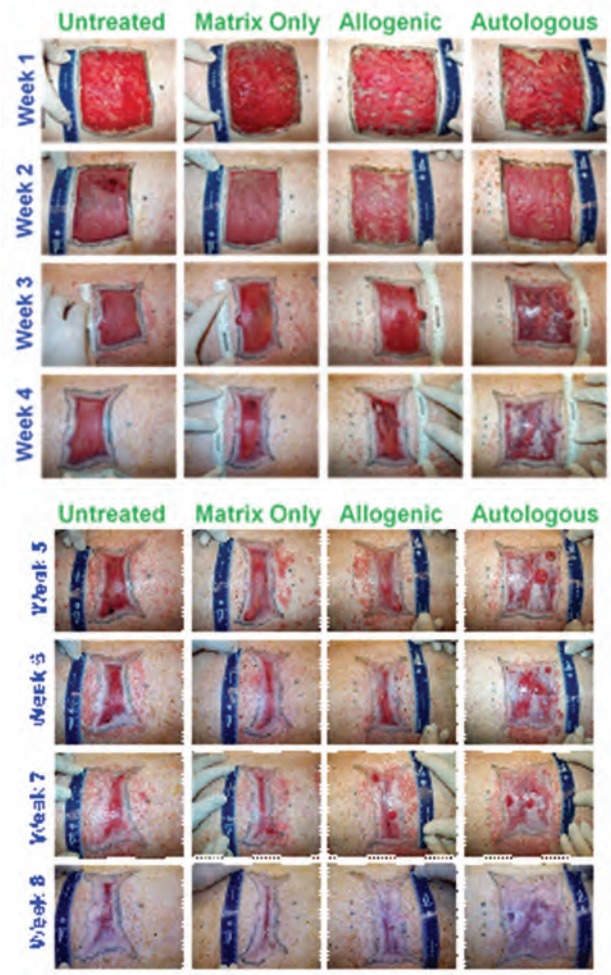

Figure 1. Gross images of wound healing over 8 weeks of study. Wounds treated with autologous cells showed complete healing by 3 weeks, where as the other treatment groups showed healing in 6 weeks.

(**Figure 1**). Wounds treated with autologous cells also showed an accelerated wound re-epithelialization and had almost 95% wound re-epithelialization by the third week of study (**Figure 2**). The amount of wound contracture observed with the autologous treatment was approximately half the amount seen with the other treatments (Figure 2). Wounds treated with allogenic cells did not show notable differences with respect to wound size, re-epithelialization and contracture when compared to controls (untreated and matrix only). Histological analyses showed a complete formation of epidermal and dermal layers within the first 2 weeks of the study in the autologous treatment group. However, other treatments showed a formation of

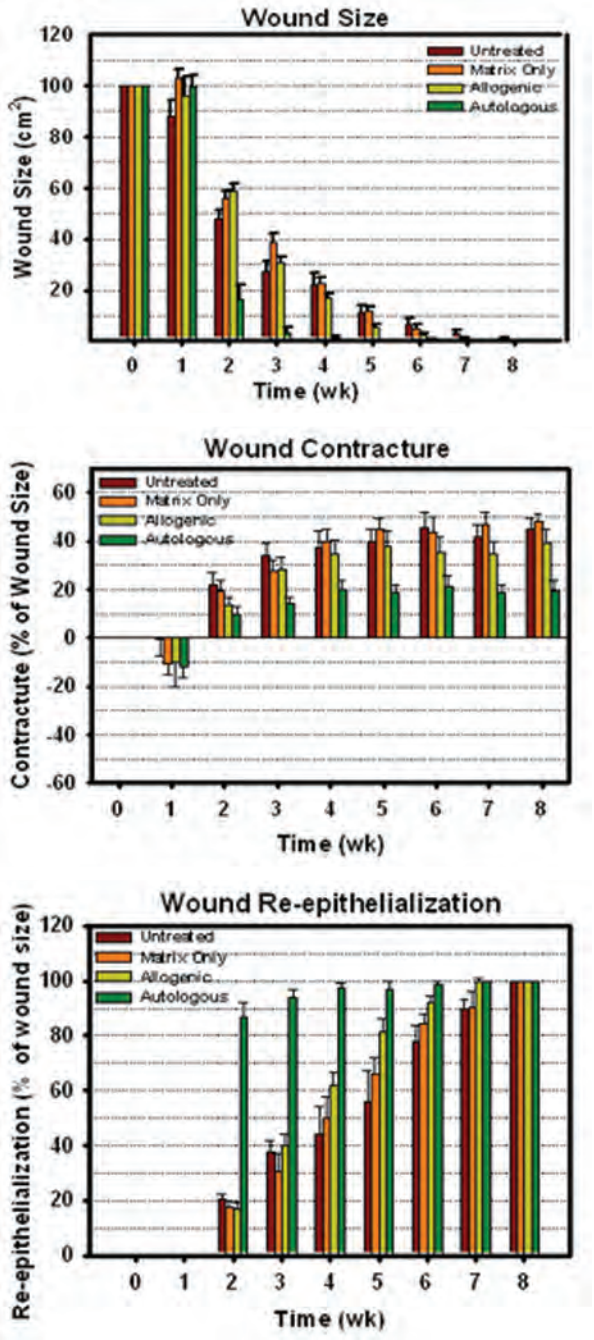

Figure 2. Wound size, contracture, and re-epithelialization of untreated, matrix only, allogenic and autologous treatments over 8 weeks of study. Wounds treated with autologous cells also showed an accelerated wound re-epithelialization and had almost 95% wound re-epithelialization by the third week of study.

epidermis and dermis by week 6 of the study (**Figure 3**). These results demonstrate the ability to regenerate skin within 2 weeks using autologous cells with minimal contraction and accelerated wound re-epithelialization.

Conclusions

The delivery of skin keratinocytes and fibroblast cells and biomaterials directly on the wound using the bioprinter was successful and effectively covered the wound defect. Delivery of autologous cells accelerated wound healing. This preclinical study suggests that the use of skin bioprinting is an alternative approach for rapid coverage of extensive skin wounds such as burn.

Research Plans for Year 5

The researchers plan to establish a third-degree full-thickness porcine burn model and complete an evaluation of bioprinted cells in the enhancement of wound healing. They will bioprint keratinocytes and fibroblast into the burn and determine the time to wound healing as well as wound contracture and wound re-epithelialization.

Planned Clinical Transitions

Although no clinical trials are currently planned under this AFIRM project, the data collected from the porcine burn model will be critical in transitioning to a future clinical trial.

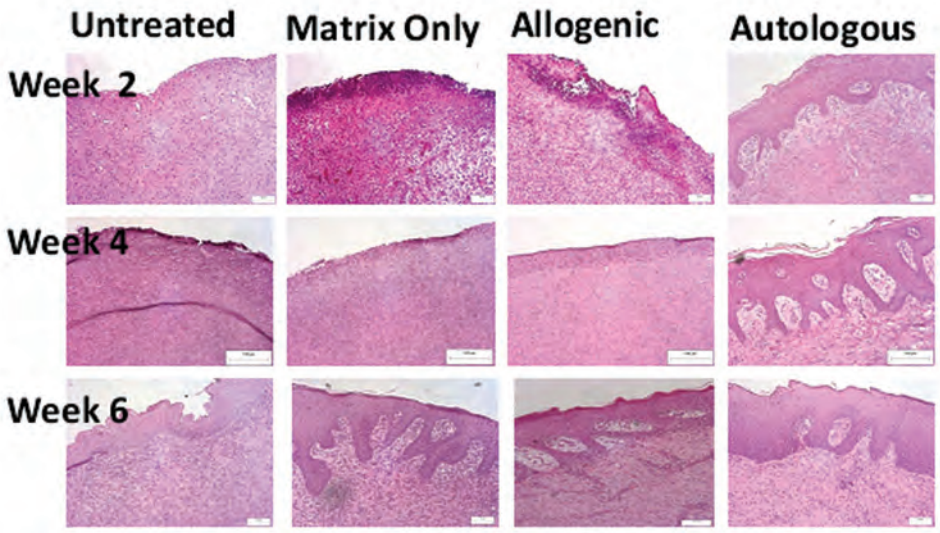

Figure 3. H&E staining of skin biopsies taken from treatments at weeks 2, 4, and 6 of the study. Complete formation of epidermis and dermis layers was observed within the first 2 weeks of study in the autologous treatments. However, other treatments showed a formation of epidermis and dermis layer by week 6 of study.

Skin Products/Substitutes

Burn Repair with Autologous Engineered Skin Substitutes

Project 4.7.2, RCCC

Team Leader(s): Steven Boyce, PhD (University of Cincinnati) and Richard Clark, MD (Stony Brook [SUNY])

Project Team Member(s): Dorothy Supp, PhD (University of Cincinnati)

Therapy: Advanced therapy for extensive, deep burns

Deliverable(s): Autologous engineered skin substitutes with pigment (ESS-P)

TRL Progress: 2010, TRL 3/4; 2011, TRL 4; 2012 (Current), TRL 4; 2013 (Target), TRL 4/5

Key Accomplishments: The researchers adapted protocols to increase the efficiency of melanocyte transplantation in their ESSs. They obtained uniform skin color with melanocyte densities that are clinically relevant. Tumorigenicity testing showed no detectable risk of tumor formation. Preliminary ultraviolet B (UVB) exposure studies showed that pigmented ESSs could protect against DNA damage from UVB radiation in sunlight.

Key Words: Burns, engineered skin, pigmentation

Introduction

Mortality and morbidity from burns, trauma, and other skin loss injuries remain significant medical and socio-economic problems estimated to cost more than $1 billion annually in treatment costs and lost productivity in the civilian population. Burns in the civilian population cause more than 900,000 hospital days in the United States annually, and full-thickness burns require treatment by excisional debridement and split-thickness skin grafting.

More than 20 years of preclinical and clinical studies have led to the development of autologous ESSs. The ESS currently consists of a lyophilized sponge of collagen and chondroitin sulfate, populated with cultured dermal fibroblasts and epidermal keratinocytes that organize into an analog of skin tissue. The device develops an epidermal barrier and basement membrane and releases high levels of angiogenic growth factors, including but not limited to, VEGF, basic fibroblast growth factor (bFGF), and transforming growth factor-beta 1 (TGF-β1). In addition, both keratinocytes and fibroblasts in culture are known to release inflammatory mediators, which promote the transient development of fibrovascular tissue.

During the first 2 years of the project, the Boyce group established advanced models of ESSs with pigmentation and vascular analogs. They also completed animal studies of human melanocyte transplantation with restoration of skin color. They developed an enzyme-linked immunosorbent assay for CD31 to track human dermal microvascular endothelial cells (HDMEC) in ESSs and transplanted human fibroblasts-HDMEC cocultures to athymic mice. In Year 3, the researchers found that they could expand sufficient numbers of autologously harvested human melanocytes in culture to seed in an ESS in a time frame sufficiently rapid to meet the surgical schedules for burn victims. They evaluated the tumorigenicity of transplanted human melanocytes and found the cells did not have tumor-forming potential in immunodeficient mice.

Research Progress – Year 4

Skin Color

During Year 4, the research approach for the project was changed with the addition of human melanocytes to the ESS, which resulted in more predictable efficiency and greater procedural reliability. **Figure 1A** shows a human ESS without melanocytes. In Figure 1B, the ESS was populated with human melanocytes and assessed for the development of skin color.

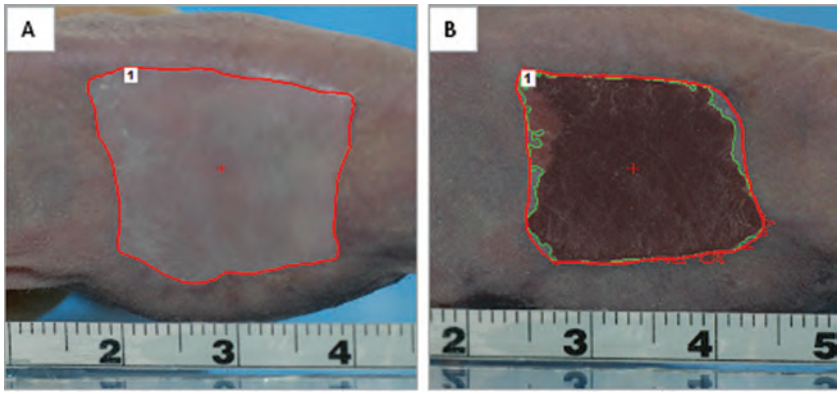

Figure 1. Comparison of inoculation methods for the addition of human melanocytes to an ESS. Red contour is the wound margin. Green contours are pigmented fields of grafted wounds. (A) No added human melanocytes. (B) Coculture of human melanocytes and human keratinocytes. The co-inoculation generated uniformly pigmented fields within the grafted wounds. Scale in centimeters.

Solar Protection

The researchers conducted preliminary studies to assess the ability of pigmented ESSs to protect against DNA damage from UVB radiation in sunlight. DNA damage was reduced by more than 50% in pigmented skin compared to healed ESSs without pigment.

Tumorigenicity Testing

The research team completed their assessment of cultured human melanocytes for tumor formation. As previously reported, no detectable tumors were found in 16 strains of cultured melanocytes from adult skin.

Conclusions

Overall, this project continues to progress toward a clinical trial with the verification of end points for safety and efficacy, and establishment of laboratory protocols that are anticipated to be compatible with the clinical care of burn patients. The researchers' advances include restoring skin color by adding melanocytes to ESSs, developing protocols for melanocyte propagation that coincide with surgical schedules for burn patients, and conducting tumorigenicity testing that suggests that transplantation of cultured human melanocytes is safe.

Research Plans for Year 5

The researchers plan to validate protocols for isolation, propagation, cryopreservation, and transplantation of normal human melanocytes as a cellular component of ESSs. They will also develop protocols for clean-room manufacture of an ESS-P and for an initial clinical study in pediatric subjects. They will coordinate with RCCC and the Clinical Trials Core at Case Western Reserve University to assemble data and protocols for submission to the FDA.

Planned Clinical Transitions

The licensee of the ESS technology will be notified of plans for an initial clinical study with ESS-Ps and will be asked to provide support for clean-room manufacturing. The FDA will be contacted for advice on the clinical study plans. The intent is to submit a Request for Designation to the FDA for a clinical study involving ESS-Ps.

Skin Products/Substitutes

Tissue-Engineered Skin Products- ICX-SKN

Project 4.2.1, WFPC

Team Leader(s): Vincent Ronfard, PhD (Healthpoint Biotherapeutics, Ltd.) and Paul Kemp, PhD (Intercytex, Ltd.)

Project Team Member(s): Dennis L. Carson, PhD, DABT and Sarah Ramsay, MS (Healthpoint Biotherapeutics, Ltd.); Kathi Mujynya Ludunge, BS/MBA (DFB Pharmaceuticals, Inc.); John Lovelady PhD, Jonathan Elwell, and Sarah Drinkwater (Intercytex, Ltd.)

Collaborator(s): Penny Johnson, PhD and Clare Lovelady, PhD (Intercytex, Ltd.)

Therapy: A permanent dermal skin graft replacement (ICX-SKN) that can be integrated and remodeled by the host for burns

Deliverable(s): Initiation of human clinical evaluation of ICX-SKN

TRL Progress: 2008, TRL 1; 2009, TRL 1; 2010, TRL 2; 2011, TRL 2/3; 2012 (Current), TRL 2/3

Key Accomplishments: Researchers at Intercytex, Ltd., and Healthpoint Biotherapeutics, Ltd., have developed the tissue-engineered skin product ICX-SKN. In Year 4, they examined the raw material requirements and determined that bovine serum and certain growth factors could be removed and the fibrin content could be reduced without adversely affecting the final product. This new version of ICX-SKN is less expensive to produce, yet has similar biocompatibility as demonstrated by the preclinical results obtained with the pig burn model.

Key Words: Burn, matrix, skin graft replacement, human dermal fibroblasts, fibrin

Introduction

The need exists for an "off-the-shelf" skin replacement that is instantly available and alleviates the need to take full-thickness skin grafts. Several FDA-approved "living skin equivalents" and "living dermal equivalents" are currently available. Although these materials, such as Apligraf®, Dermagraft®, and Orcel®, work as artificial skin grafts, in reality no current living product meets the rigorous requirements necessary to accomplish this function. Rather, the dermal component of these products is rapidly degraded in the wound environment, releasing the cells, which then contribute to wound healing by secondary intention.

In contrast to these earlier living skin equivalents and living dermal equivalents that have used either a preformed collagen matrix or biodegradable synthetic mesh as the initial support system, the intent from the start of this project was to develop a more biologically robust ECM by allowing the fibroblasts themselves to produce the material in vitro. Others have shown that fibroblasts allowed to grow to superconfluency in vitro are able to synthesize a relatively strong ECM, but the resulting material is extremely thin and fragile.

The intent of this project, therefore, was to extend the findings of Neidert et al.,[1] who have shown that cells grown within a fibrin scaffold gradually remodeled this scaffold into a cell-synthesized matrix. During the past 3 years, Intercytex and then Healthpoint developed the tissue-engineered skin product ICX-SKN. The researchers completed the extensive physical, biochemical, and biological characterization of the ICX-SKN matrix during maturation. They assessed improved methods of matrix production (e.g., ultrasound stimulation) and investigated new manufacturing processes (e.g., casting dish designs). They conducted proof-of-concept in the pig burn model using four prototypes. This extensive characterization helped to define the product for manufacturing process control and final product specifications. The intended use for burn

[1] Neidert MR, et al. 2002. *Biomaterials* 23(17):3717-31.

injury treatment is the simultaneous application of ICX-SKN and autograft in a single-step procedure.

Research Progress – Year 4

A requirement before any clinical study can begin on either a medical device or a biological is the submission of a chemistry, manufacturing, and control (CMC) dossier, and part of this is the justification of the necessity of each component in the product. For this reason and for the ongoing need to minimize cost of goods of the ICX-SKN, a series of alternate compositions was evaluated and compared.

Simple Casting Chamber for Measurement of Composition Alternatives

The dish prototype that was developed in Year 3 for production of first-in-man clinical samples (2.5 x 3.5 cm) requires 3.7 mL of cast media. This means that an extensive series of cast composition change experiments would be costly in terms of raw material and would produce constructs that were larger than needed at this stage of the process. The researchers therefore assessed a trans-well alternative that used 50% less starting material.

Manufacturing

Manufacturing process changes were made including total removal of serum and TGF-β, which reduced the process time from 7 to 5 weeks. The researchers also reduced in a stepwise manner the amount of fibrinogen and thrombin with the unexpected finding that the resulting constructs appeared to be more robust (i.e., stronger) when compared directly to those cast at the same time to the original formulation. They eliminated the consideration of freeze-drying. They determined that, once harvested after a 5-week maturation, constructs could be stored in a shipping/storage medium for up to 21 days at 2°C–8°C (in dark conditions) and retain viability as determined by Alamar Blue. Further tests are ongoing to determine if this can be extended to 28 days. In addition, the researchers will determine if viability can be maintained after storage at ambient temperature (~23°C).

Differential Scanning Calorimetry (DSC)

DSC measures the energy required to heat a sample. If the sample undergoes a phase change as happens when a collagen triple helix is denatured, then this phase change can be exothermic. Collagen denaturation is endothermic. DSC analysis of the samples produced during the compositional modification studies is ongoing.

Histology of the Construct

The new formulation of ICX-SKN was produced at Intercytex in the United Kingdom and was shipped to Healthpoint in the United States for testing in excised porcine burn wounds. Representative H&E and Masson's trichrome staining of the ICX-SKN construct is shown in **Figures 1** and **2**, respectively.

Pig Study

In alignment with the approved protocol, 16 burn wounds were generated on the dorsum of two pigs using 2 cm diameter heated brass rods. After 24 hours, the burned tissue was excised and the resultant open wounds were treated with one of five treatments. The study plan was to sample one pig after 1 week and the other after 3 weeks.

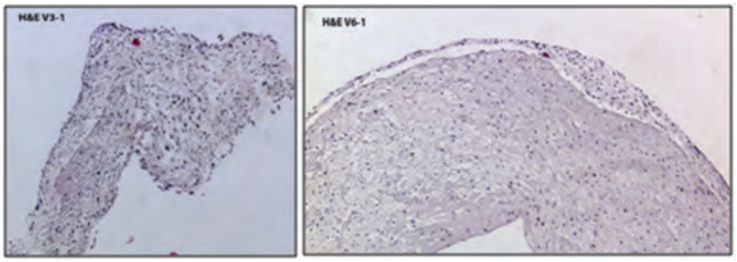

Figure 1. H&E staining of ICX V3 and V6 (100X).

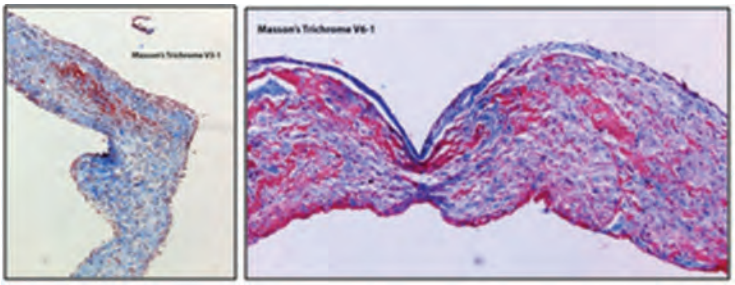

Figure 2. Masson's trichrome staining of ICX V3 and V6 (100X).

Preliminary Study Results

The burn wounding and excision process proceeded in alignment with the design and historic studies. **Figure 3** shows photographic images of wounds before treatment and after ICX-SKN treatment. H&E-stained tissues are shown in **Figure 4**.

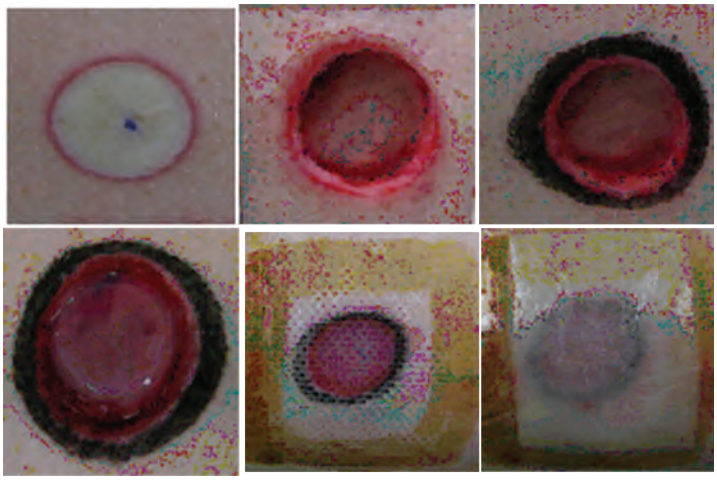

Figure 3. The upper row of photographs shows a representative burn wound, an excised wound, and the excised wound with the wound edge marked in black. The lower panel of photographs shows an ICX-SKN-treated wound with the nonstick dressing and benzoin resin applied, followed by the application of moist gauze and the transparent film dressing.

Conclusions

Important progress has been made in developing the new version of ICX-SKN. This version is less expensive to produce yet attains similar biocompatibility as demonstrated by the preclinical results obtained on the pig burn model. This gives the researchers the confidence to move forward the development of the product. They believe that the combination of cells, ECM-produced matrix, and human fibrin will provide an ideal dermal substrate allowing rapid vascularization and optimal take of skin autograft in a one-step procedure.

Research Plans for Year 5

Moving forward, Healthpoint will continue to produce ICX-SKN at two different sites. The immediate need is to pick the lead candidate and evaluate it in the pig burn model at the end of the year. The lead candidate from these studies will be selected for testing in humans. As this project moves forward, interactions with the FDA will begin as plans are finalized for an IND and the start of the clinical trial in 2013.

Planned Clinical Transitions

The project plans include evaluating the ICX-SKN in humans. Once the lead candidate is selected, the development of the IND will begin. A pre-IND meeting with the FDA is anticipated in early fall 2012.

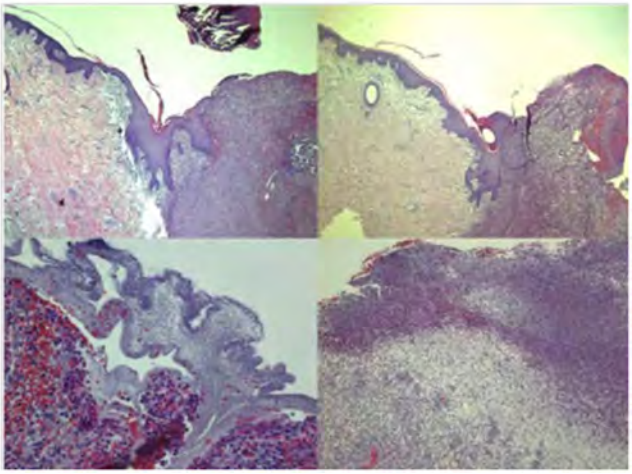

Figure 4. H&E stained tissues showing robust granulation of the wounds after 1 week (upper images, 40X), possible ICX-SKN remaining at the surface of one wound (lower left, 400X), and a region of lower cell density in a granulation tissue bed (lower right, 100X).

Skin Products/Substitutes

Fluid-Derived and Placenta-Derived Stem Cells for Burn

Project 4.2.6, WFPC

Team Leader(s): John D. Jackson, PhD (Wake Forest University)

Project Team Member(s): Chad D. Markert, PhD (Wake Forest University)

Collaborator(s): David Mack, PhD, Aleksander Skardal, PhD, and James Yoo, MD, PhD (Wake Forest University)

Therapy: Amniotic fluid-derived and placental-derived stem cells for burn

Deliverable(s): An improved "off-the-shelf" bioengineered skin product for the treatment of extensive burns utilizing broadly multipotent stem cells from perinatal sources (amniotic fluid and/or placental tissue)

TRL Progress: 2009, TRL 1; 2010, TRL 2; 2011, TRL 2; 2012 (Current), TRL 2

Key Accomplishments: After establishing full-thickness wound model in nude mice, the research team delivered amniotic fluid-derived stem (AFS) cells with and without mature skin cells (keratinocytes) in the wound. The addition of the AFS cells in this paradigm led to increased wound closure rates, increased percentage of epithelialization, and increased levels of neovascular/angiogenic activity in the regenerating skin, as compared to the gel-only control group. They found that combining AFS cells with mature keratinocytes also enhanced wound healing.

Key Words: Stem cells, trophic factors, regenerative medicine, living skin equivalents

Introduction

AFS cells possess properties found in MSC, such as multipotent differentiation, immunomodulatory activity, and the lack of significant immunogenicity. MSC have shown therapeutic potential for the repair and regeneration of tissues damaged by injury or disease. In particular, MSC treatment of acute and chronic wounds leads to accelerated wound closure and increased levels of epithelialization, granulation tissue, and angiogenesis. Given that AFS cells can be obtained less invasively than MSC and show greater proliferative capacity in culture, the researchers investigated whether they could augment wound healing with AFS cells in a similar manner as MSC.

The researchers used full-thickness skin wound model in nude mice to assess the ability of AFS cells to accelerate wound-healing (**Figure 1**). The objectives of the project were to determine whether AFS cells could augment wound-healing rates when bioprinted in the wound model and whether increased wound-healing rates might be due to integration of the AFS cells in the regenerating tissue or their secreted trophic factors. AFS cells were also bioprinted with mature keratinocytes to examine if the combination of stem cells and mature epithelial cells would enhance wound healing. Bioprinting of the AFS cells into the skin wound increased wound healing rates and

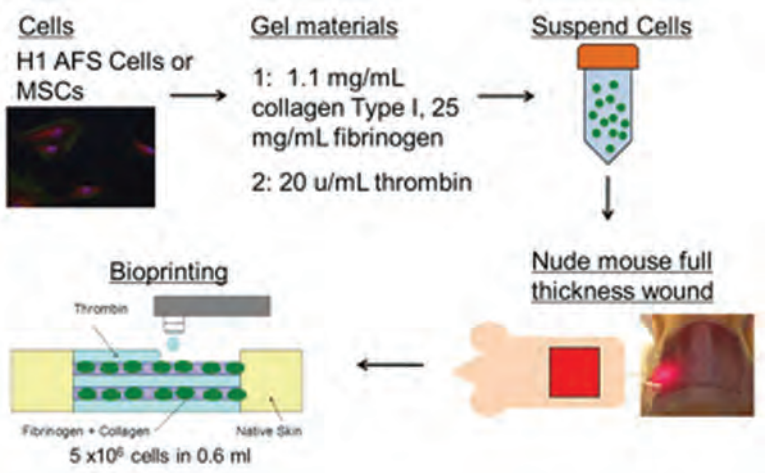

Figure 1. Method for bioprinting stem cells in full-thickness wounds.

induced the neovascularization of the wound area. Interestingly, the number of AFS cells decreased over time. This suggests that the AFS cells did not directly contribute to wound healing by being incorporated into the epidermis but influenced wound closure and vascularization potentially via the production of trophic factors.

The researchers found that directed differentiation of AFS cells presented many challenges and resulted in a lack of consistency in epithelial marker expression. Therefore, they redirected the project during the past year to focus on examining the role of undifferentiated AFS cells in wound healing. This redirection resulted in faster progress into an in vivo animal model for studying AFS cells in wound healing.

Research Progress – Year 4

The researchers measured and quantified wound size, contraction, and re-epithelialization at 1 and 2 weeks post surgery in their nude mouse full-thickness wound model. At both time points, wound closure was faster in groups treated with AFS cells and MSC, compared to the gel-only control group (**Figure 2**). Cell-treated groups showed greater levels of contraction than the gel-only group at week 1 (**Figure 3**). However, re-epithelialization levels were greater at weeks 1 and 2 in groups treated with AFS cells and MSC, compared to the gel-only group (Figure 3).

More blood vessels were seen in the groups treated with AFS cells and MSC, as compared to the gel-only group. At 1 week post treatment,

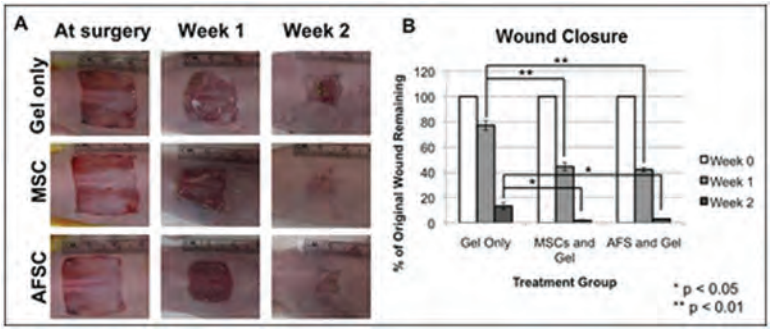

Figure 2. Wound closure after treatment with AFS cells and MSC.

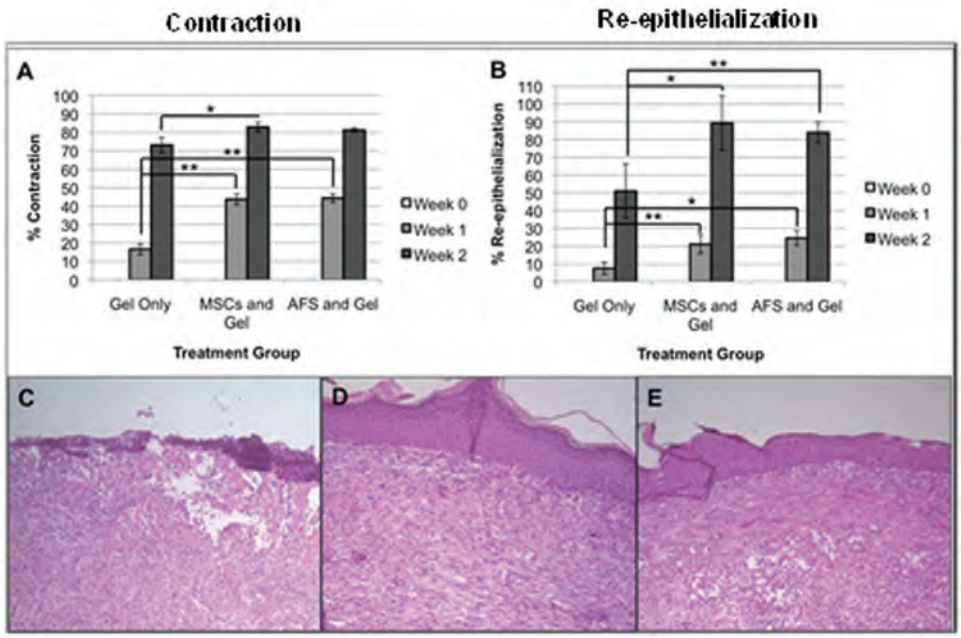

Figure 3. Wound contraction and epithelialization after treatment with AFS cells and MSC (*p<0.05).

microvessel density and blood vessel diameter were greater in the AFS cell and MSC groups when compared to the gel-only group; however, at 2 weeks post treatment, the AFS cell-treated group had greater vessel diameters than either the MSC-treated group or the gel-only group (**Figure 4**). A cell-tracking study showed the number of AFS cells and MSC decreased in the regenerating wound, which demonstrated that the stem cells did not integrate into the epithelium (**Figure 5**). The data show that AFS cells enhanced healing of the full-thickness skin wound as well as increased neovascularization activity in the wound. Because the number of AFC cells decreased over time, the increase in wound-healing activity may be due to trophic factors produced by the stem cells early in the healing process.

AFS cells and porcine keratinocytes were bioprinted onto full-thickness wounds on the back of nude mice. The cells were printed in two layers with the AFS cells on the bottom layer and the keratinocytes on the top layer (**Figure 6**). In addition, each cell type was bioprinted alone as a comparative group. Wound healing was rapid, with wound closure occurring by day 14 in all groups (**Figure 7**). AFS cells began to decrease in number by day 7 post bioprinting and were undetectable by day 14 post bioprinting. This finding confirms the earlier results of the transient nature of the AFS cells and MSC post bioprinting.

Conclusions

Deposition of AFS cells in fibrin-collagen in a nude mouse full-thickness skin wound model increased

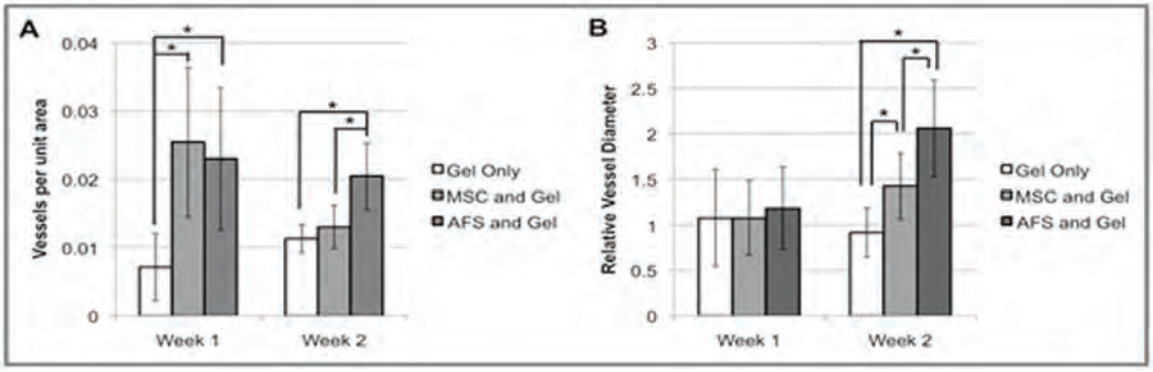

Figure 4. Microvessel density and vessel diameter after treatment with stem cells (*p<0.05).

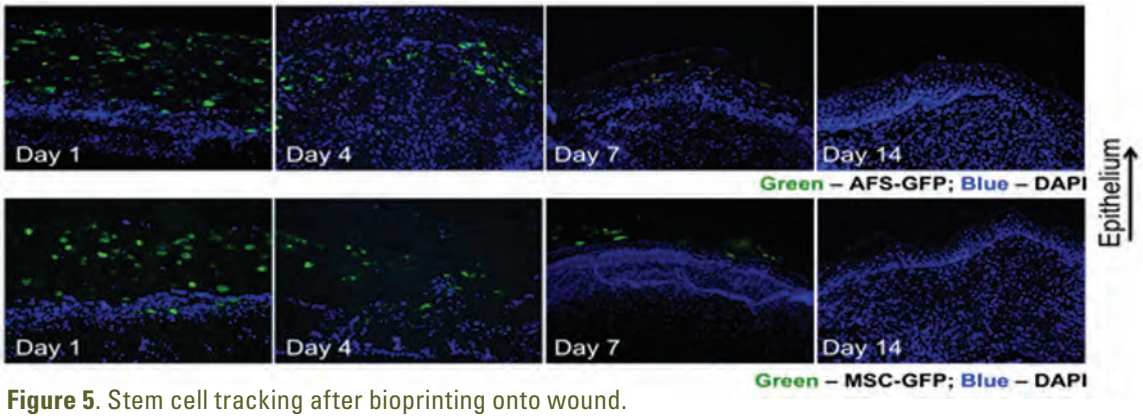

Figure 5. Stem cell tracking after bioprinting onto wound.

wound closure rates, amount of epithelialization, and levels of neovascular/angiogenic activity in the regenerating skin. The AFS cell numbers decreased over time, which suggests that the AFS cells delivered trophic factors that were important in wound healing. These results suggest that the bioprinting of AFS cells as a cellular therapy may be a potentially powerful tool for burn and wound-healing treatments.

Research Plans for Year 5

In Year 5, the researchers plan to bioprint AFS cells alone and in combination with autologous keratinocytes in a large animal (porcine) model of burn injury. They will examine similar parameters associated with wound healing including wound epithelialization, wound contracture, and vascularization.

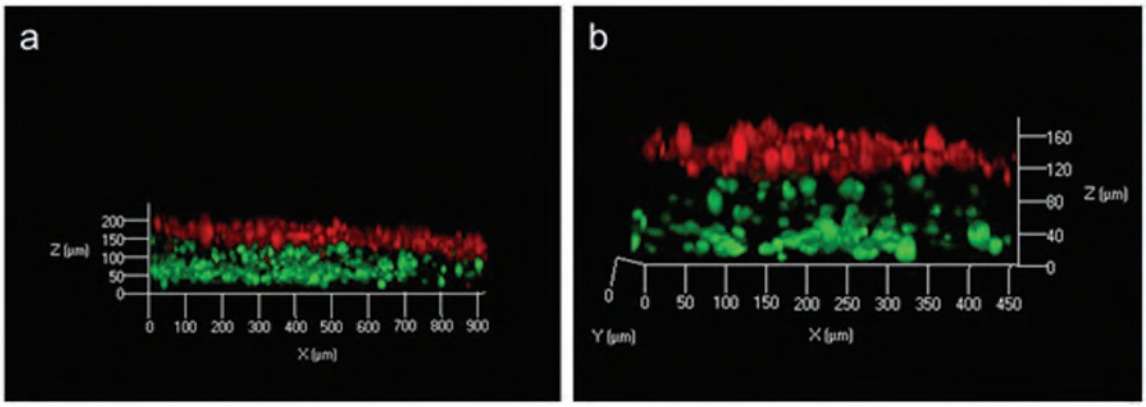

Figure 6. Tracking of GFP-lenti-labeled AFS (green) and CM-DiI-labeled KC (red) in wounds at the 4-day time point. a: Confocal microscopy showing cell distribution along the z-axis (10X objective lens). b: Confocal microscopy showing cell distribution along the z-axis (20X objective lens). AFS: Amniotic fluid-derived stem cells, KC: Keratinocytes.

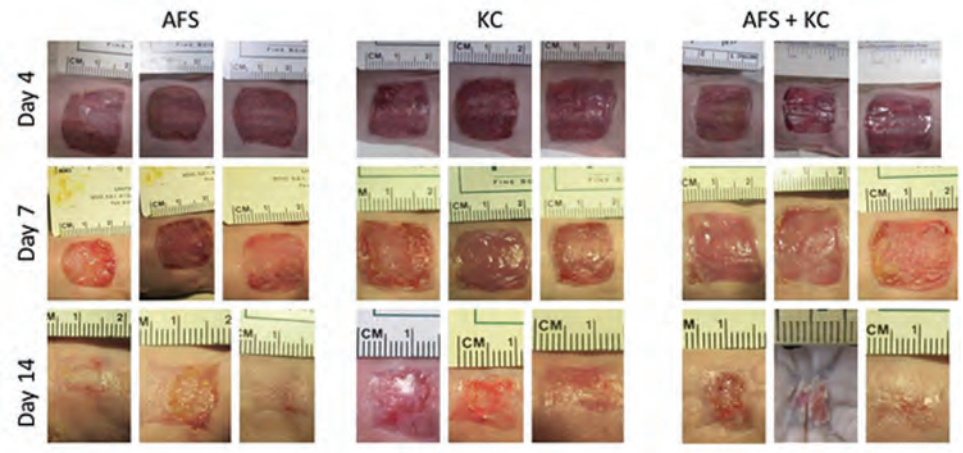

Figure 7. Wound healing over 14 days in a nude mouse excisional model. AFS: Amniotic fluid-derived stem cells, KC: Keratinocytes, AFS+KC: Both cell types applied in a stratified manner, with AFS applied first (dermal layer) and KC applied on top (epidermal layer).

Skin Products/Substitutes

In Vitro Expanded Living Skin for Reparative Procedures

Project 4.2.8, WFPC

Team Leader(s): Sang Jin Lee, PhD, James J. Yoo, MD, PhD, and James H. Holmes (Wake Forest)

Project Team Member(s): John Jackson, PhD, Hyun-Wook Kang, PhD, Peter Masso, BS, Peter Prim, BS, Justin Werker, BS, and Abner Mhashilkar, PhD (Wake Forest)

Collaborator(s): None

Therapy: Autologous skin grafts for treatment of burn injuries

Deliverable(s): Skin expansion device for expanding autologous skin grafts

TRL Progress: 2009, TRL 4; 2010, TRL 5; 2011, TRL 5; 2012 (Current), TRL 5

Key Accomplishments: The researchers have developed an in vitro tissue expander system that permits a rapid increase in surface dimensions of donor skin while maintaining tissue viability for subsequent skin transplantation. They designed an effective tissue gripper system for the device. They also built a new-generation uniaxial bioreactor system. The research team continued to optimize the skin expansion parameters and protocols and devised a strategy for performing a clinical trial.

Key Words: Autologous skin grafts, in vitro skin expander, bioreactor, burn repair

Introduction

Many reparative procedures due to battlefield trauma and burn may require additional skin for coverage. The standard of care for skin defect replacement is the use of autologous skin grafts. However, donor-site tissue availability is a major obstacle to the successful replacement of skin defects. Because of this limitation, other approaches are commonly employed to cover skin defects. These include commercially available skin products based on biomaterials and tissue engineering, allografts, and xenografts. However, these approaches also have limitations, such as the need for a concomitant autograft, insufficient mechanical properties, high cost, lack of permanence, potential for infectious disease transmission, and inadequate biocompatibility. Nevertheless, many commercial skin products are being used as acceptable skin substitutes when autologous donor tissue is unavailable.

Alternatively, subcutaneous tissue expanders or meshed split-thickness skin grafts (STSGs) are used clinically to generate larger segments of autologous skin when donor-site tissue is limited. Subcutaneous tissue expanders are balloon implants that are sequentially filled with incremental volumes of saline to increase the amount of overlying skin. The physico-mechanical stress of the tissue expander results in biologic creep, greater mitotic activity of cells, and increased vascularity, which ultimately leads to expanded skin. Subsequently, the expanded skin can be used as a tissue flap or harvested for use as a skin graft. However, the use of a subcutaneous tissue expander is associated with an additional surgical procedure(s), which increases donor site and overall morbidity. In addition, this technique requires a lengthy wait time (on the order of months) to obtain sufficient tissue for intervention. Moreover, the discomfort associated with the increasing expander volume and the frequent tissue fibrosis remains as a major limitation. Alternatively, meshed STSGs are obtained using a graft mesher that cuts the skin into a mesh pattern, which results in greater surface dimensions before application on the wound bed. However, meshed STSGs are not considered ideal for many applications because

they leave large gaps of the open wound, which requires a longer healing time and results in a cross-hatched or cobblestone pattern of healed skin as scar tissue fills the gaps.

The overall goal of this project is to provide wounded soldiers with large dimensions of autologous skin for reparative procedures. The specific aims of the project are to (1) optimize expansion parameters for maximizing surface dimensions of human skin, (2) establish SOPs for skin expansion parameters and delivery, and (3) determine the applicability in wounded soldiers through a clinical trial.

The research team has made significant progress to date toward the project goals. The team developed an in vitro tissue expander system that permits a rapid increase in surface dimensions of donor skin while maintaining tissue viability for subsequent skin transplantation. The expander system utilizes a computer-controlled bioreactor capable of providing an accurate expansion rate for yielding target skin dimensions over a defined time period. This system was successfully tested and validated on human skin samples. The group has been able to consistently double the surface area of donor skin within 2 weeks while maintaining cell viability. Viable grafts were obtained in both small (mice) and large (pig) animal models. A new bioreactor was designed for use in clinical trials and improvements to the system's tissue gripper design were investigated.

Research Progress – Year 4

The researchers continued optimization of the expansion protocol for human skin. They optimized the various expansion parameters, including magnitude, frequency, slope, and expansion and resting time. They also characterized the expanded skin matrices with histological staining (H&E and Masson's trichrome) and immunohistochemical staining for proliferating cell nuclear antigen (PCNA), and staining with the terminal deoxynucleotidyl transferase dUTP nick end-labeling (TUNEL) assay.

The research team also continued the modification of the skin expansion bioreactor system. Since the prior grip system was mechanical and damaged the tissue during expansion, the researchers are redesigning the grip system using microneedles. A new gripper system was designed and fabricated by Allied Automation to test skin in planar tension by straining the tissue (**Figure 1**). The system contains 16 individual arms with microneedles on each arm to effectively grip the skin. The system is also designed to sustain compressive force that would translate the force within the gripper to stretch the skin sample to a strain area of 100% of the original skin sample area. The researchers improved the software to control the skin bioreactor: e.g., recording expansion protocol, measuring tension, controlling temperature, and controlling oxygen and carbon dioxide levels.

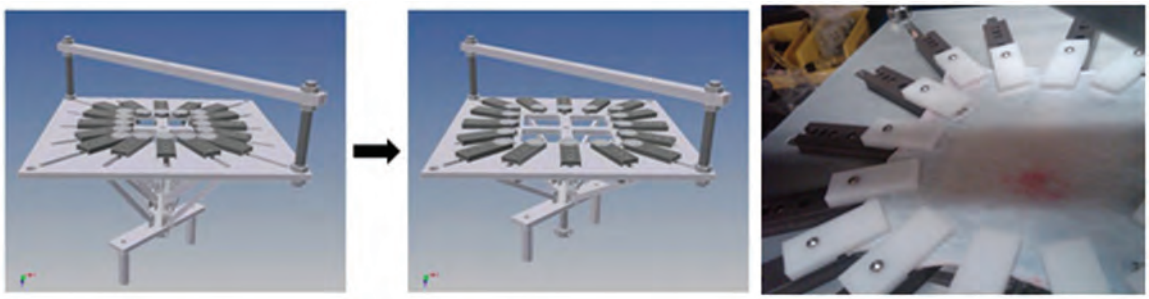

Figure 1. (Left) A new gripper system and expansion mechanism and (Right) gross appearance of gripper system with a porcine skin graft.

The research team also continued optimization of the human skin culture system using different culture medium components. The researchers evaluated human skin samples in culture at 7 days and 14 days using histology, immunohistochemistry, and TUNEL staining (as noted earlier). They continued development of a new generation of skin expander (**Figure 2**). Optimization of skin expansion parameters is ongoing. They also continued development of SOPs for skin expansion and prepared documents for an IDE/IND meeting with the FDA.

Skin matrices were placed in a sterile bioreactor for expansion. The edges of samples were clamped at multiple areas in the biaxial bioreactor. After placement, the initial dimensions were measured using a sterile ruler to obtain a baseline value. Subsequently, 300 mL of culture medium was added. Continuous flow of medium into the expansion chamber was maintained with a peristaltic pump. The bioreactor was monitored and kept at 37°C with a heated water jacket and 5% CO_2 was circulated through the unit for the entire duration of expansion. Computer software was used to monitor the temperature, position, and load of the skin throughout stretching. After stretching, the final dimensions of the expanded skin were measured. The skin sample was removed from the bioreactor in preparation for skin grafting.

Various features were considered in the process of designing a bioreactor system for a clinical trial. For example, the skin bioreactor system must be operated as a closed system to prevent potential contamination/infection and to minimize the frequency of manipulation. Medical-grade materials such as stainless steel and Teflon were used. Two stepper motors, a positioning sensor, an electric thermometer, and a force sensor were used for the construction of this fully automatic system. In addition, two circulating pumps were implemented for automatic medium exchange and temperature control. The expansion site is completely isolated from the outside environment to minimize the possibility of contamination.

Conclusions

The team continued over the past year to optimize the expansion parameters and design of the skin expansion system. Laboratory results with the

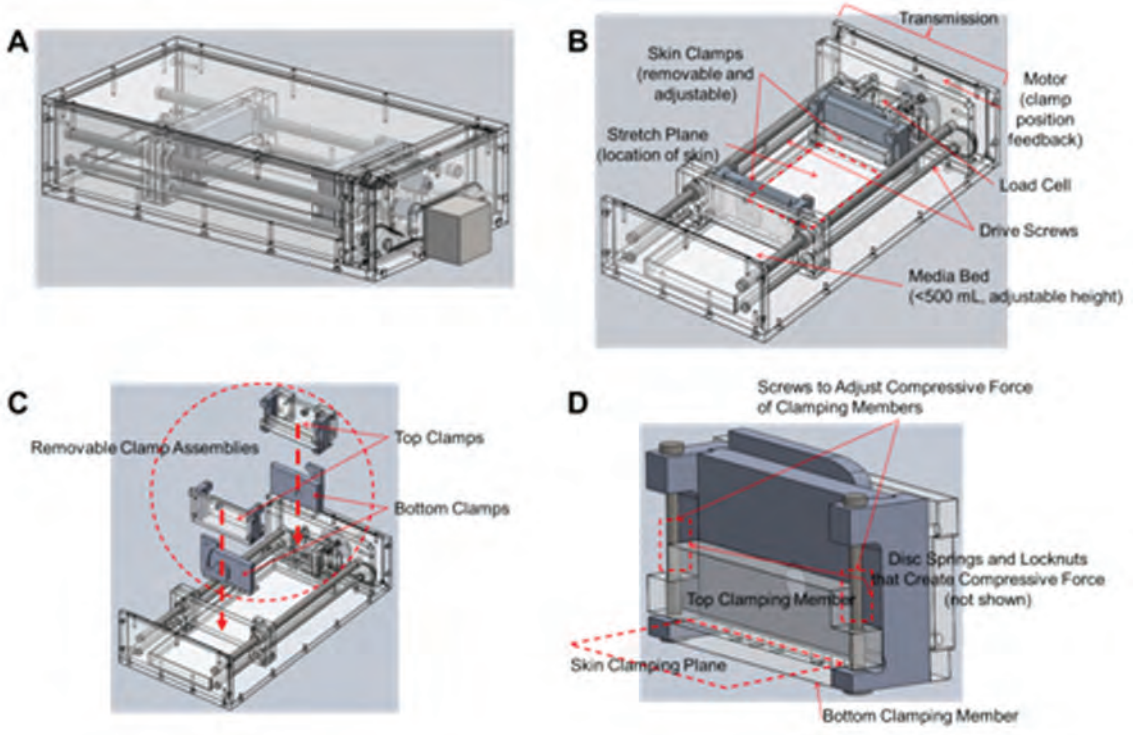

Figure 2. New generation of uniaxial skin expander. (A) Full-assembled unit, (B) open (lid and sides hidden), (C) removable clamp assemblies, and (D) adjustable clamps.

system are promising and continued progress toward initiating clinical testing is warranted.

Research Plans for Year 5

The research team will continue to move the skin expansion system project toward testing in humans. Plans are to conduct materials characterizations and biocompatibility testing and construct a clinical version of the device.

Planned Clinical Transitions

Because the skin expansion uses equipment without any cellular components, it is defined as a device and will be under regulation of the devices section of the FDA. The researchers are currently working toward obtaining an IDE through the FDA for approval of a prospective, multicenter, nonrandomized, uncontrolled pilot study of human skin expansion (Feasibility/Phase 1). IRB approval is currently being sought.

Corrections/Changes Planned in Year 5

Engineering personnel changes and challenges in designing a gripper system that minimizes tissue damage have delayed the progress of this project. The research team identified and partnered with an engineering firm to address the engineering challenges, and several gripper prototypes were built and tested. A new skin expander is being constructed for testing and validation.

Skin Products/Substitutes

Autologous Human-Debrided Adipose-Derived Stem Cells for Wound Repair in Traumatic Burn Injuries

Project 4.6.8, USAISR

Team Leader(s): Robert J. Christy, PhD (USAISR)

Project Team Member(s): Shanmugasundaram Natesan, PhD (USAISR)

Technical: Nicole Wrice (USAISR)

Collaborator(s): Laura Suggs, PhD (University of Texas); InGeneron, Inc., Houston, TX; Andre Cap, MD, PhD and Anthony Johnson, MD (USAISR)

Therapy: Tissue-engineered skin substitute for repairing burn injuries

Deliverable(s): Dermal equivalent using autologous stem cells

TRL Progress: 2010, TRL 3; 2011, TRL 3; 2012 (Current), TRL 4; 2013 (Target), TRL 5

Key Accomplishments: The research team isolated human adipose-derived stem cells (ASC) using a point-of-care device. They developed the technology to differentiate ASC into epithelial cells for use on patients so severely burned that they do not have an autologous epithelial cell source. The team also developed a strategy to induce differentiation of discarded burn skin ASC (dsASC) with ligands previously shown to induce differentiation of normal keratinocytes without the addition of any exogenous growth factors. They also demonstrated that, when exposed to the appropriate stimuli, the dsASC will differentiate into the mesenchymal cell types that correspond to the three layers of skin.

Key Words: Adipose-derived stem cells, keratinocytes, epithelial cells

Introduction

Large body surface area burns pose a significant therapeutic challenge with implications for early hemodynamic instability and sepsis, as well as later complications of scarring, contracture, and long-term disability. From a clinical standpoint, the extent and severity of burn injury determine the need for tissue-grafting or tissue substitutes. Though autografting remains the treatment of choice for excised burn wounds, this option may be severely limited in patients with extensive burns because of limited donor-site availability. Furthermore, repeat harvesting of split-thickness skin grafts from the same donor area can result in morbidity, loss of dermal thickness, excessive scarring, and increased pain.

Developing a tissue-engineered skin substitute using stem cells is a potential alternative option to regenerate skin for the treatment of extensively burned patients. ASC have great potential to regenerate skin because of their ability to differentiate into multiple cell lineages. Unfortunately, after severe burn injury, the source(s) of adipose tissue can be limited due to the availability of uninjured viable tissue and the fear of causing additional morbidity from subcutaneous liposuction. Because tangential debridement of skin often leads to debridement of some viable tissue, the Christy team has shown that stem cells can be isolated in adequate quantities from the adipose layer of dsASC. Furthermore, these cells are able to integrate within the excision wound bed of an athymic rat. Unlike other cells types, such as fibroblasts, keratinocytes, and endothelial cells, which require culture expansion, dsASC can be isolated in proportionally large numbers from patients with an increasing percentage of surface area burns. These stem cells can then be used along with collagen and fibrin-based scaffolds to develop epithelial, dermal-vascular, and hypodermal layers, which can then be used to develop a complete full-thickness skin equivalent.

In this project, the research team has used a polyethylene glycol (PEG)-fibrin biomaterial and ASC as

a strategy for the revascularization of traumatized tissue. The researchers isolated viable human ASC from debrided burn patient tissue, evaluated the cells' viability, and confirmed the multi-lineage differentiation potential of the cells. They also demonstrated the in vivo vascularization potential of an ASC-PEGylated fibrin gel using a full-thickness excision wound in a rat model. They determined that human ASC-PEG-fibrin constructs have the ability to enhance the vascularization of a healing wound better than PEG-fibrin hydrogels alone.

Research Progress – Year 4

Development of the Layers of Skin Substitute Using dsASC

A schematic diagram is shown in **Figure 1** that depicts the strategy adopted by the research team to develop a skin substitute. They used dsASC in combination with a collagen hydrogel to develop epithelial and hypodermal layers. Simultaneously, to reconstruct a vascularized dermal layer, they implemented a collagen-PEGylated-fibrin bilayer hydrogel construct.

Stem cell isolation. The hypodermal layer (10–12 g) from debrided skin or abdominoplasty was dissected, transferred to a petri dish, and finely minced with sterile scissors or manual lipoaspirate. Stem cells were isolated using the point-of-care Transpose RT™ System (InGeneron, Inc. Houston, TX) according to the manufacturer's instructions.

Epithelial construct. To develop the epithelial construct, dsASC were seeded on top of a collagen hydrogel and initially induced with all-transretinoic acid (ATRA). The dsASC seeded over the collagen matrix started to align into squamous cell-like morphology by day 4 (**Figure 2A**) and after air-lifting and fenofibrate induction were able to differentiate into epithelial-like cuboidal cell morphology by day 12 (Figure 2B). Immunocytochemical analysis of frozen sections of the epithelial differentiated dsASC on the collagen gel showed positive staining for pan cytokeratin (red, Figure 2C; nuclei are blue). These results indicate that dsASC could be differentiated into an epithelial-like phenotype on a collagen matrix without using growth factors.

Vascularized dermal construct. A vascularized dermal construct was developed by seeding dsASC within a collagen-PEGylated-fibrin bilayer hydrogel. This strategy allows for a simultaneous, bidirectional differentiation of dsASC within the bilayer construct. The dsASC exhibited fibroblast-like morphology within the collagen layer by day 6 (Figure 2D), and by day 12 the dsASC remained fibroblast-like and had proliferated and populated the entire gel (Figure 2E). In contrast, within the PEGylated-fibrin layer of the bilayered gel, the

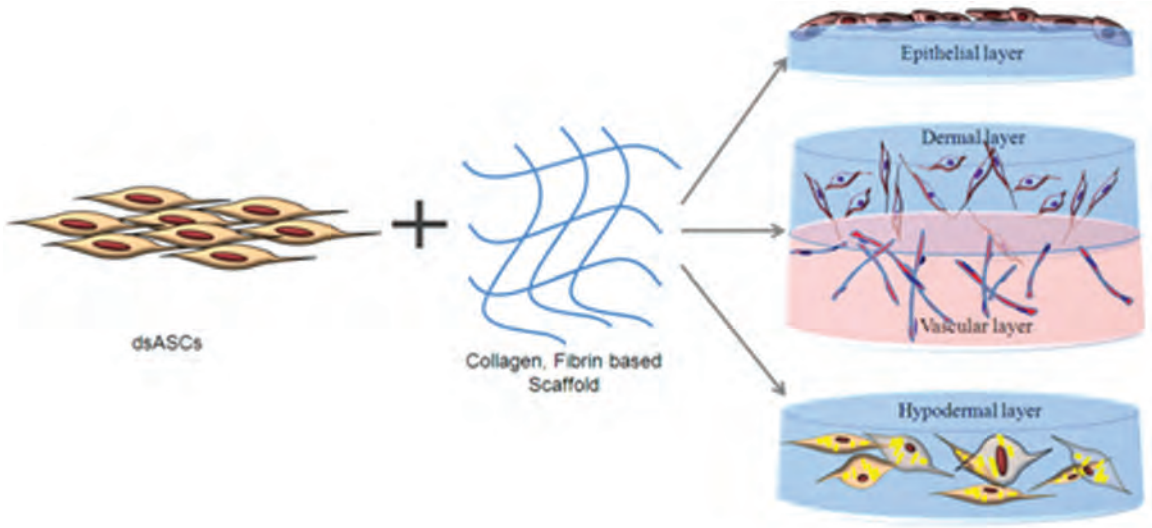

Figure 1. Schematic representation of the development of different layers of skin substitute using dsASC and hydrogel-based matrices. Epithelial and hypodermal constructs are developed using a collagen hydrogel and a vascularized dermal construct is created using a collagen-PEG-fibrin-based bilayered hydrogel.

dsASC formed distinct tubular networks by day 6 (Figure 2G) and eventually formed dense networks by day 12 (Figure 2H). Immunostained sections of the day 12 bilayered gels showed the presence of cells positive for alpha-smooth muscle actin (Figure 2F) within the collagen layer, indicating maintenance of stromal phenotype by dsASC. Tubular networks within the PEGylated-fibrin layer stained positive for NG2, which is expressed by microvascular pericytes in newly formed blood vessels, indicating PEGylated-fibrin gel supports dsASC differentiation toward a pericyte lineage (Figure 2I). Overall, these results show that dsASC within the bilayer hydrogel may be used as a vascularized dermal equivalent.

Hypodermal construct. The hypodermal construct was developed by differentiating dsASC within a collagen gel using adipogenic differentiation, media. Early during the induction of differentiation the dsASC proliferated within collagen gel, but only a few cells exhibited the presence of oil vesicles by day 7 (Figure 2J). However, by day 14 the dsASC showed a significant accumulation of lipid droplets (Figure 2K). Lipid accumulation by the differentiated dsASC within the collagen matrix

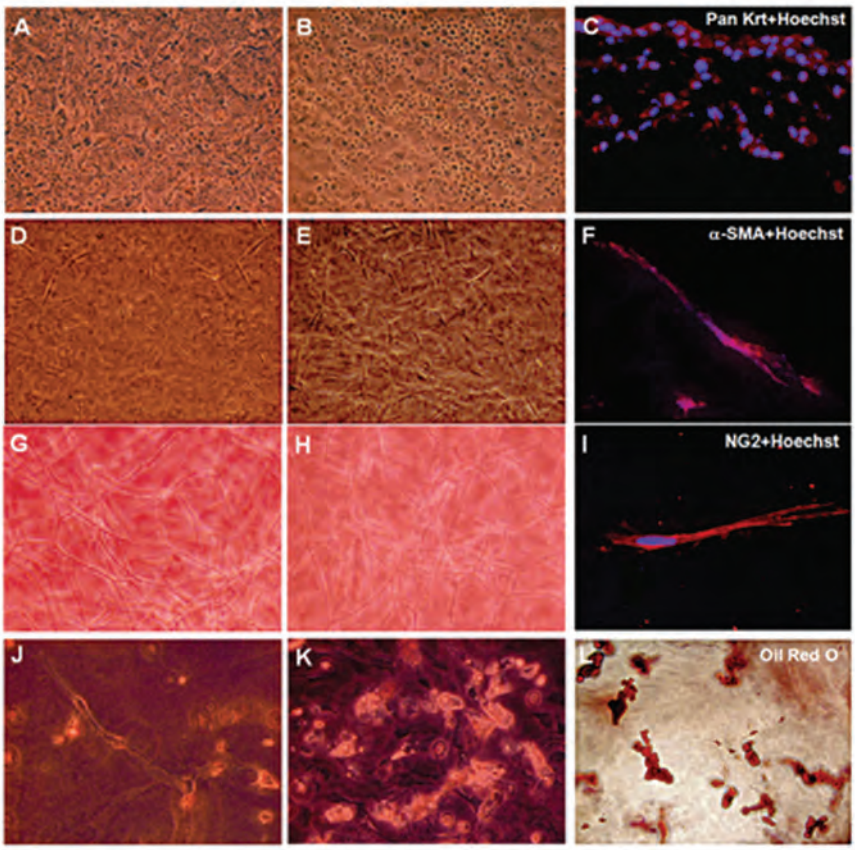

Figure 2. (A and B) Light microscopic images taken at day 4 (A) and day 12 (B) show the differentiation time course of dsASC into epithelial-like cells on a collagen hydrogel. (C) Immunocytochemical image of section from dsASC differentiated into epithelial-like cells on collagen gel (day 12) stained with pan cytokeratin. (D, E, G, and H) Light microscopic images taken at day 6 (D, G) and day 12 (E, H) show the differentiation time course of dsASC in PEG-fibrin-collagen bilayer gels exhibiting bidirectional differentiation. (F and I) Immunocytochemical image of section from bilayered hydrogel (day 12) depicting dsASC to maintain stromal phenotype with collagen layer, stained with α-smooth muscle actin (F) and differentiated to vascular phenotype, stained with NG2 (I). (J and K) Light microscopic images depicting the differentiation time course of dsASC into adipocytes on collagen. (L) Oil Red O staining of differentiated dsASC (day 14) confirming formation of mature adipocytes within collagen gel. Bright field images original magnification: X100 (A–H and L) and X200 (J, K). Immunofluorescence original magnification X400 (C, F, I).

on day 14 is shown with the positive staining with oil red O (Figure 2L), confirming the commitment of dsASC to form mature adipocytes within the collagen matrix.

Dynamic changes in morphology of dsASC and transcript levels of keratin-specific genes during differentiation with fenofibrate and all ATRA. Having previously shown that 75 µM fenofibrate induces distinct morphological changes in dsASC and expression of various keratin-specific genes, the research team investigated the effect of the combination of fenofibrate and ATRA on gene expression and phenotypic changes during the course of differentiation (days 4, 8, and 12). The control samples (without ATRA and fenofibrate induction) maintained their characteristic spindle-shaped morphology during the entire course of differentiation process (**Figure 3A-C**). The cells induced with fenofibrate and ATRA started to exhibit refractive and lenticular appearance by day 4 (Figure 3D). The cells eventually retracted their cell spreading by day 8 (Figure 3E) and formed widespread colonies of cells over the collagen matrix that exhibited distinct cuboidal morphology

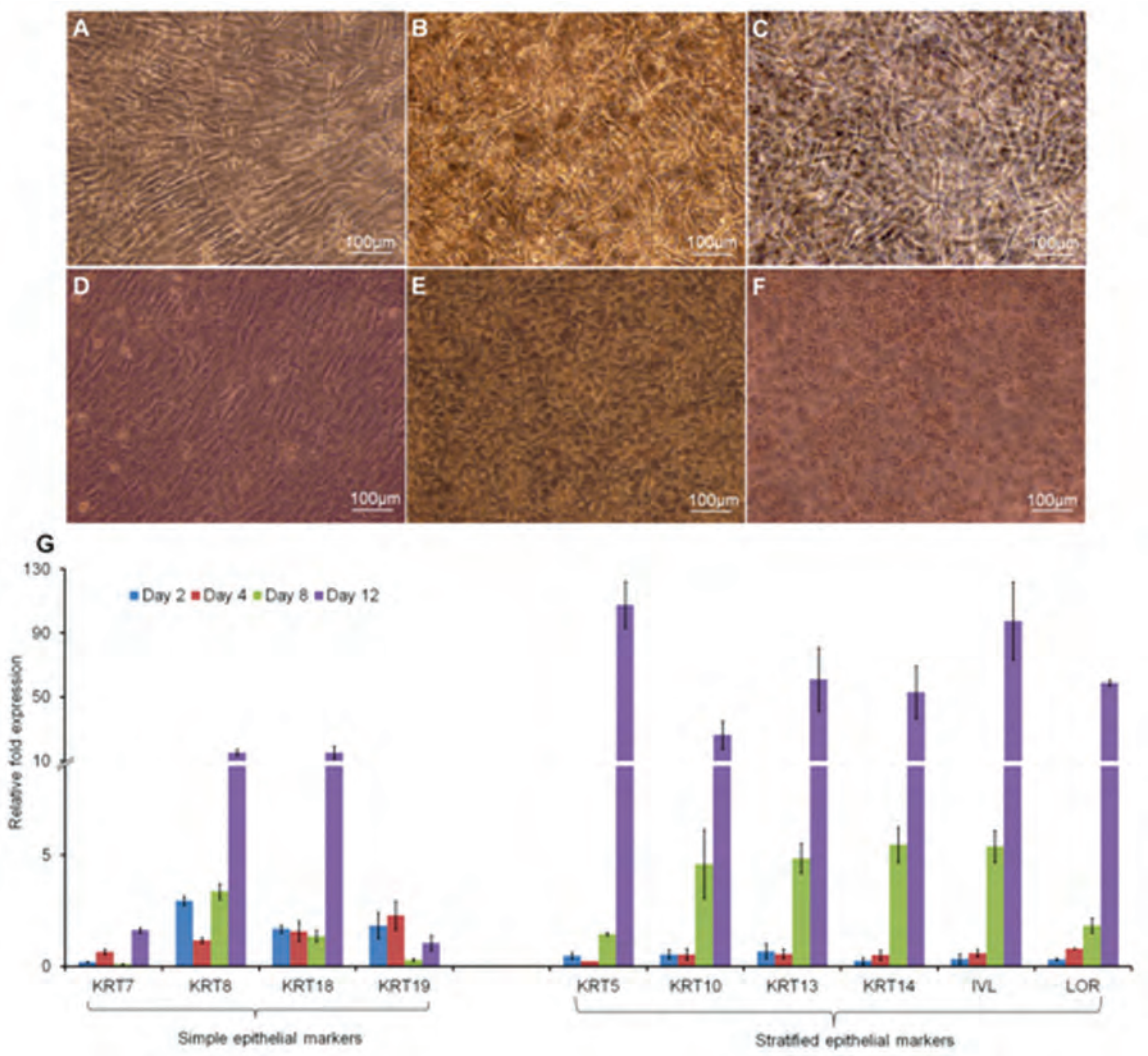

Figure 3. Differentiation of dsASC to epithelial-like cells. (A–C) Light microscopic images of undifferentiated control dsASC on a collagen hydrogel. (D–F) Light micrographs taken of dsASC fenofibnrate and ATRA differentiated dsASC into epithelial-like cells. (G) RT-PCR analysis showing ASC differentiated into epithelial-like cells showing positive expression of various cytokeratins and markers responsible for the formation of cornified envelope (stratified epithelial markers). Simple epithelial markers are expressed at low levels throughout the course of differentiation.

with a squame appearance (Figure 3F). Gene expression analysis showed that on day 4 (before fenofibrate induction and air exposure) dsASC exhibited low-level expression of all the keratin-specific genes analyzed (<3-fold). By day 8, mRNA levels of stratified epithelial-specific markers slowly started to increase, specifically KRT14 and IVL, which showed >5-fold increases, despite some of the simple epithelial genes being expressed at comparatively low levels (<4-fold). The cells by day 12 showed a significant increase in all keratin genes specific to stratified epithelial markers. Notably, KRT5 (basal keratin marker) and IVL (cornified envelope marker) robustly increased showing a >100-fold increase (Figure 3G).

Conclusions

The theoretical advantage of replacing all three anatomic layers of missing skin is to improve the quality of grafted skin long term, with need for fewer surgical revisions. While additional studies are needed to demonstrate the feasibility of this approach, the Christy team has demonstrated that viable stem cells can be harvested from the excised burn eschar and, when exposed to the appropriate stimuli, they will differentiate into the mesenchymal cell types that correspond to the three layers of skin. When mixed with the appropriate scaffolds and inducers, this source of stem cells can potentially be utilized for immediate wound coverage without the need for cell expansion. Furthermore, this approach will allow for the entire procedure to be performed within the operating room immediately after burn eschar excision for permanent wound coverage.

Alternatively, the autologous cells can be stored to be used for secondary revisional procedures. By introducing additional complexity into the coverage of a burn wound, the risks of failure naturally increases. However, the potential benefits of achieving better long-term outcomes combined with fewer operations needed for early coverage or for secondary revisions can easily outweigh that risk. The bilayer collagen-PEGylated fibrin hydrogel has the advantage of inducing robust vascularization, which facilitates incorporation and consequently may also lower the risk of infection. Further demonstration of this methodology in a preclinical model is under way.

Research Plans for Year 5

The researchers will continue to develop dermal equivalents that induce ASC to differentiate toward vascular and dermal cells via properties of the scaffolds and will integrate an epithelial cell sheet that is developed from ASC. The present strategy is expected to provide an environment for the formation of blood vessels within the matrices that will increase the viability and survival of the graft thus facilitating its integration into both the burn and/or donor-site wound beds, to improve healing with less scar tissue formation. The researchers plan to continue to use and optimize the InGeneron, Inc. point-of-care device for the isolation of ASC. This will be used for cell isolation from the debrided burn patient tissue, as well as from surgically isolated adipose tissue obtained from abdominoplasty from the approved IRB protocol using current standard of care lipoaspiration surgical techniques.

Planned Clinical Transitions

The researchers will continue to develop a more clinically relevant porcine burn model and will use this model for the development of a large (up to 20%) total body surface area burn, which will provide a stringent test for their product and other AFIRM-related skin equivalent products.

Clinical Trials

Clinical Trial: Expedited Availability of Autologous-Engineered Human Skin for Treatment of Burned Soldiers

Project 4.7.4, RCCC/USAISR

Team Leader(s): David Smith, MBA, Christine Nigida, MS, Kim Warren, PhD, and Kirstin Powel, MS (Lonza Walkersville, Inc.)

Project Team Member(s): Stanton Gerson, MD (Case Western Reserve University); Booker T. King, MD (USAISR); and Nicole Gibran, MD (University of Washington-Harborview Medical Center)

Collaborator(s)/Secondary Site(s): USAISR and Harborview Medical Center

Therapy: Treatment of deep partial and full-thickness burns (≥50% total body surface area) using skin substitutes

Deliverable(s): Engineered skin substitute

TRL Progress: 2011, TRL 5; 2012 (Current), TRL 5; 2013 (Target), TRL 6

Key Accomplishments: The researchers will compare an autologous engineered skin substitute (ESS) with a meshed, split-thickness autograft for the treatment of deep partial and full-thickness burn wounds in a clinical trial in adult patients. In preparation for the trial, the researchers completed proof-of-concept and acute toxicology animal studies and manufacturing qualification and shelf-life studies.

Key Words: Burns, skin substitutes, full-thickness, combination products, clinical trials

Introduction

From 2003–2007, the burn unit at the USAISR at Fort Sam Houston Center had 1,497 hospitalizations, including 656 military service members, 540 of who had been deployed in Iraq. Victims of large burns do not possess sufficient donor skin to complete grafting without multiple harvesting of donor sites at 7- to 10-day intervals. With each harvest, healing time increases as epithelial sources (glands, follicles) are removed, leaving wounds and donor sites susceptible to infection. Sepsis, which develops in part from microbial contamination and invasion in wounds, accounts for 75% of deaths from burn injuries and is often associated with multiple organ failure. Other major aspects of recovery from burns, including immune function, positive nitrogen balance, and physical therapy, all depend on complete wound closure. A significant source of long-term morbidity is the development of scars in two areas: (1) the original burn wounds, which have been grafted with meshed and widely expanded skin grafts, and (2) other body areas where skin was harvested to cover the burns (i.e., donor sites of skin grafts). Conversely, it is well known that grafting of wounds within a sheet format suppresses scar formation.

Prompt and effective wound closure remains a challenge in recovery from extensive, deep-burn injuries. To address this limitation, researchers have developed an autologous ESS. ESS is an autologous product prepared from cryopreserved cells from a split-thickness skin harvest area. ESS consists of cultured keratinocytes and fibroblasts attached biologically to a collagen-based matrix. The end product is a long sheet that can be placed into the burn area to be compared to a conventional split-thickness autograft. Lonza Walkersville, Inc. (LWI) has licensed this technology and completed the technology transfer and product development. This project is focused on expediting the path to an ESS clinical study for treatment of extensive burns in military populations.

Clinical Trial Status

USAISR and Harborview Medical Center in Seattle, Washington are jointly planning a 10-patient clinical trial. LWI anticipates that it will enroll 14 subjects,

upon permission by the FDA to proceed with the IND-based study. Two patients will initially be enrolled at each site for a Priming Phase. An additional 10 patients will then be enrolled for execution of the clinical trial.

Clinical Trial Plans for the Next Year

Phase 1 is to be initiated before end of 2012. Upon completion, LWI will submit an FDA proposal for a pivotal trial.

Planned Commercialization Transitions

LWI will submit a Biologics License Application to the FDA upon the conclusion of the pivotal trial.

Clinical Trials

A Comparative Study of the ReCell® Device and Autologous Split-Thickness Meshed Skin Grafting in the Treatment of Acute Burn Injuries

Project 4.2.7, WFPC/USAISR

Team Leader(s): James Holmes, MD (Wake Forest School of Medicine)

Project Team Member(s): Booker T. King, MD (USAISR); Joseph Molnar, MD (Wake Forest School of Medicine); Rajiv Sood, MD (University of Indiana); William Hickerson, MD (University of Tennessee Health Science Center); Bruce Cairns, MD (University of North Carolina at Chapel Hill); Kevin Foster, MD (Maricopa Integrated Health Systems); David Mozingo, MD (University of Florida); Marion Jordan, MD (Washington Hospital Center, DC); Richard L. Gamelli, MD (Loyola University Medical Center); David Smith, MD (Tampa General/USF); Michael Feldman, MD (VA Commonwealth University); Tina Palmieri, MD (UC Davis); and John Griswold, MD (Texas Tech University Health Science Center)

Collaborator(s): Fiona Wood, MD (Royal Perth Hospital); William Dolphin, PhD (Avita Medical Ltd); Andrew Quick, MS (Avita Medical Americas LLC); Annette Fagnant, MS (MedDRA Assistance Inc); Susanne Panzera and Maureen Lyden, MS (BioStat International, Inc); Evan Renz, MD, Leopoldo Cancio, MD, Johnathan Lundy, MD, Rodney Chan, MD, PA, James Williams, MPAS PA-C, and Michael Chambers (USAISR)

Therapy: Transplantation of autologous epidermal cells for treatment of second-degree burn injuries

TRL Progress: 2009, TRL 1; 2010, TRL 7; 2011, TRL 7; 2012 (Current), TRL 7; 2013 (Target), TRL 7

Key Accomplishments: The researchers have enrolled 63 subjects to date, 19 of whom have been followed through the 52-week endpoint. Enrollment is continuing at 12 active sites and will soon commence at one additional recently approved site.

Key Words: ReCell® system, cell spray, skin grafting, burns

Introduction

The rapid and effective management of wounds of an injured warfighter is a critical factor in the determination of wound outcome and consequential morbidity and mortality. The ReCell Device is based on previous work of Wood & Stoner[1] and the recognition that autologous transplantation of epidermal cells could offer long-term wound closure in a clinically advantageous time frame while optimizing the patient's outcome. The device is designed to provide a simple, safe technique for the harvesting of skin cells for enhancement of epidermal repair. The initial step involves harvesting a thin, split-thickness skin biopsy, followed by enzymatic and mechanical disaggregation to harvest the cells of the epidermis, dermis, and epidermal-dermal junction. The separated cells and associated signaling factors are combined into a suspension containing a mixed population of live keratinocytes, melanocytes, and papillary fibroblasts. The suspension is then sprayed onto the prepared wound bed. The cells migrate over the surface providing epidermal reconstruction with site-matched characteristics of color and texture. The applied cells are incorporated into the developing epidermis.[2] The speed of re-epithelialization is very important as the "sealing" of the skin surface limits the inflammation that has been implicated as the pivotal factor in hypertrophic scar formation. By providing a source of viable and metabolically responsive cells onto

[1] Wood F. 2003. *Wounds* 15:16-22.
[2] Stoner M, Wood F. 1999. *J. Invest. Derm.* 112:391-392.

the wound surface, the ReCell Device technology may facilitate rapid wound healing while minimizing donor-site morbidity and potentially eliminating or minimizing scar formation.

The aims of this project are to collect clinical data to demonstrate the safety and effectiveness of the ReCell Device compared with the standard of care, split-thickness meshed grafts (STMGs), for the treatment of second-degree burn wounds. The results will be used to support a premarket application to the FDA for the ReCell Device. For the regulatory application, the hypotheses to be supported are: (1) noninferiority with the primary efficacy endpoint defined as recipient site wound closure at the week 4 follow-up visit of the ReCell-treated area as compared to that of the STMG-treated area and (2) superiority in the healing of the ReCell donor site as compared to the STMG donor site at week 1. The clinical study design was modified slightly to meet requirements of the FDA's Center for Biologics Evaluation and Research (CBER). Specifically, for the regulatory endpoint, the study has been expanded from 60 patients with a 6 week follow-up to 106 patients with a 4 month follow-up. In accordance with the AFIRM grant, subjects will be followed for up to 52 weeks following randomization to collect additional data pertaining to wound healing appearance/scar formation.

During the first 2 years of this study, the researchers obtained both FDA and U.S. Army Medical Research and Materiel Command (USAMRMC) Office of Research Protections/Human Research Protection Office (HRPO) approval of the study protocol, executed contracts with key vendors for support of the clinical trial (i.e., regulatory affairs, clinical management, biostatistics, data management, and the independent reading facility for primary endpoint adjudication), and initiated subject enrollment. They enrolled 35 subjects at 6 sites, and 1 subject was followed for 1 year post treatment. FDA approval was obtained for enrollment at 6 additional sites.

Clinical Trial Status

To date, 63 subjects have been enrolled (target = 106), with 32 enrolled in the past 12 months. Nineteen subjects have been followed through 1 year post treatment. In total, 13 sites are cleared to enroll subjects, and 12 sites are actively enrolling. One of the sites is located at the USAISR Burn Center, which is the only burn center operated by the DoD and serves as the regional burn center. As such, it provides treatment for all severe burns sustained by active duty military personnel and burn victims in the San Antonio region, whether DoD beneficiaries or civilians. The USAISR received USAMRMC IRB approval in November 2011, enrolled its first subject in January 2012, and now has six subjects enrolled. Avita Medical, the study Sponsor, expects to complete study enrollment by December 2013. The USAISR site Principal Investigator is LTC Booker King.

Recruitment of subjects for the study has been slow so a number of steps were taken in an attempt to improve enrollment. During the past year, 6 additional clinical sites were approved by the FDA. Staff was trained and recruitment began, resulting in the treatment of 12 of the 32 subjects. A clinical trial subject recruitment professional was retained in late 2011 to interview coordinators and investigators at selected sites. Ongoing review and assessment of screening logs is being conducted. While no single obvious issue has impeded enrollment, the level of communication with investigators has been increased via regular contact. Investigators who attended the Southern Region Burn Conference (December 2011) were engaged one-on-one to discuss recruitment and miscellaneous training-related items while other investigators were updated via individual web-based meetings. Newsletters containing tips on recruitment and other tips were distributed in February, March, and May. The February newsletter introduced a pocket reference card for study patient selection as well as subject recruitment flyers and posters, which have been deployed as each site secures IRB approval of the material (5 sites to date). Improved surgeons' ReCell product quick reference guides and coordinators' treatment visit checklists were also distributed in February. There has been a singular focus on the recruitment of study participants; however, the average rate across 13 sites remains just two to three per month. Of note, the annual IDE progress report for the study was accepted without any questions by the FDA.

Conclusions

Informal review of the (nonblinded) site investigators' assessments of donor sites and burn wound healing (the study co-primary endpoints) for the first 23 subjects indicates that the results appear to be on track for demonstration of the effectiveness of ReCell. However, 3 subjects have experienced treatment-area healing at 8 weeks instead of the anticipated 4 weeks due to some form of re-injury on the ReCell-treated burn. Since this did not occur in the control-treated burn areas, the FDA is likely to inquire about the robustness of ReCell versus STMG.

Clinical Trial Plans for the Next Year

The researchers anticipate completing the trial enrollment goal (106 subjects) during the upcoming year. The clinical program will be transitioning from an execution phase to a final reporting phase with completion of subject accrual anticipated over the course of the next 12 to 24 months. Avita Medical will continue to be an industry collaborator on this project.

Corrections/Changes Planned for the Next Year

The program time line has been extended due to program delays as a result of the challenges of enrolling subjects in the rigorous protocol approved by FDA/CBER.

Clinical Trials

Stratatech Technology for Burns

Project 4.2.9, WFPC/USAISR

Team Leader(s): James Holmes IV, MD (Wake Forest)

Project Team Member(s): Booker T. King, MD (USAISR); Michael Schurr, MD (University of Colorado Hospital); Lee Faucher, MD (University of Wisconsin Hospital and Clinics); Kevin Foster, MD (Arizona Burn Center); and Steven Wolf, MD (University of Texas Southwestern)

Collaborator(s): B. Lynn Allen-Hoffmann, PhD, Allen Comer, PhD, and Mary Lokuta, PhD (Stratatech); Leslie Jones (Research Point); Evan Renz, MD, Leopoldo Cancio, MD, Johnathan Lundy, MD, Rodney Chan, MD, PA, James Williams, MPAS PA-C, and Michael Chambers (USAISR)

Therapy: A readily available, viable, full-thickness, allogeneic human skin substitute (StrataGraft® skin tissue) that provides immediate wound coverage and promotes the healing of severe burns and other complex skin defects

Deliverable(s): A clinical trial that assesses the safety and efficacy of StrataGraft skin tissue as an alternative to autografting for promoting the healing of deep partial-thickness burns

TRL Progress: 2009, N/A; 2010, N/A; 2011, TRL 6; 2012 (Current), TRL 6

Key Accomplishments: The first cohort of 10 subjects has been fully enrolled in the StrataGraft skin tissue clinical trial. None of the subjects treated to date has required autografting of the StrataGraft treatment site by day 28, and there has been no evidence of safety concerns or immunological responses to the skin substitute. Allogeneic DNA from the cells comprising StrataGraft tissue was not seen at 3 months. These data suggest that StrataGraft skin tissue facilitates wound closure and is replaced as the patient's own cells close the wound. Based on these data, enrollment in the second cohort, which involves treatment with larger areas of StrataGraft, was initiated in April 2012, and is ongoing with 19 subjects enrolled to date.

Key Words: StrataGraft skin tissue, burn, skin grafting, regenerative medicine

Introduction

The standard of care for both full-thickness and deep partial-thickness burns is surgical excision followed by coverage with autologous skin grafts. In large burns, the area of healthy skin is often limiting and must be used to cover areas of full-thickness injury. As a result, areas of deep partial-thickness injury must be temporarily managed with other means before definitive coverage with autograft. Alternatives to autografting the deep partial-thickness component of severe burns would expedite the healing of large burns and reduce or eliminate the morbidities associated with donor-site wounds.

Stratatech Corporation has developed StrataGraft tissue as a readily-available allogeneic skin substitute to promote the healing of complex skin defects due to burns and trauma. StrataGraft tissue is a living, meshable, suturable, human skin substitute that reproduces many of the structural and biological properties of normal human skin. The technology provides an epidermal layer composed of differentiated, multilayered, epidermal keratinocytes from a single human donor grown on a non-bovine collagen matrix embedded with fibroblasts from a second human donor. In addition to providing immediate wound coverage with robust barrier function, numerous antimicrobial peptides, growth factors, and cytokines secreted by the viable cells of StrataGraft tissue are anticipated to accelerate wound healing and reduce infection, thereby facilitating wound closure and cosmetic outcome.

Stratatech Corporation completed a Phase 1/2a clinical trial in 15 patients with severe burns and other complex skin defects, designed to assess the

safety and early efficacy of exposure to escalating amounts of StrataGraft tissue followed by removal and autografting. They found that StrataGraft tissue exhibited a good safety profile and was well tolerated with no evidence of acute immune responses.[1,2]

In this project, the researchers are clinically examining the safety and efficacy of StrataGraft skin tissue as a permanent skin replacement to promote the healing of deep partial-thickness burns without the need for autografting. Primary endpoints are: the need for autografting of the study wound by 28 days and wound closure at 3 months. Additional assessments are designed to monitor adverse events, local or systemic toxicity, immunological responses to allogeneic cells of StrataGraft tissue, and persistence of the cells from StrataGraft tissue.

Clinical Trial Status

During the past year, the research team has made excellent progress toward completion of a multicenter Phase 1b clinical trial to assess the safety, tolerability, and efficacy of prolonged exposure to increasing amounts of a single application of StrataGraft skin tissue compared to autograft in the deep partial-thickness component of complex skin defects. Following the FDA's acceptance of the study design, the researchers submitted the study protocol to the IND application that they had established with the FDA's CBER for clinical evaluation of StrataGraft skin tissue in complex skin defects. They identified six clinical sites for this study: Wake Forest University Baptist Medical Center, USAISR, University of Colorado Hospital, University of Wisconsin Hospital and Clinics, Arizona Burn Center at Maricopa Medical Center, and Parkland Health and Hospital System. Key documents for this study, including the clinical protocol, informed consent form, and investigator's brochure, have been reviewed by the IRB at each of these sites. IRB and HRPO approval for this study have been obtained at five of the six sites; approval at USAISR is anticipated shortly. Due to the pending approvals, USAISR had not enrolled any subjects as of August 2012. Complete enrollment at USAISR is anticipated by the end of 2012. The USAISR site Principal Investigator is LTC Booker King.

Stratatech Corporation has maintained a continuous production stream of StrataGraft skin tissue for the clinical trial at Waisman Biomanufacturing (Madison, WI), a cGMP-compliant contract manufacturing facility. All StrataGraft tissue lots produced for this trial have met all lot release criteria. ResearchPoint (Austin, TX) is providing clinical trial monitoring services for this trial. Activities completed during the previous year include development of the safety monitoring plan, study database, statistical analysis plan, and data management plan. Study-specific procedures and documents have been prepared and distributed to the clinical sites.

The clinical results to date have exceeded Stratatech Corporation's expectations. Enrollment in the first dose cohort was initiated in September 2011 and was completed in February 2012. The initial group of 10 study subjects was treated with up to 220 cm^2 of StrataGraft tissue. All subjects in the initial dose cohort met the primary safety and efficacy endpoints for the study. All burns treated with StrataGraft tissue healed without the need for autografting and all of these wounds remained closed after 3 months (**Figure 1**). Because the StrataGraft-treated wounds did not need to be autografted, study subjects reported less pain at the donor site that had been prospectively identified for coverage of the StrataGraft-treated site, if needed (**Figure 2**).

There were no adverse events deemed likely product-related in any of the initial subjects. In subjects evaluated to date, there has been no evidence of an acute immune response to StrataGraft tissue. Allogeneic DNA from StrataGraft tissue was not detected in tissue samples from the StrataGraft-treated site after 3 months. Unexpectedly, evaluation of scarring and cosmesis after 3 months revealed that, in many cases, the sites treated with StrataGraft were smoother, more supple, and less raised than the autograft control sites (**Figure 3**). Although these exciting observations need to

[1] Centanni JM, et al. 2011. *Annals of Surgery* 253(4):672-683.
[2] Schurr MJ, et al. 2009. *Journal of Trauma-Injury Infection and Critical Care* 66(3):866-873.

be confirmed by continued patient enrollment and long-term follow-up, the results to date have exceeded expectations and suggest that a single application of StrataGraft tissue may be able to promote the healing of deep partial-thickness burn without the need for autografting.

Following an interim analysis of data from the first subject cohort, the WFSM I-DSMB unequivocally recommended progression to the next patient cohort. Enrollment in the second dose cohort is ongoing and will be completed during the upcoming year. Subjects in this cohort will be treated with up to 440 cm^2 of StrataGraft tissue.

Conclusions

In summary, progress made during the past year has enabled initiation of a clinical trial to evaluate the safety and efficacy of StrataGraft tissue. To date, the StrataGraft clinical trial results have exceeded expectations because no StrataGraft treated wound has required subsequent autografting. Continued clinical evaluation of StrataGraft skin tissue in the current clinical study should provide a strong body of data to establish the safety and efficacy of StrataGraft skin tissue as an alternative to autografting for deep partial-thickness burns.

Clinical Trial Plans for the Next Year

The researchers plan to complete subject enrollment, follow up assessments of safety and efficacy outcomes, and prepare the study report.

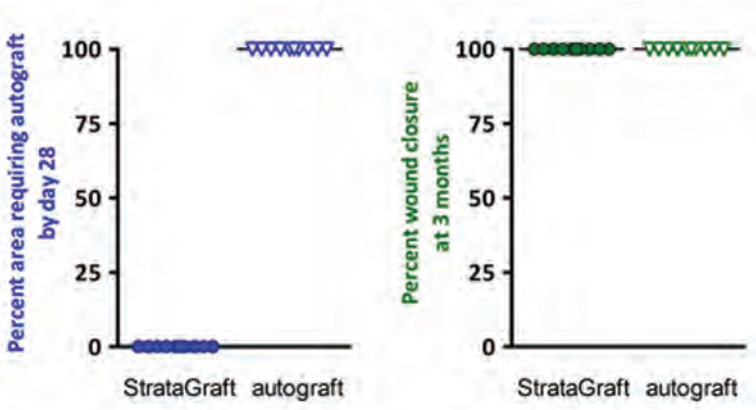

Figure 1. Autografting and wound closure assessments.

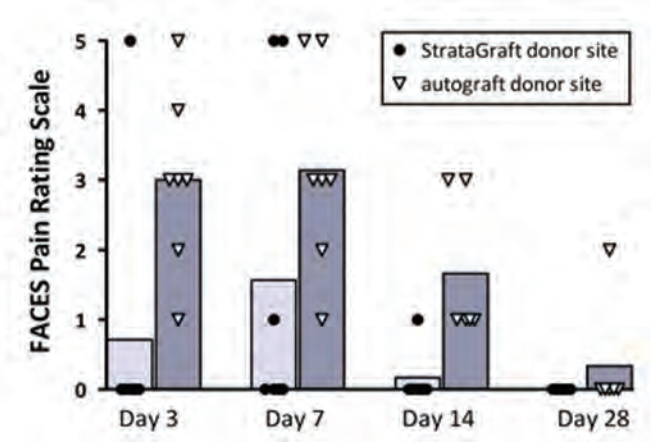

Figure 2. Donor-site pain assessments.

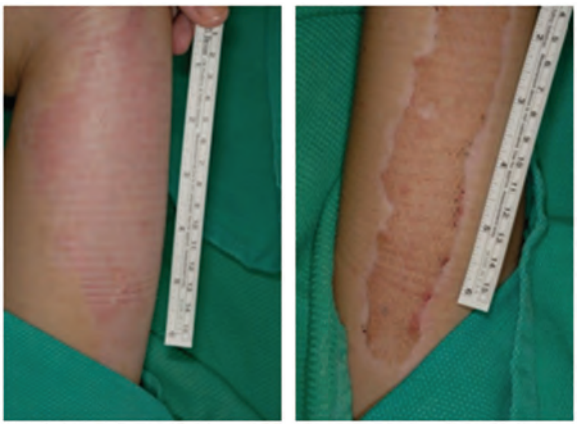

StrataGraft Tissue Autograft

Figure 3. Wound site appearance after 28 days.

VI: Compartment Syndrome

Cellular Therapy of CS

Cellular Therapy for Treatment and Consequences of Compartment Syndrome

Project 4.3.1, WFPC

Team Leader(s): Johnny Huard, PhD (McGowan Institute for Regenerative Medicine [MIRM]) and Shay Soker, PhD (Wake Institute for Regenerative Medicine)

Project Team Member(s): Burhan Gharaibeh, PhD, Nick Oyster, BS, Minakshi Poddar, MS, Johannes Schneppendahl, MD (MIRM); Tracy Criswell, PhD and Zhan Wang, PhD (WFIP)

Collaborator(s): William Wagner, PhD and Stephen Badylak, DVM, MD, PhD (WFIP)

Therapy: Cellular therapies for treatment of compartment syndrome (CS)

Deliverable(s): Muscle tissue regeneration by delivering muscle stem and progenitor cells together with angiogenic and antifibrosis factors

TRL Progress: 2008, TRL 1; 2009 CS Model, TRL 3; 2010 Progenitor cells, TRL 2; losartan, TRL 4; 2011 Progenitor cells, TRL 2; losartan, TRL 4; 2012 (Current) Progenitor cells, TRL 2; losartan, TRL 5

Key Accomplishments: The research team completed development of a small animal model of traumatic lower limb injury that features aspects of crush, ischemia-reperfusion (I/R), and CS injuries and shows significant damage to the underlying skeletal muscle, nerve, and vascular structures. They established a novel method of measuring intracompartmental pressure in the anterior compartment of rats. They created three murine muscle-derived stem cell (MDSC) lines that stably expressed LacZ, LacZ/vascular endothelial growth factor (VEGF) or LacZ/soluble fms-like tyrosine kinase 1 (sFlt-1). They characterized the cells for levels of VEGF and sFlt-1 secretion and transplanted the cells into the tibialis anterior (TA) muscle of injured athymic rats. The levels of fibrosis and necrosis that were observed post injury and cell transplantation indicate that timing the regulation of VEGF levels following CS is important in expediting skeletal muscle regeneration.

Key Words: Compartment syndrome, skeletal muscle, stem cells, fibrosis

Introduction

CS is a serious injury characterized by an increase in pressure in an enclosed space leading to compromised circulation, severe pain, and damage to muscle, nerves, and vasculature. The clinical standard of care for CS is surgical fasciotomy, which allows the compartment volume to increase. Fasciotomy is used with varying degrees of success in civilian and combat trauma centers. With fasciotomy rates increasing among U.S. armed forces casualties and the understanding that fasciotomies are often too late or insufficient to prevent CS, there is a need for an increased understanding of the damage to the underlying tissues.

In this project, the researchers aimed to create a small animal model of CS to allow for the future testing of therapies for treating CS sequelae. The researchers' model is being developed based on their expertise in contusion and laceration injury models in rodents and the use of murine skeletal MDSC therapies. Additionally, large animal models have the drawback of immune rejection during xenotransplantation, whereas the athymic rat model represents a viable cellular therapy model without the need for immunosuppressants. Furthermore, histopathological and physiological data obtained allowed for a more thorough assessment of the heterogeneity of the CS injury than has been done in other studies.

During the first 2 years of the project, the researchers created a model of CS in a rat leg muscle using a combination of a tourniquet and an external

compression device (ECD). They performed a microscopic evaluation of the model using a variety of stains. They isolated, characterized, and banked human and rodent MDSC to use in stem cell repair strategies. They found that MDSC can be implanted and tracked in the damaged muscle area and led to a significant reduction in fibrosis in the injured area. The researchers also showed that endothelial cells cocultured with myoblasts enhanced muscle fiber formation and tissue growth on collagen-based scaffolds in vivo. Finally, they showed that the angiotensin receptor II blocker losartan reduced fibrosis and improved muscle function in damaged muscle in humans. In Year 3, the researchers showed that a consistent injury can be created with the neonatal cuff as a replacement for the previously utilized ECD and that compression during ischemia (concurrent) or reperfusion (consecutive) seems to have little effect on the outcome of the injury. Reduced animal handling is the benefit of the concurrent application technique.

Research Progress – Year 4

Dr. Huard's laboratory completed development of the injury model (**Figure 1**). As part of the study, the group used a novel method to measure the intracompartmental pressure of the affected muscle (**Figure 2**). An implantable blood pressure monitor/transmitter (Data Systems International) was partially implanted into a rat prior to injury (Figure 2). For this experiment, only the probe was implanted into the muscle body while the transmitter remained outside the subject.

Following implantation into two athymic rats, the tourniquet and cuff (TKA + compression) or tourniquet alone (TKA alone) were secured over the hind limb with the monitor implanted, and the intracompartmental pressure was recorded every 10 seconds for 3 hours. The researchers found that external compression is necessary to elevate the anterior compartment pressure to the level necessary for a diagnosis of CS (Figure 2D).

Thirty-five athymic rats were injured in the Huard model and randomly assigned to one of four treatment groups: PBS, LacZ, VEGF, or sFlt-1. The last three treatment groups consisted of mouse MDSC isolated via the Huard group's preplate technique.

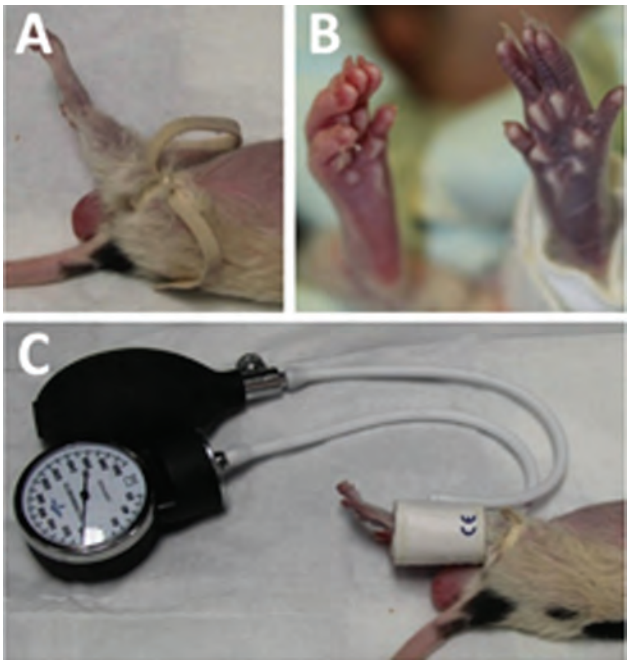

Figure 1. The CS injury model. (A) The tourniquet was placed just above the trochanter major and secured by double-knotting. (B) Venous blood flow occlusion was confirmed by a lack of pink color in the sole of the injured foot (right). (C) The neonatal cuff was secured over the lower hind limb that included the anterior compartment and inflated to a pressure above 300 mmHg. The tourniquet and cuff remained in place for 3 hours during which time the animal remained anesthetized with 2% isoflurane.

The researchers transduced mouse MDSC with LacZ retrovirus and then separated the cells into 3 groups. Two groups were additionally transduced with either VEGF or sFlt-1 retrovirus. Secreted levels of VEGF and sFlt -1 in the transduced MDSC were analyzed with an enzyme-linked immunosorbent assay (ELISA) (**Figure 3A–B**). Detectable levels of VEGF and sFlt-1 were present only in the cell lines transduced to overexpress the particular protein (either VEGF or sFlt-1). The negative values are due to the comparison to a standard curve as a linear relationship since the curve deviated from a linear relationship at low concentrations.

This group has previously shown that VEGF can have a negative effect on muscle regeneration at high concentrations. To reduce the secreted amount of VEGF to beneficial levels, the final number of injected cells consisted of 50% LacZ only and 50% VEGF-overexpressing cells. Seventy-two

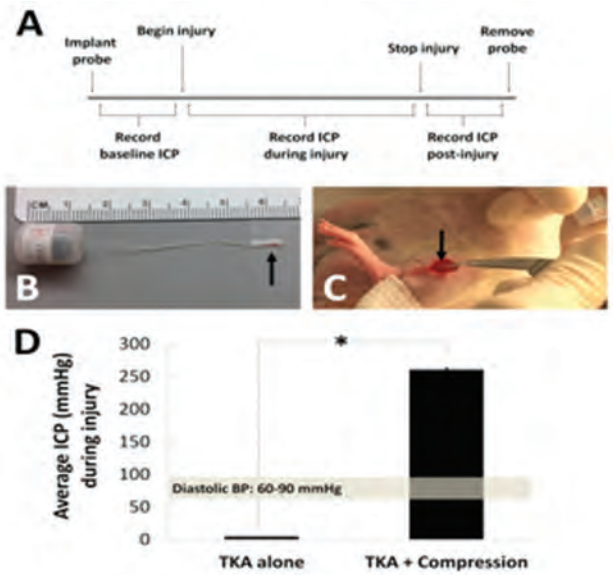

Figure 2. Intracompartmental pressure measurements during the 3-hour injury. (A) Experimental design for the measurement of compartment pressures. After implanting the tip of the catheter, baseline pressure measurements were recorded for 5–10 minutes. The injury was started by applying the tourniquet or the tourniquet plus cuff. Once the materials were secured, pressures were recorded for 3 hours. After 3 hours the tourniquet and/or cuff was removed, and pressures were recorded for another 20 minutes after which the transmitter was removed. (B) The implantable transmitter was used to measure and transmit anterior compartment pressures. It consists of a transmitter and a 5 cm catheter, the tip of which (arrow) is implanted into the muscle. (C) The tip of the transmitter is being inserted into the centroid of the TA (arrow). For these measurements only the tip was implanted while the rest of the catheter and the transmitting component were left extracorporeal. (D) The average compartment pressures were recorded inside the anterior compartment when injured with a tourniquet alone or a tourniquet plus external compression for 3 hours. The range of diastolic pressure for rats is represented by the shaded brown bar. The average pressure when the tourniquet-only is applied is 4.41 ± 0.02 mmHg. The average pressure when the cuff is applied in addition to the tourniquet is 260.70 ± 2.70 mmHg (* $p<0.05$).

hours post injury, phosphate-buffered saline (PBS) or 1 x 10^6 MDSC were injected into the injured TA muscles. Animals were euthanized 7 and 14 days after injury and the tissues were collected, frozen, sectioned, and stained to look for implanted cells (Figure 3C). The researchers assessed the function of injured anterior muscle groups using an in situ test apparatus (806D Aurora Scientific) just before euthanizing the animals. The data in Figure 3D show no significant differences in function between the treatment groups. Levels of fibrosis (Figure 3E) and necrosis (Figure 3F) indicate that timing the regulation of VEGF levels following CS is important in expediting skeletal muscle regeneration.

Conclusions

The researchers have developed a novel model of a traumatic lower limb injury that combines aspects of CS, I/R, and crush injuries to cause significant damage to the underlying skeletal muscle, nerve, and vascular structures. Mouse MDSC overexpressing VEGF or sFlt-1 transplanted into injured skeletal muscle indicate that the timing of VEGF regulation is critical in treating an injury as complex as CS.

Research Plans for Year 5

Therapies combing the benefits of MDSC and the antifibrotic effect of losartan (reported in the 2011 annual report) are being tested. Along with the previously mentioned murine cell lines, this group has created three human muscle-derived cell lines that stably express green fluorescent protein (GFP), GFP and VEGF, or GFP and sFlt-1. Dr. Huard's team previously reported on the successful transplantation of human MDSC into CS-injured athymic rats. Tests using these newly developed and characterized muscle cells will build upon Year 4's successful transplantation of murine MDSC. The researchers will optimize the timing and dosing of MDSC transplantation and losartan to better regulate VEGF and mimic the clinical setting. The data from this past year indicate that VEGF regulation is important in treating the complex tissue damage that CS creates; however, the current treatment protocol may not be ideal. Currently, both MDSC and losartan treatment is started 72 hours after

CS injury, but clinical treatments will be started immediately following fasciotomy. The injury models developed by the Huard and Soker groups mimic fasciotomy (removal of external compression) to allow for testing of a clinically relevant treatment protocol.

Planned Clinical Transitions

The researchers are proposing (though unfunded at this time) to determine the effect of losartan on tissue fibrosis and time to return to prior level of function in a limited case study of acute grade II or III hamstring strain patients. They will quantify skeletal muscle fibrosis in the injured hamstring of the subjects with a 3 Tesla magnetic resonance imaging (MRI) during the initial visit and will conduct a follow-up MRI 6-months post injury. Research subjects will be followed to determine the time to return to the prior level of sports activity, and a correlation between scarring and time to return will be determined.

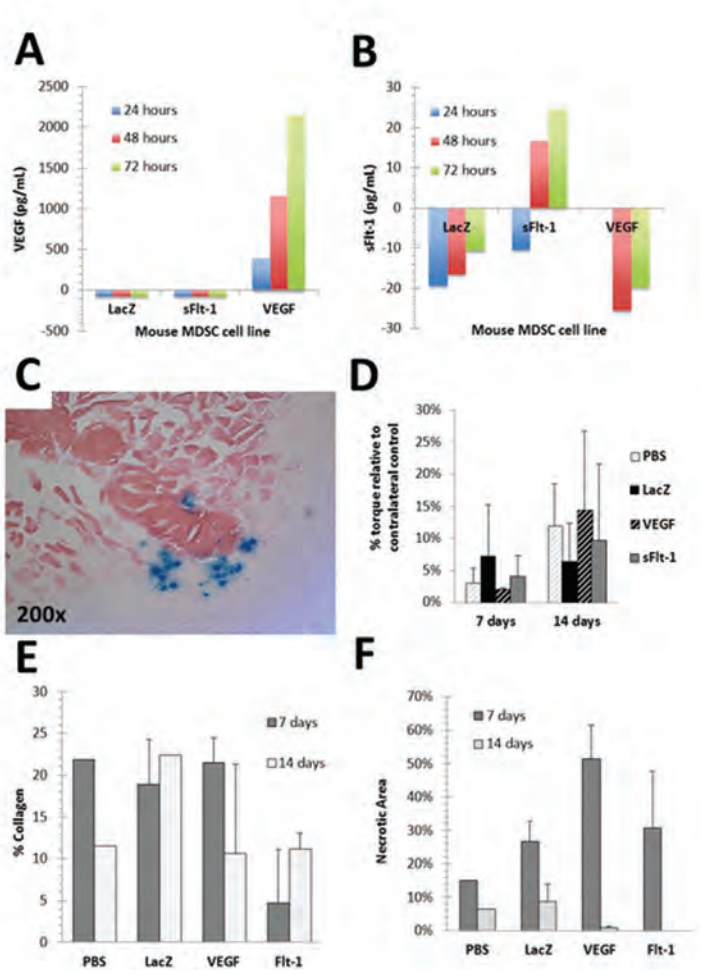

Figure 3. Transplantation of murine MDSC into injured athymic rats. (A–B) VEGF and sFlt-1 secretion levels 24–72 hours in culture. Protein concentrations were determined using ELISA kits and concentrations are presented in pg/mL based on comparison to known levels of protein standards. (C) Beta-galactosidase staining of MDSC-implanted TA 7 days after injury and 4 days after implantation. Cells are stained blue while skeletal muscle fibers are stained pink with eosin. (D) Functional testing of injured muscles showed no statistical differences between treatment groups. Data are presented as the percentage of torque generated by the injured anterior crural muscles compared to the contralateral control anterior crural muscles. (E) Fibrosis formation was analyzed by Masson's trichrome stains. Collagen levels were quantified as the percentage of positively stained pixels in the tissue area. Differences among the groups are not statistically significant. (F) Analysis of hematoxylin and eosin (H&E) stained injured tissue sections for the amount of necrotic tissue. No differences are significant; however, the trend indicates VEGF and sFlt-1-expressing MDSC reduce the amount of necrotic tissue.

Cellular Therapy of CS

Use of Bone Marrow-Derived Cells for Compartment Syndrome

Project 4.3.2, WFPC

Team Leader(s): Kenton Gregory, MD, (Oregon Health and Sciences University [OHSU])

Project Team Member(s): Bo Zheng, MD, Cynthia Gregory, PhD, Michael Rutten, PhD, Hua Xie, MD, PhD, Rose Merten, BS, Bryan Laraway, BS, Annabeth Rose, BS, James Hunt, BS, Carrie Charlton, BS, Amy Jay, BS, Cher Hawkey, BS, and Teresa Malarkey, CVT, LAT (OHSU)

Collaborator(s): OHSU Center for Regenerative Medicine; USAISR; Special Operations Medical Command-Fort Bragg; Biosafe-AmericaBiologics Consulting Group; and Torston Tonn, MD (Johann Wolfgang University, Frankfurt, Germany)

Therapy: Autologous bone marrow stem cell treatment for compartment syndrome (CS)

Deliverable(s): Develop a large-animal CS model to evaluate efficacy of multiple stem cell treatment to regenerate muscle and nerve damage in extremity wounds complicated by CS

TRL Progress: 2008, TRL 2; 2009, TRL 2; 2010, TRL 3; 2012 (Current), TRL 3–4; 2013 (Target), TRL 4–5

Key Accomplishments: During the past year, the Gregory group completed the pivotal proof-of-concept preclinical study in Sinclair miniswine to evaluate the deployment strategy of autologous bone marrow mononuclear cells (BM-MNC) to treat extremity injuries complicated by CS. They first completed a prospective, randomized, blinded, sham-controlled dose ranging study to determine a therapeutic concentration of autologous BM-MNC for treatment 1-week post CS injury. The selected concentration was used in the multidose study to determine the deployment strategy of single versus multiple cell treatments (one, two, and three cell treatments post injury). No adverse events or complications were associated with any cell treatments. Both studies showed statistically significant improvement in muscle strength and gait. Robust engraftment of transplanted cells was observed at 3 months. This study demonstrates the potential of a safe, new treatment for severe extremity injury that offers injured troops an improved functional recovery.

Key Words: Extremity compartment syndrome, autologous bone marrow-derived stem cells, porcine model, automated bone marrow stem cell separator, gait analysis, cell engraftment

Introduction

Extremity injuries are the most common battlefield wounds sustained by troops in current military conflicts. These injuries are often complicated by CS, where secondary edema and swelling increase compartment pressure until blood flow stops, resulting in ischemia and infarction of muscle and nerve tissue. Fasciotomy is required to relieve the pressure. Troops developing CS have prolonged recovery times and permanent disability is common. The goal of this project is to improve the endogenous cellular regenerative response by local treatment with autologous bone marrow stem and progenitor cells to produce an improved functional recovery.

During the first 2 years of the project, the researchers developed a large animal model of CS using Sinclair miniswine that could be used to test whether the application of bone marrow progenitor cells can enhance the healing and function of an injured limb. They created cell invasion assays as well as flow cytometry protocols to help assess the function, viability, and identification of cells used in bone marrow treatments. They also developed a cell colony-forming unit assay protocol for adult porcine bone marrow to examine the effects of stem cell colony formation in response to bone marrow cells loaded with and without the cell trackers DiI or quantum dots. They completed a comparative flow cytometry analysis of BM-MNC in uninjured and CS-injured pigs. Their preliminary

results indicated upregulated expression levels of certain identifiable cell phenotypes in CS-injured pigs. In Year 3, the researchers nearly completed a large animal pilot study using Sinclair miniswine to evaluate the effectiveness of autologous BM-MNC treatments in CS injuries. They also developed an in vivo cell tracking technique that has allowed them to demonstrate extremely robust cell engraftment up to 3 months post treatment.

Research Progress – Year 4

Preclinical Study

The researchers performed a prospective, randomized, blinded, sham-controlled study comparing treatment of CS with autologous bone marrow cells versus control (media only) in a chronic (3 month) swine model. They created a severe extremity injury with CS by infusing autologous plasma into the left hind TA muscle compartment, which resulted in elevated compartment pressures (>120 mmHg) for 6 hours and produced severe ischemia and infarction of the muscle and nerve with resultant motor and nerve deficits.

One week after CS injury, the researchers aspirated approximately 50 milliliters of bone marrow for mononuclear cell isolation using a Sepax (Biosafe, Inc.) automated cell-processing device. The cells were sampled for phenotype characterization, labeled with CM-DiI fluorescent cell tracker, and injected according to a standardized three-dimensional grid pattern throughout the injured muscle. The BM-MNC were harvested, isolated, and administered again at week 2 post injury (n=16) and at week 4 post injury (n=8). The researchers performed flow cytometry analysis for each therapeutic BM-MNC preparation, totaling either two or three autologous BM-MNC preparations per subject. In addition to assessing each preparation independently, the researchers evaluated consecutive cell preparations from the same subject for any BM-MNC morphological changes that occur between bone marrow draws.

Prior to administration to autologous recipients, aliquots of the BM-MNC were reserved for cell function analysis. The researchers assessed the functional capacity of the BM-MNC by examining their ability to invade and migrate through a Matrigel-coated membrane filter in response to a stromal cell-derived factor-1α (SDF-1α) gradient. The assays were performed using 8.0 micron Matrigel-coated trans-well filter plates.

The researchers recorded muscle and nerve function data at five time points: pre-injury, post injury, and at weeks 1, 6, and 12 post injury. Gait analysis data were acquired at 11 time points: pre-injury, at days 1–3, weeks 1–6, and at the time of sacrifice (week 12).

After sacrifice, the injured skeletal muscle was harvested and investigated for evidence of previously injected CM-DiI cells. Cryosections of the harvested muscle were fixed, and the tissue was characterized using primary antibodies against skeletal muscle myofibers, vascular-like cells, proliferation nuclear proteins, and macrophage cells. To assess the differentiation fate of the CM-DiI labeled cells that were injected into the injured muscle, a 1 cm^3 portion was taken from the injured muscle and enzymatically digested. The digested cells were then sorted using a BD-FACS Aria II into CM-DiI positive and negative CM-DiI stained cells.

Muscle function analysis. The researchers determined muscle function by dorsiflexion force measurements of the injured limb. The absolute torque suggests that the control (cell media only) animals did not clinically improve between weeks 6 and 12 while the cell treatment groups continued to improve (**Figure 1**). The normalized torque

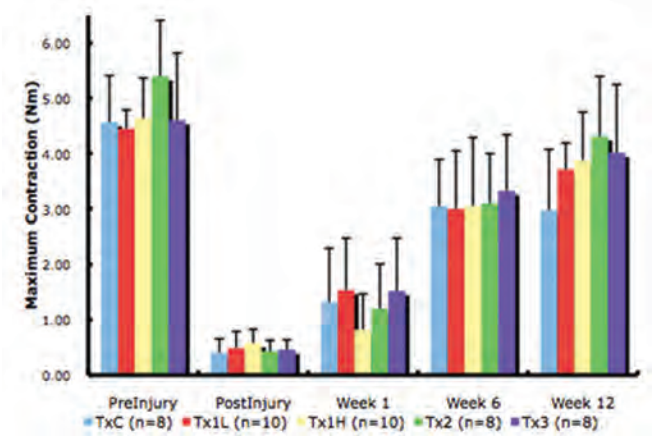

Figure 1. Absolute Torque (Nm). TxC-Control animals, cell-media only injections at week 1. Tx1L-Low cell dose (50 x 10^6 BM-MNC) single treatment at week 1. Tx1H-High cell dose (100 x 1 0^6 BM-MNC) single treatment at week 2. Tx2-High cell dose (100 x 10^6 BM-MNC) two cell treatments, weeks 1 and 2. Tx3-High cell dose (100 x 10^6 BM-MNC) three cell treatments, weeks 1, 2, and 4.

represents the quality of muscle function at week 12 by normalizing the maximum contraction to the muscle mass. **Figure 2** suggests that a single treatment with a high cell dose is the optimum cell therapy for improved muscle function as this regimen produced the maximum absolute torque of109.9 ± 28.6 Nm/kg.

Gait analysis. Gait analysis was represented by hind limb force symmetry. Immediately following injury, the animals supported most of their weight on their uninjured right side. As the animals began to improve, the researchers observed the same pattern of healing as the muscle function data where the treatment groups continued to improve clinically between weeks 6 and 12 while the control group did not (**Figure 3**).

BM-MNC characterization. Subsets of BM-MNC were detected by staining with antibodies specific for several distinct cell populations. The antibody panel was chosen to stain cell-surface determinants found on cells including mesenchymal stromal cells and endothelial/vasculature related cells, primitive stem cells, and hematopoietic lineage cells. Ongoing analyses demonstrate the presence of these BM-MNC subsets (data not shown), which is consistent with the adult Sinclair miniswine bone marrow being a multipotent cell source for injured tissue repair.

Flow cytometry assessments of the BM-MNC were monitored for viability pre- and post-CM-DiI labeling through observation of 7AAD positive cells (dead) and Annexin V positive cells (apoptotic). Additional analyses revealed that within the isolated BM-MNC population, there were three distinct populations of cells based on their size and internal granularity (i.e., their forward and side light-scattering properties, respectively). The researchers compared the data to determine whether the cell subset populations varied pre- and post-CM-DiI labeling (**Figure 4**).

Cell function assay. BM-MNC were functional in all cases, as demonstrated by their increased invasion in response to SDF-1α versus no chemokine. CyQUANT-based SDF-1α invasion assays demonstrated that all BM-MNC doses contained functional cells at the time of injection (data not shown). The researchers plan to attempt to correlate cell functionality with improvements in muscle function.

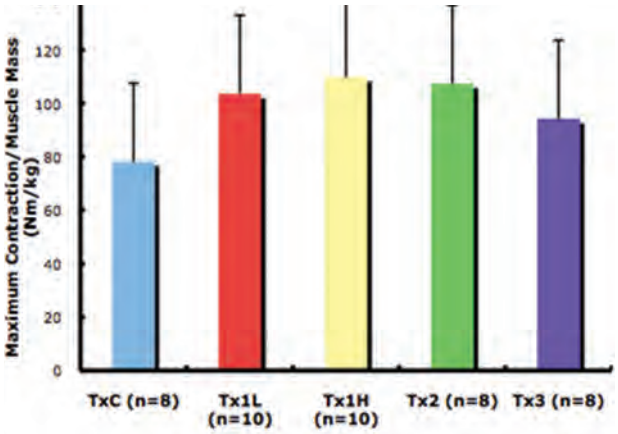

Figure 2. Normalized Torque (Nm). TxC-Control animals, cell-media only injections at week 1. Tx1L-Low cell dose (50 x 10^6 BM-MNC) single treatment at week 1. Tx1H-High cell dose (100 x 10^6 BM-MNC) single treatment at week 2. Tx2-High cell dose (100 x 10^6 BM-MNC) two cell treatments, weeks 1 and 2. Tx3-High cell dose (100 x 10^6 BM-MNC) three cell treatments, weeks 1, 2, and 4.

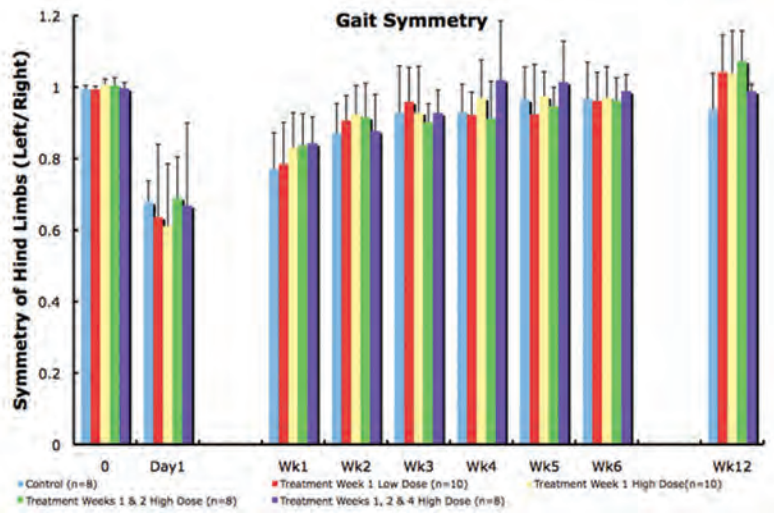

Figure 3. Gait analysis of force balance between left hind injured limb and the right hind uninjured limb. Healing appears to be uniform up to week 6 post CS injury. After week 6, all of the cell groups continue to improve while the control does not.

BM-MNC CM-DiI labeling and in vivo tracking. Evidence of successful engraftment of injected BM-MNC, as shown by CM-DiI-labeled cells (red) seen on confocal microscopy, was found at 11 weeks post injection (**Figure 5**). Skeletal muscle myofiber markers (dystrophin, desmin, and phalloidin) showed that CM-DiI-labeled cells appeared to preferentially distribute within regions of skeletal muscle fibers or reside near new regenerated myofibers (Figure 5 A, B, E). CM-DiI cells were located close to or colocalized with myogenitor antigens (MyoD and Pax7) (Figure 5 C–D) or were also found located close to neuronal type markers (β-III tublin, GFAP, CNPase, O4, and α-Bungarotoxin) (Figure 5 F–J) and to vascular structures where they expressed vascular endothelial markers (CD31, vWF, and α-SMA) (Figure 5 K–M). Some CM-DiI-labeled cells were found to be positive for the proliferation nuclear protein Ki-67 (Figure 5 N) and negative for macrophage antigen expression within the skeletal muscle tissue (Figure 5 O).

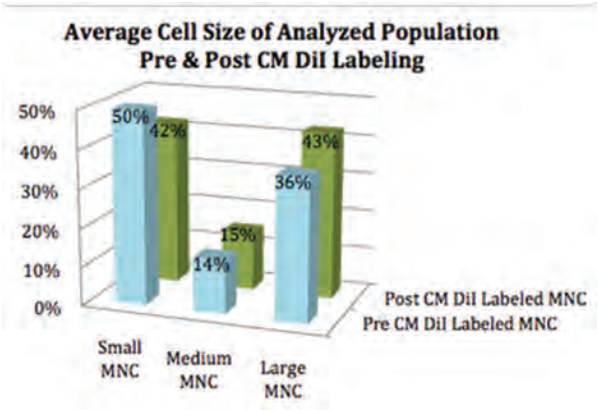

Figure 4. Analysis of cell-size subpopulations show that cell distribution is consistent pre- and post-CM-DiI labeling of the BM-MNC.

Recovery of CM-DiI-labeled cells from digested skeletal muscle tissue by cell sorting. The sorted CM-DiI-positive cells were cytocentrifuged onto glass slides (**Figure 6A**) for phenotypic characterization using confocal immunofluorescence microscopy (Figure 6B). The enzymatic digestion of two grams of TA skeletal muscle yielded on average 3.24 x 10^6 total isolated cells

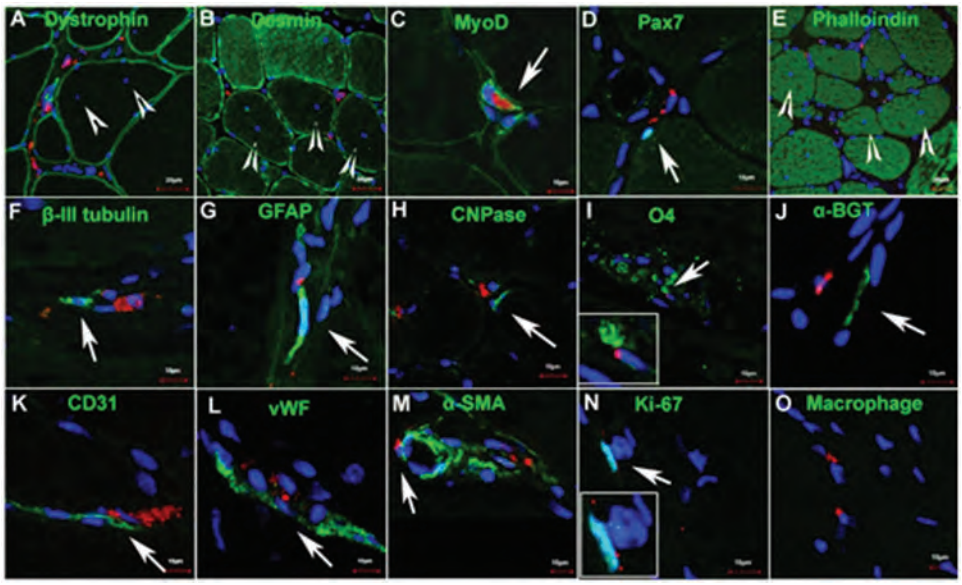

Figure 5. Representative confocal microscope images of fluorescent immunohistochemical staining of DiI-labeled cells in injured skeletal muscle at 11 weeks post injection. Data showed CM-DiI labeled BM-MNC (red cells) distributed between myofibers (green) (A) dystrophin, (B) desmin, and (E) phalloidin. (Note, newly regenerated skeletal myofibers are central nuclei arrow heads). CM-DiI cells (red, arrow) located close to or colocalized with myogenitor antigen (green, arrow) (C) MyoD and (D) Pax7, or nervous system cell-type markers (green, arrow) (F) β-II tubulin, (G) GFAP, (H) CNPase, (I) O4, and (J) α-Bungarotoxin, or with vascular relative antigen (green, arrow) (K) CD31, (L) vWF, and (M) α-SMA. Some CM-DiI-labeled cells showed positive for the proliferation nuclear protein (green, arrow) (N) ki-67 and negative for macrophage antigen (O). Nuclei (blue) were stained with DAPI. The image (left corner) was magnified by the area indictated by the arrow.

and 1.23 x 10^5 sorted CM-DiI-positive cells (n = 5). The purity of the sorted CM-DiI-positive cells was found to be 97.25% positive for CM-DiI labeling. In preliminary single-antibody staining experiments, CM-DiI-labeled cells expressed the neural markers S-100, GFAP, O4, and β -III tubulin, as well as von Willebrand factor and α-smooth muscle actin (Figure 6C). The muscle digest was completed for all animals moving forward in the pivotal study.

Conclusions

Treatment of severe TA CS muscle injury with autologous bone marrow stem and progenitor cells in a large animal model resulted in significantly improved muscle function as measured by tetanic force contraction 3 months after injury. While control animals treated with media alone stopped improving clinically 6 weeks after injury, animals stem/progenitor cell-treated continued to improve clinically through the 12-week study endpoint. Significant gait improvement and reduction of foot drop were observed at 3 months in treated animals compared to control animals. No adverse events or complications were associated with any cell treatments. This study demonstrates the potential of a safe, new treatment for severe extremity injury that offers injured troops an improved functional recovery. Important to the clinical translation of this protocol, the Sepax device is FDA-approved for human cord blood cell separation, which will allow for a shorter pathway through the FDA resulting in a cost-effective product.

Research Plans for Year 5

The Gregory group will finish their 6-month safety and efficacy study with 10 control animals and 10 treatment animals before the end of Year 5.

Planned Clinical Transitions

The Gregory group will begin a multicenter Phase 1 human clinical trial. Working closely with the commercial partner Biosafe Group SA, they plan on treating more than 20 patients with autologous BM-MNC following a CS extremity injury if funding is obtained. The FDA has granted 510(k) clearance for use of the Sepax device to separate bone marrow stem cells.

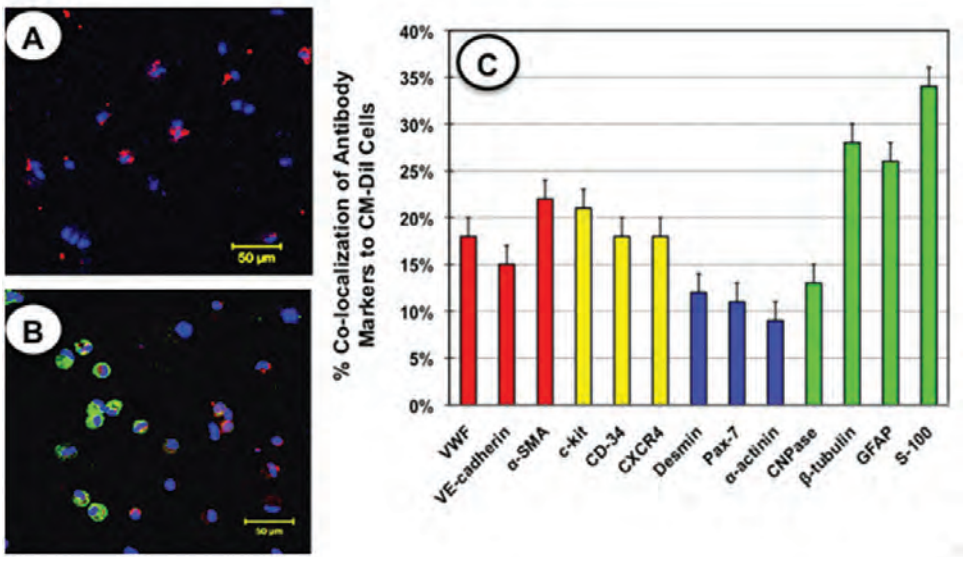

Figure 6. (A) Confocal image showing sorted CM-DiI-labeled cells; nuclei (blue) are stained with DAPI. (B) Example of CM-DiI sorted cells co-stained with a phenotypic antibody, i.e., neuronal glial fibrillary associated protein (green); nuclei (blue) are stained with DAPI. (C) Graph showing the co-localization of different phenotypic antibodies with CM-DiI sorted cells. Bars represent mean +/- SE; n = 5.

Cellular Therapy of CS

Improving Cell-Based Approaches for Extremity Trauma

Project 4.3.6, USAISR

Team Leader(s): Chris R. Rathbone, PhD and Thomas J. Walters, PhD (USAISR)

Project Team Member(s): Benjamin T. Corona, PhD and Joseph C. Wenke, PhD (USAISR)

Therapy: Adult stem cell transplantation

Deliverable: Strategy to improve the use of bone marrow-derived cells (BMC) for the treatment of ischemia-reperfusion (I/R) injury

TRL Progress: 2010, TRL 3; 2011, TRL 3; 2012 (Current), TRL 3; 2013 (Target), TRL 3

Key Accomplishments: The researchers characterized lineage-depleted BMC (LD-BMC) that were isolated from animals by flow cytometry. They determined the survival of freshly isolated LD-BMC after intramuscular injection of the cells 0, 2, 7, and 14 days after injury. They initiated experiments to determine the functional benefit of intramuscular or intravenous delivery of LD-BMC.

Key Words: Stem cells, muscle, injury

Introduction

Most combat-related extremity injuries are caused by explosive munitions, which can cause fractures, tissue loss, and vascular injury. This constellation of injury puts extremities at risk for CS and skeletal muscle I/R injury. Currently, the clinical treatment of complex I/R is insufficient. Numerous intervention strategies have been proposed aimed at reducing I/R, but pretreatments are impractical in a trauma setting and treatments applied during or immediately after ischemia are rarely feasible. A treatment that could be applied after patient stabilization would be much more practical. Cell-based therapies are an option since they can be applied after patient stabilization.

BMC containing a heterogeneous mixture of stem cells can be concentrated from bone marrow aspirate in the operating room using currently available FDA-approved point-of-care devices. The vast majority of studies utilizing cell therapies for I/R use culture-expanded cells, often mesenchymal stem cells (MSC), which makes extrapolation to the use of freshly isolated BMC derived from point-of-care devices difficult. The use of culture-expanded cells instead of freshly isolated cells leaves a significant knowledge gap with regard as to how to best utilize freshly isolated cells.

Based on the premise that freshly isolated BMC represent a means for expedited translation to the clinic and that there is a need to improve our understanding of the utility of freshly isolated BMC for I/R, the purpose of this work is to develop guidelines for use of freshly isolated BMC for treatment of I/R. Of the guidelines that need to be addressed, the mode and timing of delivery are two important considerations if freshly isolated cells are to be employed. Two logical routes of delivery are either direct intramuscular or intravenous injections.

During the first 2 years of this project, the researchers established and validated an in vitro muscle system and software to determine functional outcomes following I/R injury. They completed preliminary studies to determine the feasibility of injecting freshly isolated BMC into I/R-injured skeletal muscle. They also initiated studies to determine the effect of the timing of injection on cell engraftment.

Research Progress – Year 2 (Funded in 2010)

Adaption of point-of-care devices, originally developed for humans, to rodent models is difficult because the volume of aspirate required from

rodents for the devices to be effective is impractical. Although large animal models can be used (e.g., pig), rodent models offer the benefit of increased throughput, the potential to use transgenic animals, and greater flexibility with regard to the number of measurements that can be made. The research team used magnetic activated cell sorting (MACS) with a lineage depletion kit to deplete T cells, B cells, monocytes, granulocytes, and erythrocytes from mouse bone marrow aspirate to emulate freshly isolated cells derived from human point-of-care devices. In addition to its ability to approximate other point-of-care devices, the resulting population, LD-BMC, is enriched for stem cells and may represent a means to improve extremity trauma outcomes. In the current studies, the researchers used MACS to explore the use of LD-BMC and to aid in the development of guidelines for autologous point-of-care cellular therapies for the treatment of I/R injury.

The tibia and femur of FVB-L2G85 transgenic donor mice were flushed, and BMC were subjected to MACS with lineage depletion. Briefly, BMC were labeled with a cocktail of biotin-conjugated antibodies against lineage-specific antigens – CD5, CD45R (B220), CD11b, Gr-1 (Ly-6G/C), 7-4, and Ter-119—and then magnetically labeled with anti-biotin microbeads. The lineage-positive cells (T cells, B cells, monocytes/macrophages, granulocytes, erythrocytes, and their committed precursors) were depleted by retaining them on a MACS column in the magnetic field of the autoMACS® Pro Separator while unlabeled lineage negative cells passed through.

In a subset of animals (n = 5) flow cytometry was used to assess the presence of mesenchymal and hematopoietic stem cells within the LD-BMC. LD-BMC were blocked with FcR blocking reagent for 10 minutes and then labeled with phycoerythrin (PE) or APC-conjugated monoclonal antibodies (CD105, CD117, Sca-1; Miltenyi Biotec Inc., Auburn, CA) or isotype control antibodies (BD Biosciences, San Jose, CA). Live gating was performed with propidium iodide (Miltenyi Biotec Inc., Auburn, CA). Flow cytometry analyses were performed using MacsQuant analyzer and MacsQuantify software 2.4 (Miltenyi Biotec Inc., Auburn, CA).

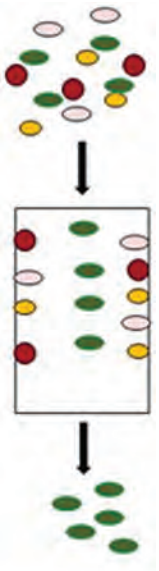

BMC
Bone marrow cavity of FVB-L2G85 transgenic donor mice flushed, centrifuged, and washed

MACS
BMC labeled with antibodies to deplete T cells, B cells, monocytes/macrophages, granulocytes, erythrocytes, and their committed precursors

LD-BMC (green cells)
CD105 – 53.4% (± 3.1)
Sca-1 – 15.8% (± 1.6)
CD117 – 48.5% (± 0.4.7)

Figure 1. Schematic to demonstrate the MACS procedure used to obtain and characterize freshly isolated LD-BMC.

One of the many outcomes that may affect the therapeutic effectiveness of the LD-BMC is cell survival. While several studies directed toward cellular therapies for muscle injury use BMC that have been culture-expanded, few have determined the potential for freshly isolated BMC to improve muscle regeneration. The first objective of this study was to determine the survival of freshly isolated LD-BMC in a mouse I/R model following intramuscular injections. Determining the best time to administer cells represents critical information for maximizing the clinical applications of this approach. Freshly isolated LD-BMC survival following intramuscular injection 0, 2, 7, and 14 days post injury was evaluated.

To determine the effect of timing of administration on the survival of LD-BMC, depleted cells were resuspended in 50 µL for cell injections. For intramuscular injections, cells were injected parallel to the long axis of the TA muscle with an insulin syringe. For in vivo bioluminescent imaging, changes in cell survivability were determined by measuring luminescence in vivo using a Xenogen box at the indicated time points.

The freshly isolated LD-BMC survived throughout the 28-day study period, regardless of whether they were delivered 0, 2, 7, or 14 days after

injury (**Figure 2**). The ability of the freshly isolated LD-BMC to survive transplantation for up to 28 days after delivery suggests they may be a therapeutic option for the treatment of I/R injury. Studies to determine if the intramuscular delivery of LD-BMC provides a functional benefit following I/R have been initiated.

Conclusions

LD-BMC obtained from MACS produce a stem cell-enriched population of cells. The use of LD-BMC for treating I/R injury is supported by the cells' ability to persist in vivo for up to 28 days after intramuscular delivery and their ability to home to the injured leg following intravenous delivery.

Research Plans for Year 4

The research team plans to compare functional recovery following the intramuscular and intravenous delivery of LD-BMC after I/R injury. The researchers anticipate that the proposed studies will provide information to complete large animal studies using suitable FDA-approved devices.

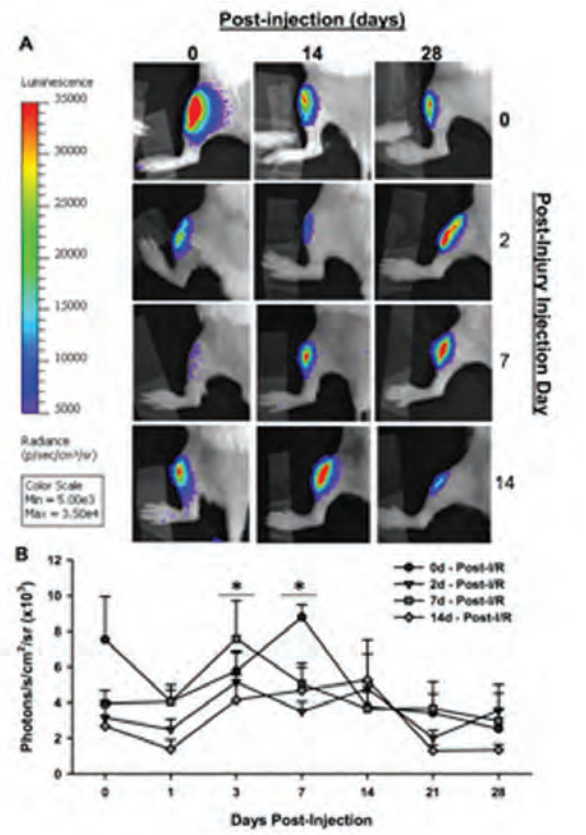

Figure 2. Representative images (A) and quantification (B) of bioluminescent imaging following intramuscular injection of cells 0, 2, 7, or 14 days after injury. Bioluminescent imaging was performed 0, 1, 3, 7, 14, 21, and 28 days after cell injection to estimate cell survival. * indicates significantly different from days 1, 21, and 28. Values are (average +/- SEM).

Biological Scaffold-Based Treatment of CS

Biodegradable Elastomeric Scaffolds Microintegrated with Muscle-Derived Stem Cells for Fascial Reconstruction Following Fasciotomy

Project 4.3.3, WFPC

Team Leader(s): William R. Wagner, PhD (McGowan Institute for Regenerative Medicine)

Project Team Member(s): Keisuke Takanari MD, PhD, Ryotaro Hashizume, MD, PhD, Yi Hong, PhD, Nicholas J. Amoroso, BSE, Tomo Yoshizumi, MD, Hongbin Jian, MD, Antonio D'Amore, PhD, and Christopher L. Dearth, PhD (University of Pittsburgh)

Collaborator(s): Stephen F. Badylak, DVM, MD, PhD and Johnny Huard, PhD (University of Pittsburgh)

Therapy: Treatment of abdominal compartment syndrome; development of fascial repair technology

Deliverable(s): Biodegradable elastomeric scaffolds for fascial reconstruction

TRL Progress: 2008, TRL 1; 2009, TRL 1; 2010, TRLs 2–3; 2011, TRL 3; 2012 (Current), TRL 3

Key Accomplishments: The researchers completed the in vivo evaluation of "sandwich" biohybrid scaffolds composed of dermal extracellular matrix (dECM) and poly(ester urethane)urea (PEUU). Applying a new "sandwich" fabrication technique provided mechanical properties that mimicked native abdominal muscle tissue and resulted in a higher deposition of collagen and a better remodeling response compared to the control biohybrid construct. In addition, the researchers began an assessment of a tissue construct composed of GFP transgenic MDSC and PEUU using a microintegration technique. They confirmed the presence of GFP-positive cells at both 4 and 8 weeks after implantation. MDSC integration into an elastic scaffold facilitated improved microvascular regeneration relative to controls in this animal model of abdominal wall repair. Biaxial mechanical properties of explanted tissue constructs were similar to native tissue.

Key Words: Abdominal compartment syndrome, biodegradable elastomer, extracellular matrix, muscle-derived stem cells, mechanical property

Introduction

A severe abdominal injury often requires decompressive laparotomy to avoid pathological levels of intraabdominal pressure and subsequent abdominal compartment syndrome. The large abdominal wall defect created due to these lifesaving laparotomies remains a challenging problem for surgeons. Common techniques used to reconstruct full-thickness abdominal wall defects utilize synthetic meshes. The disadvantages for using prosthetic materials are the risks of intestinal fistula formation, prosthetic infection, adhesions, and recurrent hernias, which are related to the foreign body response and mechanical property mismatch.

A biohybrid composite material that offers both strength and bioactivity for optimal healing toward native tissue behavior may overcome these disadvantages and would be applicable in a variety of fascial tissue repair and replacement procedures. dECM gel possesses attractive biocompatibility and bioactivity with weak mechanical properties and rapid degradation while conventionally electrospun biodegradable, elastomeric PEUU has strong mechanical properties with limited cellular infiltration and tissue integration. The Wagner group hypothesized that these two different materials could be combined in a manner that would possess both advantages.

During the first 3 years of this project, the researchers created three different designs of a novel biohybrid scaffold composed of dECM and PEUU. They implanted these constructs in a rat full-thickness abdominal wall defect model and assessed their biocompatibility and mechanical properties. They found that separation of the processing streams of dECM and PEUU resulted in better scaffold bioactivity although mechanical properties in vivo were compromised. However, development of a "sandwich" fabrication technique overcame this drawback and achieved excellent mechanical properties that mimicked native abdominal muscle tissue. The regeneration of muscle was observed by Masson's trichrome staining in a sandwich sample at the 8-week time point, which was confirmed by immunostaining for alpha-sarcomeric actin. The researchers also created a tissue construct by combining GFP transgenic MDSC and PEUU using a microintegration technique. In a pilot experiment, 14 days after implantation, GFP-positive cells were seen in abundance within the scaffold.

Research Progress – Year 4

PEUU and dECM Processed by "Sandwich" Technique

The outer layers of the scaffold sandwich were generated by electrospraying saline concurrently with PEUU electrospinning at the beginning and end of the processing period. For the middle PEUU fiber/dECM gel hybrid layer, porcine dECM gel solution was electrosprayed instead of spraying saline as was done for the outer layers. While saline was being electrosprayed, PEUU was concurrently electrospun for this middle layer (**Figure 1**). Control scaffolds were created using the same fabrication technique, except lacking the outer supportive layers

Assessments were performed using a rat full-thickness abdominal wall defect model. A lateral wall defect (1 x 2.5 cm) was repaired with the sandwich or control scaffolds. Histological assessments showed both scaffold types to have good cellular infiltration at both time points; however, the control group became thinner at the later time point (**Figure 2**).

Collagen assays showed a marked increase in total collagen content for both patch types from the time of implant to 4 and 8 weeks ($p<0.01$, **Figure 3**). The amount of collagen was higher in the sandwich versus control scaffold for both

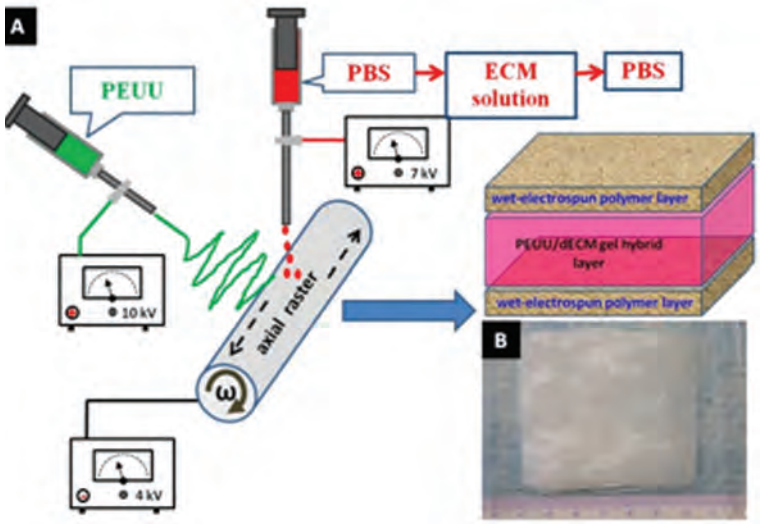

Figure 1. Schematic of the sandwich fabrication technique. The green stream represents polymer (PEUU) electrospinning and the red stream is electrosprayed with saline, followed by ECM gel, and then saline. The saline spraying results in formation of the denser upper and lower layers of the sandwich scaffold.

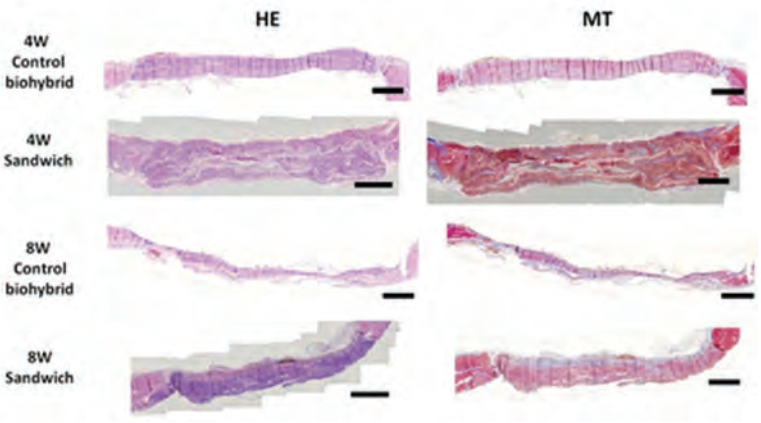

Figure 2. Representative cross-sections of implanted dECM/PEUU (control) and dECM/PEUU (sandwich process) staining with H&E, and Masson's trichrome (Scale bar = 1 mm).

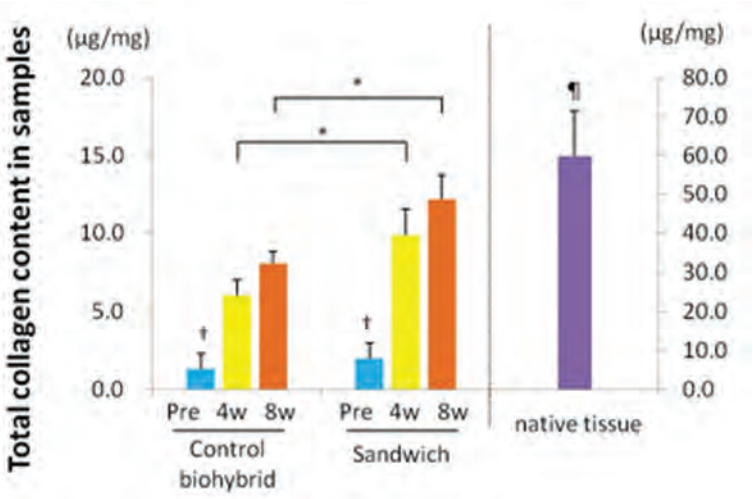

Figure 3. Collagen content in samples. *p< 0.05. † p< 0.01 compared to 4- and 8-week samples. ¶ p<0.05 compared to 4- and 8-week samples in experimental groups and p<0.01 compared to preimplant samples.

time points (p<0.05). Assessment of scaffold site remodeling with immunostaining for macrophage phenotype showed that the ratio of CD163 (M2 macrophages) to CCR7 (M1 macrophages) increased in the sandwich group from 4 to 8 weeks and at 8 weeks was greater than that observed in control biohybrid. (**Figure 4**).

MDSC Integrated Wet Electrospun PEUU

The Wagner group is currently investigating concurrent electrospinning/electrospraying to microintegrate GFP transgenic MDSC into the scaffolds. Allogenic transplantation was performed with this MDSC-integrated material (**Figure 5**). Control scaffolds were created utilizing the same method without cells. After 4 and 8 weeks, GFP-positive cells were seen in the scaffold (5.9% and 5.1% of cells, respectively). Representative cross-sections showed high cell infiltration in both groups (**Figure 6A**) and the thickness of the abdominal wall markedly increased in both scaffolds (Figure 6B), whereas the cell integrated scaffold had higher vascularity at both time points compared to the control scaffold (Figure 6C).

Conclusions

The sandwich scaffold approach overcomes previous limitations encountered with biohybrid elastomeric scaffolds, maintaining wall thickness and exhibiting higher levels of collagen production with structural and mechanical properties similar to native tissue. This technique is ready to progress to the porcine model. The results with the MDSC microintegrated scaffolds are progressing well, with further analysis ongoing. Cell survival at 8 weeks has been demonstrated along with improved vascularity.

Research Plans for Year 5

In the coming year, the Wagner group will finish its study of MDSC microintegrated scaffolds in the rat

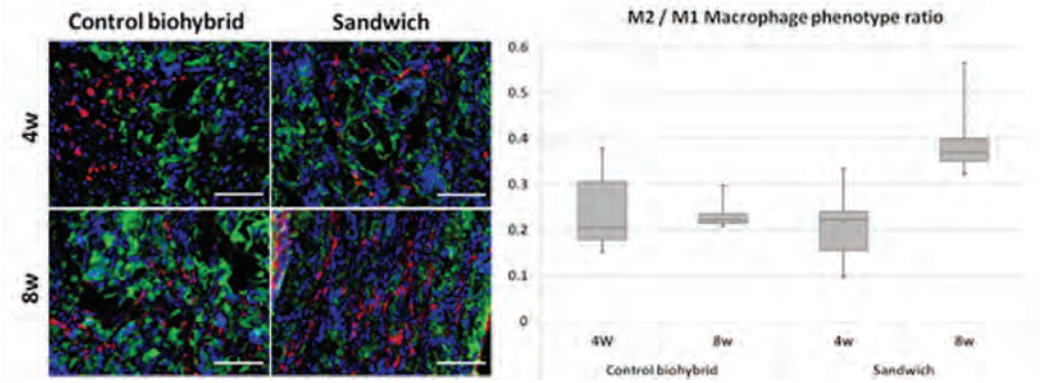

Figure 4. Immunostaining against CD163 (M2 macrophages, red) and CCR7 (M1 macrophages, green). Nuclei are stained with Hoechst (blue). Scale bar = 200 µm. Graph on right shows the ratio of M2 vs M1 macrophages.

model and potentially combine this approach with the dECM sandwich scaffold approach. Porcine trials will begin now that final animal approvals have been obtained. The developed materials will be considered for other applications. Potential applications include skin, craniofacial, and soft tissue reconstruction. When the large animal model is completed, it is anticipated that this technology may potentially be evaluated in concert with other approaches developed in the AFIRM projects.

Planned Clinical Transitions

Clinical transitions for this project are beyond the time frame of the currently funded AFIRM program. Initiation of clinical trials is not anticipated until Year 8.

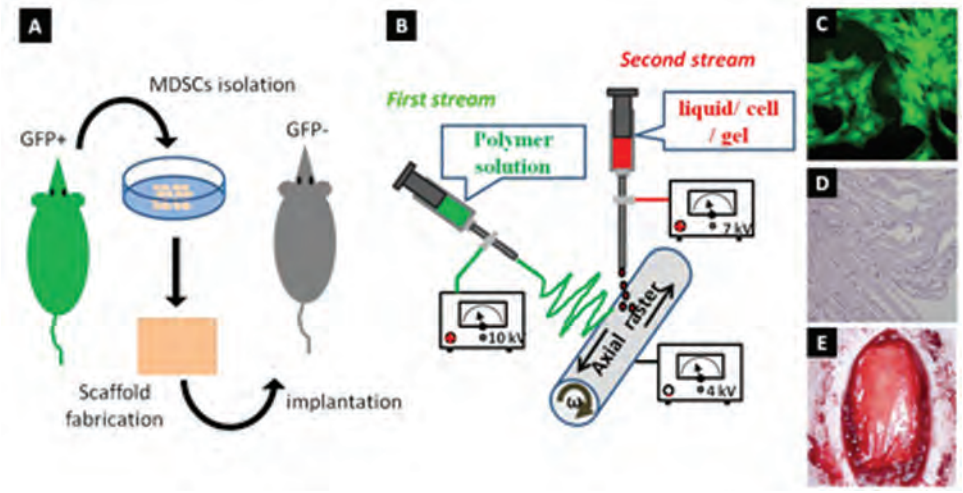

Figure 5. A. Schematic of the study design. GFP-positive MDSC were harvested, seeded in the scaffold, and implanted into an allogenic rat of the same strain. B. Scaffold fabrication method C. MDSC after 1-day culture. D. H&E staining image of the MDSC microintegrated scaffold. E. Macroscopic image of the scaffold just after implantation.

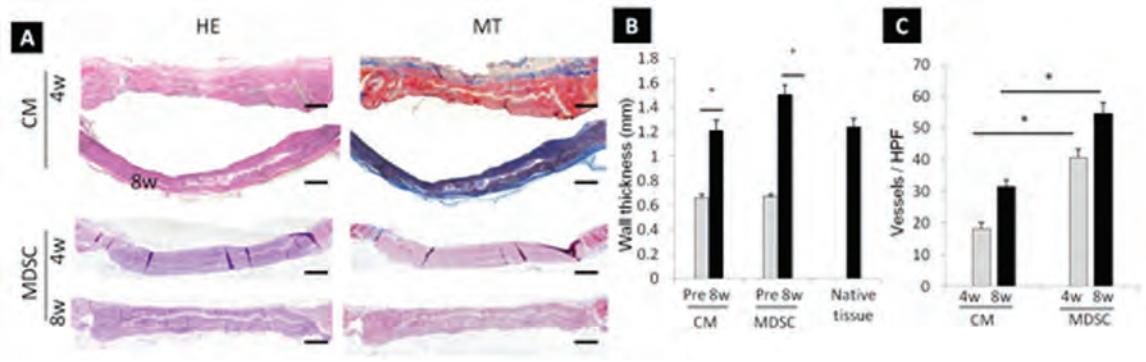

Figure 6. A. Representative cross-sections of implanted cell-integrated scaffolds at 4 and 8 weeks after implantation. Scale bar = 1 mm. B. Wall thickness of preimplant sample, 8 weeks after implantation, and native tissue. Both scaffolds showed increased thickness after 8 weeks implantation that was equivalent to the native tissue. C. Vessel number in the explanted scaffold expressed as number per high power field. MDSC integrated scaffolds had significantly greater vessel numbers compared to scaffolds utilizing culture medium alone. *$p<0.05$

Biological Scaffold-Based Treatment of CS

Use of Autologous Inductive Biologic Scaffold Materials for Treatment of Compartment Syndrome

Project 4.3.4, WFPC

Team Leader(s): Stephen F. Badylak, DVM, PhD, MD (McGowan Institute for Regenerative Medicine)

Project Team Member(s): Christopher L. Dearth, PhD, Scott Johnson, MS (McGowan Institute for Regenerative Medicine); and Matthew T. Wolf, BS (Department of Bioengineering, University of Pittsburgh)

Collaborator(s): Johnny Huard, PhD (McGowan Institute for Regenerative Medicine) and Kenton Gregory, MD (Oregon Medical Laser Center, Oregon Center for Regenerative Medicine)

Therapy: Treatment for peripheral compartment syndrome (PCS)

Deliverable(s): Reconstruction of functional compartmental tissue in animal models utilizing the inductive properties of biologic scaffolds and stem cells

TRL Progress: 2008, TRL 1; 2009, TRL 2; 2010, TRL 3; 2011, TRL 5; 2012 (Current), TRL 5

Key Accomplishments: The researchers induced PCS in rabbits and evaluated the host regenerative response after 3 and 6 months of treatment with in situ autologous compartment ECM used in conjunction with bone marrow-derived mononuclear cells. They found that the autologous compartment ECM elicited improved remodeling outcomes compared to controls. The researchers also demonstrated survival of Qdot-labeled cells 1 and 3 months post injection. They also successfully optimized methods for inducing PCS in a porcine model.

Key Words: Peripheral compartment syndrome, extracellular matrix, bone marrow derived mononuclear cells

Introduction

PCS represents a serious complication of traumatic extremity injury; especially the type of trauma sustained by soldiers in combat. Severe swelling within a confined space (compartment) is associated with increased intracompartmental pressure, which severely compromises blood flow, leading to ischemia and necrosis of all tissues within the compartment (e.g., muscle, nerves, and associated structures). The loss of functional tissue is frequently severe enough to require amputation of the affected limb. The standard of care for peripheral CS is fasciotomy with an attempt to salvage the viability of as much functional tissue as possible, though morbidity of this approach is high.

The Badylak group is investigating a method for using the inductive properties of ECM as a scaffold for constructive remodeling into functional tissue. Previous work has shown that manufactured forms of ECM (e.g., porcine small intestinal submucosa, porcine urinary bladder, porcine and bovine dermis, and pericardium) have the potential to promote constructive remodeling of damaged or missing body parts in place of inflammation and scarring. The present work extends this concept by investigating methods of deriving autologous compartment ECM from in situ decellularization of the necrotic tissue (with the presence of stem cells). Stated differently, the ECM within the compartment would be isolated from its original cell population (which has now become necrotic), and this matrix would then be used as a template for tissue reconstruction.

During the first 3 years of this project, the researchers established a reproducible model of PCS in two species (rabbit and canine). This PCS induction model has now become the basis for the current preclinical animal studies. Previous work also included optimization of compartment tissue decellularization and characterization of its

properties considered to be important for biocompatibility in vitro. In addition, the researchers initiated preclinical studies of the suitability of currently available biologic scaffolds and stem cells for treatment in their animal models.

Research Progress – Year 4

Reconstruction of Functional Compartmental Tissue in Animal Models Utilizing the Inductive Properties of Biologic Scaffolds and BM-MNC

Previously, decellularization of compartment ECM was optimized using saline, 0.1% peracetic acid (PAA), and 2% deoxycholate (DOC). The DOC treatments optimally resulted in a reduction in DNA and cellular protein but retention of growth factors. The methods for creation of autologous compartment ECM were used for treatment of PCS in a previously validated rabbit model. In addition, autologous BM-MNC were delivered to the affected compartment after decellularization of the compartment and isolation in situ of autologous ECM. This approach overcomes many of the current concerns (e.g., both the cells and ECM are autologous), thus avoiding concerns about xenogeneic sources.

PCS induction and autologous ECM treatment were completed within the past year (**Figure 1a**). CS pressures above 150 mmHg were maintained for all treatment groups, which was greater than the initial pressure prior to induction (Figure 1b). There were also no significant differences in the induction procedure between groups.

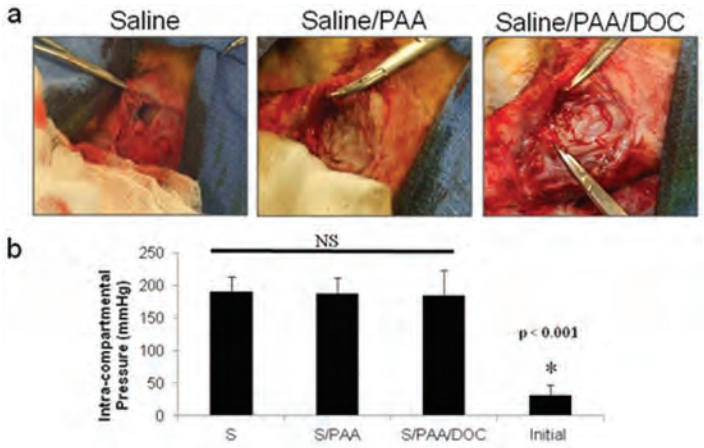

Figure 1. (A) Macroscopic images showing the creation of autologous compartment ECM by flushing of the compartment with saline, 0.1% PAA, and 2% DOC. (B) Intracompartmental pressure measurements for each of the methods showing that all were inductions were similar and significantly higher than prior to infusion.

At 3 months post treatment, fibrous tissue and new muscle cells were found in the defect area in groups treated with saline/PAA and saline/PAA/DOC while only dense fibrous tissue was present in the saline control group (**Figure 2a**). There were greater amounts of myogenesis and less dense fibrous tissue in the saline/PAA/DOC group than in the saline/PAA. Therefore, only the saline control and saline/PAA/DOC groups were continued for the 6-month time point. After 6 months, there was adipose tissue and some connective tissue in both groups. However, there were more numerous and larger islands of skeletal muscle present in the saline/PAA/DOC group.

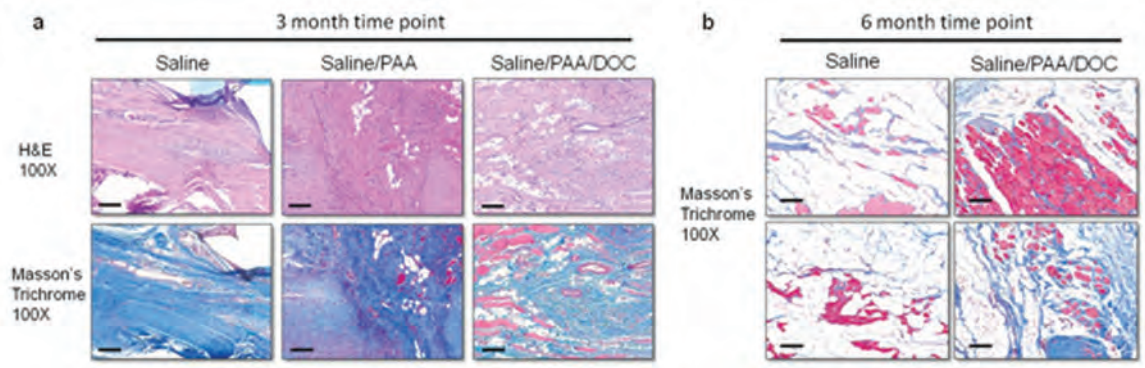

Figure 2. (A) After 3 months, the saline-only control showed only fibrous tissue while the saline/PAA and saline/PAA/DOC groups showed early evidence of myogenesis. (B) After 6 months, there was adipose tissue, fibrous tissue, and muscle tissue found in the defect saline/PAA/DOC groups but less myogenesis in the saline control.

To determine if the potential role of the autologous BM-MNC in the myogenesis seen in the saline/PAA/DOC group, BM-MNC were labeled with Qdots (Qtracker-655, Invitrogen). One month following their implantation in saline/PAA/DOC-treated animals, numerous Qdot-labeled cells were found within the remodeling tissue (**Figure 3a**, arrows). There were few cells labeled after 3 months, but they were present in remodeling tissue and around muscle fiber bundles (Figure 3b, arrows). The survival and integration of Qdot-labeled BM-MNC are currently being assessed for the 6-month time point.

Optimization of PCS Induction in a Porcine Model

PCS induction methods were translated and optimized for use in a porcine model. Cadaveric pigs were exposed to PCS conditions by exposing the anterior tibial compartment, inserting a saline infusion needle, inserting a pressure measurement needle, and tying a tourniquet around the proximal portion of the leg (**Figure 4a**). Pressure was initiated by injecting a saline bolus, which was maintained on a pressure bag drip. Elevated intracompartment pressures exceeding 300 mmHg were maintained for an extended period of time.

Conclusions

The primary accomplishments of this project to date include: (1) Completion of surgical induction and treatment of PCS using autologous compartment ECM, (2) analysis of the long-term outcome (3 and 6 months) after PCS treatment in a rabbit model using autologous compartment ECM derived in situ and autologous BM-MNC, and (3) optimization of methods to induce CS in a porcine model.

Research Plans for Year 5

In the upcoming year, the researchers will complete the final evaluation of the final 6-month time point in the rabbit (samples are due to be collected within the next 4 months). Samples will be assessed by histomorphometric staining and quantification and immunolabeling for indicators of myogenesis, innervation, and vascularization in the remodeling tissues. Qdot technology has been used to show that injected BM-MNC with autologous ECM do indeed remain and potentially participate in the constructive remodeling response.

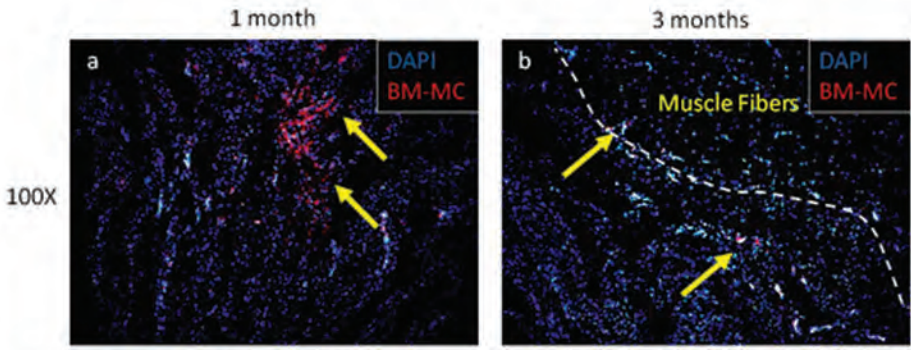

Figure 3. Saline/PAA/DOC-treated compartment tissue following injection with Qdot-labeled BM-MNC (red) after (A) – 1 month, where numerous labeled cells are present in the remodeling tissue, and (B) –3 months post treatment where there are fewer cells. Sections were counterstained with DAPI (blue).

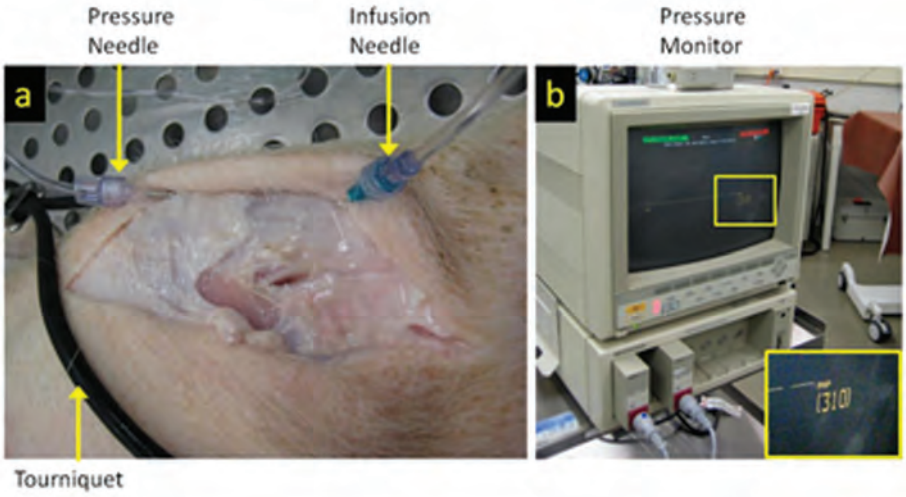

Figure 4. (A) Optimization of PCS induction in a cadaveric pig. A tourniquet was tied around the leg and a saline infusion needle and pressure monitor needle inserted into the compartment. (B) Pressure was maintained above 300 mmHg (inset) for extended periods of time using this configuration.

The fate of Qdot-labeled cells will be determined via immunofluorescent colocalization with skeletal muscle, vasculature, and putative stem cell markers. Concurrent with the final analysis of the rabbit study, PCS will be induced in the porcine model and treated with the saline/PAA/DOC method with autologous BM-MNC and compared to a saline control. The study will utilize the surgical and logistical methods optimized in Year 4.

Planned Clinical Transitions

Pending similar positive results in the large animal (porcine) preclinical studies, a human clinical trial is currently in the planning stage. It is likely that the therapeutic trial will involve the optimal methods derived from the Gregory, Huard, and Guldberg teams' projects.

Biological Scaffold-Based Treatment of CS

Material-Induced Host Cell Recruitment for Muscle Regeneration

Project 4.3.5, WFPC

Team Leader(s): Sang Jin Lee, PhD (Wake Forest)

Project Team Member(s): James J. Yoo, MD, PhD, In Kap Ko, PhD, Young Min Ju, PhD, and NaJung Kim, PhD, (Wake Forest)

Collaborator(s): Shay Soker, PhD (Wake Forest)

Therapy: Treatment of muscle injuries through in situ muscle tissue regeneration

Deliverable(s): Demonstration of in situ muscle tissue regeneration using a target-specific scaffolding system

TRL Progress: 2008, TRL 2; 2009, TRL 2; 2010, TRL 3; 2011, TRL 3; 2012 (Current), TRL 3; 2013 (Target), TRL 4

Key Accomplishments: During the past year, the research team developed novel injectable and implantable scaffolding systems using heparin-conjugated gelatin microparticles and heparin-conjugated decellularized muscle matrix, respectively. The scaffolding systems effectively released myogenic-inducing factors, which promoted myogenic cell migration and regenerated newly formed muscle tissue in vivo. Combination delivery with heparin-conjugated decellularized muscle matrices enhanced the recruitment of satellite cells and pericytes into the muscle-targeting scaffold and also facilitated more well-aligned newly formed myofibers into the interface and interior of the implants than uncrosslinked scaffolds and controls lacking a delivery system.

Key Words: Biomaterials, myogenic-inducing factor, in situ tissue regeneration, host stem cell mobilization, volumetric muscle loss, compartment syndrome, muscle regeneration

Introduction

CS is a common traumatic injury that results in muscle, nerve, and vessel damage due to increased pressure within a confined space in the body. Although CS can affect any limb or muscle compartment, including the abdomen, it frequently occurs after trauma to the lower leg such as fracture. The standard treatment is fasciotomy, which is considered as the definitive and only treatment for acute CS. Although this procedure is able to relieve immediate concerns, muscle weakness and atrophy are continued sequelae. Various management approaches have been introduced that include physical therapy, muscle transplantation, and myoblast cell therapy. However, none has entirely addressed the problems associated with the long-term consequences of CS in wounded soldiers.

In this project, the research team aims to investigate in an animal model the ability to initiate cell mobilization, recruitment, and differentiation of stem or progenitor cells residing in the host to regenerate muscle tissue through the use of a target-specific scaffolding system. This approach is based on the demonstration that almost every tissue in the body contains some type of stem or progenitor cells.

During the first 2 years of the project, the researchers introduced a variety of myogenic-inducing factors into scaffolds and tested their ability to promote host muscle satellite/progenitor cell mobilization, including migration, proliferation, and differentiation. They found that cell proliferation was significantly increased by the addition of insulin-like growth factor 1 (IGF-1), IGF-2, or basic fibroblast growth factor (bFGF), compared to controls. They also found that the these myogenic factors, along with hepatocyte growth factor, significantly increased cell migration in a Boyden chamber plate assembly when compared to controls. In Year 3, the Lee group demonstrated that PAX7-expressing cells can be mobilized into an implanted biomaterial

and that these cells are capable of differentiating into muscle cells. They also demonstrated that a novel combined system of systemic injection of substance P and local release of stromal-derived factor-1α can be a powerful tool for efficient tissue regeneration in situ.

Research Progress – Year 4

Effort during the past year focused on evaluating various myogenic-inducing factors for muscle cell migration, proliferation, and differentiation in vitro and investigating the possibility of using an appropriate biomaterial to initiate cell mobilization and recruitment in vivo.

Development of an injectable device using heparin-conjugated gelatin microparticles: To immobilize myogenic factors in gelatin microparticles, the researchers first conjugated heparin onto the 60–100 µm gelatin microparticles. Heparin, a sulfated polysaccharide, has been widely used as a surface modifier to enhance the stability of biologically important proteins such as growth factors and cytokines via binding affinity. Heparin conjugation onto the gelatin microparticles was confirmed by toluidine blue staining (**Figure 1A**).

To determine the protein release kinetics, the researchers used lysozyme as a model protein. Lysozyme was loaded onto both heparin-conjugated and unmodified gelatin microparticles using a solution dropping method. Sixty microliters of PBS containing 120 µg of lysozyme was added to the dried gelatin microparticles and the samples were allowed to react at 4°C for 12 hours to allow protein loading. The protein-immobilized gelatin microparticles were then suspended in 1 mL PBS (containing 0.1% bovine serum albumin) at 37°C. At various time points, the supernatants were collected and the amount of released lysozyme was determined by direct absorbance using a spectrophotometer (405 nm) (Figure 1B).

To evaluate the effects of myogenic factors, the researchers developed heparin-conjugated gelatin microparticles that immobilized IGF-I via electrostatic interactions. For the in vivo study, they created a traumatic defect by excising approximately 30%–40% of the TA muscle of Sprague-Dawley (SD) male rats (age: 10–12 weeks). The IGF-1-immobilized biomaterial system was implanted in the TA muscle defect injury of rats and retrieved at 1, 2, and 4 weeks after implantation (Figure 1C). The retrieved tissue samples were characterized by histological and immunohistochemical staining.

IGF-1 released from gelatin microparticles effectively promoted myogenic cell migration and regenerated newly formed muscle tissue in vivo (**Figure 2**). By the first and fourth weeks, host

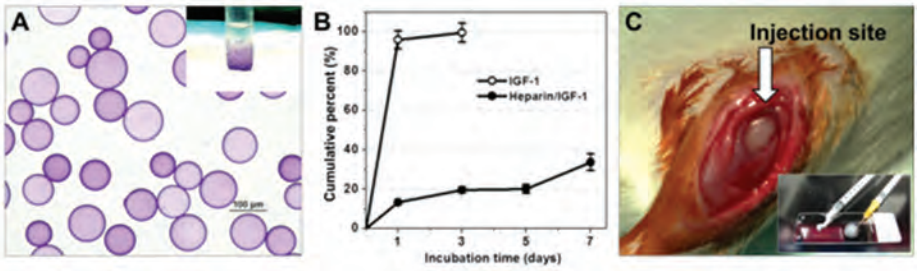

Figure 1. (A) Heparin-conjugated gelatin microparticles as confirmed by toluidine blue staining. (B) Release profiles of IGF-1 from heparin-conjugated gelatin microparticles. (C) IGF-1-immobilized gelatin microparticles were injected in the TA muscle defect injury of rats.

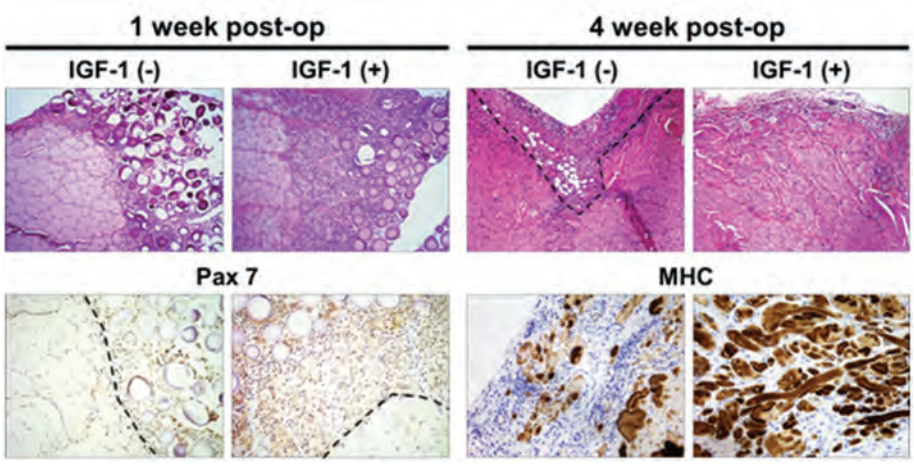

Figure 2. Histological (H&E) and immunohistochemical (Pax 7, MHC) evaluations of the injected gelatin microparticles at 1 and 4 weeks post operation (X100).

cells had accumulated within the injury region and abundant host vasculature was found within the region. H&E and immunostaining for myosin heavy chain (MHC) of representative sections after 4 weeks of injection showed the gradual build-up of a neo-muscle fiber bundle structure around the IGF-1-loaded gelatin microparticles (Figure 2).

Development of an implantable device using heparin-conjugated decellularized muscle matrix: Muscle scaffolds were fabricated by decellularization of the TA muscle of SD rats using Triton X-100 and ammonium hydroxide (**Figure 3A, B**). For efficient delivery of SDF-1α and IGF-1, heparin molecules were conjugated on the decellularized muscle scaffold using 1-ethyl-3-(3-dimethylaminopropyl)carbodiimide/N-hydroxysuccinimide (EDC/NHS) chemistry (Figure 3C).

For the in vivo study, a traumatic defect was created by excising approximately 30%–40% of TA muscle of SD male rats (age: 10–12 weeks). Combination delivery with heparin-conjugated decellularized muscle matrices were implanted in the TA muscle defect injury of rats and retrieved at 1, 2, and 4 weeks after implantation.

Their results show that the combination delivery system enhanced the recruitment of satellite cells and pericytes into the muscle-targeting scaffold and also facilitated more well-aligned newly formed myofibers into the interface and interior of the implants than uncross-linked scaffolds and controls lacking a delivery system. Furthermore, morphological integration of newly formed myofibers with host muscle was confirmed (**Figure 4**). The incorporation of multiple regulatory signals into a scaffolding system and the researchers' combined delivery may be a promising approach for more efficient and effective muscle regeneration in situ.

Conclusions

The research team developed novel injectable and implantable devices that can mobilize host muscle cells and form neo-muscle tissues in a muscle defect region in rats. They demonstrated that cells expressing muscle satellite/progenitor cell markers can be mobilized into an implanted biomaterial and that these cells are capable of differentiating into muscle cells. Therefore, it may be possible to enrich the infiltrate with specific cell types and control their fate, provided the proper substrate-mediated signaling can be imparted into

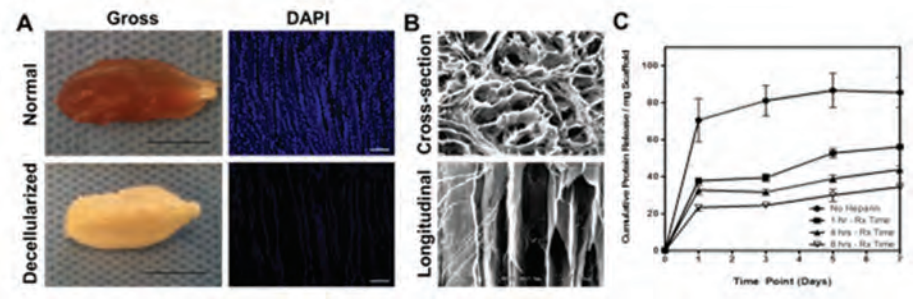

Figure 3. (A) Complete decellularization of the TA muscle, confirmed by DAPI staining while (B) maintaining of structural integrity of the TA muscle. (C) Release profiles of protein released from heparin-conjugated decellularized muscle matrices.

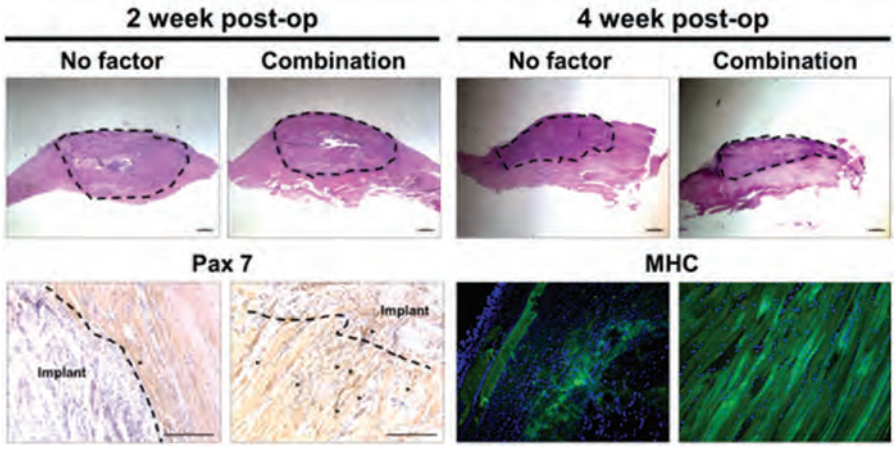

Figure 4. H&E staining of the harvested TA muscle tissue. The implants are identified by circled areas in the low magnified images. Immunohistochemical staining for Pax 7 for host stem cells infiltrated into the implants at 2 weeks. Immunofluorescent staining for MHC to identify mature muscle fibers adjacent to the implants. The combination delivery system induced efficient integration of newly formed myofibers in the interior sites with the host muscle tissue.

the scaffold. Thus, in situ regeneration of functional muscle tissue through host cell recruitment may be possible.

Research Plans for Year 5

The research team plans to continue long-term in vivo evaluation of the myogenic-inducing factor incorporated biomaterials and the development of a smart scaffolding system for application. In vivo studies investigating in situ muscle tissue regeneration in a CS rat model are also planned for Year 5.

Planned Clinical Transitions

This basic research project is not slated for clinical trials during the first 5 years of the award.

Acronym List

2D ..... two-dimensional
3D ..... three-dimensional
α-SMA ..... alpha-smooth muscle actin
ABP ..... allograft bone particles
ACB ..... autogenous cancellous bone
ACBG ..... autogenous cancellous bone graft
ACURO ..... Animal Care and Use Review Office
AE ..... adverse event
AFIRM ..... Armed Forces Institute of Regenerative Medicine
AFS ..... amniotic fluid-derived stem
AFT ..... autologous fat transfer
AFT-SPAR ..... autologous fat transfer for scar prevention and remodeling
ALP ..... alkaline phosphatase
ANOVA ..... analysis of variance
ARRI ..... Automation & Robotics Research Institute
ASC ..... adipose-derived stem cells
ASTM ... American Society for Testing and Materials
ATRA ..... all-trans retinoic acid
AWP ..... autologous wound paste
BAM ..... bladder acellular matrix
BCP ..... biphasic calcium phosphate
bFGF ..... basic fibroblast growth factor
BIODOME ..... biomechanical interface for optimized delivery of MEMS orchestrated mammalian epimorphosis
BMA ..... bone marrow aspirate
BMC ..... bone marrow-derived cells
BM-MSC ..... bone marrow-derived mesenchymal stem cells
BMP-2 ..... bone morphogenetic protein 2
BMSC ..... bone marrow stromal cells
BOD ..... Board of Directors
BTCMP ..... β-tricalcium phosphate
BUN ..... blood urea nitrogen
CAD ..... computer-aided design
CaP ..... calcium phosphate
CBER ..... Center for Biologics Evaluation and Research
CC ..... Cleveland Clinic
CCTD ..... chronic caprine tibial defect
CCT-eta ..... chaperonin-containing T-complex polypeptide
CDRH ..... Center for Devices and Radiological Health
CFMD ..... canine femoral multidefect
CFR ..... craniofacial reconstruction
cGMP ..... current Good Manufacturing Practice
chABC ..... chondroitinase ABC
CHO-K ..... Chinese hamster ovary-K
CMAP ..... compound muscle action potential
CMF ..... cranio-mandibulo-maxillofacial
CMU ..... Carnegie Mellon University
CRMRP ..... Clinical and Rehabilitative Medicine Research Program
CS ..... compartment syndrome
CSD ..... critical-size defect
CSS ..... cell stablilization solution
CTA ..... composite tissue allograft
CTP ..... connective tissue progenitor
CTP-O ..... connective tissue progenitor cells
DE 1 ..... dose escalation cohort
dECM ..... dermal extracellular matrix
DFO ..... desferrioxamine
DIC ..... digital imaging correlation
DMC ..... Data Monitoring Committee
DMEM ..... Dulbecco's modified eagle medium
DOC ..... deoxycholate
DoD ..... Department of Defense
DS ..... density separation
dsASC ..... discarded burn skin ASC

Appendix

DSC ..... differential scanning calorimetry

DTD DD ..... desaminotyrosyl-tyrosine dodecyl dodecanedioate

DTE .....N-dithiocarbonyl ethoxycarbonyl

E12..... embryonic day 12

E15..... embryonic day 15

EC.....endothelial cell

ECD .....external compression device

ECM..... extracellular matrix

EDC/NHS ..... 1-ethyl-3-(3-dimethylaminopropyl) carbodiimide/N-hydroxy-succinimide

EDXA..... energy dispersive x-ray analysis

ELISA .....enzyme-linked immunosorbent assay

EMB..... explantable microvascular beds

EMG .....electromyography

EO ..... ethylene oxide

ePTFE .....expanded polytertafluoroethylene

ERK .....extracellular signal-regulated kinase

ES.....electrospun

ESS .....engineered skin substitutes

ESS-P.....engineered skin substitutes with pigment

FAK.....focal adhesion kinase

FDA .....U.S. Food and Drug Administration

FGF .....fibroblast growth factor

FGF9 .....fibroblast growth factor 9

FLIR.....forward looking infrared

G+.....gram-positive

G- ..... gram-negative

GAG..... glycosaminoglycan

GAPDH..... glyceraldehyde 3-phosphate dehydrogenase

GDNF .....glial cell-line derived neurotrophic factor

GFP .....green fluorescent protein

GLP ..... Good Laboratory Practice

GMP .....Good Manufacturing Practice

H..... human

H&E .....hematoxylin and eosin

HA ..... hyaluronic acid

hASC .....human adipose-derived stem cells

HDMEC ..... human dermal microvascular endothelial cells

HGF .....hepatic growth factor

HLA ..... human leukocyte antigen

hNSC..... human neural stem cell

hpf..... high power field

HRPO ..... Human Research Protection Office

HTR .....hard tissue replacement

hVEGF ....human vascular endothelial growth factor

IACUC ..... Institutional Animal Care and Use Committee

IDE ..... Investigational Device Exemption

IED.....improvised explosive device

IGF .....insulin-like growth factor

IGF-1.....insulin-like growth factor 1

IND ..... Investigational New Drug

iPSC .....induced pluripotent stem cells

IPT ..... Integrated Project Team

I/R.....ischemia-reperfusion

IR..... infrared

IRB .....Institutional Review Board

ISO ..... International Organization for Standardization

IV .....intravenous

KC.....keratinocyte

KO .....knockout

LD.....latissimus dorsi

LD-BMSC .....lineage-depleted bone marrow-derived stem cells

LWI .....Lonza Walkersville, Inc.

M..... million

MACS ..... magnetic activated cell sorting

M/C .....mucocutaneous

MCA..... mineralized cancellous allograft

MC .....Mayo Clinic

MCC .....multipotent cell cluster

MCP1.....monocyte chemoattractant protein-1

MDSC ..... muscle-derived stem cells
MFI ..... mean fluorescence intensity
MGH ..... Massachusetts General Hospital
MHC ..... myosin heavy chain
microCT ..... microcomputed tomography
MIRM ..... McGowan Institute for Regenerative Medicine
MIT ..... Massachusetts Institute of Technology
MPC ..... muscle progenitor cells
MRI ..... magnetic resonance imaging
MS ..... magnetic separation
MSC ..... mesenchymal stem cells
MSD ..... molecular surface design
NGF ..... nerve growth factor
NHP ..... nonhuman primate
NIH ..... National Institutes of Health
NMJ ..... neuromuscular junction
NSAIDs ..... nonsteroidal anti-inflammatory drugs
OHSU ..... Oregon Health and Sciences University
OPF ..... oligo(poly(ethylene glycol) fumarate)
OSMEA ..... organic, stretchable microelectrode array
PA ..... peptide amphiphile
PAA ..... peracetic acid
PBS ..... phosphate-buffered saline
PCL ..... poly(ε)-caprolactone
PCLF ..... polycaprolactone fumarate
PCNA ..... proliferating cell nuclear antigen
PCR ..... polymerase chain reaction
PCS ..... peripheral compartment syndrome
PDGF ..... platelet-derived growth factor
PDGF-BB ..... platelet-derived growth factor-BB
PDGF-β ..... platelet-derived growth factor-beta
PDO ..... polydioxanone
PEG ..... polyethylene glycol
PEUU ..... poly(ester urethane)urea
PGE2 ..... prostaglandin E2
PLA ..... polylactic acid
PLGA ..... poly(lactic-co-glycolic acid)
PLLA/PLCL ..... poly(L-lactide)/poly(ε-caprolactone)
PMMA ..... poly(methyl methacrylate)
PMO ..... Project Management Office
POG ..... particulate oxygen generator
PPF ..... poly(propylene fumarate)
PTD-A ..... potentially therapeutic dose-A
PUR ..... polyurethane
PVA ..... polyvinyl alcohol
PY ..... program year
QSR ..... Quality System Regulation
RBC ..... red blood cells
RCCC ..... Rutgers–Cleveland Clinic Consortium
RGD ..... arginine-glycine-aspartic acid
rhBMP-2 ..... recombinant human bone morphogenetic protein-2
ROS ..... reactive oxygen species
SAE ..... serious adverse event
SBM ..... synthetic bone mineral
SC ..... spinal cord
SCID ..... severe combined immunodeficient
SD ..... Sprague-Dawley
SDF-1α ..... stromal cell-derived factor-1α
SEM ..... scanning electron microarray
siRNA ..... small interfering RNA
SOP ..... standard operating procedure
SR ..... selective retention
SSD ..... silver sulfadiazine
STMG ..... split-thickness meshed grafts
STSG ..... split-thickness skin graft
SVF ..... stromal vascular fraction
TA ..... tibialis anterior
TBSA ..... total body surface area
TCR ..... T-cell receptor
TCP ..... tri-calcium phosphate
TEMR ..... tissue-engineered muscle repair
TENG ..... tissue-engineered nerve grafts
TGF ..... transforming growth factor

Appendix

TGF-β ..... transforming growth factor-beta
TLI ..... therapy to limit injury
TNF-α .....tumor necrosis factor-alpha
TRL.....Technology Readiness Level
TUNEL.....terminal deoxynucleotidyl transferase dUTP nick end-labeling
TyrPC.....tyrosine-derived polycarbonate
UBM ..... urinary bladder matrix
UCB ..... umbilical cord blood
UCSB ..... University of California, Santa Barbara
UF .....University of Florida
UMDNJ..... University of Medicine and Dentistry of New Jersey
USAMRMC..... U.S. Army Medical Research and Materiel Command
USAISR ... U.S. Army Institute of Surgical Research
USPTO ..... U.S. Patent and Trademark Office
UVA .....University of Virginia
UVB .....ultaviolet B
VA.....Department of Veterans Affairs
VCA ..... vascularized composite allograft
VEGF.....vascular endothelial growth factor
VML ..... volumetric muscle loss
WFIRM ..... Wake Forest Institute for Regenerative Medicine
WFPC ..... Wake Forest–Pittsburgh Consortium
WFSM.....Wake Forest School of Medicine
XPS ..... x-ray photoelectron spectroscopy

Proud Sponsors of the AFIRM

The Armed Forces Institute of Regenerative Medicine establishes national teams that are collaborating including leading scientists in the field of regenerative medicine. For more information about the AFIRM, please contact:

Ms. Kathleen Berst
AFIRM Acting Director
kathleen.berst@us.army.mil